The dynamic temporal and spatial regulation of BMP signalling during early vertebrate development

Sabine Reichert

University College London

and

Cancer Research UK London Research Institute

PhD Supervisor: Dr. Caroline S. Hill

A thesis submitted for the degree of

Doctor of Philosophy

University College London

September 2013

Declaration

I Sabine Reichert confirm that the work presented in this thesis is my own. Where information has been derived from other sources, I confirm that this has been indicated in the thesis.

Abstract

During embryonic development multipotent cells are specified to give rise to the different tissues of the body. This process depends on a tightly controlled network of signalling pathways. Importantly, tissues, which require differential activity of these pathways, can be induced in close proximity, thus suggesting an intricate spatial and temporal control of pathway activation. One of the pathways crucial for tissue specification is the bone morphogenetic protein (BMP) signalling pathway. Its role in the patterning of the ectoderm is well understood during gastrulation but unclear for later stages of development.

Using zebrafish and *Xenopus* as model organisms, I investigated the spatial and temporal control of BMP activity after gastrulation at the border of the neural plate as progenitor cells emerge that give rise to cell types such as melanocytes and smooth muscle cells, as well as the olfactory epithelium and the lens. I identified new players that regulate the formation of distinct domains of BMP signalling and thereby enable the specification of adjacent tissues with different requirements for BMP activity.

Previously, Snw1 was identified as a crucial factor for neural crest specification during development. Overexpression and depletion of Snw1 in *Xenopus* and zebrafish embryos leads to a loss of the neural crest cell population. Snw1 was identified as a regulator of BMP activity at the neural plate border, but not as a core component of the pathway downstream of the receptor. Snw1 is involved in a step between transcription and expression of the BMP ligands and since depletion of Snw1 in zebrafish increases *bmp2b* ligand transcription but prevents expression of the protein. I have further dissected the function of Snw1 and shown that Snw1 is in a complex with components of splicing machinery, as well as several chromatin remodeling and transcriptional elongation factors. I have used RNAseq to identify additional Snw1 targets.

“So long, and thanks for all the fish.”

Douglas Adams, *The Hitchhiker's Guide to the Galaxy*

Acknowledgements

Embarking on a PhD is an exciting but equally challenging journey. Like any big journey it is not to be undertaken lightly and great travel companions are indispensible for guidance, support and the occasional good laugh.

My love for science was first sparked by my encouraging and inspirational mentor Dr. Helen Morrison at the Fritz Lipmann Institute in Jena/Germany. Helen taught me to trust my scientific instincts and to strive to be the best scientist I can be. With her support I swapped the calm, leafy peacefulness of central Germany for the big city excitement of London to work at the CRUK London Research Institute in Dr. Caroline Hills lab. It has been a wonderful time, during which I have met amazing scientists and friends. I want to thank Caroline for giving me the opportunity to work in her lab. I learned so much and I very much appreciate the time and effort you have put into teaching me and supporting my projects. Also thanks to Claire (for more than one Wednesday night), Becky, MC, Daniel, Debi, John, Mary, Jo, Ana, Tessa, Ilaria, Eva, Ele and Marco, with whom I had the pleasure to work. We always had such a great atmosphere in the lab and that makes even the scientific lows bearable, you are truly more than just colleagues. Special thanks to my long-term fellow Eastern Block residents Pedro and Thijs. You guys have been the greatest support and inspiration a young PhD student could wish for.

Science does not live in a nutshell and sharing it with the outside world is important. I want to thank my thesis committee, Taija Makinen and Nic Tapon, as well as all members of the Developmental Biology interest group for brilliant scientific discussions and advice.

I also would like to thank the fantastic LRI service laboratories for support, in particular the microscopy department, the Advanced Sequencing facility and the Bioinformatics department, especially Richard Mitter. As any development biologist I would be nothing without my favourite model organism. Thanks Phil Taylor, Darren Martin and Chris Sergeant for keeping the fish facility up and running so smoothly and for always trying to accommodate all my individual requests.

I know that my roots give me the foundation to feel secure in life. So last but not least, I want to thank my amazing family and friends. You know how much you mean to me without me having to spend many words on it.

Table of Contents

Table of figures

List of tables

Abbreviations

APC	adenomatosis polyposis coli
BAMBI	BMP and activin membrane-bound inhibitor
BCIP	5-Bromo-4-chloro-3-indolyl phosphate
BIO	6-BromoIndirubin-3′-Oxime
BMP	bone morphogenetic protein
CDK	cycline-dependent kinase
CMP	counts per million
COSMIC	catalogue of somatic mutations in cancer
CR	cysteine rich
cm	centimetre
DFISH	double-fluorescent *in situ* hybridisation
DNA	deoxyribonucleic acid
Dpp	decapentaplegic
DTT	dithiothreitol
DV	dorsoventral
eGFP	enhanced green fluorescent protein
EtOH	ethanol
Fdx	fluorescein isothiocyanate–dextran
FGF	fibroblast growth factors
FDR	false discovery rate
Fwd	forward
GSK3	glycogen synthase kinase 3
HAT	histone acetylase
HDAC	histone deacetylase
HSPGs	glycosylphosphatidylinositol- anchored heparan-sulphate proteoglycans
HUVEC	human umbilical vein endothelial cells
IF	immunofluorescence
IP	immunoprecipitation
ISH	whole-mount *in situ* hybridisation
kb	kilobase

LEF	lymphoid enhancer-binding factor 1
LRP	lipoprotein receptor-related protein
mA	milliampere
MAB	maleic acid buffer
MAD	mothers against decapentaplegic
MAPK	mitogen-activated protein kinases
MBT	mid-blastula transition
Met	methionine
MeOH	methanol
MH2	MAD homology 2
Min	minute
mm	millimetre
MO	morpholino
mRFP	monomeric red fluorescent protein
NE	neural ectoderm
NEB	New England Biolabs
NC	neural crest
NNE	non-neural ectoderm
NICD	Notch intracellular domain
NPB	neural plate border
O/N	overnight
PCP	planar cell polarity
PCR	polymerase chain reaction
PFA	paraformaldehyde
PI	protease inhibitors
Rev	reverse
RNA	ribonucleic acid
RNAPII	RNA polymerase II
RT	room temperature
qRT-PCR	quantitative real time PCR
scw	screw
SDS-PAGE	SDS polyacrylamide gel electrophoresis
snRNP	small nuclear ribonucleic particles
Sog	short gastrulation

SUMO	small Ubiquitin-like Modifier
TCF	T-cell factor
Tg	transgenic
TGF-β	transforming growth factor β
Tsg	twisted gastrulation
V	volts
X. laevis	*Xenopus laevis*

Chapter 1. Introduction

1.1 Embryonic patterning

During vertebrate embryogenesis the early embryonic cells are induced to form the three germ layers - endoderm, mesoderm and ectoderm - in a process of cell differentiation and morphogenesis. The different germ layers are then further specified to give rise to the tissues and organs. The endoderm develops into the inner lining of the respiratory and digestive systems. The mesoderm gives rise to several organs (kidney, heart, gonads), connective tissue (bone, muscles, blood vessels) and blood cells. The ectoderm first differentiates into the non-neural ectoderm (NNE), the preplacodal ectoderm (PPE), the neural crest (NC) and the neural plate (NP), which together will form the epidermis and the nervous system. Thus during embryonic development cells progressively loose their pluripotency as they become specified into the various cell types.

Understanding the mechanisms underlying these cell fate decisions and subsequent organ formation is crucial and has implications beyond deciphering normal developmental processes. Many of the pathways that regulate tissue specification are deregulated in diseases such as cancer (Kho et al., 2004, Dreesen and Brivanlou, 2007) and studying developmental processes has led to the identification of novel genes, signal transduction pathways and regulatory mechanisms that are implicated in the development of malignancies. An example is the transforming growth factor β superfamily (TGF-β) signalling pathway. Although the pathway was first described in a tissue culture context, the main effectors of the TGF-β signalling pathway, the Smad transcription factors, were first described in the fruit fly *Drosophila melanogaster* (Sekelsky et al., 1995). Subsequently many other components of the pathway were identified in a developmental context such as the negative regulators Chordin and Noggin in *Xenopus laevis (X. laevis)* (Sasai et al., 1994, Smith and Harland, 1992). Another example is the Hippo signalling pathway, which is required for organ size control and cell fate decisions during normal development. First identified in *Drosophila,* Hippo signalling was subsequently shown to be evolutionary conserved in mammals and has been extensively implicated in cancer development (Harvey and Tapon, 2007). Similarly, the hedgehog pathway (Hh), also first described in *Drosophila*, plays a role in the

development of several cancers (McMillan and Matsui, 2012, Nusslein-Volhard and Wieschaus, 1980). Numerous drug development programs in both academia and industry have been and are directed to identify pathway inhibitors for cancer treatment (Perrot et al., 2013, Yun et al., 2012). These examples demonstrate the impact studying signalling pathway regulation in development can have on understanding and treating disease.

Another incentive to understand how tissues are specified from pluripotent progenitor cells is to enable the construction of tissues and organs from stem cells for medical therapies. Today, we rely on organ and tissue donations to replace damaged organs. However, although the numbers of donations in the UK have been increasing over the past years, the number of people waiting for a transplant still exceeds the number of available donors (NHS Blood and Transplant (NHSBT),Organ Donation and Transplantation Activity Report 2012/13). Moreover, rejection of donated transplants as a result of an immune response can lead to transplant failure and requires the use of immunosuppressive drugs. Therefore, using stem cells as a renewable source for tissues is a promising approach for treatment of diseases. The development of such methods necessitates a detailed understanding of how different tissues are normally specified during embryonic development.

Tissue specification and patterning in developing embryos is known to require networks of tightly-regulated signalling pathways, such as those activated by the TGF-β, Wnt, FGF and Notch ligands (Stuhlmiller and Garcia-Castro, 2012a, Tzahor, 2007). In the following sections I will introduce the current understanding of how these pathways are spatially and temporally regulated to orchestrate growth and differentiation during ectodermal patterning with an emphasis on BMP signalling during NC development.

1.1.1 Ectodermal patterning

During vertebrate ectodermal patterning progenitor cells are initially specified along the dorsoventral (DV) axis with the neural plate (NP) on the dorsal side, the neural plate border (NPB) adjacent and epidermal progenitors in the non-neural ectoderm (NNE) ventrally (Figure 1.1)(Hammerschmidt and Mullins, 2002). These relatively uncommitted progenitors are then further specified along the DV, as well as the

rostro-caudal axis, and the ectoderm differentiates into 4 main functional entities: the central nervous system (CNS), the NC and cranial placodes at the NPB, which together give rise to structures of the peripheral nervous system, and the skin (Figure 1.1)(Kwon et al., 2010). The NC differentiates into craniofacial cartilage and bone, melanocytes, smooth muscle and cells of the peripheral nervous system. In contrast, the PPE contributes to cranial sense organs such as the eye, the ear and the olfactory epithelium (Streit, 2007, Dupin et al., 2006).

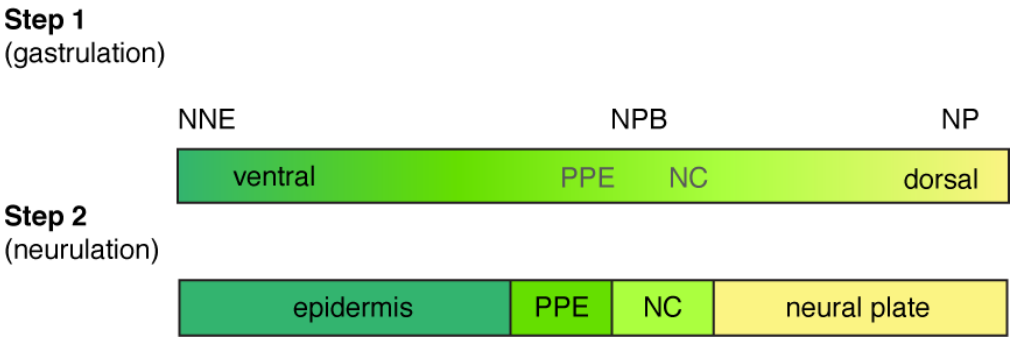

Figure 1.1 Ectodermal patterning

Ectodermal progenitors are progressively specified during ectodermal patterning along the DV axis.

Ectodermal differentiation requires a network of signalling pathways, which is temporally and spatially highly dynamic. Moreover, the cellular identity is not only determined by exposure to a signalling molecule, but depends on the concentration and the combination of signals and whether a cell is competent to respond to the signal exposure at a given time. Therefore, it is thought that tissue specification occurs in several phases and is conferred by a dynamic network of signalling pathways. Thus the changing requirements of tissues for pathway activity can be met as progenitors become increasingly specified.

In the following section I will introduce the main signalling pathways involved in ectodermal patterning, namely Wnt, FGF, Notch and BMP signalling.

1.1.2 Wnt signalling

The Wnt pathway plays an important role during embryonic development and is implicated in diverse processes such as cell fate decisions, polarity, migration and proliferation (Grigoryan et al., 2008, Logan and Nusse, 2004). In the canonical Wnt

signalling pathways secreted Wnt proteins bind to Frizzled and LRP family cell surface receptors, which ultimately leads to the stabilisation and nuclear accumulation of β-catenin (Kim et al., 2013) (Figure 1.2). In the nucleus, β-catenin then interacts with transcription factors belonging to the TCF/LEF family to modulate gene expression. In the absence of Wnt signalling β-catenin is phosphorylated by GSK3β, which is in a protein complex with APC and Axin, and is targeted for ubiquitination-dependent proteasomal degradation by the E3 ligase β-TrCP. Upon ligand binding, however, the cytosolic adaptor protein Dishevelled is activated and the β-catenin destruction complex inhibited.

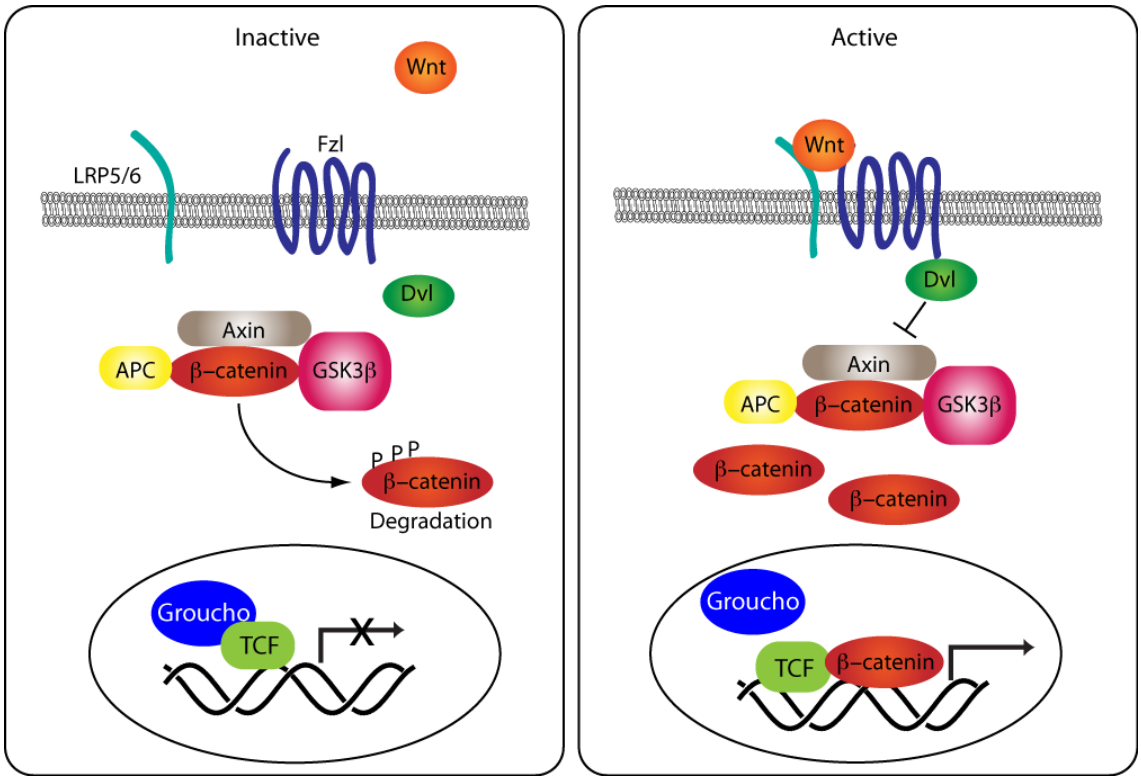

Figure 1.2 The canonical Wnt signalling pathway

In the absence of Wnt-signal, β-catenin is targeted and phosphorylated by the APC/Axin/GSK3β complex leading to its ubiquitination and proteasomal degradation. In the presence of Wnt ligand, the co-receptor LRP5/6 is brought in complex with Wnt-bound Frizzled. This activated Dishevelled (Dvl), the β-catenin destruction complex is inhibited and β-catenin translocates to the nucleus. The Groucho/HDAC co-repressor complex is subsequently displaced and β-catenin acts a co-activator for TCF/LEF-mediated transcription

The non-canonical Wnt signalling pathways are β-catenin independent (van Amerongen, 2012). In the non-canonical planar cell polarity (PCP) pathway Wnt signals are transduced via small G-proteins such as Rho/Rac resulting in cytoskeletal changes. In a second main alternative pathway, Wnt assists in regulating intracellular calcium levels by regulating the calcium release from the endoplasmic reticulum.

Wnt activity has a long been proposed as positive regulator of NC induction in several species. Analyses predominantly in *X. laevis* has suggested that activation of Wnt in combination with attenuation of BMP signalling can induce NC (Abu-Elmagd et al., 2006, LaBonne and Bronner-Fraser, 1998, Steventon et al., 2009, Litsiou et al., 2005). Co-expression of Wnt1 or Wnt3a together with the BMP inhibitors Noggin or Chordin in *X. laevis* animal caps leads to the ectopic expression of the NC markers such as *slug* (Saint-Jeannet et al., 1997). Furthermore, overexpression of these ligands in the whole embryos causes an expansion of NC marker expression. Knockdown of Wnt3 and Wnt8 and expression of a dominant negative Wnt construct suppresses the induction of several NC and NPB markers (Elkouby et al., 2010, Hong et al., 2008, Steventon et al., 2009). Wnt8 has also been implicated in NC development in zebrafish. Injection of a morpholino against *wnt8.1* delays, but does not abolish, the expression of the NC markers *pax3*, *foxd3* and *sox10* (Lewis et al., 2004). Furthermore, expression of downstream components of the canonical Wnt signalling pathway such as Frizzled3, Frizzled7, LRP6 and β-catenin result in ectopic NC induction in *X. laevis* (Abu-Elmagd et al., 2006, Deardorff et al., 2001, LaBonne and Bronner-Fraser, 1998, Tamai et al., 2000) and depletion of Dishevelled 1 or 2 leads to a suppression of *snail2* and *twist* expression (Gray et al., 2009).

In the chick, addition of Wnt3a to prospective neural epiblast explants promotes the expression of NC markers (Patthey et al., 2009, Wilson et al., 2001) and inhibition of Wnt signalling in prospective NC explants results in loss of NC markers (Patthey et al., 2009). The role of individual Wnt ligands in chick NC development has not been studied, but *wnt3a* and *wnt8a/c* expression patterns during blastula stages suggest and involvement in NC induction (Skromne and Stern, 2001, Wilson et al., 2001).

In the mouse, Wnt1 and Wnt3a are dispensable for the initial expression of *ap2* but required for NC marker expression during migration. Double-homozygous

null mutants for Wnt1/Wnt3a display severe defects in NC derivatives (Ikeya et al., 1997). In a transgenic $Wnt1^{Cre}$ mouse line, cells deriving from the neural crest are targeted (Danielian et al., 1998). Depletion of β-catenin in the region of Wnt1 expression affects NC development and thus leads to a failure of craniofacial development (Brault et al., 2001). However, the observed phenotype might be due to impaired cell adhesion.

Taken together, there is circumstantial evidence that Wnt signalling is a positive regulator of NC induction mostly from overexpression of or treatment with Wnt ligands. It remains to be determined, which specific ligands are required for Wnt signalling and Wnt8 as well as Wnt3 are possible candidates.

1.1.3 Fibroblast growth factor signalling

Fibroblast growth factors (FGFs) are a family of growth factor required for a variety of developmental and homeostatic processes such as mesoderm induction, neural development and wound healing (Dorey and Amaya, 2010, Turner and Grose, 2010, Ford-Perriss et al.). FGFs bind to receptor tyrosine kinases (FGF receptors) assisted by cell surface associated heparin sulphate proteoglycans. Upon ligand binding FGFRs dimerise, which triggers tyrosine kinase activation leading to autophosphorylation of the intracellular receptor domain (McKeehan et al., 1998). This autophosphorylation regulates the protein tyrosine kinase activity of the receptor and leads to the activation of one or more intracellular signalling cascades such as the MAPK, PLCγ/Ca^{2+} and PI3 kinase/Akt pathway (Dorey and Amaya, 2010).

In *X. laevis*, the role of FGF signalling in early patterning and tissue induction has been studied extensively. As the main focus Fgf8a has emerged as a NC inducer. Depletion of Fgf8a using a morpholino approach abolishes the expression of the NC markers *ap2*, *snail2*, *sox8/10*, *hairy2*, *pax3* and *msx1* and Fgf8 overexpression expands NC marker domains (Hong et al., 2008, Hong and Saint-Jeannet, 2007, Monsoro-Burq et al., 2005, Nichane et al., 2008a). In contrast to the Wnts, Fgf8 is able to induce transient NC marker expression in animal cap assays without simultaneous inhibition of BMP activity (Monsoro-Burq et al., 2003). Fgf8 is also required for the induction of preplacodal markers, while ectopic

expression of Fgf8 in chick induces expression of *eya2,* but no other PPE specific marker (Ahrens and Schlosser, 2005, Litsiou et al., 2005, Brugmann et al., 2004).

NC formation requires Fgfr1, but not Fgfr4a, expression. It has been suggested that FGF indirectly regulates NC development acting to induce *wnt8* expression (Hong et al., 2008). Fgf8 cannot rescue the NC phenotype in *wnt8* or *β-catenin* morphants, whereas overexpression of Wnt8 or β-catenin restores NC marker expression in *fgf8* depleted *X. laevis* embryos. Furthermore, Fgf8 is required for *wnt8* expression in the paraxial mesoderm at late gastrula stages and Fgf8 overexpression expands the *wnt8* expression territory. Interestingly, Fgf8 acts on NC development in a dose-dependent manner; targeted injection of low doses of *fgf8a* mRNA enhances the expression of several NC markers, whereas NC induction is inhibited at higher doses. Thus similar to BMP signalling, which I will discuss in detail later, there appears to be a specific window of FGF signal strength that allows NC development.

In zebrafish, the contribution of FGF signalling to NC induction has not been extensively studied. Inhibition of FGF activity, beginning at the onset of gastrulation, inhibits the expression of the NPB marker *pax3*, which in turn regulates NC induction (Garnett et al., 2012, Meulemans and Bronner-Fraser, 2004, Sato et al., 2005). In contrast, overexpression of Fgf8 in zebrafish leads to an expansion of the *ap2* expression domain at the NPB (Furthauer et al., 1997, Furthauer et al., 2004). However, FGF/MAPK signalling is also required for DV patterning by contributing to the BMP activity gradient formation, thus could indirectly determine NC induction.

In chick, inhibition of FGF signalling by targeted expression through electroporation of a dominant negative Fgfr1 or the MAPK signalling inhibitor Mkp3 during gastrulation impairs *pax7* and *snail2* expression (Stuhlmiller and Garcia-Castro, 2012b). Electroporation after gastrulation did not result in any effect, again suggesting a possible indirect role for FGF signals in NC induction by antagonizing BMP signals during DV axis formation. This study indicates, since expression of the truncated Fgfr1 acts cell-autonomously, a direct ectodermal requirement for FGF as opposed to an indirect role by inducing Wnt signals in the paraxial mesoderm, which is suggested in *X. laevis* (Hong et al., 2008). Moreover, Fgfr1 and Fgfr4 are expressed in the prospective NC epiblast but are absent from the mesoderm (Lunn et al., 2007, Stuhlmiller and Garcia-Castro, 2012b).

In mouse, no FGF pathway component has been directly linked to NC development. Knockouts of Fgfr1 and Fgf8 die before NC induction, as they fail to gastrulate properly (Deng et al., 1994, Meyers et al., 1998, Sun et al., 1999, Yamaguchi et al., 1994). Later in development, Fgfr1 is expressed in the NC-derived palate mesenchyme and mice carrying $Wnt1^{Cre}$ and $Fgfr1^{flox}$ transgenic alleles display severe craniofacial defects (Wang et al., 2013). All other FGF knockouts generated so far do not display defects in NC induction (Itoh, 2007).

Taken together, FGF signalling is required for NC development with Fgf8 being the ligand most likely conferring FGF activity in this process. Several lines of evidence support a role for the FGF receptor Fgfr1 during NC induction. It will have to be clarified if FGF activity directly regulates NC cell fate or whether the observed phenotypes are an indirect result of dorsal patterning defects.

1.1.4 Notch signalling

Notch proteins span the cell membrane and are activated by the binding of transmembrane ligands, Delta or Delta-like (Dll) and Serrate (Jagged in mammals), on the surface of adjacent cells. Upon ligand binding proteolytic cleavage releases the Notch intracellular domain (NICD), which translocates to the nucleus to activate gene transcription (Fiuza and Arias, 2007)(Figure 1.3). Notch is plays an important role in cell-cell communication and is required for cell fate decisions and boundary formation for example during neural development (Andersson et al., 2011).

In *X. laevis* NC development, Notch/Delta signalling appears to play an essential role. However, there is some controversy about the timing of activity and the sequence of NC inducing events. One study has demonstrated that inducible expression of NICD at late gastrula stages results in an expansion of NC markers similar to the effect of NC targeted overexpression of *hairy2* (Glavic et al., 2004b). The authors show that Notch activates the transcription of *hairy2*, which acts as a transcriptional repressor for *bmp4.* This would modulate BMP activity to a level that allows for NC induction, as NC is induced at specific levels of BMP activity (1.1.5). However, in the experimental setup, BMP inhibition occurs in a second phase after NC induction when NC progenitors have to be maintained, a process that requires active BMP signalling. A different study subsequently provided contradicting evidence suggesting that *hairy2* is not regulated by Notch but is induced by BMP

inhibition, canonical Wnt signalling and Fgf8 (Nichane et al., 2008a). The authors suggest that Hairy2 maintains undifferentiated NC progenitors, as overexpression of *hairy2* represses NC and induces NPB markers. It was then demonstrated that Hairy2 acts upstream of Notch by activating Delta1, which in turn upregulates *id3*, *snail2* and *sox9* (Nichane et al., 2008b).

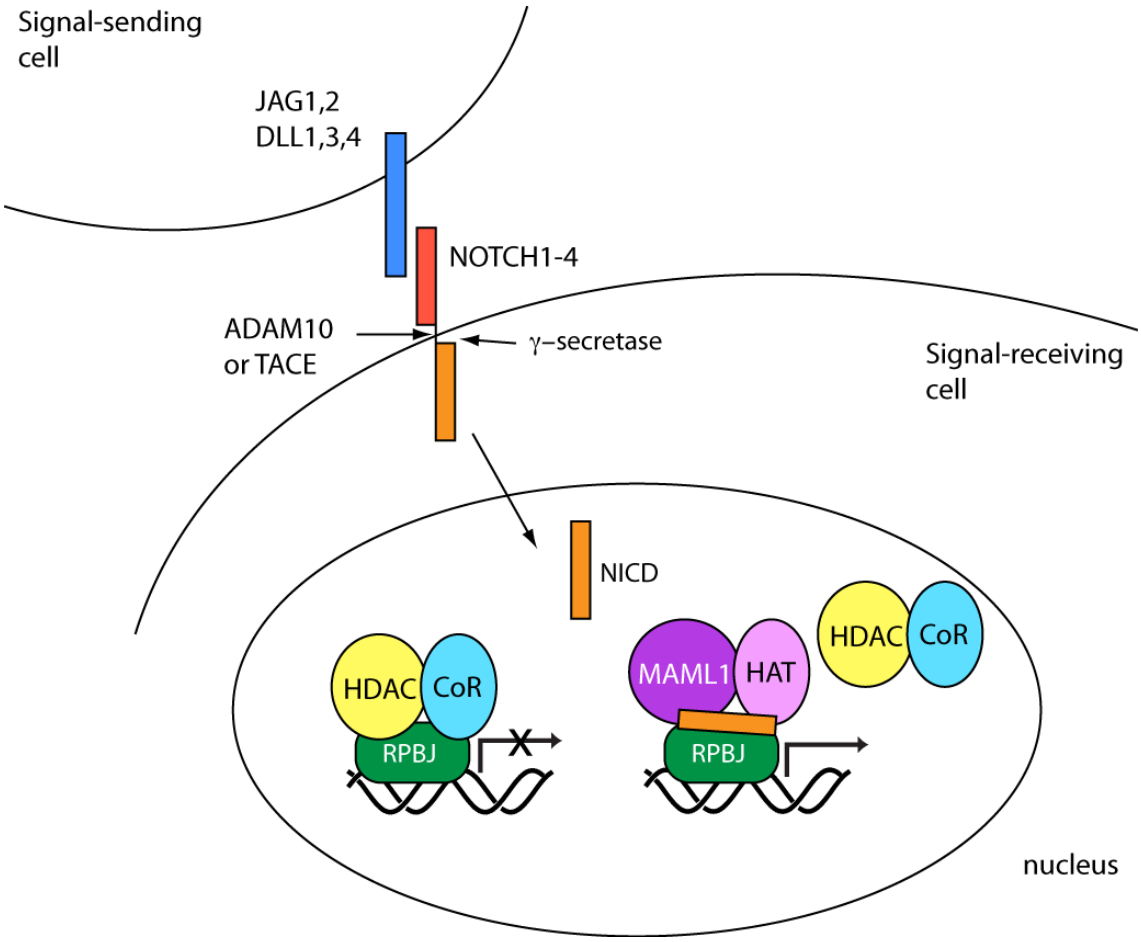

Figure 1.3 Core-components of the canonical Notch signalling pathway

Ligands of the Jagged (JAG1 and JAG2) and Delta-like (DLL1, DLL3, DLL4) families interact with Notch family receptors (NOTCH1-NOTCH4). Proteolytic processing by ADAM10 or TACE and γ-secretase releases the NICD, which enters the nucleus where it forms a complex with RPBJ thus displacing a histone deacetylase (HDAC)-co-repressor (CoR) complex. Activating factors such as MAML1 and histone acetyltransferases (HAT) are recruited to the NICD-RPBJ complex leading to the activation of Notch target genes.

In chick, overexpression and depletion of Notch represses *bmp4* and *snail2* expression (Endo et al., 2002). The Notch inhibition phenotype, however, can be rescued by Bmp4 expression, indicating that Notch acts indirectly by modulating BMP activity to permissive levels.

In zebrafish embryos, Notch seems to act mainly by defining the NPB. In the Delta/Notch mutant *mindbomb,* NC derivatives are reduced, whereas NP derivatives are increased (Jiang et al., 1996). More recent data indicates that Delta/Notch restricts the neural domain by negatively regulating the transcription factor Prdm1a. Prdm1a is required for NPB specification and antagonises Olig4 function, which defines the border of the NP and promotes neural cell fates (Hernandez-Lagunas et al., 2011).

In mouse there so far is no indication of Notch acting at the step of NC induction. *Delta1* null mutants display aberrant trunk NC migration, but no defects in NC induction, arguing for a later role of Notch signalling (De Bellard et al., 2002).

In summary, a direct role of Notch signalling in NC induction has yet to be demonstrated. The data so far rather suggests an indirect role by modulating BMP activity levels.

1.1.5 BMP signalling

Another pathway that is crucial for embryonic development and whose deregulation is also implicated in human disease is the bone morphogenetic protein (BMP) signalling pathway (Blanco Calvo et al., 2009, Lowery and de Caestecker, 2010, Wu and Hill, 2009). BMPs, together with the growth and differentiation factors (GDFs), form a subfamily of the transforming growth factor β (TGF-β) superfamily (Schmierer and Hill, 2007). For activation of the canonical BMP signalling pathway, BMP ligands bind as homo- or heterodimers to type I–type II serine/threonine kinase receptor complexes (Figure 1.4). Upon ligand binding, the constitutively active type II receptor phosphorylates the type I receptor within a glycine-/serin-rich motif. This activates the type I receptor and promotes the binding and phosphorylation of the main signalling effectors, the receptor-regulated Smads (R-Smads) at a C-terminal SSXS motif in the MH2 domain. In response to BMP and GDF signalling the R-Smads activated in particular, Smad1/5. Phosphorylated

Smad1 and Smad5 then form complexes with the co-Smad, Smad4, which accumulate in the nucleus, where they regulate gene expression.

In addition to C-terminal phosphorylation, the R-Smads can also be phosphorylated in the linker region between the N-terminal MH1 and the MH2 domain. The phosphorylation sites are important for the regulation of Smad activity and specific to distinct pathways (Kamato et al., 2013)(Figure 1.4).

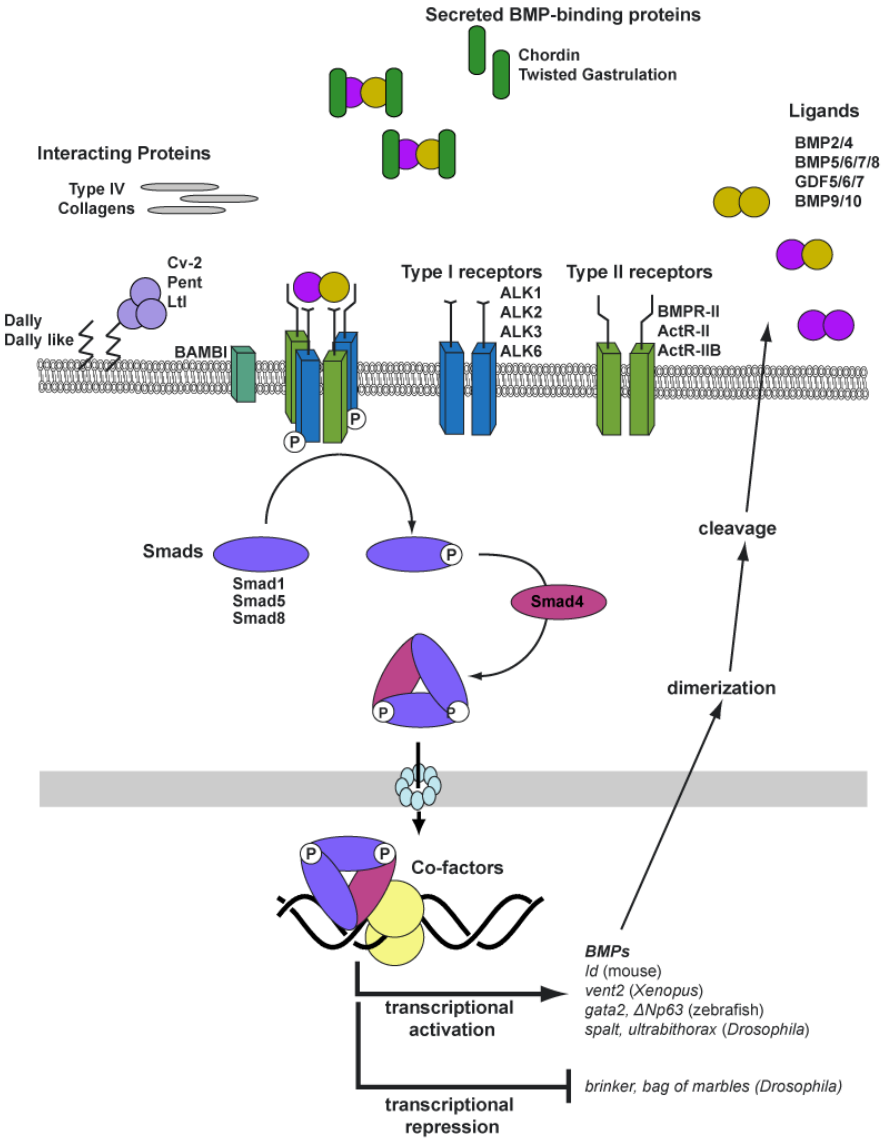

Figure 1.4 The BMP signalling pathway

Schematic of the core BMP signalling pathway. Additional secreted and membrane-bound BMP-binding proteins are depicted and will be mentioned throughout the Introduction. Adapted from (Ramel and Hill, 2012).

MAPK-dependent phosphorylation of Smad1, for example, inhibits Smad1 activity by attenuating the nuclear accumulation of Smad1 (Kretzschmar et al., 1997, Sapkota et al., 2007).

BMPs have historically been described as morphogens and gradients of BMP signalling can be observed in many species such as sea urchins, *Drosophila*, *X. laevis*, zebrafish and mouse (Ramel and Hill, 2012). Signalling gradients confer positional information in a dose-dependent manner thus giving rise to different progenitor cells according to the strength of the signal. With regard to BMP activity this is important in many processes such as wing and lens development or the establishment of the DV axis (Nellen et al., 1996, Wilson et al., 1997, French et al., 2009).

BMP signalling is crucial for ectodermal patterning as the BMP gradient is absolutely required for the establishment of the DV polarity and BMP activity promotes epidermal over neural cell fates (Nguyen et al., 1998, Wilson et al., 1997). Since NC and the PPE are induced at the border between neural and non-neural ectoderm it is suggested that this process requires intermediate levels of BMP activity with slightly higher activity required in the PPE. Indeed, treatment of explanted *X. laevis* ectoderm with the BMP inhibitor Noggin results in the induction of epidermal, NC or neural cell fates in a dose dependent manner (Marchant et al., 1998, Tribulo et al., 2003). A similar model has been proposed in zebrafish (Mullins et al., 1996 {Barth, 1999 #397}) and analysis of BMP pathway mutants supports the idea of initial NC induction requiring intermediate BMP signalling levels (Schumacher et al., 2011). Recent evidence from zebrafish indicates that the BMP gradient is required for the inductive process of NC and adjacent PPE progenitors at late blastula/early gastrula stages (Kwon et al., 2010).

The establishment of the DV gradient has been studied in great detail. In a simplified model, a combination of high BMP ligand expression ventrally and dorsal expression of BMP antagonists from the organiser such as *chordin* and *noggin* results in graded BMP activity levels. Recent studies have added great detail to this model. In zebrafish, directly after mid-blastula transition (MBT) the ligands *bmp2b*, *bmp7a* and *bmp4* are ubiquitously expressed, whereas maternally deposited *β-catenin* is concentrated to the future dorsal side of the embryo (Schier and Talbot, 2005). At sphere stage, the transcriptional repressor Dharma is expressed dorsally and mediates the earliest DV asymmetry by directly repressing *bmp2b* transcription

(Koos and Ho, 1999, Leung et al., 2003). This initiating event is subsequently followed by dorsal FGF activity, which appears to inhibit *bmp* ligand transcription in a dose-dependent manner (Furthauer et al., 2004, Ramel and Hill, 2013). In addition, *chordin* and *noggin1* are dorsally secreted to inhibit BMP ligand activity, but *chordin* seems to be essential for this process whereas *noggin1* acts to enhance the effect (Dal-Pra et al., 2006)(1.2.2.2). The combination of these instructive signals results in a graded expression of *bmp* ligands themselves at the end of the blastula stage (Furthauer et al., 2004, Sidi et al., 2003). Interestingly, during this process BMP ligands do not seem to act as morphogens in the classical sense of generating a gradient through extracellular diffusion, as it has been demonstrated in *Drosophila* (Zhou et al., 2012b). In contrast, the zebrafish DV BMP signalling gradient is formed from an initially ubiquitous BMP activity (Ramel and Hill, 2013). Importantly, the graded expression of the *bmp* ligands is initially established through dorsal transcriptional inhibition by Dharma and FGF signalling.

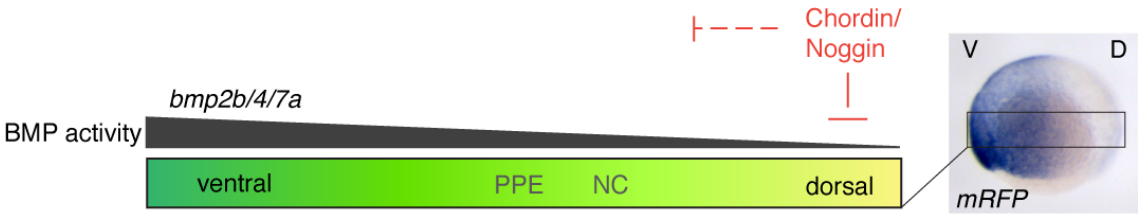

Figure 1.5 BMP activity gradient during gastrulation

BMP activity is initially inhibited by the dorsal expression of BMP antagonists such as Chordin and Noggin. At gastrula stages expression of the BMP ligands is autoregulated and thus graded with higher expression levels ventrally. Along this BMP gradient cell types such as PPE and NV are initially specified.

From about 60% epiboly, *bmp* ligand transcription is autoregulated by BMP signalling thereby maintaining the graded ligand expression (Figure 1.5) (Kishimoto et al., 1997, Nguyen et al., 1998, Schmid et al., 2000). Thus, the combination of these transcriptional inputs is the gradient forming factor rather than actual diffusion or redistribution of Bmp proteins. This is also indicated by immunostaining against Bmp2b in zebrafish embryos, where no BMP activity could be observed outside of Bmp2b expression domains, as would be expected if BMP proteins could not diffuse from their site of expression (Ramel and Hill, 2013). This observation

supports other data, which, using mosaic experiments, shows that Bmp2b acts cell autonomously during zebrafish ectodermal patterning (Nikaido et al., 1999). Similarly, studies in *X. laevis* determined that in contrast to Activin, Bmp4 expression does not have any long-range effects on surrounding tissues (Jones et al., 1996). Notably, *X. laevis* Bmp4 is suggested to be functionally equivalent to zebrafish Bmp2b (Kondo, 2007).

As mentioned above this initial gradient with discrete levels of BMP activity along the DV axis defines the position of ectodermal derivatives such as the PPE, the NC and the NP (Nguyen et al., 1998). This gradient model is sufficient to explain the requirements for progenitor cell induction during gastrulation, but later specification processes cannot be explained. For example, during zebrafish PPE formation, which is located adjacent to the NC, BMP signalling is required only during late blastula stages, but is no longer needed after the onset of gastrulation (Kwon et al., 2010). The same study suggested that BMP activity is not only dispensable for further PPE induction, but that in fact full attenuation of BMP signalling is necessary during late gastrulation, presumably through localized expression of BMP antagonists. Indeed, ectopic sources of BMP inhibitors result in an expansion of PPE marker expression (Ahrens and Schlosser, 2005, Glavic et al., 2004a, Litsiou et al., 2005).

Experiments in chick support the idea that BMP signalling acts in two phases during DV patterning. Treatment of prospective neural crest explants with Noggin shows that for NC development BMP signalling is not required during early blastula stages to induce NC, but is required from the late blastula stage onwards (Patthey et al., 2009). Also, inhibition of BMP signalling after gastrulation results in the loss of NP border markers and BMP activity is required for the expression of NC specifiers at later stages (Selleck et al., 1998). Thus, the requirement of BMP activity in NC and PPE development differs significantly over time. Interestingly, a recent study has demonstrated the loss of the BMP gradient after gastrulation and BMP activity becomes localised to the NPB (Wu et al., 2011). How this process is regulated and how distinct signalling domains are regulated is not understood.

Studies concerning the contribution of BMP signalling components in mice have been complicated by the fact that BMP signalling is essential for early developmental processes. Knockout mice for the type I receptors *Alk2* and *Alk3,* type II receptor *Bmpr2*, and *Bmp4* die before gastrulation (Beppu et al., 2000,

Fujiwara et al., 2002, Gu et al., 1999, Mishina et al., 1999, Mishina et al., 1995). Heterozygous Bmp4 mutants, however, display craniofacial defects indicating perturbed NC development (Dunn et al., 1997). To circumvent this problem Wnt1-Cre lines have been generated. Due to the onset of Wnt1 expression after NC induction these lines cannot give any information on early events but they are useful tools to analyse later events. Mice with signalling components such as *Alk2, Alk3, Alk5* and *Smad4* conditionally knocked down all display craniofacial, pharyngeal and cardiac defects indicating a role in NC development (Dudas et al., 2004, Jia et al., 2007, Kaartinen et al., 2004, Ko et al., 2007, Nie et al., 2008, Stottmann et al., 2004, Wang et al., 2006).

Taken together, the importance of BMP signalling for NC development has been convincingly demonstrated. There appears to be differential requirements for BMP activity at the different stages of DV patterning. How BMP activity is temporally and spatially regulated during this process *in vivo*, especially after gastrulation, is yet to be addressed.

1.1.6 Integration of the signalling pathways in NC and PPE induction

As indicated in the previous sections, the signalling processes implicated in NC development and ectodermal pattering are not isolated events but form an intertwined, dynamic network. This permits the induction and specification of many progenitor cell types with a relatively restricted number of pathways. The molecular events and the timings that lead to tissue specification might vary slightly between organisms, but an overall model for neural crest induction can be deduced.

Current data indicates that the in zebrafish initial induction of NPB cell fates occurs at the late blastula/early gastrula stage with different continued signalling for maintenance and specification of these progenitors cells at later stages. A first phase requires at least partial inhibition on BMP signalling, as high levels of BMP activity favour epidermal cell fates. In a later phase BMP signalling must be inhibited for PPE development and activated for NC progenitor maintenance. BMP signalling also continues to be inhibited in the NP for neural specification. Attenuation of BMP activity is achieved through several means. For the early BMP activity gradient formation, dorsal FGF signalling is crucial to inhibit *bmp* ligand

transcription, although it is not yet clear how FGF achieves that. In addition to the limited expression of Bmp ligands secreted BMP antagonists such as Noggin and Chordin help to reinforce and stabilise the gradient. A recent study in chick suggested that Wnt signalling temporally regulates BMP activity at the NPB. Exposure of gastrula stage prospective neural explants with *Wnt3* induces Bmp4 expression, whereas treatment of prospective NC explants with a Wnt inhibitor leads to the downregulation of *Bmp4* and loss of NC markers (Patthey et al., 2009). Similarly it has been demonstrated in *X. laevis* that the first NC inductive step requires Wnt activation and BMP inhibition, but the later maintenance phase requires both signals (Steventon et al., 2009). Whether this hold true in other species remains to be tested.

FGF signalling is required for the initial induction of NPB markers, however it has an important role in many processes such as DV patterning, mesoderm induction and gastrulation movements, all of which could influence NC induction. As mentioned above, FGFs are able to regulate Wnt and BMP signalling. During early DV axis formation FGF negatively regulates BMP activity. Within the NPB FGF signalling is required to inhibit epidermal development and BMP activity prevents the generation of neural cells (Patthey et al., 2009, Sjodal et al., 2007, Stuhlmiller and Garcia-Castro, 2012b).

In zebrafish, intermediate levels of BMP activity establish expression of the NPB markers *zic3* and *pax3a* and this is enhanced by Wnt and FGF signals during mid to late gastrulation (Garnett et al., 2012). By integrating these signals through different enhancers a sharp expression domain at the NPB can be achieved. Moreover, this study demonstrates a Wnt-independent function of FGF signals in zebrafish NPB induction.

Taken together, increasing evidence has been gathered as to how different signalling pathways are integrated to give rise to the cell types specified during ectodermal patterning. It is still a challenge to decipher the contribution of the implicated signalling pathways to the patterning process. It will be important in the future to directly monitor signalling activity in time and space in order to understand the crosstalk between pathways. Moreover, it is important to manipulate pathway with regard to the temporal requirements of signalling activity. With the emergence of novel tools to manipulate and monitor spatial and temporal signalling events,

such as transgenic reporter lines and inducible expression systems, more insight will be gained in how signals are orchestrated *in vivo* at a molecular level.

1.2 Spatial regulation of BMP activity

BMP activity can be spatially regulated at different levels from transcriptional control of the pathway to localised modulation of ligand activity. In the section I will give an overview of some of the regulatory mechanisms and how they contribute to localised pathway activity. I will introduce how BMP signalling can be modulated on the level of the Smad transcription factors as well as the processing of the BMP ligands and the regulation of their activity in the extracellular space.

1.2.1 Regulation on Smad transcriptional level

The Smad transcription factors are ubiquitously expressed in most tissues, but Smad protein activity can be regulated through post-translational modifications. Smad proteins are highly conserved within their N-terminal MH1 and C-terminal MH2 domains (Attisano and Lee-Hoeflich, 2001). Between these two MH domains lies a non-conserved linker region. Smads are activated by ligand-induced phosphorylation of the C-terminal MH2 domain in their –SSXS motif by type I receptors. However, the linker region can also be phosphorylated on Ser or Thr by other kinases such as Erk MAPK, cyclin-dependent kinases (CDKs) or GSK3 (Alarcon et al., 2009, Fuentealba et al., 2007, Pera et al., 2003, Wang et al., 2009). This can both affect protein stability and recruitment of cofactors to regulate gene transcription and these processes are interregulated. CDK8 and CDK9, for example, can phosphorylate the linker region of Smad1, which results in the recruitment of the Hippo pathway transcriptional coactivator YAP (Alarcon et al., 2009, Aragon et al., 2011). YAP binding enhances Smad-mediated transcription, but ultimately the linker phosphorylation is recognised by the ubiquitin ligase Smurf1, which is thought to lead to Smad degradation. Similarly it was shown in *X. laevis* that the duration of activity of Smad1, phosphorylated in is MH2 domain, was regulated by sequential Smad1 linker phosphorylation and subsequent targeting for proteasomal degradation by Smurf1-induced polyubiquitination (Fuentealba et al.,

2007). MAPK and GSK3 inhibition prolonged BMP activity in response to ligand exposure by stabilising Smad1. Mutation of the Mad, the *Drosophila* R-Smad, GSK3 linker phosphorylation sites in the *Drosophila* wing disk results in a phenotype consistent with increased BMP activity (Eivers et al., 2011). Regulation of Smad activity through linker phosphorylation has important developmental implications, for example, during patterning of the zebrafish DV and anteroposterior (AP) axes (Hashiguchi and Mullins, 2013). DV patterning by BMP signalling along the AP axis is temporally coordinated with AP patterning by FGF, Wnt and retinoc acid (RA) signalling. The temporal coordination is partly mediated by FGF/MAPK-dependent phosphorylation of the PSmad1/5 linker. This negatively regulates PSmad1/5 function in the ventral vegetal (posterior) region of the gastrula stage embryo and alteration of the MAPK phosphorylation sites results in precocious patterning of DV tissues. This, however, is independent of an altered Smad stability and the authors propose an independent mechanism possibly affecting Smad1/5 activity directly. Exploiting a different mechanism, the Nemo kinase can inhibit BMP activity. *Drosophila* Nemo phosphorylates Mad in the N-terminal MH1 domain, thus resulting in an increased nuclear export (Zeng et al., 2007). Taken together, this indicates that Smad-mediated BMP signalling can be regulated by kinases other than the BMP receptors.

Smad activity can be modulated by other posttranslational modifications apart from phosphorylation, for example, SUMOylation. SUMO (ubiquitin-related modifier) proteins are small proteins, which resemble the three-dimensional structure of ubiquitin (Geiss-Friedlander and Melchior, 2007). They are conjugated to a substrate through an enzymatic cascade including E1, E2 and E3 enzymes. SUMOylation can have different effects on targets ranging from alterations to protein activity to changes in subcellular localisation and protein stability. In *Drosophila*, SUMOylation of Medea (Med, co-Smad) negatively regulates the Dpp signalling range by promoting the nuclear export of Med (Miles et al., 2008). This study proposes that interaction with pMad delays the SUMOylation of Med upon entry to the nucleus, thus allowing for the formation of active Smad signalling complexes in response to BMP signals.

The tissue and stage specific expression/activity of transcriptional co-regulators is another mean to spatially control BMP signalling. A well-studied example is the Smad1/Smad4 interacting protein Schnurri. Schnurri's activating

and repressing function has been mostly investigated in *Drosophila* and it can act directly, as well as indirectly, on gene transcription. Schnurri, for example, has a direct role in the activation of the *ubx* and *race* target gene expression (Dai et al., 2000, Wharton et al., 2004, Torres-Vazquez et al., 2000?). In an indirect step, Schnurri can control BMP target gene transcription by binding in a Smad/Schnurri repression complex to the promoter of the brinker gene. Brinker is a transcriptional repressor, thus Brinker inhibition results in an upregulation of BMP-dependent gene expression (Pyrowolakis et al., 2004). Interestingly, the worm homologue of Schnurri also confers tissues specific responses to BMP pathway activation (Liang et al., 2003). The vertebrate homologue is yet to be identified

1.2.2 Spatial regulation of BMP ligand activity

BMP ligand activity can be regulated at an intracellular level through altering transcription levels as well as the processing of BMP ligands. As secreted ligands, Bmp ligand activity is also coordinated through binding of activating or inhibiting factors in the extracellular space. In the following sections, I will introduce several known mechanisms.

1.2.2.1 Intracellular regulation of BMP ligand production/activity

In zebrafish, early zygotic *bmp* ligand transcription is under the control of the maternally deposited BMP ligand *radar/gdf6a* (Goutel et al., 2000) and the maternal transcription factor Pou2/Oct4 (Reim and Brand, 2006). As described earlier, after an initial phase of ubiquitous expression, *bmp2b* is then repressed on the dorsal side by FGF signalling and the localised transcriptional repressor dharma (Furthauer et al., 2004, Leung et al., 2003). Later on, *bmp* transcription is under BMP signalling autoregulation and mutants for *bmp2b* and *bmp7a* lack BMP activity after mid-gastrulation (Schmid et al., 2000).

Bmp ligands are initially synthesised as large inactive precursors and have to undergo proteolytic cleavage in the Golgi apparatus by pro-protein convertases to obtain the biologically active mature form (Zhou et al., 2012a). There are two major cleavage sites, S1 and S2. Cleavage at S1 liberates the mature ligand, but cleavage at S2 facilitates the release of the pro-peptide (Cui et al., 2001). In the

intracellular compartment, the pro-domain regulates the correct folding, dimerization, cleavage, and secretion of the mature BMP thus tissue specific cleavage can regulate localised BMP activity (Harrison et al., 2011). In *Drosophila*, for example, the BMP type ligand Decapentaplegic (Dpp) is cleaved at two sites in the wing but only at S1 in the midgut (Sopory et al., 2010). Cleavage at both sites appears to increase the stability of the mature ligand, thus modifying signal intensity and range. How the cleavage is tissue-specifically regulated is still unknown. A Bmp4 precursor that cannot be cleaved at S2 has been shown to stay attached to the pro-domain and as a result is targeted for degradation and thus less active when overexpressed in *X. laevis* (Cui et al., 2001). Mutation of this cleavage site in mice results in the severe loss of BMP4 activity in some tissues, whereas other tissues developed normally indicating a tissue specific requirement for S2 cleavage (Goldman et al., 2006).

BMP ligands bind to receptors as homo-or heterodimers in *Drosophila*, *X. laevis*, mouse and tissue culture cells whereas heterodimers are have a higher signalling potency (Butler and Dodd, 2003, Nishimatsu and Thomsen, 1998, Shimmi et al., 2005, Valera et al., 2010). In contrast, heterodimer formation of Bmp2b and Bmp7a is absolutely required for signalling in zebrafish (Little and Mullins, 2009). During ectodermal patterning in *Drosophila, dpp* mRNA expression is repressed by the transcriptional repressor *dorsal* in the ventral half of the embryo and thus Dpp is expressed dorsally, whereas *screw* (*scw,* another BMP family ligand in *Drosophila*) is expressed ubiquitously (Wolpert et al., 2007). Facilitated transport by the extracellular proteins Short gastrulation (Sog) and Twisted gastrulation (Tsg), which have a higher affinity for Dpp/Scw heterodimers results in a dorsal accumulation of heterodimers compared to broadly distributed Dpp homodimers, thus allowing for the patterning of two different dorsal tissues (Shimmi et al., 2005). The Dpp/Scw heterodimer also has a higher ability of stimulating Sog cleavage by the protease Tolloid (Tld), which allows for the release of the ligand complex and receptor binding. In the developing zebrafish embryos, *bmp2b* and *bmp7a* are expressed in similar domains during gastrulation and mutants of both ligands show similar phenotypes (Schmid et al., 2000). Interestingly, it has been elegantly demonstrated that injection of a recombinant BMP2/BMP7 heterodimer, but not a BMP2 homodimer, can rescue bmp2b/swirl mutants (Little and Mullins,

2009). Thus, only in the presence of both ligands signalling can occur, providing an additional level of BMP activity regulation in zebrafish.

1.2.2.2 Regulation of BMP ligand activity in the extracellular space

A plethora of secreted proteins have been implicated in the modulation of BMP ligand activity. Some of these regulatory factors are membrane bound and can either act to concentrate ligand activity or retain them whilst inhibiting signalling. In *Drosophila* the two activating proteins Dally and Dally-like, which are glycosylphosphatidylinositol- anchored Heparan-Sulphate Proteoglycans (HSPGs), are believed to counteract endocytosis of Dpp and increase Dpp concentration of the cell surface (Raftery and Umulis, 2012). However, if levels of, for example Dally, are high this may result a sequestering of Dpp and inhibition of its diffusion (Fujise et al., 2003).

As mentioned above, patterning of the dorsal ectoderm in *Drosophila* requires a BMP signalling gradient, which is formed by an intricate network of regulators. The Dpp/Scw heterodimer is bound by Sog/Tsg, which prevents ligand binding to the receptors and transport towards the dorsal midline, whilst Tld releases Dpp/Scw by Sog cleavage and thus allows for signalling. An additional regulatory layer for gradient formation involving collagens has been identified (Wang et al., 2008). The authors propose a model, in which Sog and the Dpp/Scw heterodimer independently bind the type IV collagen Viking (Vkg). This facilitates the formation of a Dpp/Scw/Sog/Tsg complex and directional movement of the complex to the dorsal midline. Tld triggers the cleavage of Sog and the release of the ligands complex, which can form a new inhibitory complex in the presence of Sog in lateral regions. In the absence of Sog, the ligand complex binds to receptors for activation. Type IV collagens are able to augment Dpp signalling in Drosophila embryos, in a process that requires Dpp/Collagen IV interaction.

The BMP and Activin membrane-bound inhibitor BAMBI acts a pseudoreceptor and was first identified in *X. laevis* (Onichtchouk et al., 1999). BAMBI resembles a type I receptor, but lacks the intracellular kinase domain. BAMBI expression inhibits BMP activity through its intracellular domain, which is similar to the type I receptor homodimerisation interface. Ligand induced

incorporation of BAMBI in type I receptor complexes hinders signalling. In zebrafish, two BAMBI homologues exist, Bambi-A (Nma) and Bambi-b. Ectopic expression of *bambi-a* in *X. laevis* and zebrafish inhibits the expression of known BMP target genes (Tsang et al., 2000), suggesting the role of BAMBI is conserved across species. A role for Bambi-b has not yet been identified. In mice, BAMBI is required for vascular development and BAMBI knockdown in HUVEC cells promoted basal and TGF-β induced phosphorylation of SMAD1/5 (Guillot et al., 2012).

Some of the molecules that modulate BMP activity are secreted and diffusible and may even facilitate the transport of BMP ligands across the extracellular space. The diffusible factors Noggin and Chordin (Sog in *Drosophila*) are important for DV patterning in vertebrate embryos (1.1.5) and inhibit BMP activity by binding the BMP ligands and inhibiting their interaction with the BMP receptors. After initial inhibition of *bmp2b* transcription by Dharma, dorsally expressed Noggin1 and Chordin inhibit BMP signalling, thus contributing to the gradient formation. Tolloid together with the metalloproteinase Bmp1 degrade Chordin in Bmp/Chordin complexes, thus restoring BMP signalling through the receptors and allowing for DV pattern formation (Piccolo et al., 1997). Twisted gastrulation also promotes BMP activity by facilitating this cleavage (Larrain et al., 2001, Jasuja et al., 2006).

Crossveinless2 (Cvl2) is another secreted protein that regulates BMP activity during development. As the name suggests, Cvl2 was first described in Drosophila wing development (Bridges, 1920) and later implicated as a direct positive regulator of BMP signalling often co-expressed with *bmps* (Conley et al., 2000, Matsuda and Shimmi, 2012, Serpe et al., 2008). In contrast to Chordin and Tsg, Cvl2 acts at a short range and is tethered to the membrane by HSPGs (Serpe et al., 2008). Cvl2 contains N-terminal cysteine-rich domains (CR), similar to Chordin/Sog, and a C-terminal von Willebrand factor D (vWFD) domain. In *Drosophila*, Cvl2 has been clearly demonstrated to positively regulate BMP signalling during wing vein patterning. During this process Dpp and another ligand, Glass bottom boat (Gbb), are produced in the longitudinal veins. Sog and Cvl2 then facilitate the transport of the Bmps into the posterior crossvein (PCV), where Sog is cleaved by Tolloid-related and the ligands are freed. Cvl2 is also expressed in the PCV and assists the ligands binding to the BMP receptors similar to a co-receptor. A similar positive role for Cvl2 has been demonstrated in loss-of-function studies in

mouse and zebrafish (Ikeya et al., 2006, Moser et al., 2007, Rentzsch et al., 2006) and mouse and chick Cvl2 enhances BMP4-mediated Smad1 phosphorylation in tissue culture (Kamimura et al., 2004).

During zebrafish gastrulation, Cvl2 acts as a positive feedback regulator, which is partly accomplished by competing with Chordin for binding of Bmp ligands (Rentzsch et al., 2006). This study also suggests that proteolytic cleavage can convert Cvl2 from a pro- to and anti-BMP factor. Indeed, in different contexts Cvl2 has been described as a negative regulator of BMP signalling. Overexpression of Cvl2 (Bmper) in *X. laevis* antagonises BMP activity and inhibits BMP-2 and BMP-4 dependent osteogenic differentiation of in the mouse chondrogenic cell line ATDC5 (Binnerts et al., 2004, Moser et al., 2003, Ambrosio et al., 2008). Ambrosio et al. propose that *X. laevis* Cvl2 forms a ternary complex containing BMP4 and Chordin. This on one hand enhances Chordin function and thus inhibits BMP signalling, but on the other hand might in conjunction with Tolloid have a pro-BMP effect ventrally ensuring that BMPs are freed for receptor binding (Zhang et al., 2010).

A later study suggests that a pro-Bmp affect requires binding of Chordin. Whether this interaction facilitates the loosening of a BMP/Chordin interaction thus allowing the binding of BMPs to the receptor facilitated by Cvl2 or whether a Tolloid-dependent mechanism exists is still under debate. The observation that loss of Cvl2 enhances and overexpression of Cvl2 inhibits BMP signalling in some contexts suggests a possible dose dependent role. Indeed, in fly wing development overexpression of Cvl2 could activate or antagonise BMP signalling, depending on the level of expression (Serpe et al., 2008). A modelling approach suggests that not only levels of the signalling components, but also the affinity of different ligands and receptors for Cvl2 binding can influence the choice between and activating or inhibiting function of Cvl2. They also demonstrate that Cvl2 regulation in a positive feedback could be a mechanism to refine positional BMP signalling. Thus, the function of Cvl2 in modulating BMP signalling appears to be context-dependent and regulated by the relative expression levels of the players involved. This interplay of secreted and membrane-bound BMP activity modulators allows for robust but flexible regulation of localised BMP signals, even if the ligands themselves are uniformly expressed.

The mechanisms I described above are examples of an even more complex interplay of positive and negative BMP signalling regulators. As BMP activity during

developmental processes such as ectodermal patterning has to be tightly regulated to allow for the specification of diverse cell types, an intricate network of factors is involved in such processes. Great progress has been made in understanding the interplay between activating and inhibiting molecules as well as different BMP ligands to achieve spatial and temporal signalling control. Still, a lot more research is needed to shed light on the regulatory process, especially in vertebrate development.

1.3 The *Tg(BRE:mRFP)* transgenic zebrafish line

The investigation of spatiotemporal BMP signalling dynamics during ectodermal patterning requires a robust readout for BMP activity. Traditionally, staining for C-terminally phosphorylated Smad1/5 (PS1/5) has been used to detect domains of BMP activity during embryogenesis. This, however, only allows for the detection of strong signals, such as the DV BMP activity gradient during gastrulation (Tucker et al., 2008). Moreover, it has been demonstrated that Smad1/5 are not exclusively phosphorylated in response to BMPs/GDFs, but also in a non-canonical fashion upon stimulation with TGF-β (Goumans et al., 2002). Thus, PSmad1/5 is not an exclusive readout for BMP activity.

To overcome these limitations, the Hill lab generated a transgenic zebrafish BMP reporter line (Wu et al., 2011, Ramel and Hill, 2013). The *Tg(BRE:mRFP)* expresses monomeric red fluorescent protein (mRFP) under the control of a well-characterised BMP responsive element from the mouse *Id1* enhancer (Korchynskyi and ten Dijke, 2002). This line faithfully reports BMP activity in tissues where BMP signalling was expected such as the somites, the dorsal retina and the tail bud (Esterberg et al., 2008, French et al., 2009, Pyati et al., 2006). mRFP fluorescence can only be detected from 6 somite stage onwards, with a strong signal in the tail bud and in the presomitic mesoderm, as during earlier stages mRFP protein levels are too low (Ramel and Hill, 2013). In contrast, *mRFP* mRNA can be detected in 8-cell stage embryos and thus ISH can be used as a readout for earlier BMP activity. Moreover, *mRFP* mRNA is much less stable than mRFP protein with a half-life of less than 20 minutes compared to a protein half-life of more than 12 hours.

Therefore, mRFP ISH can be used as a more dynamic representation of BMP signalling events.

It has been demonstrated that *Tg(BRE:mRFP)* transgenic zebrafish are a *bona fide in vivo* reporter for BMP/GDF activity using several approaches. Overexpression of the BMP inhibitors *noggin* or *chordin* substantially reduces the levels of detected *mRFP* at 75% epiboly (Ramel and Hill, 2013, Wu et al., 2011). In contrast, activation of BMP signalling by knockdown of *chordin* or overexpression of the ligand *bmp2b* and the constitutively active receptor CA-Alk8 leads to increased *mRFP* expression. In genetic approach using Bmp2b-deficient *swirl (swr)* embryos (Mullins et al., 1996) the same study demonstrated a strong reduction of *mRFP* expression in homozygous *swr*^{TA72A} embryos compared to wild-type or heterozygous siblings. BMP activity in the dorsal retina is known to be conferred by Gdf6a expression (French et al., 2009) thus *mRFP* expression in this tissue is likely to result from Gdf6a ligand activity. Indeed, *mRFP* expression levels as well as mRFP fluorescence are reduced in *gdf6a* morphants, confirming that the *Tg(BRE:mRFP)* line is also a sensitive readout for GDF subfamily mediated signalling (Ramel and Hill, 2013). Finally, inhibition of BMP signalling using the chemical inhibitors Dorsomorphin and LDN-193189, which target the type I BMP/GDF receptors, resulted in reduced mRFP expression measured by Western blot analysis (Ramel and Hill, 2013, Sanvitale et al., 2013).

Taken together, the *Tg(BRE:mRFP)* transgenic zebrafish line is a genuine readout for BMP/GDF activity. It thus provides a sensitive and accurate tool to investigate the dynamic changes in BMP signalling during ectodermal patterning and NC development *in vivo*.

1.4 Snw1

As described above, BMP signalling and ligand activity can be modulated at many levels. So far, there are no reports on co-transcriptional regulation of BMP ligand expression or the existence alternative splice variants of BMP ligands. However, it has recently been demonstrated that the known splicing factor Snw1 is a potent regulator of BMP signalling at the NPB and is required for NC development in *X. laevis* and zebrafish (Wu et al., 2011). Through which mechanism Snw1 confers

this regulation is not understood. Snw1 depletion results in a loss of BMP signalling after gastrulation, however, *bmp* ligands can still be detected by whole-mount *in situ* hybridisation (ISH). Tissue culture experiments in this study indicate that Snw1 is not part of the core BMP signalling pathway downstream of the receptors. Moreover, the observed phenotype can be rescued by targeted injection of a *bmp2b* cDNA in *X. laevis*, indicating that the cells at the NPB are still responsive to a BMP stimulus. Taken together, the data so far indicate that Snw1 regulates BMP activity at a level upstream of the BMP receptors and downstream or at the level of *bmp* ligand transcription.

Snw1 is an essential protein in many species and is extremely conserved from yeast to human (Wu et al., 2011). The *X. laevis* Snw1 protein, for example, is 88% identical to human SNW1, 83% identical to zebrafish Snw1 and 62% identical to the *Drosophila* homologue Bx42. The alternative name Skip (Ski-interacting protein) is often used and the *S. cerevisiae* orthologue is called Prp45. There appears to be only one gene per genome, which encodes for a 60-80 kDa nuclear protein. The name Snw1 is derived from the conserved sequence motif “SNWKN” (Folk et al., 1996), which is identical in all genera. The basic structure, starting from the N-terminus, contains the following motifs: a glycine-rich box, a proline-rich box (possibly presents a binding site for WW and SH3 domain containing proteins), the SNWKN signature domain, highly conserved amphiionic helical repeats, a species-specific insert and the region of similarity to the N-terminal half of SH2 domains (Figure 1.6) (Folk et al., 1996). Overall the protein structure of Snw1 seems to be very suitable for the binding of a great variety of interaction partners and the high conservation of the Snw1 protein sequence indicates an evolutionary role of Snw1 in multiple interactions. However, none of these motifs have yet been functionally tested. Part of the structure might exist in a natively unfolded state as data from *Dictyostelium* SnwA suggests (Uversky et al., 2000). Such regions can be found in proteins that have a high interaction flexibility such as the human papilloma virus (HPV)-16 E7 (Alonso et al., 2002).

Snw1 was first described as the *Drosophila* homologue Bx42 and was found to be a specific protein in a series of transcriptionally-active puffs on salivary gland chromosomes (Saumweber et al., 1990). The homologs in *Saccharomyces cerevisiae* (Prp45), *Schizosaccharomyces pombe* (Snw1p)and *Drosophila* are required for cell survival, splicing (Ambrozkova et al., 2001, Gahura et al., 2009,

Makarov et al., 2002), and nuclear export of spliced mRNAs (Farny et al., 2008) and Snw1 has been reported to interact with an extensive list of partners. I will discuss the evidence for a role of Snw1 in processes such as splicing and transcriptional regulation in the following sections.

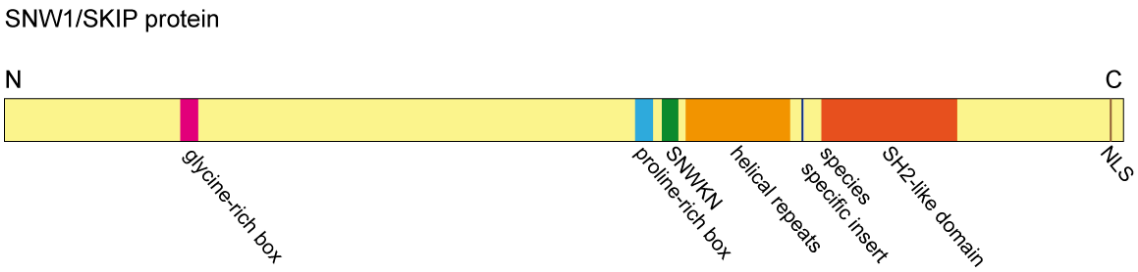

Figure 1.6 Overview of the conserved domains of the Snw1 protein

1.4.1 A role of Snw1 in pre-mRNA processing

Pre-mRNA transcribed by RNA polymerase II has to undergo several processing steps to become a mature mRNA that can be exported from the nucleus and translated. One of these processes is splicing, in which introns are removed and exons are joined. Splicing is a two step *trans*-esterification reaction catalyzed by the spliceosome. In the first step, a specific adenine nucleotide at the branch point (indicated in red), 18-40 nucleotides upstream of 3' splice site, attacks the 5' splice side and cuts the sugar backbone at that point. The loose 5' end is then covalently linked to the adenine nucleotide, creating the lariat intermediate. The free 3'OH of ExonA reacts with the start of the next exon sequence, joining the exons together and releasing the Intron lariat. The spliceosome is a large ribonucleoprotein complex of five uridine-rich small nuclear RNAs (snRNA) and around 200 additional proteins. The assembly of the spliceosome occurs in a stepwise manner and large rearrangements of the spliceosome orchestrate the different splicing steps (Makarov et al., 2002). For the first splicing step the U1snRNP together with the splicing factors U2AF and SF1 bind the 3' splice site (complex E), which promotes the recruitment of the U2snRNP to the branch point in an ATP-dependent manner (complex A). Subsequently the so-called complex B is formed by binding of the U4-

U6-U5 tri snRNP, which leads to major RNA/RNA and RNA/protein rearrangements and the release of U1- and U4snRNP. The resulting complex C is the complex that is responsible for catalysing the formation of the lariat, intron excision and exon-exon ligation. The mRNA is then released and the spliceosome dissembles and is recycled for another round of splicing.

Snw1 has been identified as a component of the activated spliceosome in *S.cerevisiae, S.pombe* and *H.sapiens* in several independent screens (Neubauer et al., 1998, Ajuh et al., 2000, Gavin et al., 2002, Ohi et al., 2002, Zhou et al., 2002). More specifically, Snw1 was identified as component of the CDC5/P19 subcomplex, which is part of the B* and C complexes and the post-spliceosomal species (Albers et al., 2003, Makarov et al., 2002).

In a yeast two-hybrid screen using Prp22 (DHX8 in humans), also part of the CDC5 complex, as a bait, Prp45 and Prp46 (PLRG1 in humans) were identified as interaction partners (Albers et al., 2003). Both proteins are associated with the spliceosome throughout the splicing process and bind low levels of U2-, U5- and U6-, but not U1- and U4- snRNP. Importantly, this study demonstrated that in yeast depletion of Prp45 results in splicing defects *in vivo*.

A role of SNW1 in human pre-mRNA splicing has been suggested by a study, in which a dominant negative truncated version of SNW1 was expressed in tissue culture cells (Zhang et al., 2003). This study demonstrated the transient accumulation of unspliced transcripts from a human growth hormone reporter gene cassette upon disruption of native SNW1 function. In fission yeast the Snw1 homologue spSNW1 has previously been shown to interact with the U2AF35 subunit (Ambrozkova et al., 2001) and recombinant SNW1 has been reported to bind U2AF65 from HCT116 nuclear extracts (Chen et al., 2011). This interaction is thought to gene specifically facilitate the co-transcriptional loading of U2AF65 onto the unspliced pre-mRNA in a gene-specific manner. In response to DNA damage stress SNW1, as well as DHX8 and Prp19, are required for the splicing of *p21* but not other p53-induced targets such as *PUMA* (Chen et al., 2011).

There have been suggestions of a role for Snw1 at other stages of pre-mRNA processing. For example, Snw1 binds the poly(A)-binding protein 2 (PABP2), which contributes to mRNA nuclear export (Calado et al., 2000, Kim et al., 2001). In *Drosophila*, Bx42/Snw1 was identified in a genome-wide RNAi screen to be required for poly(A)-mRNA export from the nucleus (Farny et al., 2008).

More research is required to determine the function of Snw1 in pre-mRNA processing. Snw1 is part of the activated spliceosome but does not seem to have any catalytic activity itself. Interestingly, a recent study demonstrated by (NMR) that the large intrinsically disordered region in Snw1 undergoes a disorder-order transition upon binding of peptidylprolyl isomerase-like protein 1 (PPIL1) (Wang et al., 2010a). PPIL1 is recruited by Snw1 to the spliceosome by a region other than the peptidylprolyl isomerase active site and thus it still functions as a peptidylprolyl cis/trans-isomerase when part of the spliceosome. In summary, the unorder region of Snw1 is proposed to act as an 'interaction platform' that is required to facilitate the large structural rearrangements during the splicing process.

1.4.2 Snw1 as a transcriptional coregulator

Transcriptional coregulators interact with transcription factors to enhance or repress the transcription of specific genes. Snw1 has been associated with many different pathways and may act as a coactivator as well as a corepressor. It seems unlikely that a single factor is involved in the regulation of such a diversity of processes. The recruitment of endogenous levels of Snw1 to the spliceosome has been satisfactorily demonstrated using various approaches, as explained above. In contrast, most of the interactions and the subsequent implication of Snw1 in transcriptional pathway regulation stems from overexpression studies. As I will further elaborate on in Chapter 5, Snw1 appears to be prone to unspecific protein interactions, thus not all of the proposed functions of Snw1 may validate in the future. However, in the following paragraph I will introduce a selection of signalling processes Snw1 has been implicated in to date.

1.4.2.1 Vitamin D receptor (VDR)/Retinoic acid (RA) signalling

The vitamin D receptor (VDR) belongs to the thyroid hormone/retinoid receptor subfamily of nuclear receptors and functions as a heterodimer with retinoid X receptor (RXR) in vitamin D3-dependent transcription (Thompson et al., 1998). Human SNW1 was identified as an interaction partner of VDR using yeast two-hybrid and in vitro immunoprecipitation and subsequently named Nuclear Receptor Coactivator of 62 kDa (NCoA-62), as it augmented VDR-activated transcriptional processes in transient reporter gene assays (Baudino et al., 1998, Zhang et al.,

2001). SNW1 interacts selectively with the VDR-RXR heterodimer and forms a ligand–dependent ternary complex with steroid receptor coactivator (SRC) proteins to synergistically act on promoting VDR-dependent transcription. It was later shown that human sirtuin 1 (SIRT1), a NAD(+)-dependent deacetylase, associated with SNW1 and modulates its activity (Kang et al., 2010). As previously reported, SNW1 in cooperation with SRC-1 enhanced the transcriptional activity of the retinoic acid receptor (RAR). In contrast, overexpression of SIRT1 inhibited transcriptional transactivation in a luciferase assay and Sirt1 and SNW1 compete for RAR binding. Thus SIRT1 and SNW1 have reciprocal role during RA-induced neuronal differentiation of P19 cells.

1.4.2.2 Delta/Notch signalling

Delta/Notch signal transduction controls differentiation and proliferation responses by converting the transcriptional repressors of the CSL family (CBF1, Supressor of Hairless, Lag-1) to activators (Bray and Furriols, 2001, Bresnick et al., 2000). Upon ligand binding the intracellular domain of the Notch receptor (NotchIC) is cleaved and translocates to the nucleus where is binds to CSL family members like CBF1. This leads to a replacement of the silencing mediator for retinoic acid and thyroid hormone receptor proteins (SMRTs) / histone deacetylase (HDAC) complex and thus allows for transcription to start at CBF1-controlled promoters. Protein interaction assays showed an interaction between SNW1 and SMRTs, CBF-1 as well as NotchIC and the biological activity of NotchIC depends on binding of SNW1 (Leong et al., 2004, Zhou et al., 2000).

In *Drosophila*, global loss of Bx42/Snw1 is embryonic lethal and tissue specific depletion phenotypically resembles some classes of *Notch* mutants suggesting a contribution of Snw1 to the Notch pathway (Negeri et al., 2002). Overexpression of the CBF1 homologue Suppressor of Hairless in the wing disc results in defects in the vein architecture (Furriols and Bray, 2000). This phenotype is strongly enhanced by Bx42/Snw1 RNAi arguing for an interaction of both factors in the Notch pathway (Negeri et al., 2002). The same study goes on to demonstrate that Snw1 depletion affects Notch target gene expression. Moreover, Snw1 RNAi

expression in the eye disc leads to an eye to antenna transformation similar to what is observed upon overexpression of dominant negative forms of Notch.

Taken together, the data to date argues for a function of Snw1 as a coactivator of the Notch signaling pathway.

1.4.2.3 Wnt signalling

Another signalling pathway Snw1 has been suggested to modulate is the canonical Wnt signalling pathway. As mentioned above, upon Wnt stimulation, β-catenin translocates to the nucleus and binds TCF/LEF transcription factors to initiate target gene expression (1.1.2). In the absence of Wnt signalling, TCF/LEF act as transcriptional repressors on target genes by binding to the transcriptional co-repressors Groucho-HDAC (Billin et al., 2000). A previous study suggested that Snw1 forms a ternary complex with the transcription factor LEF1 and HDAC1 to mediate target gene repression (Wang et al., 2000). The authors demonstrate that overexpressed Skip interacts with co-transfected Lef1, Tcf1, Tcf3 and Tcf4c as well as HDAC1 and β-catenin. Using a 2-step IP assay, they further show SNW1, LEF1 and HDAC1 to be part of one complex. Expression of SNW1 in HEK293T cells inhibits TOPflash reporter activity in response to co-transfected β-catenin in a dose-dependent manner and overexpression of Snw1 in *X. laevis* embryos abolishes NC development. Interestingly, knockdown of SNW1 in HEK293T cells also impaired Wnt target gene expression downstream of β-catenin as well as NC induction in *X. laevis*. Wang et al. suggest that Snw1 acts as a scaffold protein in canonical Wnt signalling. Overexpressed Snw1 enhances the formation of a Lef1/HDAC1 repressive complex thus inhibiting target gene expression. In addition, Snw1 might be required for the β-catenin-dependent conversion of TCF/LEF proteins to co-activators, which is why Snw1 depletion also reduced Wnt reporter activity.

Taken together, Snw1 is proposed to regulate Wnt signalling at a transcriptional level. This function is important in *X. laevis* development for NC induction.

1.4.2.4 TGF-β signalling

In a yeast two-hybrid screen SNW1 was identified to interact with SKI (hence its alternative name Ski interacting protein, SKIP) (Dahl et al., 1998) and SKI/SnoN were subsequently shown to be a transcriptional repressor of the TGF-β signalling pathway (Akiyoshi et al., 1999, Luo et al., 1999). Ski and SnoN bind to the Smad transcription factors and inhibit TGF-β-dependent transcription through the recruitment of a nuclear co-repressor complex. In yeast and mammalian cells, Snw1 was demonstrated to interact with Smad2 and Smad4 by yeast two-hybrid and using purified proteins (Leong et al., 2001). Moreover, overexpression of SNW1 in COS1 cells along with Smad3 augments TGF-β-dependent transactivation. However, in another study SNW1 was stably overexpressed in C2C12 cells without addition of the Smads (Figueroa and Hayman, 2004). In this experimental setup SNW1 was not sufficient to enhance TGF-β dependent gene reporter activity.

TGF-β inhibits myotube formation during muscle development by the functional repression of myogenic transcription factors such as MyoD probably mediated by Smad3-dependent transcriptional repression (Liu et al., 2001). Since SKI has been implicated in muscle development as well (Engert et al., 1995) the link between Smad3, SNW1 and SKI appears to be a possible explanation for the molecular function of SKI on MyoD-dependent genes. As mentioned in a previous section (1.4.1) SNW1 binds the poly(A)-binding protein 2 PABP2, required for nuclear export. Interestingly, SNW1 and PABP2 were identified in a ternary complex with MyoD and act together to stimulate its transcriptional activity (Kim et al., 2001).

In summary, Snw1 has been implicated in TGF-β signalling as a transcriptional activator. However, data generated in our lab does not support an interaction of Snw1 with either Smads or Ski and tissue culture experiments indicate that Snw1 is not part of the core signalling pathway downstream of receptor activation.

1.4.3 Transcriptional elongation

Snw1 has been implicated in the regulation of several signalling pathways as well as splicing. Evidence suggests that Snw1 acts as a platform/scaffold in these processes to allow for the rearrangement of large protein complexes such as the spliceosome and ternary complexes of transcription factors. By allowing the interaction with components of different molecular 'machineries', Snw1 might act as a mediator between different processes such as transcription initiation and splicing and be required for their functional coupling.

Recent research supports this hypothesis. Brès *et al.* demonstrated SNW1 associated with P-TEFb transcriptional elongation complex in a step that is required for HIV-1 Tat transactivation (Bres et al., 2005). Moreover, SNW1 associates with U5snRNPs and a more active C-terminal truncated SNW1 enhances the use of alternative HIV-1 Tat splice sites. SNW1 also associates with c-Myc and Menin, a subunit of the MLL1 histone methyltransferase (H3K4me3) complex, which is necessary for HIV-1 Tat transactivation (Bres et al., 2009). Interestingly, SNW1 and PTEF-b are dispensable for UV stress induced HIV-1 transcription, thus the elongation step requiring SNW1, c-Myc and Menin is bypassed under DNA damage stress. However, SNW1 is required for basal and stress induced splicing of *p21* mRNA (1.4.1) (Chen et al., 2011).

In summary, this suggests that depending on the cellular and physiological context, Snw1 may adopt different functions to regulate transcription/co-transcriptional processes. As mentioned at the beginning of this section, many of the data that has been generated to identify the molecular role of Snw1 comes from yeast two-hybrid screens and overexpression studies. Although these are valid approaches, the obtained data has to be rigorously validated in endogenous assays. Interaction studies, for examples, that use overexpression of both proteins may lead to false positive results and identification of binding partners that do not exist in a normal cellular context.

As mentioned before, Snw1 was identified as a regulator of BMP activity at the NPB and thus NC induction (Wu et al., 2011). Knockdown of Snw1 in tissue culture cells did not impair their ability to respond to a BMP stimulus. The proposed interaction of Snw1 and the Smads as well as the transcriptional repressor Ski

could not be verified. Thus, we suggest that Snw1 regulates BMP activity not on a transcriptional level after receptor activation on BMP target genes. In contrast, Snw1 might act at the level or downstream ligand transcription, possibly transcriptional elongation and co-transcriptional splicing.

1.5 Aim of the thesis

Studying tissue specification during developmental processes provides novel insights into how signalling pathways are regulated and integrated to give rise to a variety of tissues. Ectodermal patterning is a crucial early event during development that defines neural and non-neural progenitors. It has long been known that BMP activity is indispensible for this process. Direct evidence for the spatial and temporal sequence of the activation of BMP signaling during ectodermal patterning, especially after gastrulation, however is scarce. Furthermore, much of the data available has been generated from phenotypical analyses of BMP mutants such as the zebrafish *swirl* (*bmp2b)*, *snailhouse* (*bmp7*) and *somitabun (smad5)* mutants (Nguyen et al., 1998, Mullins et al., 1996). These mutants, however, lack early BMP signalling required for initiation of DV patterning and can therefore only provide limited information on the specific requirements of NC and PPE for BMP activity during later stages.

It was therefore the aim of my PhD thesis to investigate BMP signalling dynamics during ectodermal patterning using the transgenic zebrafish *Tg(BRE:mRFP)* reporter line. I then further investigated the mechanism regulating localised BMP activity or inhibition in different tissues thus identifying a BMP regulatory network that can explain the changing signalling requirements during NC and PPE development.

In a second part I aimed to identify the role of the nuclear protein Snw1 in regulating BMP activity and NC induction. As mentioned above, it was previously demonstrated that Snw1 must act at the level or downstream of ligand transcription and upstream of receptor activation (Wu et al., 2011). At what step Snw1 acts however and whether it only targets BMP signalling at the NPB is not understood. It has also been demonstrated that Wnt signalling is perturbed in Snw1 *X. laevis* morphants. However, whether that is the cause for the defect in NC development is

still under debate as a different study identified Snw1 as a regulator of Wnt activity, which also contributes to NC development (Wang et al., 2010b). I therefore used a combination of embryological and molecular approaches to elucidate the molecular function of Snw1.

In summary, my aims were to contribute to the understanding of the spatiotemporal regulation of BMP signalling during vertebrate development. I hope the results of this work will have implications beyond understanding normal developmental processes and further our insight into how BMP signalling is perturbed in disease.

Chapter 2. Materials & Methods

General laboratory chemicals were purchased from Sigma-Aldrich, Roche or Fisher Scientific unless otherwise stated. Standard laboratory solutions including 10 x TAE, 10 x TBE, 5 M sodium chloride, 0.5 M EDTA (pH 8), 1 M Tris-HCl (pH 7.8 or 8), 10 x PBS, 1 x PBS and autoclaved water were prepared by Cancer Research UK Laboratory Services.

2.1 Embryology

2.1.1 Fish maintenance and strains used

The zebrafish colony was maintained by the fish facility staff Phil Taylor, Darren Martin and Chris Sergeant at 27.5°C as described (Westerfield, 2000). The fish were kept in dechlorionated water on a 14/10 hour light/dark cycle and embryos were collected from spontaneous spawning. The staging was conducted according to Klimmel *et al.* (Kimmel et al., 1995). The embryos were kept in Petri dishes containing autoclaved water supplemented with a 500x "fish water mix" diluted to 1x up to 5 days post fertilisation The mutant lines used were: *Tg(hsp70l:dnXla.Bmpr1a-GFP)* (Pyati et al., 2006) and *Tg(BRE:mRFP)* (Wu et al., 2011) .

500x fish water mix

6 g	Instant Ocean salts
0.2 g	methylene blue
	up to 200 ml with H_2O

2.1.2 *X. laevis* husbandry

All adult *X. laevis laevis* specimens were obtained from Nasco (Fort Atkinson, WI, USA). Male and female frogs were maintained in separate tanks.

2.1.2.1 Materials and solutions

10x Normal Amphibian Medium (NAM) Salts

1.1 M NaCl	64.28 g
20 mM KCl	1.49 g
10 mM $CaNO_3$	2.36 g
20 mM $MgSO_4$	2.4 g
1 mM EDTA	2 ml 0.5 M EDTA pH 8.0
	Up to 1 litre with H_2O
	Filter sterilised, stored at room temperature

10 M NaOH

40 g NaOH
Up to 100 ml with H_2O
Stored at room temperature

1 M HEPES pH 7.6

59.58 g HEPES
pH to 7.6 with 10 M NaOH
Up to 250 ml with H_2O
Filter sterilised, stored at room temperature

0.1 M $NaHCO_3$

2.1 g $NaHCO_3$
Up to 250 ml with H_2O
Filter sterilised, stored at room temperature

1 x NAM

100 ml 10 × NAM Salts
2 ml 1 M HEPES (pH 7.5)
10 ml 0.1 M $NaHCO_3$
Up to 1 litre with H_2O
Stored at room temperature

10 % NAM

20 ml 10 × NAM salts
4 ml 1 M HEPES (pH 7.5)
Up to 2 litres with dH_2O
Stored at room temperature

50 % NAM

200 ml 1 x NAM
200 ml H_2O
Stored at room temperature

75 % NAM + 2 % (w/v) Ficoll

150 ml 1 x NAM
50 ml H_2O
4 g Ficoll® 400, Type 400-DL
Made up to 24 hours before use

2 % (w/v) Cysteine

4 g L-Cysteine (Fluka)
195 ml 10% NAM
pH to 7.8 with 10 M NaOH, up to 200 ml with H_2O
Made fresh before use

10 x Modified Barth's Saline (MBS) salts

880 mM NaCl	25.71 g
10 mM KCl	0.373 g
10 mM $MgSO_4$	0.6 g
25 mM $NaHCO_3$	1.05 g
	pH to 7.8 with 10 M NaOH
	Up to 500 ml with dH_2O
	Stored at room temperature

1 M $CaCl_2$

11.1 g $CaCl_2$
Up to 100 ml with H_2O
Filter sterilised, stored at 4ºC

1 x high salt MBS

25 ml 10 × high salt MBS
1 ml 5 M NaCl
175 µl 1 M $CaCl_2$
Up to 250 ml with H_2O
Filter sterilised, stored at room temperature

0.2 % (w/v) Ethyl 3-aminobenzoate methanesulfonate salt (MS222)

4 g MS222
Up to 2 litres with H_2O
pH to 7.5 with 10 M NaOH
Stored at room temperature for up to 1 week

10 x MEM

1 M MOPS	104.63 g
20 mM EGTA	3.8 g
10 mM $MgSO_4$	0.6 g
	pH to 7.4 with 10 M NaOH
	Up to 500 ml with H_2O
	Filter sterilised, stored at 4ºC

1x MEMFA

5 ml 10 x MEM
5 ml 37% formaldehyde solution
Up to 50 ml with H_2O
Made fresh before use

Pregnant Mare Serum Gonadotropin (PMSG) solution

5000 IU of PMSG-Intervet (Intervet) was dissolved in 20 ml of accompanying solvent
This provides a 250 units per ml solution
Stored in aliquots at -20ºC

Human Chorionic Gonadotropin (HCG) solution

10,000 IU of HCG was dissolved in 8 ml sterile dH_2O
This provides a 1,250 units per ml solution
Stored in aliquots at -20ºC

2.1.2.2 Collecting mature oocytes

Adult female *X. laevis* animals were injected into the dorsal lymph sac 3-7 days before the induction of ovulation with 200 µl of a 250 units/ml solution of pregnant mare serum gonadotropin (equivalent of 50 units of PMSG, a substitute for Follicle Stimulating Hormone) to stimulate follicle and oocyte maturation. Ovulation was induced 14-20 hours before oocyte collection by injection of 400 µl of a 1,250 units/ml solution of human gonadotropin (equivalent of 500 units of HCG). The mature oocytes were collected manually by holding the female frog over a clean Petri dish and gently massaging the abdomen of the frog to stimulate egg-laying.

2.1.2.3 Isolating testes

Male frogs were sacrificed by submerging in a bath of 0.2 % (w/v) Ethyl 3-aminobenzoate methanesulfonate salt (MS222) for 20-30 minutes. In addition, following the Schedule I procedure, the neck was severed prior to dissection to obtain testes. Testes were stored in 70 % L-15 (Leibovitz) medium (Gibco) at 15ºC for up to 72 hours.

2.1.2.4 In vitro fertilisation

Sperm was obtained by crushing a testis in 1 ml 1x high-salt MBS using a pellet mixer (Anachem). The sperm solution was evenly pipetted over the unfertilised eggs in Petri dishes. To activate the sperm the dish was flooded with 10 % NAM. Successful fertilisation leads to the contraction of the animal hemisphere (pigmented half of the egg) resulting in the rotation of eggs within the vitelline membrane so that the animal hemisphere faced upwards approximately 30 minutes post flooding.

2.1.2.5 Dejellying

Embryos are covered with a protective jelly that must be removed prior to most micromanipulation procedures. For that purpose the 10 % NAM was replaced with a 2 % (w/v) solution of cysteine, the contents of the Petri dish carefully transferred into a beaker and gently swirled for several minutes. The jelly was sufficiently removed when the embryos started to sit packed against each other as they settled on the bottom of the beaker. This had to be carefully monitored as excessive exposure to cysteine damages the embryos. The cysteine solution was then removed and the embryos washed five times with large volumes of 10 % NAM. Finally, the embryos were gently poured into clean Petri dishes filled with fresh 10 % NAM. The embryos were then sorted prior to injections, with fertilised embryos being firm and resistant to pressure when gently touched with a hair loop. Soft, unfertilised embryos were discarded.

2.1.3 Capped *mRNA* preparation for injections

To prepare capped mRNA for microinjections the required plasmid was digested with the appropriate restriction enzyme (2.2.6). 1 µl of the digest was run on a 1% agarose gel to check for efficiency of the digestion. The digested DNA was then cleaned using QIAquick PCR purification kit.

The following reaction mix was prepared:

1 µg	DNA template
5 µl	10x polymerase buffer (NEB)
3.125 µl	DTT 200 mM
5 µl	ATP 10 mM (Roche)
5 µl	UTP 10 mM (Roche)
5 µl	CTP 10 mM (Roche)
2.5 µl	GTP 1 mM (Roche)
2.5 µl	CAP analogue (10 mM stock) (NEB)
2.5 µl	RNasin (Promega)
to 40 µl	H_2O

5 µl T7,SP6 or T3 polymerase were added and incubated for 30 min at 37°C. Then 5 µl 10 mM GTP were added and incubated another hour at 37°C.

Add:	50 µl	50TE (50 mM TrisHCl pH 7.5, 1 mM EDTA)
	1.25 µl	Ca/Mg/DTT mix (5 µl CaCl2 1 M, 10 µl MgCl2 1 M, 10 µl DTT 200 mM)
	0.5 µl	RNasin
	2µl	Dnase I

and mix was incubated 30 min at 37°C and mixed once in between. 1 volume phenol/chloroform were added, and the solution well mixed and spun 30 min at 4°C, 13,000 rpm in a microcentrifuge. The aqueous phase was transfered into a new tube, 25 µl ammonium acetate (4 M, pH 5.2) and 300 µl cold 100% ethanol added and the RNA precipitated for 20 min on dry ice. The tube was spun for 20 min at 4°C, 13,000 rpm and the supernatant discarded. This was followed by another short centrifugation and the remaining supernatant was removed. The pellet was dissolved in 100 µl RNase-free water. The RNA concentration was determined by measuring the OD using a NanoDrop™ 1000 spectrometer. To check the RNA quality, 1 µl of RNA was added to 5 µl formamide buffer (95% formamide, 20 mM EDTA). The mix was heated for 3 min at 95°C and run on a 1% agarose gel (2.2.5).

2.1.4 Microinjections

X. laevis

Glass capillaries (INTRAFIL, 1 mm x 0.58 mm) were pulled into fine needles. They were calibrated under a microscope using fine pointed forceps to inject a 4 nl sized drop. The injection mix was prepared in RNase-free water and the embryos were injected using a Narishige IM-300 microinjector in 3% Ficol/ 75% NAM to facilitate a faster healing. Embryos were usually injected at the 1-cell stage or, if even spread of the injected RNA was crucial, into both cells at the 2-cell stage. For the targeting experiments the embryos were injected into the desired blastomere according to the developmental fate map. 3 hours after injection the embryos were transferred into dishes containing 1/10 NAM. The embryos were fixed for immunostaining or *in situ* hybridisation in MEMFA for 2 hours at room temperature (RT) or overnight at 4°C. For immunostaining, the embryos were stored in PBS, for *in situ* hybridisation the embryos were dehydrated in a series of PBS/MeOH and stored in 100% MeOH at -20°C.

Zebrafish

Glass capillaries (Harvard Apparatus, 1 mm x 0.58 mm) were pulled into fine needles. They were calibrated under a microscope using fine pointed forceps to inject a 2 nl sized drop. The injection mix was prepared in RNase-free water. Fertilised zebrafish embryos were injected using a Picospritzer III (Parker) between 1- and 4-cell stage into the yolk cell, raised at 28°C to the desired stage and fixed in 4% PFA/PBS for 3-10 days. Embryos intended for protein or RNA expression analysis were transferred in a microcentrifugation tube, snap frozen on dry ice and stored at -80°C.

2.1.5 Probe preparation for *in situ* hybridisation (ISH) (*X. laevis*)

For antisense probe preparation the plasmid encoding the probe was digested at 37°C with the appropriate restriction enzyme. 1 µl of the digest was run on a 1% agarose gel to check for efficiency of the digestion. The digested DNA was then

cleaned using QIAquick PCR purification kit. The following reaction mix was prepared for probe synthesis:

2 µl	linearised DNA template (2 µg)
5 µl	10 x polymerase buffer
10 µl	5 x rNTP mix
5 µl	100 mM DTT
1 µl	RNasin (Promega)
5 µl	SP6, T7, or T3 RNA polymerase as appropriate
22 µl	H_2O

The reaction mixture was incubated at 37ºC for 2 hours, then 2 µl DNaseI (2.7 units/µl, Worthington) were added and the reaction incubated for another 30 minutes at 37ºC to remove the DNA template. The transcribed RNA was extracted by adding an equal volume of 25:24:1 Phenol:Chloroform:Isoamyl alcohol (Sigma), the mix was vortexed and left to incubate at room temperature for 5 minutes before the tubes were centrifuged at 12,000 rpm for 10 minutes at 4ºC. The aqueous phase containing the RNA was transferred to a fresh tube. The RNA was then ethanol precipitated by adding 5 µl 3M NaOAc pH 5.2 and 165 µl 100 % ethanol. Tubes were left at -20ºC for 20 minutes before centrifuging at 12,000 rpm for 10 minutes at 4ºC (Biofuge fresco Heraeus). The RNA pellet was washed with cold 80% ethanol and allowed to air dry for 5 minutes before being dissolved in 20 µl H_2O. To check the RNA quality 1 µl samples were run on a 1 % agarose gel using the 6 x RNA formamide loading dye (2.2.5). Finally, the RNA concentration was measured (2.2.3) and the sample diluted to 10 µg/ml (10 x stock) with hybridisation buffer (2.1.7).

5x rNTP mix

2.5 mM rATP (Roche)	5 µl of 100 mM rATP
2.5 mM rCTP (Roche)	5 µl of 100 mM rCTP
2.5 mM rGTP (Roche)	5 µl of 100 mM rGTP
1.625 mM rUTP (Roche)	3.25 µl of 100 mM rUTP
0.875 mM Digoxigenin-11-UTP (Roche)	17.5 µl of 10 mM Stock
	Up to 200 µl with dH_2O
	Stored at -20ºC

2.1.6 Probe preparation for *in situ* hybridisation (ISH) (zebrafish)

The probe preparation was essentially performed as described in section 2.1.5. For probe synthesis the following reaction mix was prepared:

1 µg	DNA template
2 µl	0.1M DTT
2 µl	dig-NTP or DNP-NTP mix
0.5 µl	RNase inhibitor
2 µl	10x transcription buffer
1 µl	RNA polymerase as appropriate
to 20 µl	H_2O

The reaction was well mixed, spun down and incubated for 2-4 hours at 37°C. 80 µl 1x TE and 1 µl DNase were added and incubated for 20 min at 37°C. The RNA probes were then cleaned up using the ZYMO RNA clean up kit and eluted in 25 µl RNase free water. Probes were stored at -20°C.

5 mM dig-NTP or DNP-NTP mix

25.7 µl	H_2O
2 µl	100 mM (C,G,A)TP each
1.3 µl	100 mM UTP
7 µl	10 mM dig-11-UTP or DNP-11-UTP

2.1.7 Whole-mount *in situ* hybridisation (ISH) (*X. laevis*)

On the first day, the embryos were rehydrated in a series of EtOH washes followed by three washes with PBST (all washes were 5 min unless otherwise stated). The embryos were then bleached for 10 minutes (solution specified below) with exposure to a bright light source, such as a light box. This was followed by three washes in with PBST before 20 minutes of refixation using a 4% formaldehyde solution made in PBS (a 16% solution from Agar Scientific was diluted 4-fold in PBS). The embryos were again washed three times with PBST and then equilibrated in 25 % Hybridisation buffer and 75 % PBST. Finally, the embryos were allowed to pre-hybridise in 100 % hybridisation buffer for 3–5 hours at 65ºC in a hybridisation oven. After pre-hybridisation, embryos were incubated a 1 x solution

of the probe of interest diluted in preheated hybridisation buffer. The embryos are left to hybridise overnight at 65ºC.

On the following day, the probe was removed and stored at -20ºC for future use (up to 10 times). The embryos were washed for 10 minutes in fresh pre-heated hybridisation buffer at 65ºC before three 20 minute washes using 2 x SSC + 0.1 % (v/v) Tween-20, also at 65ºC, followed by three final 10 minute washes at 65ºC in 0.2 x SSC + 0.1 % (v/v) Tween-20. The embryos were then washed three times at room temperature in Malic Acid Buffer (MAB) before 1–3 hours of incubation in blocking buffer. After blocking, the embryos were left in a 1:2000 dilution of anti-DIG Alkaline phosphatase-conjugated antibody in blocking buffer overnight at 4ºC.

The next day the embryos were washed in MAB + 0.2 % (v/v) Tween-20 6–8 times for an hour for each wash. The embryos were washed overnight in more fresh MAB + 0.2 % (v/v) Tween-20 at 4ºC.

On day four, the embryos were equilibrated by washing three times in freshly made Alkaline Phosphatase buffer before incubation with a BM purple solution (Roche). The Alkaline Phosphatase reactions were left at room temperature and monitored hourly. In case the staining was very weak, the BM purple solution was renewed and the reactions were moved to 4ºC and left overnight. The reactions were stopped with 3 washes of PBS-Tween and the embryos refixed using 4 % formaldehyde.

Bleaching solution

1 % (v/v) H_2O_2	333 µl 30 % (v/v) H_2O_2
5 % Formamide	50 µl 100 % Formamide
0.5 x SCC	25 µl 20 x SSC
	Up to 1 ml with H_2O

100x Denhart's Solution

2 % (w/v) BSA	2 g BSA
2 % (w/v) polyvinylpyrrolidone	2 g polyvinylpyrrolidone
2 % (w/v) Ficoll	2 g Ficoll
	Up to 100 ml with H_2O
	Stored at -20ºC

Hybridization buffer

50 % (v/v) Formamide	50 ml 100 % Formamide
5 x SCC	2.5 ml of 20 x SSC
1 mg/ml Yeast RNA (torula)	100 mg Yeast RNA (torula)
100 µg/ml Heparin	10 mg Heparin
1 x Denhart's Solution	1 ml of 100 x Denhart's Solution
0.1 % Tween-20	100 µl of 100 % Tween-20
10 mM EDTA	5 ml of 0.5 M EDTA, pH 8.0
0.1 % (w/v) CHAPS	100 mg CHAPS
	Up to 100 ml with dH_2O
	Stored at -20 ºC

5 x MAB

750 mM NaCl	43.83 g NaCl
500 mM Maleic Acid	58.03 g Maleic Acid
	Up to 800 ml with dH_2O
	pH to 7.5 with NaOH
	Up to 1 litre with dH_2O
	Autoclaved and stored at RT
	Diluted to 1x with H_2O

Blocking buffer

2% Blocking reagent (Roche)	2 g
	Up to 90 ml with 1 x MAB
	Heat on a hot plate while stirring to dissolve
10 % FBS	10 ml after the solution has cooled to room temperature

Alkaline Phosphatase Buffer

100 mM Tris pH 9.5	10 ml 1 M Tris-HCl pH 9.5
50 mM $MgCl_2$	5 ml 1 M $MgCl_2$
100 mM NaCl	2 ml 5 M NaCl
0.1% (v/v) Tween	500 µl 20 % (v/v) Tween
	Up to 100 ml with dH_2O
	Made fresh before use

2.1.8 Whole-mount *in situ* hybridisation (ISH) (zebrafish)

Prior to ISH, embryos were fixed at the appropriate stage for 3-10 days in 4% PFA/ PBS. Embryos were then dechorionated, dehydrated in a graded methanol/PBST series and stored in methanol for a minimum of 12 hours at -20°C. Embryos were transferred to a 3 ml vial, rehydrated and washed in PBST (0.1% Tween20 in PBS). All washing and incubation steps were performed with light agitation. If embryos were older than bud stage they were treated with proteinase K (at 10 µg/ml) for 30 s (for somite stage embryos) or 3 min (24 hour old embryos). After two 5 min washes in PBST, embryos were post-fixed in 4% PFA/PBS for 20 min and rinsed again twice in PBST. Hybridisation buffer was prewarmed to room temperature and 600 µl added to vial and the embryos pre-hybridised for at least one hour at 67°C. After this the hybridisation buffer was replaced with 400 µl probe solution and embryos were incubated over night. The next day the probe solution was removed and stored for reuse at -20°C. The embryos were washed with wash buffers 1-4 for one hour each at 67°C followed by two 10 min washes in PBST at room temperature. Next the embryos were incubated in blocking solution (10% FBS in PBST) for one hour at room temperature. After removal of the blocking solution, the anti-DIG-AP antibody was diluted 1:2000 in blocking solution and 400 µl was added to vial. The embryos were incubated in the antibody over night at 4°C. The next morning the antibody solution was removed and the embryos washed in PBST at least four times for a minimum 15 min/each washing step. They were then equilibrated in staining buffer with two 10 min washes. Subsequently, the ISH staining was developed using SIGMA *FAST*™ BCIP/NBT (1 tablet in 10 ml of water). When the staining was sufficiently strong the staining solution was replaced initially by 50% methanol/PBS. Embryos were then stored in 100% methanol. For taking pictures, the embryos were rehydrated and then taken through a series of glycerol/PBS gradients to a final concentration of 80% glycerol/H_2O.

Hybridisation buffer (50 ml final volume):

25.0 ml	formamide
12.5 ml	20x SSC
0.5 ml	tRNA (stock: 10 mg/ml)
50 µl	heparin (stock: 10 mg/ml)
460 µl	1M citric acid
250 µl	20% Tween20
11 ml	using fine pointed forceps

Probe solution:

Hybridisation buffer was complemented with 5% dextran sulphate. 1 µl of RNA probe was added to 400 µl buffer.

Wash buffers:

1: 50% formamide, 2x SSC, 0.1% Tween20, H_2O
2: 25% formamide, 2x SSC, 0.1% Tween20, H_2O
3: 2x SSC, 0.1% Tween20, H_2O
4: 0.2x SSC, 0.1% Tween20, H_2O

Staining buffer

5 ml	1 M Tris pH 9.5
12.5 ml	1 M $MgCl_2$
1 ml	5 M NaCl
250 µl	20% Tween20
	to 50 ml with H_2O

2.1.9 Double-fluorescent *in situ* hybridisation (DFISH)

Double-fluorescent *in situ* hybridisation was essentially performed as described above for ISH using a combination of dig- and DNP-labelled RNA probes. For double *in situ* the embryos were incubated in probe solution containing dig- and DNP labelled RNA probes at the same time. After standard ISH washes embryos were incubated in 2% H_2O_2/PBST to inhibit endogenous peroxidase activity. The embryos were then washed twice in PBST for 10 min and then blocked in 10% FBS/PBST for at least one hour at room temperature. To visualise the dig-labelled probes the embryos were incubated over night at 4°C with anti-DIG-HRP antibody (1:1000 in blocking solution) and the embryos were then washed in PBST at least

four times for a minimum 15 min. Fluorescein-tyramide was added at 1:100 to 1:500 in PBST depending on the strength of the probe and the embryos incubated for 20 min at room temperature. For the colour reaction H_2O_2 was added to a final concentration of 0.001% for 30 – 40 min. To kill the peroxidase activity of the HRP the embryos were incubated in 3% H_2O_2 for one hour. Antibody incubations and washes were performed as above. Anti-DNP-HRP was added 1:250, Cy3-tyramide was used at 1:100. After the second colour reaction embryos were washed extensively in PBST, usually at least five times for one hour or over night at 4°C. Embryos were then mounted in 0.8% low melting temperature agarose and imaged using a LSM 780 confocal microscope (Zeiss).

Fluophore tyramide synthesis

Solutions:

- 10 mg/ml fluorescein-NHS ester (Pierce) or Cy3-NHS (Amersham) stock solution in dimethyl formamide (DMF) (Sigma)
- DMF-TEA solution (1 ml DMF, 10 µl triethylamine (TEA))
- Tyramide solution (10 mg tyramide, 1 ml DMF-TEA)

Reaction:

4 ml of 10 mg/ml fluorescein-NHS/DMF and 1.37 ml tyramide solution were mixed and incubated in the dark for 2 hours at RT before adding 4.6 ml ethanol. Aliquotes were stored in the dark at 20°C.

Cy3-tyramide synthesis was performed as above but reaction mix was 100 µl Cy3-NHS in 33 µl tyramide solution. 1.2 ml ethanol were added after the room temperature incubation step.

2.1.10 Immunofluorescence in embryos

Embryos were rehydrated, washed in PBST (0.1% Tween20 in PBS) and blocked for >1 hour in blocking solution at RT. The embryos were then incubated in a 1:100 dilution of antibody in blocking solution overnight at 4°C and washed the next day for 4 x 15 min in PBST. This was followed by a 1 hour incubation in a 1:500 dilution of Alexa Fluor 488-conjugated antibody and repeated washed. Finally, the nuclei

were stained using DAPI (Roche) and the embryos were mounted in 0.8% low melting agarose. Images were obtained using a LSM 780 confocal microscope (Zeiss).

Blocking solution

10% FBS
1% DMSO
0.1% Tween20
in PBS

2.1.11 Alcian blue staining

For alcian blue staining the embryos were fixed in 4% PFA/PBS at the indicated stage for 5 days. They were initially dehydrated in first 50% EtOH/H_2O and then in 100% EtOH. They were then left at -20°C for 24 hours. The embryos were transferred into staining solution and incubate for 24 hours at room temperature with mild agitation. To neutralise, they were washed in saturated sodium borate solution for 9-12 hours. The embryos were then bleached in 3% hydrogen peroxide/ 1% potassium hydroxide for about 20 min. For preservation and imaging the embryos were transferred through a series of glycerol/water containing 1% potassium hydroxide and store in 100% glycerol.

Staining solution for 100 ml final volume:

70 ml 100% EtOH
30 ml acetic acid
20 mg Alcian blue

2.1.12 Embryo extracts

Embryos were stored at -80°C. Extract buffer was prepared fresh before every use. 10 µl of buffer were used per whole embryo, which meant that the protein concentration between different samples was similar. The embryos were homogenised using a pestle. The suspensions were then centrifuged at 13,000 rpm for 10 minutes at 4ºC (Biofuge fresco Heraeus benchtop centrifuge). In general 2

embryo's worth of extract supplemented with 4x sample buffer were used per Western blot.

Embryo extract buffer

100 µl 1 M Tris pH 8.0
20 µl 0.5 M EDTA pH 8.0
250 µl 10 % (v/v) NP-40
100 µl 1.25 M sodium β-glycerophosphate
500 µl 1 M NaF
5 µl 20 µM Calyculin A
250 µl 200 mM Na-Pyrophosphate
0.5 ml complete mini protease inhibitor (Roche, 1 tablet dissolved in 1 ml H_2O)
Up to 5 ml with H_2O

2.2 Molecular biology

2.2.1 Bacterial transformation and culture

For plasmid amplification the chemically-competent *Escherichia coli* strain TG1 was transformed, unless Dam methylation was a problem in which case JM101 competent cells were used. The competent cells were prepared by Dr. Becky Randall in the lab. After slowly thawing 50 µl of chemically-competent *E. coli* strain on ice either 100 ng of plasmid DNA or a 10 µl ligation reaction were added to the cells. The reaction was incubated on ice for 15 min and afterwards heat-shocked for 1 min at 37°C. After placing the bacteria on ice for a further 2 min, 150 µl LB medium (prepared in house) were added. The bacteria were then shaken at 37°C for 30-60 min and plated on agar plates containing the suitable antibiotic (ampicillin 50 µg/ml or Kanamycin 50 µg/ml as appropriate) to select for the transformed bacteria. Agar plates were incubated at 37°C overnight to allow for the growth of bacterial colonies.

2.2.2 Plasmid preparation

2.2.2.1 Maxipreparation

E. coli containing the desired plasmid were grown in 200 ml LB medium with the appropriate antibiotic over night at 37°C with vigorous shaking. Plasmids were isolated from recombinant *E. coli* using the GenElute™ HP Plasmid Maxiprep Kit according to the manufacturer's instructions. This kit is based on the method originally published by Binboim and Doly (Birnboim and Doly, 1979) and works with the lysis of bacteria under alkaline conditions in the presence of SDS. Under these conditions, both chromosomal DNA and plasmid DNA are denatured. However, upon neutralization, plasmid DNA is selectively renatured whereas chromosomal DNA remains insoluble. Soluble (plasmid) DNA is subsequently purified by anion exchange chromatography. The final purification of the DNA involves the precipitation with isopropanol. The precipitate is washed and air-dried before being dissolved in H_2O (volume depended on the size of the pellet).

2.2.2.2 Minipreparation

For plasmid isolation QIAprep® spin miniprep kits (Qiagen) were used. The procedure is based on alkaline lysis of bacterial cells followed by adsorption of DNA onto silica in the presence of high salt. A single bacterial colony was picked from a selective agar plate and inoculated in 3 ml LB medium with the appropriate antibiotic over night at 37°C with vigorous shaking.1.5 ml of this culture were taken to perform the miniprep according to the manufacturer's instructions. The samples were eluted in 40 µl H_2O.

2.2.3 Nucleic acid concentration

The concentration of the isolated DNA or RNA was determined using a NanoDrop™ 1000 spectrometer (ThermoScientific). After calibration with the elution solution, 1 µl sample was pipetted onto the measurement pedestal and the nucleic acid concentration measured. To calculate the concentration the machine takes optical density (OD) readings at the wavelengths of 230 nm (phenol), 260 nm (nucleic acids), 280 nm (proteins) and 320 nm (background). An OD_{260} reading of 1 is equivalent to 50 µg/ml for DNA and 40 µg/ml for RNA. The concentration is then calculated based on the equations:

DNA: $(OD_{260} - OD_{320}) \times 50\ \mu g/ml$

RNA: $(OD_{260} - OD_{320}) \times 40\ \mu g/ml$

2.2.4 Polymerase chain reaction (PCR)

Standard PCR was performed using *GoTaq*® DNA Polymerase. As a template, 50 ng DNA were used in case of plasmid DNA. For PCR reaction from cDNA, the cDNA reaction was performed as explained in 2.2.9 and 2 µl of a 1:20 cDNA dilution were used.

25 µl reaction mix:

5 µl	5x buffer
0.5 µl	dNTP mic (20 mM)
0.5 µl	forward primer (10 µM)
0.5 µl	reverse primer (10 µM)
1 µl	$MgCl_2$ (25 mM)
0.12 µl	GoTaq polymerase
x µl	template
up to 25 µl	H_2O

In general, the PCR reaction was performed in a thermal cycler as follows:

95°C	2 minutes	
95°C	30 seconds	⎫
55°C	5 seconds	⎬ x 30 cycles
72°C	1 minute/kb	⎭
72°C	5 minute	
4°C	∞	

The sample was then run on a 1-2% agarose gel (depending on the product size) as specified in 2.2.5. The size of the PCR product was confirmed by comparison to standard DNA markers (New England Biolabs; NEB) and the appropriate band excised. The DNA was extracted using QIAquick Gel Extraction kit (Qiagen) using the microcentrifuge protocol according to the manufacturer's instructions and eluted in 30 µl of H_2O. For sensitive protocols the DNA was further purified with the QIAquick PCR purification kit (Qiagen) and again eluted in 30 µl of H_2O.

2.2.5 Agarose gel electrophoresis

Agarose (Invitrogen) gels of the appropriate percentage were prepared in 1 x TAE with 1 µl/50 ml ethidium bromide to visualise nucleic acids. The molten gel was poured into a sealed gel tray with the desired gel comb and allowed to set at room temperature. Gels were run in 1 x TAE with a Lambda DNA-BstEII digest or 1kb DNA ladder (NEB) at 80-120 volts for 15-45 minutes depending on the size of the

gel. To visualise and document the nucleic acids the gels were exposed to ultraviolet illumination with a Bio-Doc-It™ Imaging system (UVP, LLC).

2.2.6 Restriction enzyme digest

All restriction enzymes used were purchased NEB and used according to the manufacturer's protocol. Typically, 1 unit enzyme per 1 µg DNA was used in a 20/50 µl reaction mix. The reaction mix was then incubated at the relevant temperature for 2 hours – overnight. To check for efficient and complete digestion by the restriction enzyme 1 µl of digested sample was run alongside 1 µg of undigested plasmid DNA on a 1% agarose gel (2.2.5). The remainder of the sample was cleaned up using the QIAquick® PCR purification kits (Qiagen) according to the manufacturer's protocol.

2.2.7 Ligations

A molecular ratio of usually 1:2 (vector:insert DNA) was ligated using 1 µl T4 DNA ligase (NEB) and 1x T4 DNA ligase buffer (NEB) in a total volume of a 10 µl reaction. A control sample lacking the T4 ligase was used as a control for vector re-ligation. The samples were incubated for a minimum of 3 hours or overnight at RT and then transformed into TG1 bacteria (2.2.1). The transformed bacteria were then plated on LB-agar plates containing the appropriate antibiotic and incubated overnight at 37°C to allow colonies to grow. Colonies were then picked and the plasmid DNA isolated by minipreparation (2.2.2). To test correct insertion of the PCR product, the isolated plasmids were tested by restriction enzyme digest and positive samples were sequenced as described below to verify the DNA sequence.

2.2.8 Sequencing

For sequencing 200 ng of DNA template were mixed with 10 ng primer and 8 µl BigDye® Terminator v2.0/v3.1 (Applied Biosystems) in a final volume of 20 µl. The sequencing reaction was carried out using the following standard sequencing conditions:

96 °C	10 seconds	⎫	
50 °C	5 seconds	⎬	x 30 cycles
60 °C	4 minutes	⎭	
60 °C	1 minute		
10 °C	∞		

To remove unincorporated dye-terminators from samples, the Dyex 2.0 Spin Kit (Qiagen) was used and purified DNA was subsequently dried using a vacuum centrifuge. Samples were then submitted to the Cancer Research UK Equipment Park for capillary sequencing.

2.2.9 Total RNA isolation

Embryos were homogenised in 800 µl TRIzol® (Invitrogen) and lysed for 10 min at RT. 160 µl of chloroform were added, the samples vortexed thoroughly and incubated for another 3 min at RT. Samples were then spun for 15 min at 4°C at 13,000 rpm. The aqueous phase was moved into a new tube containing 10 µg of glycogen (Ambion) as well as 400 µl isopropanol and the mixture incubated for 10 min at RT. To precipitate the nucleic acids, the samples were centrifuged for 20 min at 4°C at 13,000 rpm. After the removal of the supernatant, the pellet was washed in 80% EtOH, dried and resuspended in 95 µl of RNase-free water, 1 µl RNasin (Promega), 2 µl DNase salts (5 µl $CaCl_2$ 1 M, 10 µl $MgCl_2$ 1 M, 10 µl DTT 200 mM) and I µl DNaseI (Worthington). To efficiently eliminate genomic DNA contaminations, the samples were incubated for 30 min at 37°C. 300 µl of RNase-free water was added and the RNA was extracted by addition of 400 µl phenol:chloroform:isoamyl alcohol (Sigma), vortexing and spinning for 10 min at 13,000 rpm. The aqueous layer, containing the RNA, was transferred to a new microcentrifugation tube, mixed with equal amounts of 100% EtOH and precipitated on dry ice for 30 min. The RNA pellet was obtained by centrifugation at 13,000 rpm for 20 min and washed with 1 ml of 80% EtOH. The pellet was then dried and resuspended in 30 µl RNase-free water. The RNA was stored at -80°C. The quality of the RNA was assessed by agarose gel electrophoresis (2.2.5).

2.2.10 RNA sequencing

The RNA sequencing was performed by the LRI Advanced Sequencing facility. A high quality of the submitted RNA was first confirmed using a Bioanalyzer RNA kit (Agilent Technologies). The libraries for sequencing were prepared with TruSeq Stranded mRNA Sample Prep Kit (Illumina) using 1 µg of total RNA as starting material. The data was subsequently analysed in collaboration with Richard Mitter (LRI Bioinformatics department).

36bp single end reads generated on the Illumina GAII were assessed for quality (i.e. base quality scores, duplication rates, number of reads, adapter contamination) using FastQC v0.10.0. Reads were aligned to the Danio rerio Zv9/danRer7 genome using Tophat2 v2.0.8 with default parameters expect for the specification to align first to the Ensembl 68 transcriptome. *(Only the reads that did not fully map to the transcriptome were then mapped on the genome. The reads that did map to the transcriptome were converted to genomic mappings (spliced as needed) and merged with the novel mappings and junctions in the final tophat output.).*

Differential expression analysis was conducted using the Bioconductor package edgeR. A matrix of gene-level read counts was created by assessing the overlap between the co-ordinates of mapped reads and Ensembl 68 exon positions. Sample library size was normalised using the default TMM method. The estimates for the common, trended and tagwise dispersion were calculated using edgeR's default methods. *(This is basically estimating acceptable levels of variation - see here for more details http://www.bioconductor.org/packages/release/bioc/vignettes/edgeR/inst/doc/edgeRUsersGuide.pdf)*

An empirical Bayes generalised linear model was used to assess differential expression between replicate groups at the gene level. A false discovery rate (FDR) controlled pvalue of <=0.05 combined with an absolute fold change of >=2 and minimum read count of 200 was set as the threshold for significance.

Heatmaps of log counts per million (CPM) values were used to visualise the expression changes of selected genes across samples. Genes were hierarchically clustered based on a Euclidean distance metric and Ward method.

2.2.11 Quantitative real time PCR (qRT-PC)

For reverse transcription cDNA synthesis the AffinityScript RT-PCR kit (Agilent Technologies, Inc.) was used. The reaction mix was as follows:

10X Buffer	2 µl
DTT (100 mM)	2 µl
dNTPs (25 mM each)	0.8 µl
Primers	3 µl
AffinityScript RT	1 µl
RNase inhibitor	0.5 µl
RNA (1 µg)	x µl
Final volume	20 µl

As a control to assess genomic DNA contaminations, a synthesis reaction without addition of the reverse transcriptase (-RT) was included for each sample. The cDNA reaction mix was then prepared in a thermal cycler using the following program:

25ºC	5 minutes
42ºC	20 minutes
55ºC	15 minutes
95ºC	5 minutes
4ºC	∞

The cDNA was diluted 1:20 in H_2O. For the qRT-PCR reaction a mix was prepared and pipetted into 96 well optical plates (Applied Biosystems):

2.5 µl	diluted cDNA
5 µl	Express SYBR green master mix (invitrogen)
0.25 µl	forward primer (10 µM stock)
0.25 µl	reverse primer (10 µM stock)
2 µl	H_2O

For each sample, triplicates were measured. *odc* or *ef1*α were used for input normalisation. The qRT-PCR was performed using an ABI 7500 Fast Real time PCR machine. The PCR machine carries out 40 rounds of cDNA amplification by first denaturing all DNA at 95ºC, then reducing the temperature to 60ºC for amplification. At the permissive temperature of 60ºC, as double stranded DNA is synthesised by DNA Polymerase, SYBR Green® binds the double stranded DNA and the resulting SYBR Green®-DNA complex is capable of emitting green light

(~522 nm wavelength) when excited by light with a wavelength of 497 nm. Thus, during each round of amplification, the amount of green light emitted should effectively double. The machine tracks the amount of fluorescence and plots it on a log-scale in order to identify the Ct value, which is set to 10-fold above a threshold value (the average baseline or background fluorescence) in the linear range of amplification (before any component becomes limiting and the signal plateaus). The higher the level of cDNA found in a sample, the fewer the rounds of amplification are required for the fluorescence to reach the Ct value. The machine then provides a list, indicating the cycle number when each sample has reached the Ct value. Samples with Ct values over 30 were not taken into account and the revelant mRNA was considered not to be expressed. The relative amount of cDNA present in a sample was calculated using the equation:

$$[cDNA]_{relative} = 2^{Ct(control)- Ct(Gene\ of\ interest)}$$

The calculation was performed for each of the triplicates and then the mean and the standard deviation determined. The Ct values of the –RT control samples provides information about possible contamination by genomic DNA. Finally a melting curve for each primer pair was determined to ensure that the primers were specific and did not amplify multiple products.

2.2.12 *In vitro* protein translation

For in vitro translation, the TNT® Coupled Reticulocyte Lysate Systems (Promega) was used according to the manufacturer's instructions.

12.5 µl	TNT
1 µl	Buffer
0.5 µl	Amino acids (+/- Met)
0.5 µl	RNA guard
0.5 µl	Polymerase (T3, T7 or SP6)
9 µl	H_2O
1 µl	DNA template (1 µg/µl)

The mix was incubated for 1.5 hours at 30ºC and aliquots stored at -80ºC. For analysis by SDS-PAGE (2.2.16) usually 1 or 3 µl of the reticulocyte lysate supplemented with 4x sample buffer was processed. The proteins could then be detected using Western blot analysis.

In order to generate ^{35}S-labelled proteins 1 µl amino acids without Met replaced amino acids +Met. Then 1 µl ^{35}S-Met was added on the expense of H_2O. Proteins were also separated by SDS-PAGE and the gel dried. To detect the radioactive protein bands the gel was exposed to an X-ray film (SuperRX, Fujifilm) overnight inside a sealed cassette.

2.2.13 Bandshift assay

2.2.13.1 Probe synthesis

For generating labelled DNA probes the following reaction mix was prepared:

2 µl	5x GoTaq PCR buffer
0.4 µl	$MgCl_2$ (25 mM)
1 µl	fwd oligo (50 ng/µl)
1 µl	rev oligo (50 ng/µl)
0.5 µl	DNA template (100 ng/µl)
1 µl	dATP [α-^{32}P] (3000Ci/mmol, 10mCi/ml)
1 µl	dCTP [α-^{32}P] (3000Ci/mmol, 10mCi/ml)
0.5 µl	dGTP (0.5 mM)
0.5 µl	dTTP (0.5 mM)
0.5 µl	dATP (50 µM)
0.5 µl	dCTP (50 µM)
0.5 µl	GoTaq polymerase
0.6 µl	H_2O

The PCR was carried out using the following standard conditions:

94 °C	3 minute	
94 °C	25 seconds	⎫
37 °C	25 seconds	⎬ x 31 cycles
72 °C	25 minutes	⎭
72 °C	3 minute	
10 °C	∞	

After the probe synthesis, 1 µl of the reaction mix was kept for later quantitation. The remainder of the samples were run on a 5% (w/v) acrylamide gel, assembled with 0.4 mm spacers and comb. The gel was run at 150V and 150 mA in 0.5x TBE for 1 hour. The gel was then exposed to a film (SuperRX, Fujifilm) to identify the

position of the labelled bands on the gel. The probe bands were cut using a scalpel and transferred into a microcentrifugation tube. 350 µl elution buffer were added, the samples vortexed and the probes eluted overnight at 37°C. The next day 350 µl phenol were added and the samples well mixed prior to a 3 min centrifugation step at 13,000 rpm. The upper aqueous phase was transferred into a new tube and the DNA probes precipitated by adding 1 µg tRNA (Roche) and 700 µl cold 100% EtOH and incubating mix for 20 min on dry ice. Next, the samples were centrifuged for 20 min at 13,000 rpm at 4°C, the EtOH removed and the pellet rinsed with 350 µl cold 100% EtOH (centrifugation was repeated for an additional 5 min). After removal of the EtOH the pellets were allowed to dry on the bench. The pellet was the resuspended in 30 µl TE and quantitated.

All probes used in bandshift reactions were dissolved to 0.2 ng/µl. In order to calculate the isotope incorporation and thereby quantitate the probes, 1 µl of the TE-resuspended probe was counted in the scintillation counter (Beckman LS 6500 multi-purpose scintillation counter) along with 1 µl of the original pre-PCR probe mix. The probe was then quantitated as follows:

From comparing the count numbers of the original PCR mix and the eluted probes the % incorporation of radioactivity in the probe were determined. Then the maximum possible yield of a probe in moles and ng was calculated by working out how much dATP and dCTP was in the reaction (hot + cold), as this was the limiting. This then allowed the prediction of how many labelled As and Cs were incorporated per probe, and taking the molecular weight of each probe into account it was possible to calculate the total ng of probe synthesised and to dilute the probes accordingly.

$$(\%\ \text{incorporation}) \times \frac{(\text{no. moles dATP + dCTP in reaction}) \times \text{mol wt probe}}{10^9 \times (\text{no. As and Cs in probe})}$$

5% (w/v) acrylamide gel (25 ml)

3.125 ml 40% (w/v) acrylamide
2.15 ml 2% (w/v) bisacrylamide
1.25 ml 10 x TBE
Up to 25 ml with deionised water

25 ml gel mix is polymerised with 60 µl 20% (w/v) APS and 50 µl Temed

Elution buffer

0.3 M Na acetate (pH 5.2)
0.1 % (w/v) SDS
1 mM EDTA

2.2.13.2 Bandshifts using whole cell extracts

In the absence of a suitable Dlx3b antibody, a Flag-tagged version of Dlx3b was transfected in HEK293T cells. Control cells were transfected with pcDNA3. The cells were harvested with D0.4 lysis buffer (2.3.4), centrifuged for 10 min at 13,000 rpm and the protein concentration determined (2.2.15). 5 µg of control extract as well as 2.5 µg and 5 µg of Flag-Dlx3b extracts were diluted to a volume of 10 µl in D0.4. They were then pre-incubated with or without 1 µl anti-Flag antibody for 5 min at RT prior to addition of 10 µl probe mix. The samples were briefly centrifuged and incubated for 15 min at RT.

Probe Mix (10 µl)

1 µl 200 mM KCl
1 µl 110 mM $MgCl_2$
1 µl probe (0.2 ng/µl)
1 µl pdI-dC (1 mg/ml stock) (Sigma)
4 µl 50 % (v/v) glycerol
2 µl H_2O

To prepare the bandshift gel two glass plates (19 cm x 20 cm) were assembled using 1.5 mm spacers and sealed using tape. The non-denaturing gel mix was poured between the plates and a 1.5 mm comb inserted. The bandshift gels were pre-run at 150 V and 150 mA for 1-2 hours in 0.5 x TBE prior to loading. The wells were then rinsed with 0.5 TBE and the samples loaded onto the gel. The gels were run for 2 hours 45 min at 150 V and 150 mA and the transferred on Whatman

paper to be dried on a gel drier. The bandshift was visualised by overnight exposure to an X-ray film (SuperRX, Fujifilm) at room temperature.

Non-denaturing acrylamide gel mix

6.25 ml 40 % (w/v) acrylamide
3.125 ml 2 % (w/v) bisacrylamide
2.5 ml 10 x TBE
2.5 ml 50 % (v/v) glycerol
Up to 50 ml with deionised water

50 ml gel mix is polymerised with 125 μl 20 % (w/v) APS and 100 μl Temed

2.2.14 Mass Spectrometry analysis

LRI Cell services grew up and harvested 30 large (T175) tissue culture flasks of HEK393T cells expressing Flag-SNW1 (2.3.3) or Flag (obtained from LRI Cell services) by itself. All steps were carried out at 4°C to avoid protein degradation. The cells pellet was resuspended in 28 ml benzonase lysis buffer supplemented with protease inhibitors (PI) and left on a nutator for 10 min prior to a 10 min centrifugation step at 300 g. An aliquot of the cytoplasmic extract (supernatant) was kept for expression analysis by Western blot. The pellet was resuspended in 5x the pellet volume with benzonase buffer + benzonase nuclease (25 μl/10 ml) (Novagen) + PI and left rotating for 20 min. The NaCl concentration was then adjusted to 450 mM and the samples rotated for another hour in the cold room. The extracts were centrifuged for 10 min at 3500 rpm using a Beckman Coulter Allegra X-15R centrifuge and an aliquot of the nuclear extract taken for expression analysis. For the following dialysis step the nuclear extracts were transferred into 6-8 kDa molecular weight cut-off dialysis tubing (Spectra/Por), which was tightly sealed to avoid leaking of the extracts into the buffer. The tubes were then placed into 1 litre of buffer D + PI and left under gentle stirring for 3-4 hours. The solution was then replaced with 2 litres of fresh buffer and the extracts further dialysed overnight.

The following day the extracts were divided into 2 ml centrifugation tubes and spun for 20 min at 13,000 in a microcentrifuge. A 100 μl aliquot was taken as an input control for Western blot. 600 μl slurry of M2 Flag agarose beads (Sigma)

were washed twice with cold PBS in 15 ml Falcons. The amount of slurry used was increased for large volumes of nuclear extracts. After the washes the nuclear extract was added to the beads and the samples incubated for 4 hours on a wheel at about 10 rpm. This was followed by a 10 min centrifugation step at 300 g. A 100 µl aliquot was taken to assess the binding efficiency of Flag-Snw1 to the Flag beads using Western blot. The beads were then washed twice with 15 ml cold WB150 (+ TritonX) with 10 min on the wheel between washes. This wash was repeated with 15 ml cold WB100. The last wash, including the beads, was loaded on autoclaved Poly-Prep Biorad chromatography columns. Flag-Snw1 and the control Flag-tag including the associated proteins were released from the beads by the addition 3xFlag peptide (prepared by LRI peptide synthesis laboratory) in 5 elution rounds. For each round 300 µl of 400 µg/ml 3xFlag peptide diluted in WB100 were added to the beads and incubated for 15 min. The tap on the columns was released and the eluate collected in a centrifugation tube. 5 µl of each fraction were analysed by Western blot to ensure that the samples were not degraded, and to assess which fraction should be pooled for mass spectrometry analysis (2.2.20). Generally, fractions 2, 3 and 4 were combined and concentrated using Ultracell centrifugal filter units (10K, Millipore). 4x sample buffer was added to the columns, the samples boiled and eluted by centrifugation, as specified in the manufacturer's manual.

Next the samples were run on a 12.5% SDS-PAGE and Coomassie stained. For further analysis the lanes were cut into 1 mm thick stripes using a razor blade and each strip transferred into a 96-well plate (provided by the Mass Spectrometry facility) containing 100 µl H_2O.

To avoid contamination all surfaces and tools were carefully cleaned and only fresh and filtered solutions were used.

Benzonase lysis buffer

25 mM Tris (pH 7.5)
40 mM NaCl
2 mM $MgCl_2$
0.5 % (v/v) NP-40

25 mM NaF, 25 mM sodium β-glycerophosphate, 0.4 mM Pefabloc SC, 1 mM DTT, and 1 x Protease Inhibitors were freshly added (Roche).

Buffer D

20mM HEPES pH 7.9
0,1 M KCl
0.2 mM EDTA pH 8
0.2 mM EGTA pH 8
20% Glycerol
1 mM Benzamidine
0.5 mM DTT
0.4 mM Pefabloc

WBX (X= 150 mM KCl or 100 mM KCl)

20mM HEPES pH 7.9
X M KCl
0.5 mM EDTA
10% Glycerol
+PI Roche tablets
NO DTT or Pefabloc

3xFlag peptide

The Flag peptide was dissolved at 8mg/ml in 200 mM Tris HCl pH 7.9 and aliquots and store at -80°C.

2.2.15 Measuring protein concentration

The protein concentrations in lysates were determined using the Bradford method. A standard curve to calculate protein concentrations of the lysates was determined using 1 µg increments of 0 – 5 µg of BSA (NEB) in a flat bottom 96-well plate. Duplicates of 1 µl of each lysate sample was pipetted into subsequent wells of the 96-well plate before pipetting 200 µl of 1x BioRad Protein Assay solution (Biorad) into all the wells to be read. The absorbance at 595 nm was measured on a SpectraMax Plus Spectrophotometer (Molecular Devices) and the protein concentrations of lysate samples were determined from the BSA standard curve.

2.2.16 SDS polyacrylamide gel electrophoresis (SDS-PAGE)

Proteins were separated by size using SDS polyacrylamide gels.
The gels were usually prepared in the lab using the following recipes:

15 % resolving gel mix

5.625 ml 40 % (w/v) acrylamide
0.645 ml 2 % (w/v) bisacrylamide
3.75 ml 1.5 M Tris-HCl pH 8.8
Up to 15 ml with H_2O
Mix well
40 µl of 20 % (w/v) APS and 30 µl TEMED were added before pouring

Stacking gel mix

0.625 ml 40 % (w/v) acrylamide
0.333 ml 2 % (w/v) bisacrylamide
0.625 ml 1.5 M Tris-HCl pH 6.8
Up to 5 ml with H_2O
Mix well
Add 15 µl of 20 % (w/v) APS and 10 µl TEMED before pouring

After the gel polymerised it was inserted into an electrophoresis apparatus (Cambridge Electrophoresis Ltd.) and the reservoirs filled with 1x SDS running buffer.

5x SDS Running buffer

1.92 M Glycine	1440 g
250 mM Tris	300 g
0.5 % (w/v) SDS	250 ml 20 % (w/v) SDS
	up to 10 litres with H_2O

The protein samples in 1x sample buffer were boiled for 5 min before loading. To determine the presence of specific proteins in cell lysates, usually 30 µg of total protein were loaded. Molecular weight markers were loaded on the same gel to estimate the protein size. The gel was then run at 230 V and 45 mA for around 1 hour 40 min (depending on the size of the proteins to be detected). The gel was

then either Coomassie stained (2.2.17) or specific proteins detected by Western blotting (2.2.20)

4x sample buffer

4 ml 20 % (w/v) SDS
2 ml 1 M Tris-HCl (pH 6.8)
4 ml 100 % glycerol
0.4 ml 2-mercaptoethanol

Molecular weight markers

50 μg/ml each of myosin (212 kDa), β-galactosidase (116 kDa), phosphorylase (97.5 kDa), BSA (66.5 kDa), catalase (57.8 kDa), glutamate dehydrogenase (55.5 kDa), GAPDH, ovalbumin (42.7 kDa), carbonic anhydrase (28.9 kDa), SBTI (20 kDa) and RNaseA (13 kDa) in 1 x SDS running buffer. Prepared by Dr. Debipriya Das.

2.2.17 Coomassie staining

For Coomassie staining the gel was incubated in staining solution for around 15 min and then destained in destaining solution for about 1 hour under gentle rocking. The destaining solution was refreshed several times until the blue background staining was sufficiently reduced to clearly visualise the specifically stained protein bands.

Coomassie stain

0.5 % (w/v) Coomassie blue R-250 (Merck)
45 % (v/v) methanol
10 % (v/v) acetic acid

Destain

25 % (v/v) methanol
7 % (v/v) acetic acid

The gel was than scanned and dried using a vacuum gel drier for preservation if required.

2.2.18 Direct antibody coupling to beads

For endogenous SNW1 IP the rabbit anti-Nco62A antibody (Bethyl Laboratories) was crosslinked to Protein A beads to minimise nonspecific binding. Per 30 µl of Protein A sepharose bead slurry (Sigma), 5 µl antibody was used. First the Protein A slurry was transferred into a 15 ml tube and washed twice with 10 ml PBS. All centrifugation steps were performed at 4°C for 2 min at 230 g. The bead pellet was resuspended in 10 ml PBS, the antibody added and incubated for 1 hour at RT with gentle rocking. The beads were then washed twice in 0.2 M Sodium Borate (pH 9.0) and resuspended in 10 ml 0.2 M Sodium Borate. Prior to 30 min incubation at RT, 0.05 g dimethylpimelimidate (DMPD) were added to a final concentration of 20 mM. The beads were washed twice in 0.2 M Ethanolamine (pH 8.0) to quench the crosslinker and incubated for 2 hours in 0.2 M Ethanolamine in a third washing step with gentle mixing. This was followed by 2 wash steps in PBS. Beads were then resuspended in PBS supplemented with 0.02% sodium azide using 10x the volume of the initial slurry input. Beads are stored at 4°C. The crosslinking efficiency was tested by Western blotting.

2.2.19 Immunoprecipitation (IP)

Cells were washed with cold PBS and lysed in Co-IP lysis buffer. They were transferred into a 1.5 ml centrifugation tube and sonicated for 13 seconds on ice. The samples were then centrifuged at 13,000 rpm for 10 min at 4°C before the protein concentration of the supernatant was measured by Bradford assay (2.2.15). 35 µg were retained as the input control and usually 300 µg of total proteins were used per IP and incubated with 5 µl of antibody for 2 hours on ice. If the antibody had not been crosslinked to beads, depending on the source of the antibody 30 µl protein G (mouse) or protein A (rabbit) beads, that were pre-equilibrated in Co-IP buffer, were added and incubated for 2 hours at 4°C with rotation. In case of Flag-IPs (Flag M2 agarose beads, Sigma) or IPs using beads with crosslinked antibody the cell lysate supernatant was directly added to these beads, also equilibrated in Co-IP buffer, for incubation. After incubation with cell lysates the beads were washed a minimum of 3 times with Co-IP buffer, resuspended in 4x sample buffer and the experiment analysed by Western blot (2.2.20).

Co-IP lysis buffer

20 mM Tris, pH 7.5
150 mM NaCl
0.5% NP-40
10% glycerol
1 mM DTT
25 mM NaF
25 mM Na β-glycerophosphate
complete mini protease inhibitors (Roche)

2.2.20 Western blot analysis

For Western blotting, proteins were transferred from an SDS gel onto PVDF membrane. For that purpose 3 mm Whatman® Paper and Immobilon™-P PVDF 0.45 µm membrane (Millipore) was cut into pieces slightly larger than the gel. One piece of PVDF membrane was first activated in 100% MeOH and the soaked in 1x Transfer buffer. Two pieces of Whatman® Paper were incubated in Transfer buffer as well. The transfer itself was performed using a SemiPhor Transfer Unit (Hoefer). First, two pieces Whatman® Paper were placed in the transfer unit, the PVDF membrane and then the gel were added on top. Finally two more pieces of Whatman® Paper were added. Throughout the whole process the inclusion of bubbles was avoided, as this disturb the transfer process. A roller was also used to remove any air bubble before closing the transfer apparatus. Proteins were transferred for 1 hour 30 min at 0.8 mA/cm^2 of gel.

After the transfer, the apparatus as dissembled and the blot soaked in Ponceau S solution (Sigma) until protein bands were visible. The blot was then quickly washed in consecutive rounds of water until the background staining was removed. The molecular weight marker sizes were labelled with a pen and the membrane cut in appropriate pieces for further analysis. The membranes were then blocked in the blocking solution containing 5 % (w/v) skimmed milk in PBS-Tween or 5% BSA in PBS-Tween for about 30 min at room temperature. After blocking, the blot was left rocking in primary antibody diluted in blocking solution for 1 hour at room temperature or overnight at 4ºC. The following day the blot was washed a minimum of 3 x 10 min with PBS-Tween before incubation in the

appropriate HRP-conjugated secondary antibody. The blot was then again washed in PBS-Tween as previously described. The HRP was detected using Luminata western HRP substrate (Millipore) and blots were exposed to an autoradiography film (SuperRX, Fujifilm) inside sealed cassettes. The film was developed using a JP-33 Automatic X-Ray Film Processor (Jpi).

10x Transfer buffer

1.5 M Glycine	1126 g
200 mM Tris	242 g
0.1 % (w/v) SDS	50 ml 20 % (w/v) SDS
	Up to 10 litres with dH_2O
	Stored at room temperature.
	Dilute fresh to make a 1x solution containing 20 % methanol.

PBS-Tween

1 x PBS	1 litre 10 x PBS
0.2 % (v/v) Tween®-20	20 ml Tween-20
	Up to 10 litres with H_2O
	Stored at room temperature

2.3 Cell culture

2.3.1 General culture conditions

Human Embryonic Kidney 293T (HEK293T) cells were cultured in DMEM supplemented with 10 % FBS, 100 units/ml Penicillin, and 100 µg/ml Streptomycin on plastic dishes or flasks of tissue culture grade (Corning®, Falcon®, NUNC™) at 37ºC with 10 % CO_2 in HeraCell incubators (Heraeus). To isolate individual cells in suspension, cells were washed once with PBS before treating with a trypsin/versene solution for 2-3 minutes. The trypsin was inactivated by adding four times the same volume of DMEM with all supplements.

2.3.2 Plasmid transfections

The following protocol describes transfection for 10 cm plates. If transfections were performed in a different format, the volume of reagents was accordingly scaled.
Cells were seeded in a 10 cm plate to be 80% confluent at the time of the transfection. Usually a maximum of 6 µg of DNA were transfected per 10 cm dish. If the experiment required transfection with different plasmids in various ratios, the same amount of plasmid was transfected in all conditions and differences balanced by adding pcDNA3 as an empty vector. In a sterile centrifugation tube, 500 µl Opti-MEM® I Reduced Serum Medium (Invitrogen) was combined with 125 µl FuGENE HD transfection reagent (Roche) and incubated at RT for 5-10 minutes. The DNA was added, everything well mixed and left at RT for another 15 min. The transfection mixture was then added dropwise to the cells on a 10 cm dish with 4 ml DMEM/10% FBS. The next morning fresh medium was added to the cells. 1-2 days after transfection, the plates were washed with cold PBS and harvested as outlined in section 2.3.4

2.3.3 Cell line generation

To generate stable cell lines that expressed Flag-SNW1, HEK293T cells were transfected as described above with pcDNA3 Flag-SNW1 and pSuperRetro (to convey puromycin resistance) in a 10:1 ratio. After 48 hours of transfection the cells were trypsinised and very sparsely seeded on 15 cm dishes to obtain single cell

colonies. The medium was supplemented with 0.8 µg/ml puromycin. This dose was previously determined by performing a concentration-killing curve experiment. When the single cell colonies reached a sufficient size, the cells were expanded and analysed for Flag-SNW1 expression by Western blot.

2.3.4 D0.4 whole cell extracts

Prior to harvesting, cells were washed with cold PBS and all liquid removed carefully. The cells were scraped with the appropriate amount of D0.4 buffer, collected in a microcentrifugation tube and sonicated for 30 s on ice. The extracts were then centrifuged in a cold centrifuge at 13,000 rpm for 10 min to remove cell debris. The protein concentration was measured as described in section 2.2.15.

D0.4 Buffer

20 mM HEPES, pH 7.5
10% (v/v) glycerol
0.4 M KCl
0.4 % (v/v) Triton X-100
10 mM EGTA
5 mM EDTA
Add fresh 25 mM NaF, 25 mM sodium β-glycerophosphate 1 mM DTT, 1 x Protease Inhibitors, 0.4 mM Pefabloc SC, 20 µg/ml Pepstatin.

2.4 Reagents

2.4.1 Morpholinos

Gene	Morpholino sequence	Position in gene	Reference
Human β-*globin*	CCTCTTACCTCAGTTACAATTTATA	Negative control MO	GeneTools LLC
cvl2 MO1	TTACTGGAGGAGACAGACACAGCAT	+1 to +25	(Rentzsch et al., 2006)
cvl2 MO2	CTA AAT TCG CTC CAG ACG CAC GGG	-25 to -2 in the 5'UTR	(Rentzsch et al., 2006)
cvl2 MO3	CCAAAGTATCCCAAGCCTGTAGAAA	-72 to -48 in the 5'UTR	(Moser et al., 2007)
dlx3b	TTTCCAAGGCAGACCGAAGCAAGTC	-64 to -40 in the 5'UTR	(Solomon and Fritz, 2002)
dlx4b	TCAGACATGAAACTCATAGACATCA	+2 to +26	(Solomon and Fritz, 2002)
bambi-b	CACACACTTTTCCTCTCAGATTCGC	-36 to -11	(Reichert et al., 2013)
p53	GCGCCATTGCTTTGCAAGAATTG	-16 to +7	(Robu et al., 2007)
gdf6a MO1	GCAATACAAACCTTTTCCCTTGTCC	exon1/intron1 boundary	(Sidi et al., 2003)
gdf6a MO2	GAGATCGTCTGCAAGATAAAGAGAA	intron1/exon2 boundary	(French et al., 2009)
bmp6	GCGCTCGTCATATTTACATCCAGTC	-14 to +11	(Reichert et al., 2013)
snw1	ACAGCTTCTCTGCGTCTTACCTTGT	exon1/intron1 boundary	(Wu et al., 2011)

2.4.2 Plasmids

2.4.2.1 For ISH probes

Unless stated, all probes are against zebrafish transcripts.

Construct	Usage	Constructed by/ obtained from	Reference
pExpress-1 bambi-b	linearise with EcoRV, transcribe with T7 RNA polymerase	Source BioScience	Image clone ID 7038842
pGEMT-zBMP2bp	linearise with NotI, transcribe with T7 RNA polymerase	M.C. Ramel	(Wu et al., 2011)
pGEMT bmp6	linearise with NcoI, transcribe with SP6 RNA polymerase	S. Reichert	(Reichert et al., 2013)

pCS2+-zBMP7	linearise with EcoRI, transcribe with T7 RNA polymerase	From A. Lekven	(Schmid et al., 2000)
pCS2+ cvl2	linearise with BamHI, transcribe with T7 RNA polymerase	From M. Hammerschmidt	(Rentzsch et al., 2006)
dlx3b	linearise with SalI, transcribe with T7 RNA polymerase	From Westfield	(Akimenko et al., 1994)
pGEMT eya1	linearise with NotI, transcribe with T7 RNA polymerase	S. Reichert	(Reichert et al., 2013)
pGEMT gdf6a	linearise with NcoI, transcribe with SP6 RNA polymerase	S. Reichert	(Reichert et al., 2013)
pSK-EGFP	linearise with BamHI, transcribe with T7 RNA polymerase	From A. Lekven	
hgg	linearise with NcoI, transcribe with SP6 RNA polymerase	From A. Meng	(Thisse et al., 1994)
pGEMT easy kctd15a	linearise with KspI, transcribe with Sp6 RNA polymerase	From I. Dawid	
pGEMT kctd15b	linearise with SalI, transcribe with T7 RNA polymerase	From I. Dawid	
pBluescriptKS-krox20	linearise with PstI, transcribe with T3 RNA polymerase	From M. Mullins	(Oxtoby and Jowett, 1993)
pGEMT mRFP	linearise with NotI, transcribe with T7 RNA polymerase	M.C. Ramel	(Wu et al., 2011)
myod	linearise with XbaI, transcribe with T7 RNA polymerase	From P. Ingham	(Weinberg et al., 1996)
pCS2+-zNCADHERIN	linearise with XhoI, transcribe with Sp6 RNA polymerase	M.C. Ramel	(Wu et al., 2011)
pGEMT six4.1	linearise with NotI, transcribe with T7 RNA polymerase	S. Reichert	(Reichert et al., 2013)
snai1b	linearise with XbaI, transcribe with T7 RNA polymerase	From P. Scotting	(Thisse et al., 1995)
sox10	linearise with SalI, transcribe with T7 RNA polymerase	From C. Linker	(Dutton et al., 2001)
pMX363-Xl Slug (in pSP72)	linearise with BglI, transcribe with SP6 RNA polymerase	From M. Sarget	(Mayor et al., 1995)

pGEMT Xl sox9	linearise with NotI, transcribe with T7 RNA polymerase	From C. LaBonne	(Spokony et al., 2002)

2.4.2.2 For mRNA synthesis

Construct	Usage	Constructed by/ obtained from	Reference
pCS2+ mCherry H2B	linearise with NotI, transcribe with SP6 RNA polymerase	From S. Woolner	(von Dassow et al, 2009)
pCS2+ GFP	linearise with NotI, transcribe with SP6 RNA polymerase	From P. Blader	Image clone ID 5083691
pCS2+GFP bmp6 Mo binding side	linearise with NotI, transcribe with SP6 RNA polymerase	R.A. Randall	(Reichert et al., 2013)
pCMVSport6 XlSKIP	linearise with ClaI, transcribe with SP6 RNA polymerase	GeneService	
pCS2+ Xl noggin	linearise with NotI, transcribe with SP6 RNA polymerase	From R. Harland	(Smith and Harland, 1992)
pCS2+ Xl dkk1	linearise with NotI, transcribe with SP6 RNA polymerase	From Heasman	(Krupnik et al., 1999)
pFTX4K EGFPC1 SNW1	linearise with XbaI, transcribe with T7 RNA polymerase	S. Reichert	

2.4.2.3 Other constructs and cloning strategy

Construct	Constructed by/obtained from	Reference
pCDNA3 Flag hSNW1	From F. Oswald	
pEF Flag hSNW1 S224A	R.A. Randall	
pCDNA3	Invitrogen	
pCS2+ Flag dlx3b	S. Reichert	(Reichert et al., 2013)
pGL3 basic Flag 5'upstream bambi-b long	S. Reichert	(Reichert et al., 2013)
pGL3 basic Flag 5'upstream bambi-b long mut	R.A. Randall	(Reichert et al., 2013)

The 5' upstream bambi-b region was initially cloned into pGL3 basic using the primers indicated in section 2.4.3.2 by introducing SacI and SmaI binding sites. The Dlx3b binding sites were then mutated by R.A. Randall.

2.4.3 Primers

2.4.3.1 *qRT-PCR primers*

Target	Primer sequence
bambi-b (fwd)	CCCAAAGCACGAACTCTCCT
bambi-b (rev)	GTGCAATCACATGACGGCTG
bmp6 (fwd)	GGCTTCGCATCATGACACTG
bmp6 (rev)	TGGGATCTGGGACAGGTTGA
ef1a (fwd)	TGCTGTGCGTGACATGAGGCAG
ef1a (rev)	CCGCAACCTTTGGAACGGTGT
gdf6a (fwd)	TCAATGCGAGCTTTTTCCGC
gdf6a (rev)	TCTTCGCAAAGGAGAGAGCG
odc (fwd)	ACACTATGACGGCTTGCACCG
odc (rev)	CCCACTGACTGCACGATCTGG
gdf6a (fwd) to test Mo	TCAATGCGAGCTTTTTCCGC
gdf6a (rev) to test Mo	TCTTCGCAAAGGAGAGAGCG
bambi-b (fwd) to test Mo2	GCGATGGCTCTTCTCCTCAC
bambi-b (rev) to test Mo2	TTCAGCTCCGACTTGCACAT
bmp2b (fwd) ex1	TGCGATCTCGCGCTGTCACTT
bmp2b (rev) ex1	CGTCGCAGCTCAAGTCGCCT
bmp2b (fwd) ex1/2	GCGACGACTCTCTGTCGTGGG
bmp2b (rev) ex1/2	AACAGCACCGTGAGAGCGCG
bmp2b (fwd) ex1-int	GACGACGGGAACGCAGACCG
bmp2b (rev) ex1-int	GGCACGCACACGCAGTGATG
bmp2b (fwd) int-ex2	GTTCACTGTGGGCCCTAAAAAGGT
bmp2b (rev) int-ex2	CGGACCACGGCGACCATGAT
bmp2b (fwd) ex2-int	GCCAGCAGAGCAAACACGATACG
bmp2b (rev) ex2-int	CCAAACGGTTGCATCACATCATTCC

bmp2b (fwd) int-ex3	ATCCAGCGCAGGCCAGACCA
bmp2b (rev) int-ex3	TCAGGCTGGACAGTGCCTCGAA
bmp2b (fwd) ex2/3	AGGGCAGCCAGCAGAGCAAA
bmp2b (rev) ex2/3	GCGGAGATCAGCTCCTCGCC
bmp2b (fwd) ex1	AAAGCGGCAGGCTCGACGAG
bmp2b (rev) ex1	GGCGGTGCCACGATCCACTC
dlx3b (fwd) ex1	GATGGGGGCAACACCCGGAG
dlx3b (rev) ex1	TGTGGTGGCGTCTGCAGGTC
dlx3b (fwd) ex3	CCCCCAGCCACCCCTCAGTT
dlx3b (rev) ex3	ATACACGGCCCCCACGCTCT
bmp2b (rev) int1	TCACAACAGACTTGCGGTCGCT
dlx3b (fwd) int1	CGTGACATCTAGCCTACACCGAGC
bmp2b (rev) int2	ACTGCCACTTGGCATTGCGT
dlx3b (fwd) int2	GCGGGCAATGACATTTCAACACA
foxi1 (fwd) ex2	CGAGGACGCGCTTAAATTGG
foxi1 (rev) ex2	TGGAAGTCGGGGAGTTTTGG
gadd45aa (fwd) 5'	CGGTGACAGCCAGAGAAAGA
gadd45aa (rev) 5'	TGCATGTAAAATCCAGAACGGAC
gadd45aa (fwd) 5'	CTGAGAGTTCAGACCGGACG
gadd45aa (rev) 5'	CGTCCTCAGAAAGTCCCACA
rbl2 (fwd) ex8	AGAAGACATCGGCACACCAG
rbl2 (rev) ex8	CATCGAGTTCTGCAGTGGGT
rbl2 (fwd) 3'	TGCTGACCGCGATACCATTT
rbl2 (rev) 3'	GCTCCGTGAAGACTGCTCAA
rbl2 (fwd) int9	ATCTTTGCTCGGGCACTTCA

rbl2 (rev) int9	GGGCCTTCACCTGAGACATT
foxo3b (fwd) ex2	GTGGCCAGTCAACAGCAAAC
foxo3b (rev) ex2	GTCTCTTGTCAGGGGTGCTC
foxo3b (fwd) ex2	GGCTTGGAATCTGTCACCCT
foxo3b (rev) ex2	ACGTCACAATCCAGACTGCC
mdm2 (fwd) ex8	TCGGACAGCTTTTCCCTGAC
mdm2 (rev) ex8	TTTGCATCCGAAGACTCGCT
mdm2 (fwd) ex11	GCTTTCCATCTCCTGCCACT
mdm2 (rev) ex11	GGGTCTCTTCCTGACTGCTG
mat2al (fwd) ex9	ACAGCCTGCTATGGACACTT
mat2al (rev) ex9	AGCACGTCTTCATCTTGAGGG
phlda2 (fwd) ex1	AGCTCAAGCTGCAGTCCATT
phlda2 (rev) ex1	TCTTCTCGTCCGAGCACCTA
rasl11b (fwd) 5'	TTGCTTTTACGGCGTCTGTG
rasl11b (rev) 5'	GCTCGGGTACTCCGCAATAG
rasl11b (fwd) 3'	AGGAGCAGATCTCCAGAGCA
rasl11b (rev) 3'	ATCAGAGGTCAGGTTTCGGG
dem1 (fwd) ex6	CCTACTGGACGGGACAGAGA
dem1 (rev) ex6	GAATGAGCCGCTTGTTGGTC
p21 (fwd) ex1	TCCCGAAAACACCAGAACGA
p21 (fwd) ex1	GTTGGTCTGTTTGCGCTTCA
ccng1 (fwd) ex3	TCAGGATCAGCCAGAATCGC
ccng1 (rev) ex3	AAGTGAAGAGCAGTCGGAGC
sesn3 (fwd) ex1	GACCAACACACCGTCTGTGA
sesn3 (rev) ex1	TCGTGTTTCGGCAGTGGTTA

sesn3 (fwd) 3'	AGAATTGTGGGTGAGCAGTCA
sesn3 (rev) 3'	TCAGGCCAAGTCCAAGGAT
sesn3 (fwd) int9	GGTGCCCGTTATGCTTGTTT
sesn3 (rev) int9	CTGCTTGTGAAGCCCTGTTG
rps6ka3a (fwd) ex17	TGATGGCCGATCAGTGTACC
rps6ka3a (rev) ex17	AGCGCTTGCTTCTCTCTCAG
rps6ka3a (fwd) 3'	GCAGCCACTTATTCAGCCCT
rps6ka3a (rev) 3'	CAGCTTTTTGAGACCACGGC
rps6ka3a (fwd) 5'	TCCGCGATTGAATTACGGGT
rps6ka3a (rev) 5'	TTTAACTTACGGTCGCCCCG
lnx1 (fwd) ex2	AGTGATCAAGAAGAGGCGGG
lnx1 (rev) ex2	TGTGGCAGAGATCAGGAGGA
lnx1 (fwd) ex2	CACTAACCCCACACTAGGGG
lnx1 (rev) ex2	GCTCCCGAAGTGCAGTCTTT

2.4.3.2 Primers for cloning

Construct	Primer sequence	Comments
GFP-Snw1 (fwd)	CCGGGTCGACGATGGCGCTAGCCAGTTTTTTG	insertion of SalI restriction site for cloning into pFTX4K EGFPC1
GFP-Snw1 (rev)	CCGGACTAGTTCACTCCTTCCTGCGCTTCTTCATATC	insertion of SpeI restriction site for cloning into pFTX4K EGFPC1
Flag-Dlx3b (fwd)	CCGGGAATTCTTAATACACGGCCCCCACGCTCTGCGG	N-terminal Flag-tag, pCS2+
Flag-Dlx3b (rev)	CCGGGGATCCATGAAGGACTACAAGGACGACGATGACAAGGCCATGAGTGGACCGACATATGACAGGAAGATAC	N-terminal Flag-tag, pCS2+
Flag-Bambi-b (fwd)	CCGGGGATCCATGCAGCGGAACAGCAGTCTCG	C-terminal Flag-tag, pCS2+
Flag-Bambi-b (rev)	CCGGGAATTCTCAGGCCTTGTCATCGTCGTCCTTGTAGTCCTTCACAAACTCCAGCTTTCCTCGGTTGCTGTAC	C-terminal Flag-tag, pCS2+

Bambi-b 5' (fwd)	CCGGGAGCTCGCTTTTCTATACCGTG ACTCA	For cloning a 1800 bp fragment of the Bambi-b 5' upstream region containing two Dlx3b binding site
Bambi-b 5' (rev)	CCGGCCCGGGACACTTTTCCTCTCAG ATTCGC	For cloning a 1800 bp fragment of the Bambi-b 5' upstream region containing two Dlx3b binding site
Bambi-b (fwd)	TAATACGACTCACTATAGGG	ISH probe, pGEMT
Bambi-b (rev)	GGATCCATTAACCCTCACTAAAGGGAA GTTTCGCTCCGGAATTCCCGGG	ISH probe, pGEMT
Bmp6 (fwd)	GTGGAGCTGTTGTTTGGCAG	ISH probe, pGEMT
Bmp6 (rev)	ATGAGCCGGTCCCTTTGATG	ISH probe, pGEMT
Eya1 (fwd)	GCCGAGTAAGTGGAAGCAGT	ISH probe, pGEMT
Eya1 (rev)	CCCGACGCAATCGATCTGAA	ISH probe, pGEMT
Gdf6 (fwd)	CGAGTTTCGTGGACAAGGGA	ISH probe, pGEMT
Gdf6 (rev)	GAGTTTTGTGGGGACGCAAC	ISH probe, pGEMT
Six4.1 (fwd)	GCCAAGAGGACTTGTCACCA	ISH probe, pGEMT
Six4.1 (rev)	ACATCGGAGTTGGAGAGGGT	ISH probe, pGEMT

2.4.3.3 Primers for Bambi-b bandshift probes

Construct	Primer sequence	Comments
Bambi-b probe1 (fwd)	GACGAAAATGTTACTAAAGGT	Primer to generate bandshift probe 1
Bambi-b probe1 (rev)	CGAAAATACTGTCCACGATGAC	Primer to generate bandshift probe 1
Bambi-b probe2 (fwd)	CTTTTGCTTGGCCCACATGC	Primer to generate bandshift probe 2
Bambi-b probe2 (fwd)	AAGCCAGACTAGGTCCAATCA	Primer to generate bandshift probe 2

2.4.4 Antibodies

2.4.4.1 Primary antibodies

Antibody	Company	Catalogue number
Actin	Sigma	A3853
Cdcl5	abcam	ab129114
zBmp2	AnaSpec	55708
Bmp2	abcam	ab17885
Dhx8	abcam	ab70588

Flag	Sigma	F7425
Flag-HRP	Sigma	A8592
GFP	Roche	11814460001
HA-HRP	Roche	12013819001
Helic2	Santa Cruz	sc-68563
Mcm6	Santa Cruz	sc-9843
NcoA62 (Snw1)	Bethyl Laboratories	A300-785A
Prpf8	abcam	ab157114
Ski	Santa Cruz	sc-9140
PSmad1/5	Cell signaling Technology	9511L
Smad5	GeneTex	GTX124559
Snw1	Santa Cruz	sc-30139
Tubulin	Roche	ab6160
Xab2	abcam	ab57515

2.4.4.2 Secondary antibodies

Antibody	Company	Catalogue number
rabbit-HRP	DakoCytomation	P0448
mouse-HRP	DakoCytomation	P0450
goat-HRP	DakoCytomation	P0049
DNP-HRP	PerkinElmer	FP1129
Dig-HRP	JacksonImmunoResearch	200-032-156
Dig-AP	Roche	12486523
Alexa Fluo 488	invitrogen	A11008

Chapter 3. A BMP regulatory network controlling ectodermal cell fate decisions at the neural plate border

3.1 Introduction

Embryonic development requires the tight control of a combination of signalling pathways in order to convey the temporal and spatial information that is necessary for processes such as organ patterning and organ size control. An example of this is the patterning of the ectoderm in the early vertebrate embryo that gives rise to progenitor cells such as the NC and the PPE. Extensive research has given insight into which signalling pathways and transcription factors are required for this process. However, the timing and localisation of the signalling output of pathways, such as BMP signalling, is not well understood.

To study BMP signalling during development our lab generated a transgenic BRE-mRFP zebrafish line (*Tg(BRE:mRFP)*) that expresses monomeric red fluorescent protein (mRFP) under the control of a well-characterised BMP responsive element from the mouse *Id1* enhancer (Ramel and Hill, 2013). Here I explore BMP signalling dynamics during ectodermal patterning in the developing zebrafish embryo and develop a new 2-step model outlining differential BMP activity requirements for different tissues during and after gastrulation. I also give mechanistic insight into the intricate spatio-temporal regulation of BMP activity during this process.

3.2 Results

3.2.1 Distinct domains of BMP activity at the NPB

To investigate the dynamic temporal and spatial regulation of BMP signalling during ectodermal patterning that leads to the specification of distinct progenitor cells at the NPB I used the *Tg(BRE:mRFP)* transgenic zebrafish line (Ramel and Hill, 2013, Wu et al., 2011). At early developmental stages the fluorescence generated in response to BMP signalling is too weak to be detected, which is why I used ISH for the *mRFP* mRNA as a dynamic readout for pathway activity.

ISH performed at different developmental stages revealed a very dynamic nature of BMP activity during gastrula and neurula stages. During gastrulation (80% epiboly) I detected a clear ventral to dorsal gradient as has been previously reported (Ramel and Hill, 2013) (Figure 3.1.A).

As morphogenetic movements shape the embryo, cells converge to the dorsal side and this gradient is lost. By the onset of somitogenesis the gradient

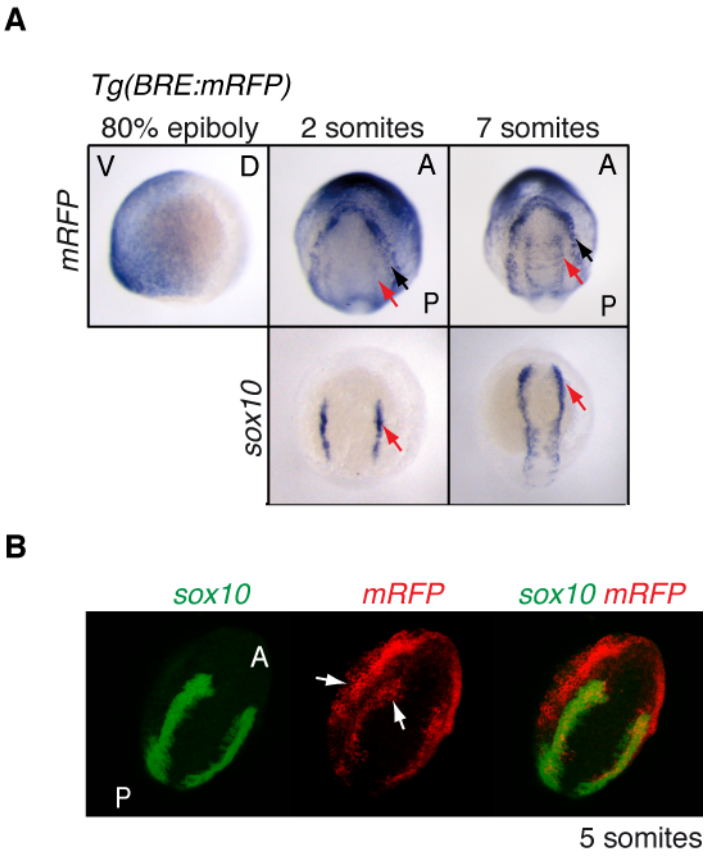

Figure 3.1 Dynamic domains of BMP activity during ectodermal patterning

(A) *ISH for mRFP in Tg(BRE:mRFP) embryos. A clear ventral to dorsal gradient is detected at 80% epiboly (lateral view, ventral to the left). During somitogenesis stages an outer horseshoe-shaped domain of BMP activity is visible at the NPB and an inner domain that resembles the neural crest domain. Depicted is a dorsal view with anterior to the top. In the lower panel ISH for sox10 on embryos at the respective stages in the same orientation as above is shown. The black arrow indicates the outer domain whereas the red arrow marks the inner NC domain.*
(B) *DFISH using probes against mRFP (Fast Blue, red) and sox10 (Fluorescein-TSA, green). The white arrow indicates the two distinct domains of BMP activity. Dorsal view with anterior to the top.*

reshapes into a distinct horseshoe-shaped domain of BMP activity at the neural plate border, which then further evolves into a distinct inner and an outer domain. I noticed that the inner domain resembles the pattern of the NC population, which can be visualised using ISH against NC markers such as *sox10* (Figure 3.1.A). To verify this, I performed DFISH using probes directed against *mRFP* and *sox10,* revealing that indeed the inner BMP activity domain coincides with the NC cell populations (Figure 3.1B).

Prior to the generation of this zebrafish line immunofluorescence staining for nuclear PSmad1/5 was primarily used to detect localised BMP activity. To compare the sensitivity of ISH against *mRFP* and to substantiate my results, I performed immunostaining for PSmad1/5 on 80% epiboly and 5 somite stage embryos (Figure 3.2). At 80% epiboly I could detect a ventral to dorsal BMP gradient as described above. At the 5-somite stage, nuclear PSmad1/5 was present at the neural plate border confirming the results using *Tg(BRE:mRFP)* embryos. The inner NC domain of BMP activity, however, could not be detected, suggesting that ISH against *mRFP* on *Tg(BRE:mRFP)* is a more sensitive readout for BMP pathway activity during zebrafish development.

Next I wanted to investigate the precise requirements for BMP signalling during NC induction and specification. For that purpose I made use of a transgenic zebrafish line that expresses GFP-tagged dominant negative BMP type I receptor (dnBMPR1a) in response to heat-shock (*Tg(hsp70l:dnXla.Bmpr1a-GFP)*) (Pyati et al., 2006). This enabled me to perturb BMP activity at specific critical developmental stages around 1.5 hours after the initial heat-shock (Hashiguchi and Mullins, 2013). The robust inhibition of BMP activity was confirmed by loss of PSmad1/5 in embryos expressing GFP-dnBMPR1a (Figure 3.3.A).

Early inhibition of BMP signalling initiated at 30% epiboly, when the BMP gradient is first established (Ramel and Hill, 2013), resulted in a loss of ventral tissues, an expansion of the neuroectoderm (shown by the hindbrain rhombomere 3 and 5 marker *krox20)* as well as NC, demonstrating the requirement of the BMP signalling gradient for the initial ventral to dorsal patterning.

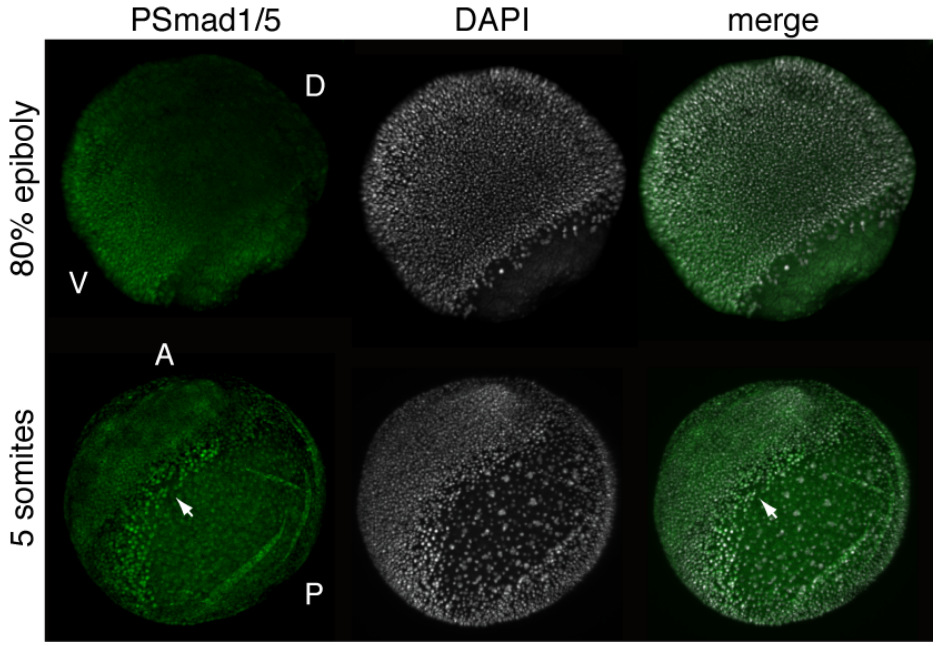

Figure 3.2 PSmad1/5 staining detects the strong outer domain of BMP signalling at the 5 somite stage
Immunofluorescence staining using an antibody against PSmad1/5 at the two developmental stages indicated. Nuclei were visualised using DAPI Lateral view of 80% epiboly stage embryos with ventral to the left. The embryo at 5 somites was mounted to centre the NPB. Anterior is to the top, dorsal to the left.

In contrast, embryos that were heat-shocked at early gastrula stages (60% epiboly) displayed only a slight expansion of the *krox20* expression domain, demonstrating that by 70-80% epiboly DV specification is mostly completed. Expression of *sox10,* however, was reduced indicating that BMP signalling is necessary during NC induction. Most importantly, inhibition of BMP signalling from early somitogenesis onwards also led to a decrease in *sox10* expression, demonstrating a requirement for BMP activity in the maintenance of the NC cell population and the importance of the inner BMP signalling domain detected in *Tg(BRE:mRFP)* embryos.

Interestingly, the induction of dnBMPR1a expression in *Tg(hsp70l:dnXla.Bmpr1a-GFP)* x *Tg(BRE:mRFP)* embryos at bud stage also resulted in a reduction of the *mRFP* staining at the three somite stage (Figure 3.4), arguing for a short half-life of the *mRFP* mRNA, and justifying *mRFP* ISH as a dynamic readout of BMP activity. This is also supported by the observation that during the establishment of the early BMP activity gradient *mRFP* transcripts are

cleared with 20 min of the gradient detection by PSmad1/5 immunostaining (Ramel and Hill, 2013). The staining for *mRFP* is not completely lost as crossing the two transgenic backgrounds leads to a reduced copy number of both transgenes. Thus BMP signalling is not as efficiently blocked compared with *Tg(hsp70l:dnXla.Bmpr1a-GFP)* incrosses.

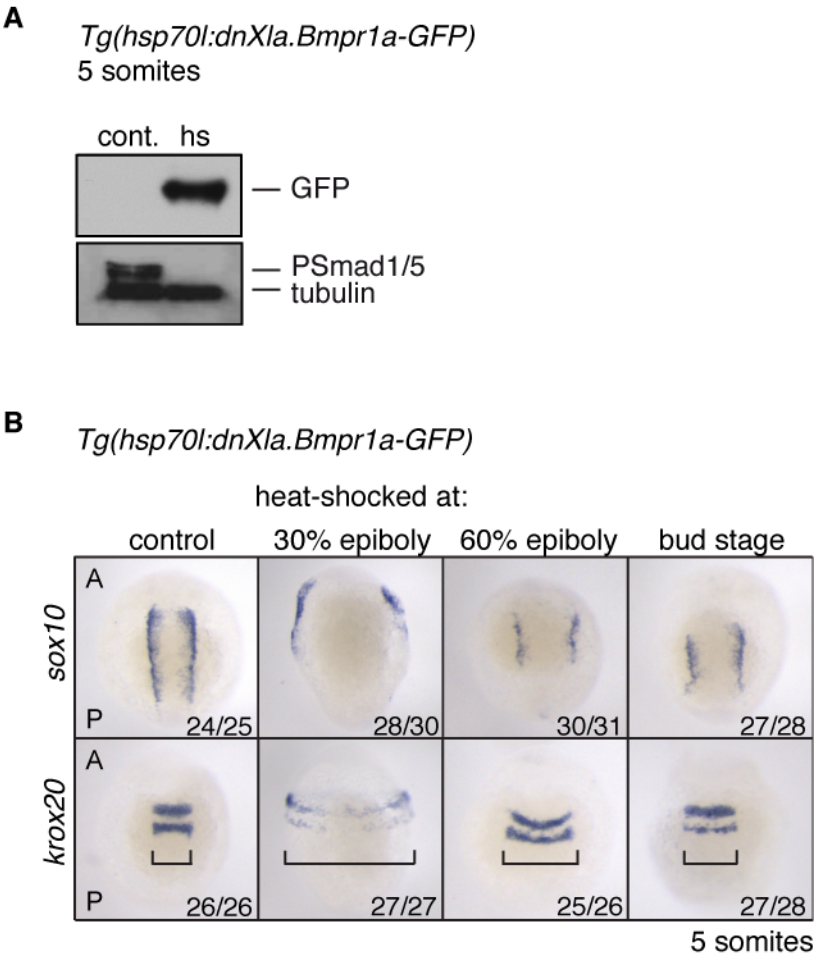

Figure 3.3 BMP activity is required for NC development at several embryonic stages

(A) *Western blot analysis of 5 somite stage Tg(hsp70l:dnXla.Bmpr1a-GFP) embryos heat-shocked at bud stage confirms the loss of PSmad1/5.*

(B) *sox10 and krox20 ISH on Tg(hsp70l:dnXla.Bmpr1a-GFP) embryos heat-shocked at indicated stages. Brackets indicate the width of the neural ectoderm marked by krox20. Numbers indicate the embryos with the observed phenotype for a representative experiment.*

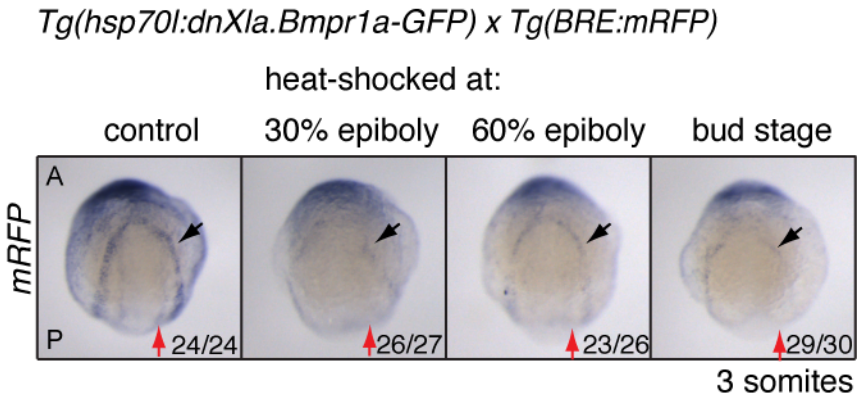

Figure 3.4 *mRFP* has a short half-life

ISH for mRFP on Tg(hsp70l:dnXla.Bmpr1a-GFP) x Tg(BRE:mRFP) embryos, heat-shocked at indicated stages, demonstrates inhibition of BMP signalling. Black arrows indicate outer domains and red arrows indicate inner domains of BMP activity. Note the inhibition of BMP signalling as read out by mRFP expression shown here is not as strong as in Figure 3.3, as the embryos from the Tg(hsp70l:dnXla.Bmpr1a-GFP) x Tg(BRE:mRFP) cross have less copies of the dnBMPR1a compared with the incrosses used in Figure 3.3. Numbers indicate the embryos with the observed phenotype for a representative experiment.

The BMP ligands *bmp2b* and *bmp7a* are expressed at the NPB and have been implicated in NC induction in several organisms (reviewed in (Stuhlmiller and Garcia-Castro, 2012a)). However, neither *bmp2b* nor *bmp7a* mRNA were detected in the inner domain of BMP activity during NC maintenance, suggesting the involvement of alternative ligands (Figure 3.5A).

BMP6, BMP7, GDF5 and GDF6 can all induce differentiation of rat cortical neural stem cells into various NC lineages (Gajavelli et al., 2004). To examine a possible function for these ligands *in vivo* in NC development, I assessed their temporal and spatial expression patterns at different developmental stages. *gdf5* is only expressed from 40 hpf onwards (Bruneau et al., 1997), and was therefore not further investigated. In contrast, *bmp6* and *gdf6a* were both detected by qRT-PCR at the end of gastrulation (bud stage) (Figure 3.5E), when the horseshoe-shaped domain of BMP activity at the NPB is first formed. To confirm the presence of these ligands during somitogenesis, I cloned ~1000 bp cDNA fragments to generate RNA probes and performed ISH on embryos after gastrulation. *bmp6* is expressed at the border with the epidermis after the end of gastrulation (Figure 3.5B), with an expression pattern similar to the outer domain of BMP activity. *gdf6a*, on the other

hand, is expressed in the NC and the anterior NPB at the 6 somite stage, as confirmed by DFISH using probes against *sox10* and *gdf6a* (Figure 3.5C and D). Thus, *bmp6* and *gdf6a* are likely candidates to be involved in the localised regulation of BMP signalling at the NPB after gastrulation.

To test this hypothesis, I knocked down *bmp6* and *gdf6a* using a morpholino (MO) approach. *bmp6* morphants displayed no reduction in *sox10* staining and *mRFP* expression was not inhibited, indicating that Bmp6 activity is not essential for formation of the outer horseshoe-shaped domain of BMP signalling (Figure 3.6A). To test whether this is due to an inability of the *bmp6* MO to block Bmp6 expression, I tested the MO efficiency *in vitro*. For this purpose Becky Randall in the lab cloned the morpholino binding site from the *bmp6* transcript in front of GFP. I then tested whether GFP expression could be blocked in a rabbit reticulocyte *in vitro* translation assay. Indeed, increasing amounts of the *bmp6* MO were able to efficiently inhibit GFP expression (Figure 3.6B). Thus the lack of phenotype is likely not to be due to a lack of knockdown efficiency

In contrast, injection of two distinct splice blocking *gdf6a* MOs (Sidi et al., 2003) (French et al., 2009) resulted in loss of BMP activity in the inner NC domain and drastically reduced the number of *sox10* positive cells (Figure 3.6C). As both morpholinos prevent splicing of the *gdf6a* transcript, I could confirm the knockdown efficiency by qRT-PCR using intron spanning primers (Figure 3.6D).

Taken together, these data provide direct evidence for the remodelling of the BMP gradient after gastrulation. Two distinct domains of BMP activity are formed at the NPB. The inner domain of BMP signalling, which corresponds to the NC, requires the BMP/GDF ligand, Gdf6a, which in turn is essential for NC development.

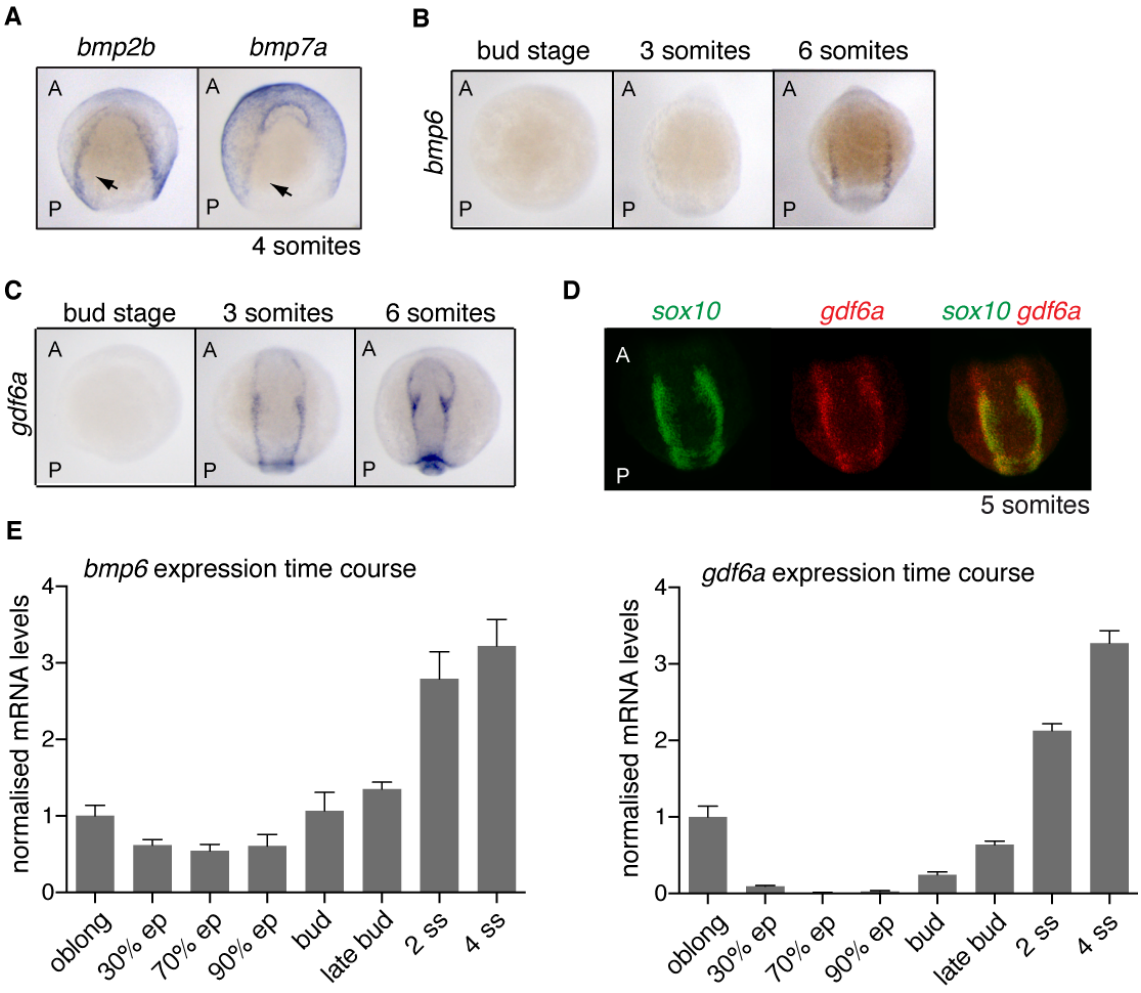

Figure 3.5 Ligands required for the BMP signalling domains at the NPB

(A) *ISH for bmp2b and bmp7a. The black arrow indicates the position of the neural crest at this developmental stage.*
(B) *ISH for bmp6 at indicated developmental stages.*
(C) *ISH for gdf6a at indicated developmental stages.*
(D) *DFISH for sox10 (NC, green) and gdf6a (red) shows expression of gdf6a in the NC cell population.*
(E) *qRT-PCR time course assessing the expression profiles of bmp6 and gdf6a during early zebrafish development at the indicated stages. mRNA levels were normalised to ODC expression.*

Embryos are dorsal anterior view with anterior to the top.

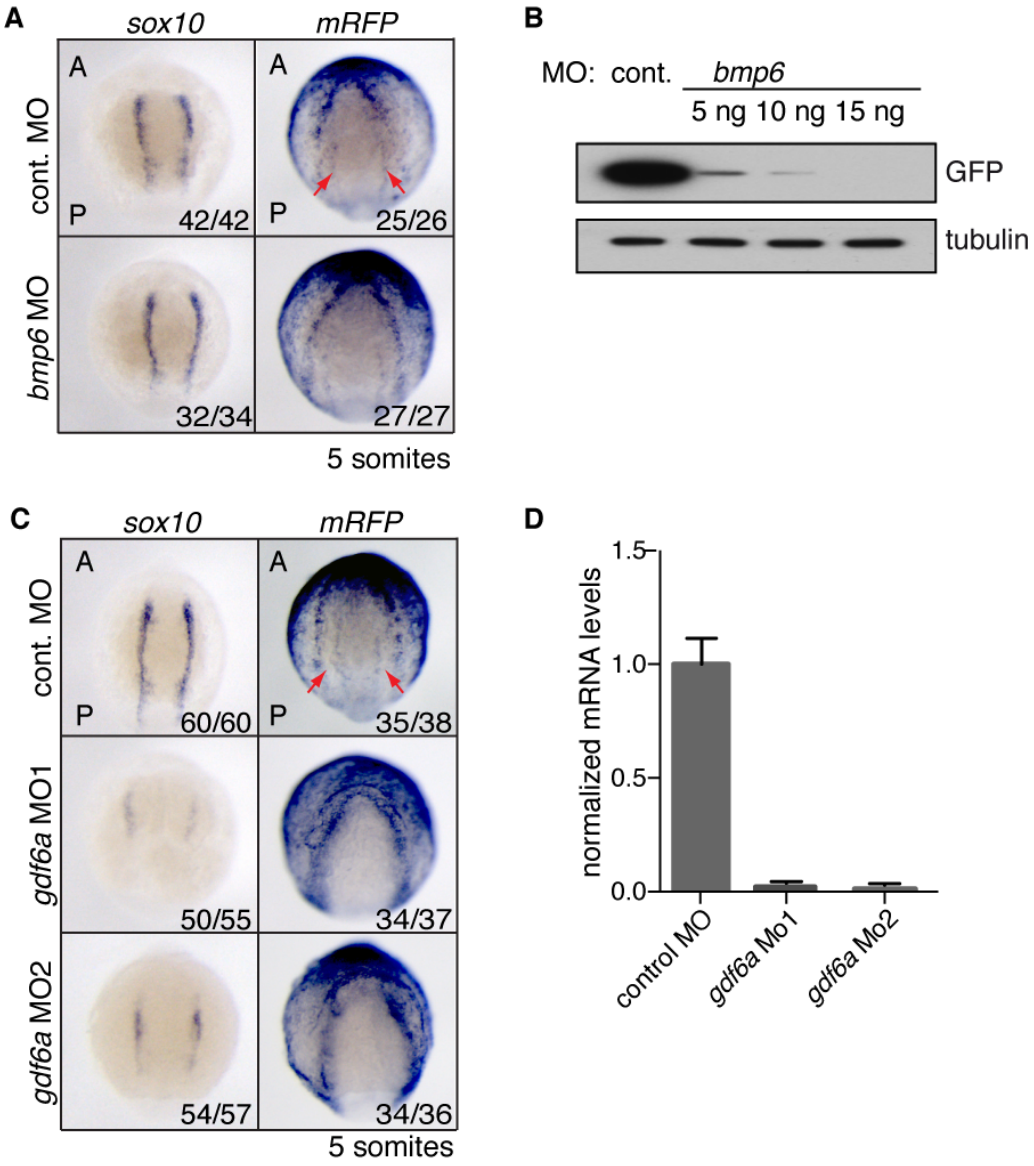

Figure 3.6 *gdf6* but not *bmp6* is essential for BMP activity at the NPB

(A) *Wild type or Tg(BRE:mRFP) embryos were injected with 10 ng of bmp6 MO and stained for sox10 or mRFP. Red arrows indicate the inner domain of BMP signalling as visualised by mRFP.*
(B) *Rabbit reticulocyte in vitro translation assay to test bmp6 MO efficiency. The amounts (ng) of MO indicated have been adjusted to correspond to the amounts generally injected into embryos scaling the input proportional to reaction volume.*
(C) *Wild type or Tg(BRE:mRFP) embryos were injected with 10 ng of the indicated MO and stained for sox10 or mRFP. Red arrows indicate the inner domain of BMP signalling*
(D) *qRT-PCR to confirm MO efficiency using intron spanning primers. gdf6a mRNA levels were normalised to ef1α mRNA expression levels.*

Numbers indicate the embryos with the observed phenotype for a representative experiment.

3.2.2 *cvl2* expression coincides with BMP activity domains

As mentioned above, both Bmp2b and Bmp7a are required for normal NC induction (reviewed in (Stuhlmiller and Garcia-Castro, 2012a)) at the NPB and null mutants of both ligands, *swirl* (*bmp2b*) and *snailhouse* (*bmp7a*), display defects in the ectodermal patterning and hence specification of the NC domain (Nguyen et al., 1998, Schmid et al., 2000). ISH analysis of *bmp2b* and *bmp7a* mRNA indicates their presence at the NPB. However, both ligands are expressed in the entire non-neural ectoderm, whereas BMP activity is tightly restricted to the NPB, where the NC is located (Figure 3.5A, Figure 3.7A). This suggests that a mechanism exists to "concentrate" the activity of these ligands at the NPB by the onset of somitogenesis.

To determine spatial regulators that might promote localised BMP signalling, I reviewed the expression of known BMP modulators, and identified the secreted BMP binding factor Crossveinless2 (Cvl2) as a possible candidate. Cvl2 is a known positive regulator of BMP signalling during zebrafish gastrulation (Rentzsch et al., 2006, Conley et al., 2000). Functionally, Cvl2 is thought to enhance BMP activity predominantly by increasing the availability of BMP proteins for receptor activation (Rentzsch et al., 2006, Serpe et al., 2008).

The expression pattern of *cvl2* overlaps with domains of BMP activity in a ventral to dorsal gradient during epiboly stages (Figure 3.7B) (Rentzsch et al., 2006). Similarly, ISH revealed that *cvl2* mRNA is detected in an outer horseshoe-shaped domain and an inner NC-like domain during somitogenesis (Figure 3.7A and B), very reminiscent of the pattern of BMP activity described above. I confirmed that *cvl2* was expressed in the horseshoe-shaped BMP signalling domain by performing DFISH using probes against *mRFP* and *cvl2* (Figure 3.7C). In addition, DFISH showed that the inner *cvl2* expression territory is localised to the NC (Figure 3.7D).

These findings demonstrate that *cvl2* expression overlaps with domains of BMP activity during ectodermal patterning. Given the described function of Cvl2, this suggests that Cvl2 may stabilise domains of BMP signalling by concentrating ligands at the receptors at early somitogenesis stages. As a result, despite the broad expression of *bmp2b* and *bmp7a*, BMP signalling would only be active in a discrete domain at the NPB.

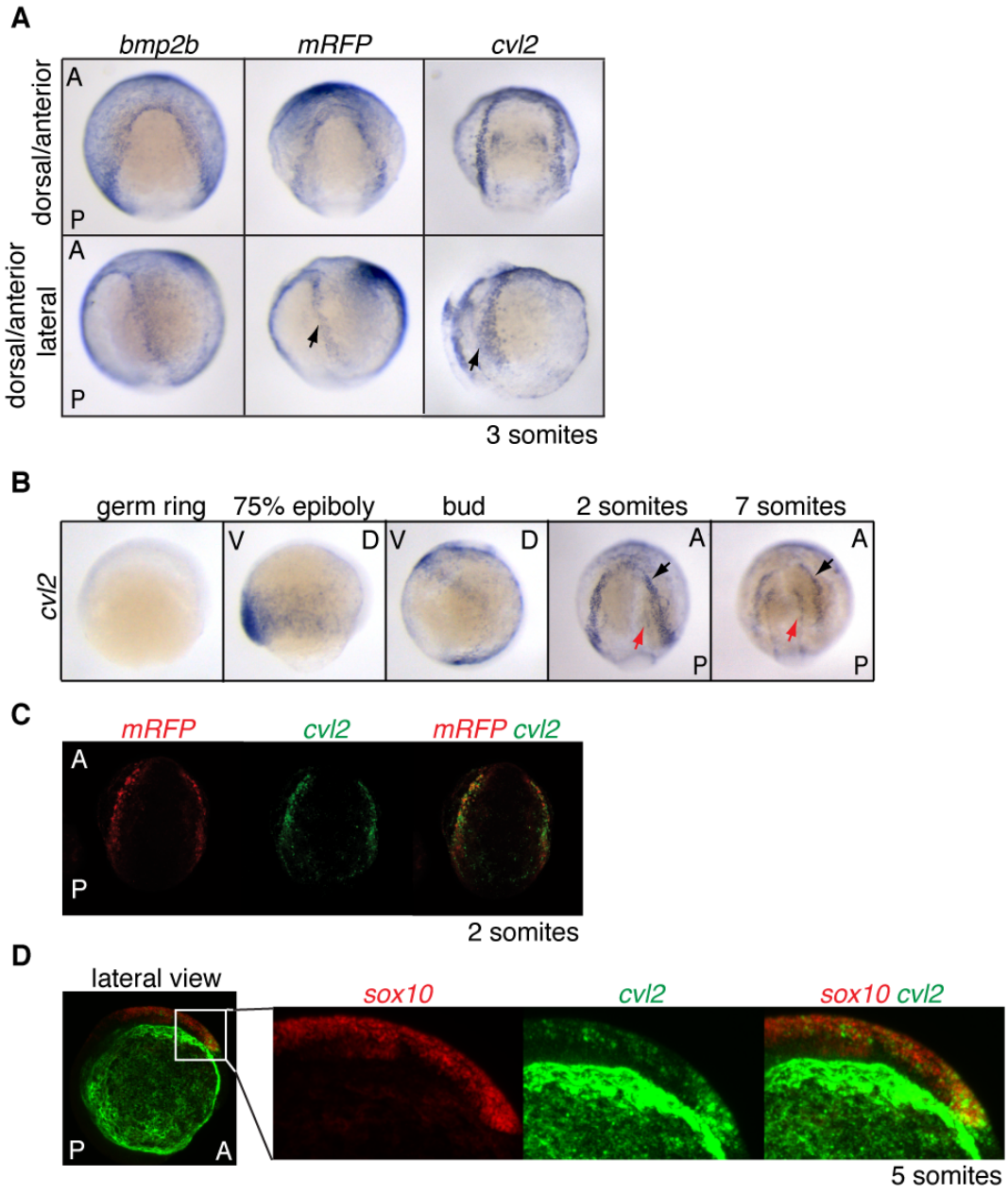

Figure 3.7 *cvl2* co-localises with domains of active BMP signalling and NC

(A) *ISH for bmp2b, mRFP and cvl2. Upper panels: dorsal anterior view; lower panels: the same embryo turned 45° to the left. Black arrows mark the sharp expression domain of mRFP and cvl2 at the NPB.*

(B) *Time course of cvl2 expression. Arrows indicate the two domains of cvl2 expression.*

(C) *DFISH reveals co-localisation of mRFP (red) and cvl2 (green) at the NPB, dorsal anterior view.*

(D) *DFISH for sox10 (red) and cvl2 (green). Strong green staining reveals the outer domain of cvl2 expression (white arrow). Weaker green staining is visible in the NC (sox10) (red arrow).*

3.2.3 cvl2 is required for localised BMP activity and NC development

The presence of *cvl2* in the NC suggested a role for Cvl2 in BMP-dependent NC development. I therefore carried out loss-of-function experiments using a translation-blocking MO against *cvl2* (Rentzsch et al., 2006). At both doses of the MO used, I observed a dramatic loss of *mRFP* expression in *Tg(BRE:mRFP)* embryos, as well as reduced levels of PSmad1/5 and loss of NC markers *sox10* and *snai1b* (Figure 3.8A, B and C). Importantly, these effects were not due to an

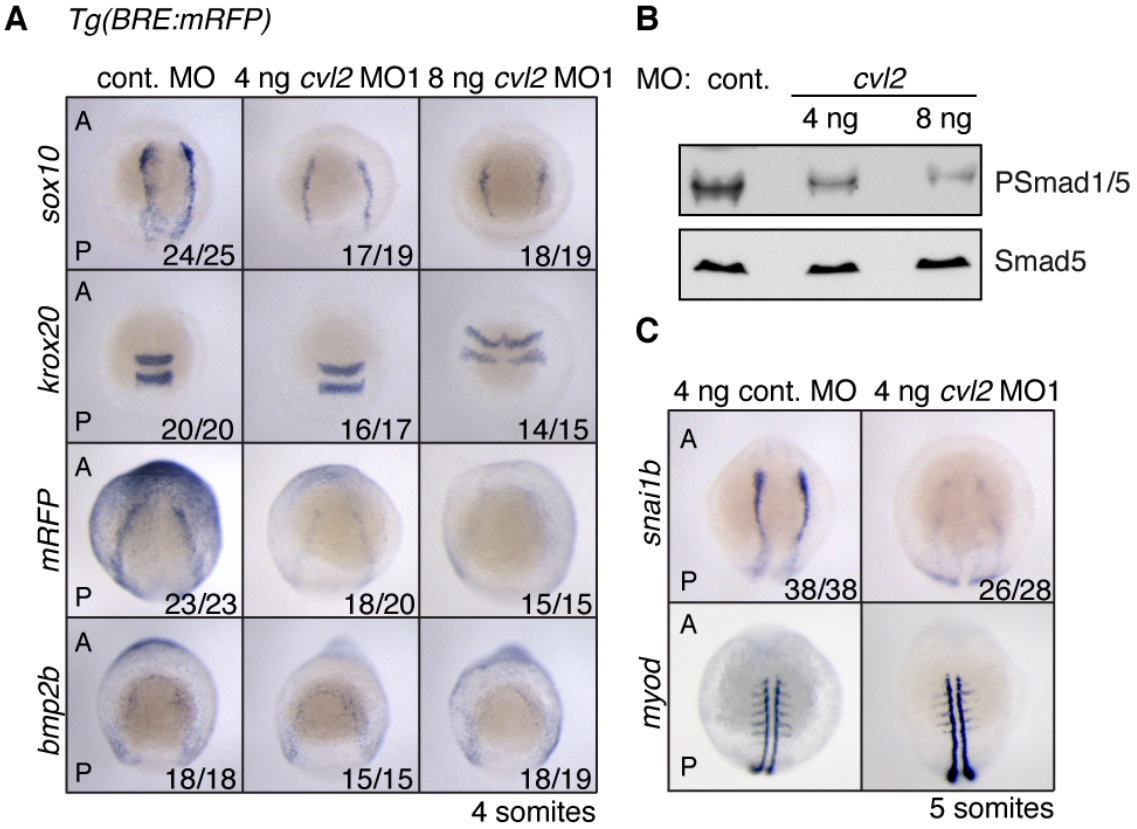

Figure 3.8 cvl2 is required for NC induction

(A) *ISH on Tg(BRE:mRFP) embryos injected with either 4 ng or 8 ng of cvl2 MO1. Dorsal anterior views, with anterior to the top.*
(B) *Western blot analysis showing dose-dependent reduction of PSmad1/5 levels in the 80% epiboly cvl2 morphants. Smad5 is used as the loading control.*
(C) *ISH analysis of control embryos and cvl2 morphants using probes against the neural crest marker snai1b and the myogenic marker myod.*
Dorsal anterior views, anterior to the top.

Numbers indicate the embryos with the observed phenotype for a representative experiment.

early defect in DV patterning (Rentzsch et al., 2006), as the *krox20* expression domain was not substantially ventrally expanded at the 4 ng dose of MO (Figure 3.8A). Interestingly, expression of the *bmp2b* ligand was unaffected by Cvl2 knockdown, supporting a role for Cvl2 at the level of Bmp2b protein (Figure 3.8A). To ensure that the observed loss of NC markers was not a result of a developmental delay, I performed ISH for *myod* on 5 somite stage embryos injected with either control or *cvl2* MO. *myod* is a marker for satellite cells during muscle development (Koishi et al., 1995) and can therefore be used to visualise and compare the number of somites in control and morphant embryos. The analysis shows that the embryos were assayed at the same somite stage ruling out that the phenotypes observed are due to a developmental delay of the morphants Figure 3.8C).

To substantiate my data and to exclude that the observed phenotype is due to off target effects of the morpholino initially used, which potentially could result in

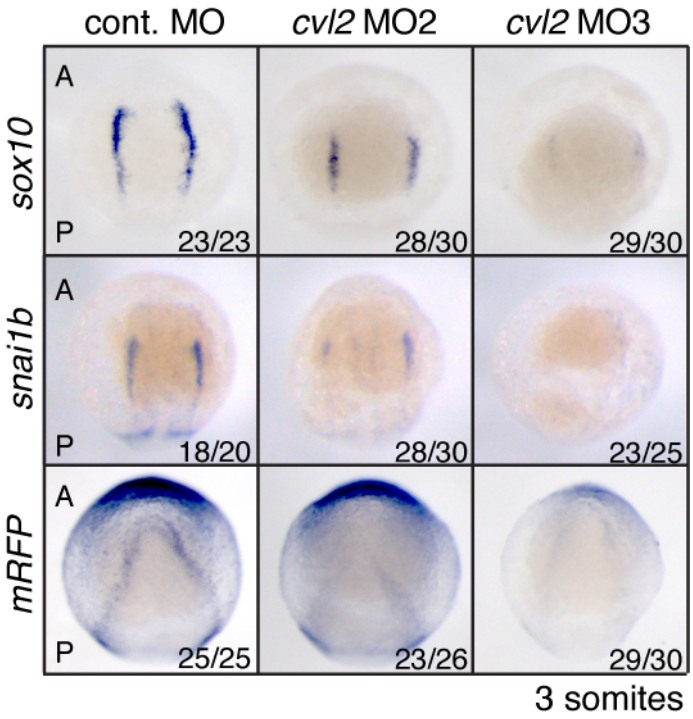

Figure 3.9 *cvl2* regulates NC development
ISH on Tg(BRE:mRFP) embryos injected with 4 ng control or 4 ng of the indicated cvl2 MO using probes again the NC markers sox10 and snai1b or mRFP.

Numbers indicate embryos with the observed phenotype for a representative experiment.

a loss of the NC cell population, I decided to corroborate the data using two additional, independent MO against *cvl2* (*cvl2* MO2 and MO3). Injection of 4 ng of either MO phenocopied the effects of *cvl2* MO on the expression of NC cell markers as well as BMP activity (Figure 3.9). Similarly, I assayed *cvl2* morphants at later times for NC derivatives. Alcian blue staining on 5-day-old embryos revealed the malformation of craniofacial cartilage confirming inhibition of NC development (Figure 3.10A and B). In order to prevent apoptotic effects a *p53* MO was coinjected. However, there seemed to be extensive cell death occurring in the *cvl2* MO1 injected embryos indicated by the much smaller head and eye size (Figure 3.10A). This might contribute to the radical loss of craniofacial cartilage in these *cvl2* morphants. The pigmentation of the embryos was not substantially perturbed (data not shown).

In various systems *cvl2* is regulated in a positive feedback loop and its expression depends on BMP signalling (Ramel and Hill, 2012). To test whether that holds true in our experimental setup I inhibited BMP signalling using the *Tg(hsp70l:dnXla.Bmpr1a-GFP)* transgenic line and confirmed that indeed *cvl2* mRNA levels were dramatically reduced in treated embryos (Figure 3.9A).

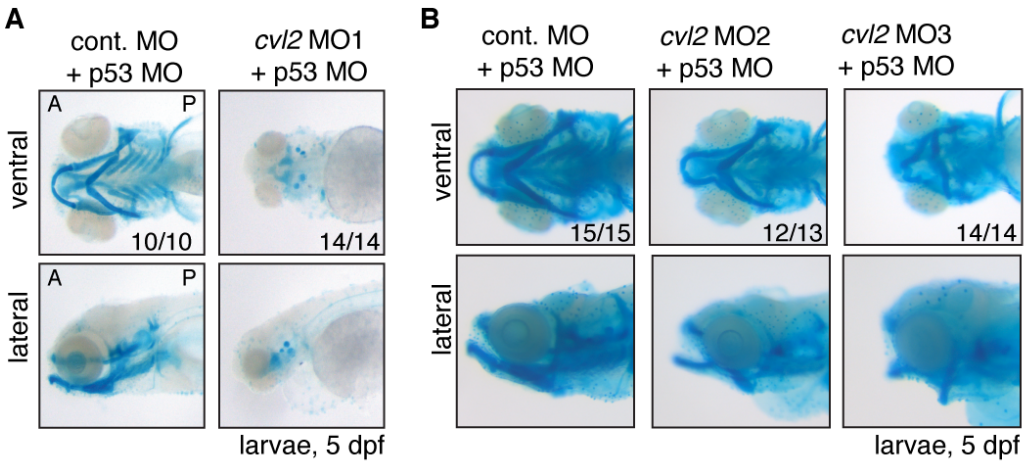

Figure 3.10 *cvl2* is required for NC development
(A) *Alcian blue cartilage staining of 5-day old zebrafish larvae, injected with 2 ng p53 morpholino (Robu et al., 2007) and either 4 ng control or 4 ng cvl2 MO.*
(B) *Alcian blue cartilage staining as described above using cvl2 MO2 and MO3.*
Numbers indicate embryos with the observed phenotype for a representative experiment.

Thus, the data demonstrates a requirement for Cvl2 in NC formation, presumably by focusing BMP signalling activity into distinct domains at the NPB. In this process Cvl2 and BMP signalling are likely to act in a positive feedback loop thereby stabilising distinct BMP activity domains.

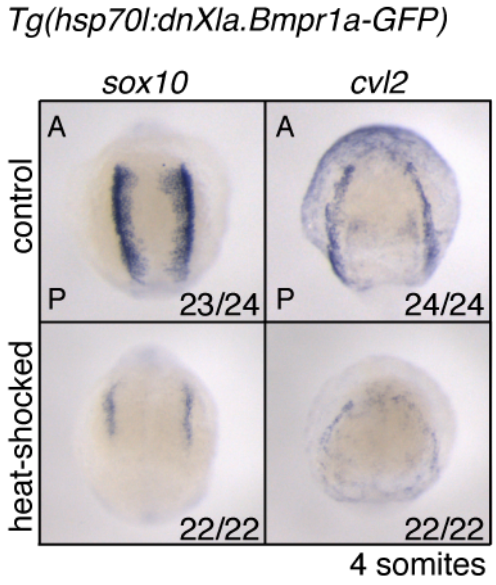

Figure 3.11 BMP signalling regulates *cvl2* expression
ISH of Tg(hsp70l:dnXla.Bmpr1a- GFP) embryos heat-shocked at bud stage using probes against sox10 and cvl2.
Numbers indicate embryos with the observed phenotype for a representative experiment.

3.2.4 Temporal and spatial analysis of the formation of distinct BMP signalling domains

Ectodermal patterning requires discrete levels of BMP signalling for the induction of cell fates such as the PPE and NC at the NPB. NC development depends on BMP activity during induction and specification (Figure 3.3B) whereas specification of the PPE requires complete inhibition of BMP activity after gastrulation (Kwon et al., 2010). This inhibition of BMP signalling has previously been postulated to be mediated by an antagonistic role of Cvl2 on BMP signalling (Esterberg and Fritz, 2009). That study suggested that the functionally-redundant Distalless transcription factors Dlx3b/4b, which are considered to be PPE markers, activate the expression of *cvl2* in the PPE. In contrast, our data points to Cvl2 being a positive regulator of BMP activity during ectodermal patterning (Figure 3.8A and B, Figure 3.9B). In addition, I hypothesise that *dlx3b* and *cvl2* are not expressed in the same domains at the NPB. The reasoning comes from the observation that *cvl2* is localised to the territories of BMP activity (Figure 3.7); the inner coinciding with the NC, and the outer at the border with the epidermis. In between is a region devoid of BMP

signalling, which is likely to be the *dlx3b*-expressing PPE. This would suggest that the PPE is specified in the gap between the two domains of BMP activity/*cvl2* expression.

To determine the exact spatial and temporal expression pattern of NC and PPE markers during ectodermal patterning I performed DFISH with a number of probe combinations at different somitogenesis stages. I visualised the neural plate by staining for *n-cadherin* (*n-cad*), and used *dlx3b* as a PPE marker. The analysis showed that the NC, marked by *sox10* expression, is specified adjacent to the neural plate and is ventrally bordered by the PPE (Figure 3.12A). The inner domain of *cvl2* expression could not be visualised by DFISH during early somitogenesis, as the expression in the NC is still weak (Figure 3.7B). However, at a later somite stage, *cvl2* expression was visible in the NC, and *dlx3b* was clearly expressed in the region between the two *cvl2* expression domains (Figure 3.12B).

Judging from their expression patterns, *cvl2* and *dlx3b* are likely to be co-expressed during epiboly stages (Figure 3.7B) (Akimenko et al., 1994). To clarify this and to analyse the establishment of distinct cell populations after gastrulation, I monitored *dlx3b*/*cvl2* expression at four stages from the end of gastrulation to the formation of the first somite (Figure 3.13). At 95% epiboly it is not entirely clear whether *cvl2* and *dlx3b* are co-expressed or expressed in intermingled cells, but it is apparent that both are present in the same domain (Figure 3.13). At later times however, as *dlx3b* expression sharpens to the NPB, the *cvl2* and *dlx3b* expression domains become increasingly separated, until two clearly distinct domains are visible at the one-somite stage (Figure 3.13).

Analysis of *Tg(BRE:mRFP)* embryos using *mRFP* DFISH in combination with *dlx3b* showed that formation of the outer *mRFP* expression domain follows a similar pattern to that of the outer *cvl2* expression domain (Figure 3.14A). A dorsal anterior view of one-somite stage embryos revealed that compared with *cvl2* and *dlx3b,* the *mRFP* horseshoe-shaped domain at the NPB was transiently slightly broader, with the outer edge co-localising with *cvl2* expression, and the inner edge overlapping with *dlx3b* (Figure 3.14B). At later stages, however, *mRFP* co-localised exclusively with *cvl2* (Figure 3.7C).

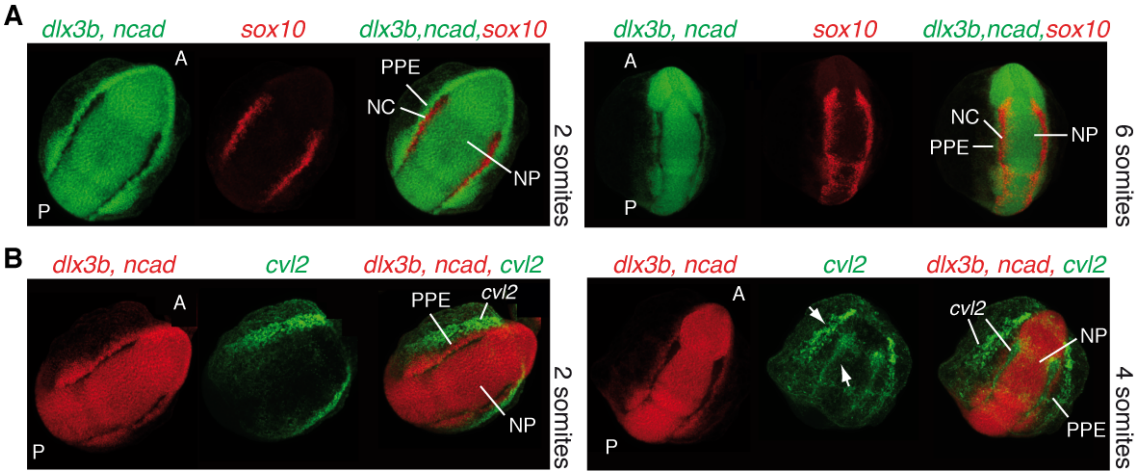

Figure 3.12 *dlx3b*, *cvl2* and *mRFP* are expressed in distinct domains at the NPB
(A) *DFISH to visualise expression pattern of sox10 (red, NC), dlx3b (green, PPE) and n-cad (green, NP) in early (left panel) and later (right panel) somitogenesis.*
(B) *Expression pattern analysis of cvl2 (green), dlx3b (red, PPE) and n-cad (red, NP) at same stages as A. White arrows indicate the two cvl2 expression domains.*
All views show dorsal anterior view with anterior to the top, or to the top right.

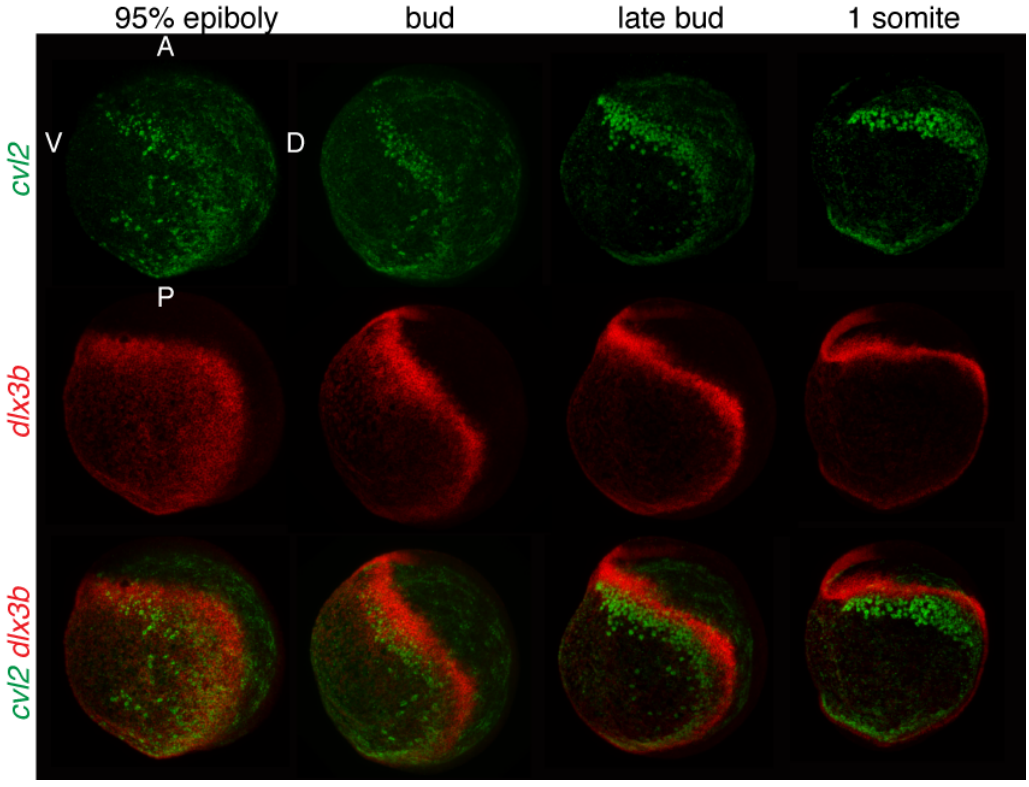

Figure 3.13 *cvl2* and *dlx3b* expression increasingly separates into distinct domains at the end of gastrulation
DFISH of cvl2 and dlx3b. Lateral views, with dorsal (NP) to the right. Developmental stages as indicated.

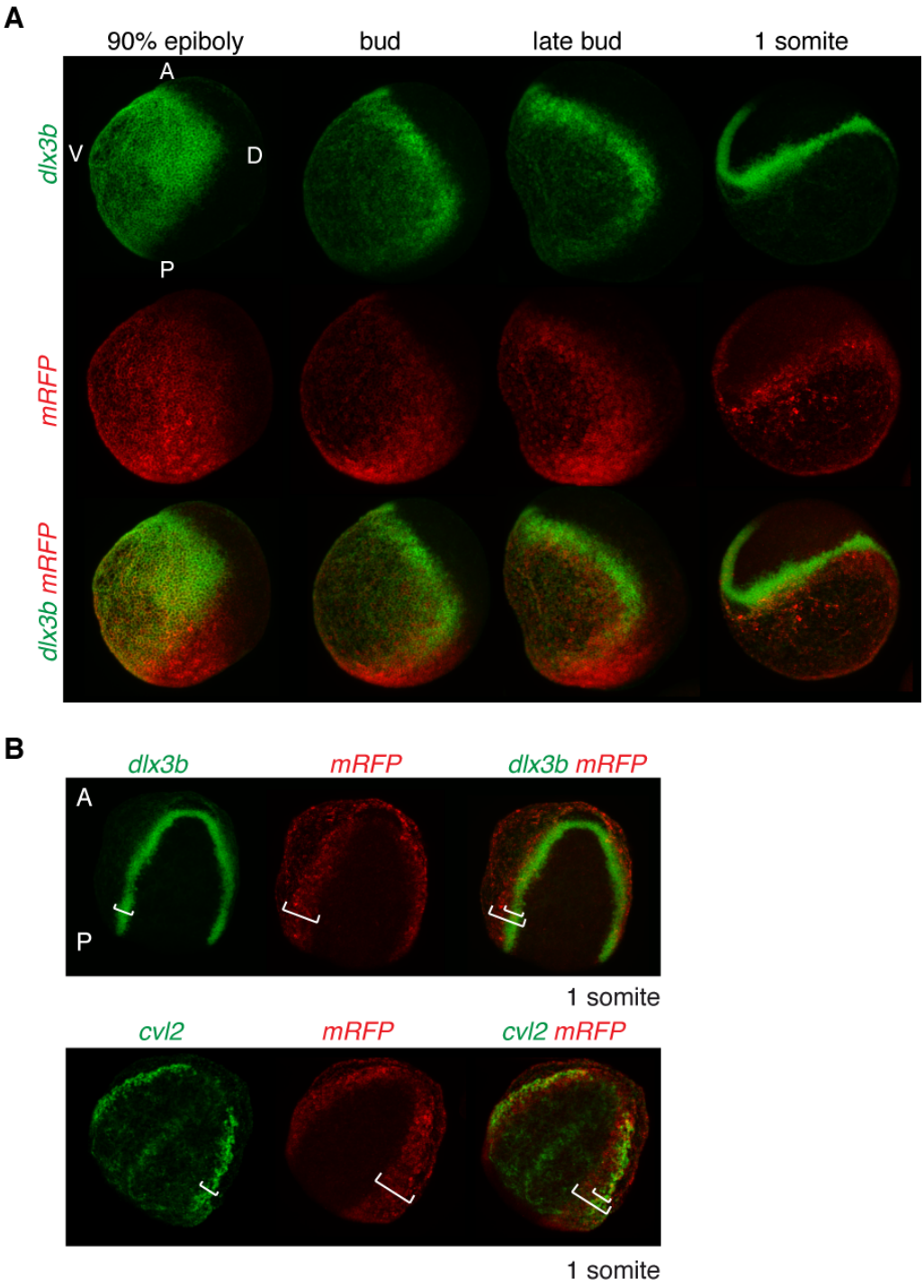

Figure 3.14 Formation of domains of *dlx3b*, *mRFP* and *cvl2* expression at the NPB

(A) *DFISH for dlx3b/mRFP and cvl2/mRFP at different developmental stages. Dorsal anterior view, with anterior to the top. Developmental stages are indicated at the top.*
(B) *dlx3b/mRFP and cvl2/mRFP DFISH at the one-somite stage. White brackets indicate width of the respective mRNA expression domains. Dorsal view; anterior to the top.*

Taken together, these data show that although *cvl2, dlx3b* and *mRFP* are initially expressed in the same territories during gastrulation, distinct expression domains form by the onset of neurulation. The PPE separates the two domains of BMP activity, confirming an absence of BMP signalling in the PPE at somitogenesis stages.

3.2.5 *dlx3b/4b* are required for BMP activity in the NC

The expression of *dlx3b* between the two domains of BMP activity/*cvl2* expression and the known requirement for Dlx3 in NC induction in *X. laevis* (Pieper et al., 2012) prompted me to investigate the role of Dlx3b in regulating BMP activity at the NPB. Knockdown of *dlx3b* in conjunction with the functionally-redundant *dlx4b* (Solomon and Fritz, 2002) resulted in reduced *sox10* expression (Figure 3.15A). This phenotype cannot be attributed to a developmental delay as shown by ISH for *myod* (Figure 3.15B). Contrary to previous reports I did not observe a general reduction of *cvl2* mRNA levels (Esterberg and Fritz, 2009), but a specific loss of the inner *cvl2* expression domain (Figure 3.15A). I went on to investigate whether this holds true on the level of BMP activity as well. Indeed, I could no longer detect the NC domain of BMP activity in *dlx3b/4b* morphants of *Tg(BRE:mRFP)* embryos (Figure 3.15A).

To exclude the possibility that this effect is due to an expansion of neural tissue and hence a loss of the tissue competent for NC specification, I performed DFISH of *cvl2* and *n-cad* on *dlx3b/4b* morphants embryos. This analysis confirmed the absence of the inner *cvl2* expression domain and revealed that the NP (*n-cad*) is not expanded upon *dlx3b/4b* depletion (Figure 3.15B). Moreover, ISH for other PPE markers (*eya1, six4.1*) showed that they were still present in *dlx3b/4b* morphants (Figure 3.16A), suggesting a direct effect of *dlx3b/4b* knockdown on BMP activity, rather than a loss of PPE *per se*. Our results therefore show that *dlx3b/4b* in the PPE are essential for formation of the neighbouring inner BMP signalling domain and hence the NC.

Previous data has suggested that expression of *dlx3b* depends on BMP signalling during early stages, as *bmp2b* mutant embryos lack *dlx3b* mRNA expression (Nguyen et al., 1998).

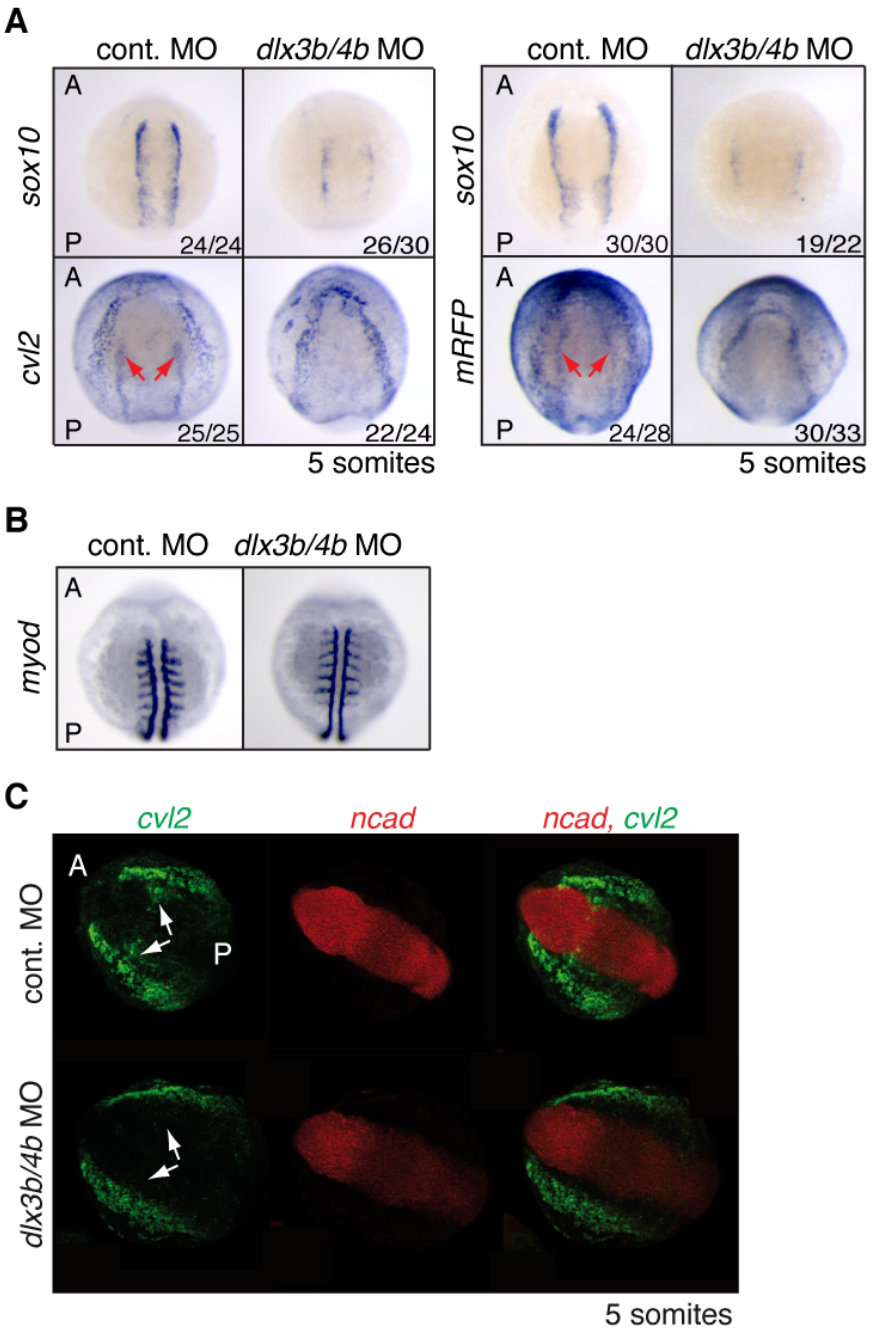

Figure 3.15 *dlx3b/4b* are required for NC induction and formation of the NC BMP signalling domain

(A) *sox10 and cvl2 ISH on wild-type embryos (left panels) and sox10 and mRFP ISH on Tg(BRE:mRFP) embryos (right panels). Embryos were injected with 14 ng control MO or 7 ng each of MOs against dlx3b and dlx4b. Red arrows, inner expression domain of cvl2 and mRFP.*

(B) *myod ISH of dlx3b/4b morphants.*

(C) *Analysis of expression domains at the NPB in dlx3b/4b morphants compared to control MO-injected embryos using DFISH against n-cad and cvl2. White arrows, inner cvl2 expression domain. Dorsal anterior view, anterior to top left.*

Numbers indicate embryos with the observed phenotype for a representative experiment.

The observation that *dlx3b/4b* morphants lacked NC therefore prompted me to re-analyse the *cvl2* morphants to exclude the possibility that the NC phenotype we observed in these embryos was due to inhibition of early BMP activity and a concomitant loss of *dlx3b* expression. However, I could show that levels of *dlx3b* were not diminished in the *cvl2* morphants, demonstrating a direct effect of Cvl2 on NC (Figure 3.16B).

Taken together these data suggest that the requirement of *dlx3b/4b* for NC development depends on the ability of *dlx3b/4b* to regulate localised BMP activity.

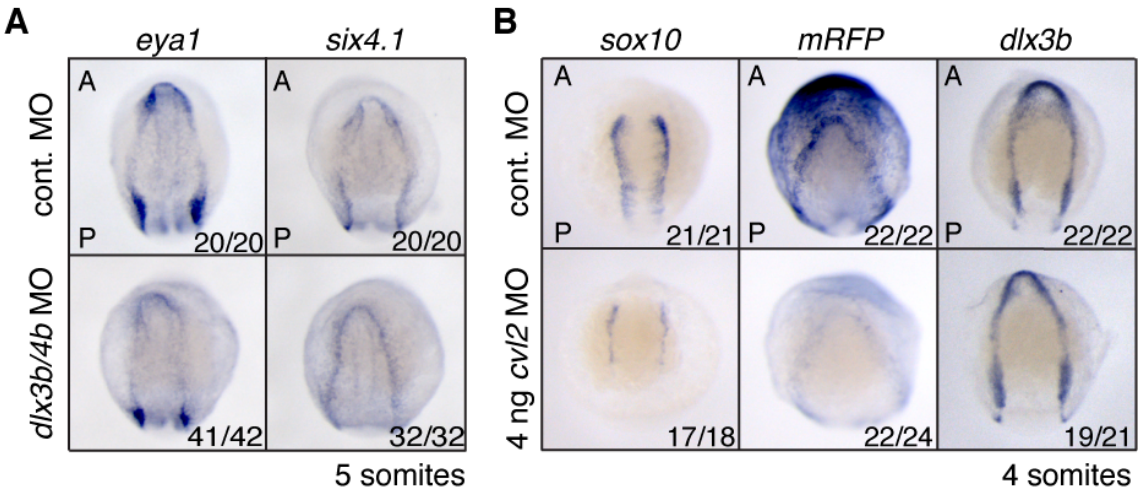

Figure 3.16 PPE markers are still present in dlx3b/4b morphants and dlx3b expression does not depend on BMP activity
(A) *ISH on embryos injected with dlx3b/4b or control MOs using probes directed against PPE markers eya1 and six4.1. Dorsal anterior view, anterior to the top.*
(B) *sox10, mRFP and dlx3b ISH on embryos injected with 4 ng cvl2 or control MO. Numbers indicate embryos with the observed phenotype for a representative experiment.*

3.2.6 *Dlx3b* regulates expression of the BMP inhibitor *bambi-b* in the PPE

cvl2 and *dlx3b* are expressed in similar domains during gastrulation, but then become mutually exclusive at the onset of somitogenesis with *dlx3b* situated between the outer and inner domains of *cvl2* expression/BMP activity. This observation suggests an active inhibition of BMP signalling in the PPE, as the process of domain formation is rapid and spatially, tightly regulated. Such an inhibition could be achieved by the localised expression of BMP antagonists in the

PPE. As Dlx3b is a transcription factor, its loss-of-function phenotype might be at least partially be explained by the loss of a localised BMP inhibitor that is under the transcriptional control of *dlx3b* at the onset of neurulation.

Analysis of the expression patterns of potential BMP inhibitors led me to identify *bambi-b* (BMP and activin membrane-bound inhibitor) as being expressed at the right time and place to locally attenuate BMP signalling at the onset of neurulation. This putative membrane-spanning protein is highly similar to the *X. laevis* BAMBI, which has been shown to function as a pseudoreceptor, inhibiting BMP activity in a cell autonomous manner (Onichtchouk et al., 1999). BAMBI resembles a TGF-β-family type I receptor but lacks an intracellular kinase domain. Functionally, it inhibits the formation of active signalling complexes by sequestering TGF-β-family type II receptors (Onichtchouk et al., 1999). qRT-PCR analysis revealed the onset of *bambi-b* expression at the end of gastrulation (Figure 3.17A). At bud stage *bambi-b* is weakly expressed in the non-neural ectoderm. From the onset of somitogenesis a new stripe of *bambi-b* mRNA

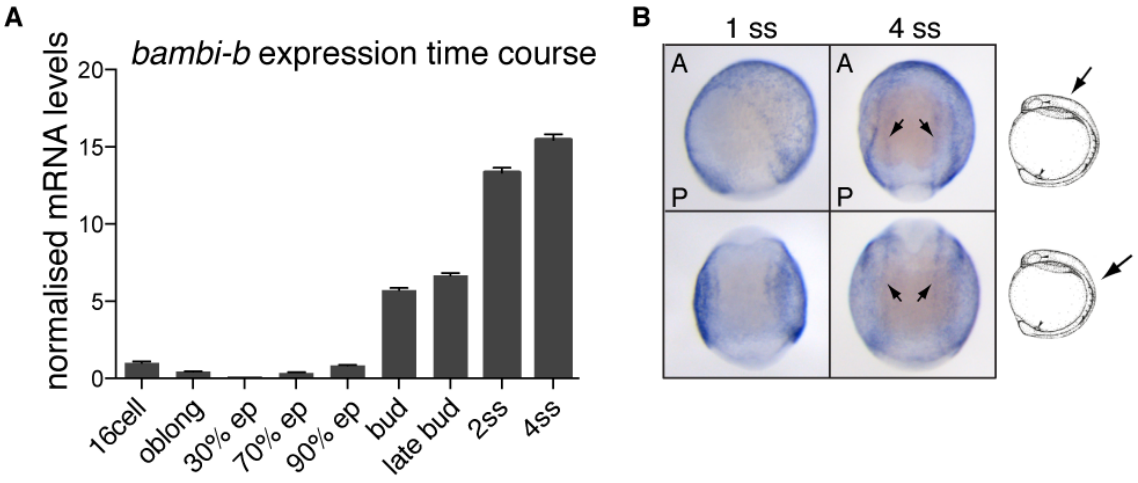

Figure 3.17 Temporal *bambi-b* expression analysis
(A) *qRT-PCR for bambi-b at indicated stages.*
(B) *ISH for bambi-b. Orientation of the embryos is indicated by arrows on cartoon embryos. Anterior view with anterior to the top. The bottom row of embryos shows a different orientation of the same embryos shown in the top row. Black arrowheads indicate stripe of bambi-b expression at the NPB.*
ss – somite stage

expression was detected in a similar territory to *dlx3b* expression, and this expression domain was still present at the four-somite stage (Figure 3.17B). As mentioned above, zebrafish Bambi-b is highly similar to human and *X. laevis* BAMBI, but had not been previously been shown to act in the BMP pathway. To test whether Bambi-b can indeed inhibit BMP signalling I cloned a FLAG-tagged Bambi-b for overexpression in tissue culture cells. Becky Randall then demonstrated that expression of Bambi-b in HEK293T cells inhibited BMP-induced phosphorylation of Smad1/5, particularly when cells were exposed to low levels of BMP4 (Figure 3.18A).

Mechanistically, *X. laevis* BAMBI has been shown to function by forming a non-productive signalling complex with the BMP type I receptors. Similarly, I could demonstrate that Bambi-b interacted with the BMP type I receptor ALK3 (Figure 3.18B). To test the requirement for Bambi-b during embryonic development for domain formation I performed loss-of-function studies using a translation-blocking MO. The functionality of this MO can be demonstrated in a rabbit reticulocyte *in vitro* translation assay, in which expression of [^{35}S]-methionine labelled Bambi-b is inhibited in the presence of the *bambi-b* MO (Figure 3.19A). The expression of the NC marker *sox10* is significantly reduced in the *bambi-b* morphants and the inner NC *cvl2* expression domain can no longer be detected (Figure 3.19A). This phenotype is similar to the observed *dlx3b/4b* phenotype, suggesting that *bambi-b* may be downstream of *dlx3b*. I therefore tested whether *dlx3b* is in fact required for induction of the stripe of *bambi-b* expression. Knockdown of *dlx3b/4b* led to a loss of this specific *bambi-b* expression domain (Figure 3.19B). Importantly, expression in the non-neural ectoderm, where *dlx3b/4b* are not expressed, was not affected.

myod ISH on *bambi-b* morphants shows that the reduction in NC is not due to a developmental delay of the *bambi-b* MO injected embryos (Figure 3.19C). To confirm that *bambi-b* is indeed required for PPE development I analysed *bambi-b* morphants for phenotypes in PPE derivatives such as the otic vesicle. *dlx3b* is necessary for otic placode development and loss of *dlx3b* results in otic vesicle defects (Figure 3.20. (Solomon and Fritz, 2002)). Similarly, knockdown of *bambi*-b affects otolith formation in the otic vesicle indicating that indeed *bambi-b* is involved in PPE development (Figure 3.20).

Finally, I investigated whether Dlx3b might be directly responsible for regulating *bambi-b* expression. I used PreMoTF (Predicted Motifs for Transcription

Factors) to predict the DNA-binding specificity of Dlx3b (Christensen et al., 2012), which was identified as TAATTG/A (Figure 3.21A). I found two possible sites in the *bambi-b* gene and flanking region: one in the 5'-UTR (+199 to +204, probe 1) and the other is upstream of the start of transcription (-851 to -846 bp; probe 2). In a bandshift assay I could demonstrate direct binding of FLAG- tagged Dlx3b to both of these sites, that supershifted with an anti-FLAG antibody, and was abolished by specific mutation of the binding site (Figure 3.21B).

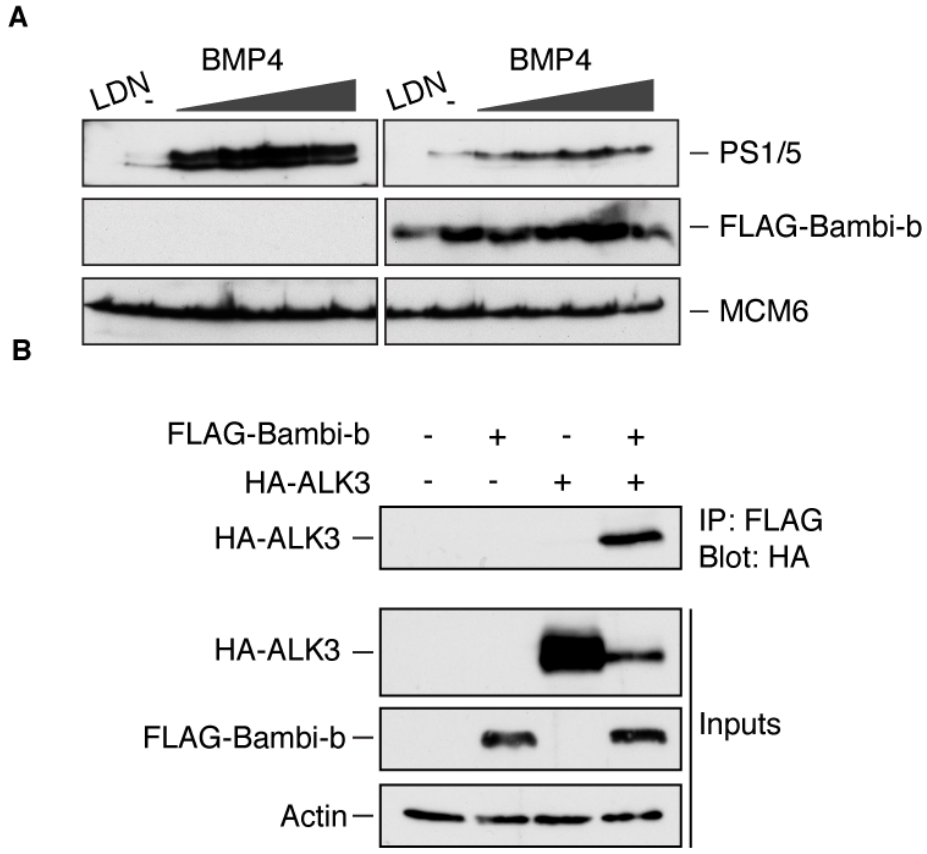

Figure 3.18 *bambi-b* inhibits BMP signalling in tissue culture and binds ALK3
(A) *HEK293T cells transfected with control plasmid or pCS2+-FLAG-Bambi-b were treated with different concentrations of BMP4 (2 ng/ml, 4 ng/ml, 10 ng/ml and 20 ng/ml) for 1 h, or with the BMP receptor inhibitor LDN-193189 for 3 h. Whole cell extracts were Western blotted using the indicated antibodies.*
(B) *HEK293T cells were transfected with control plasmid or pCS2+-FLAG-Bambi-b or HA-ALK3. FLAG-Bambi-b was immunoprecipitated from whole cell extract and the immunopreciptates were Western blotted for HA. The inputs are also shown. Actin is a loading control.*

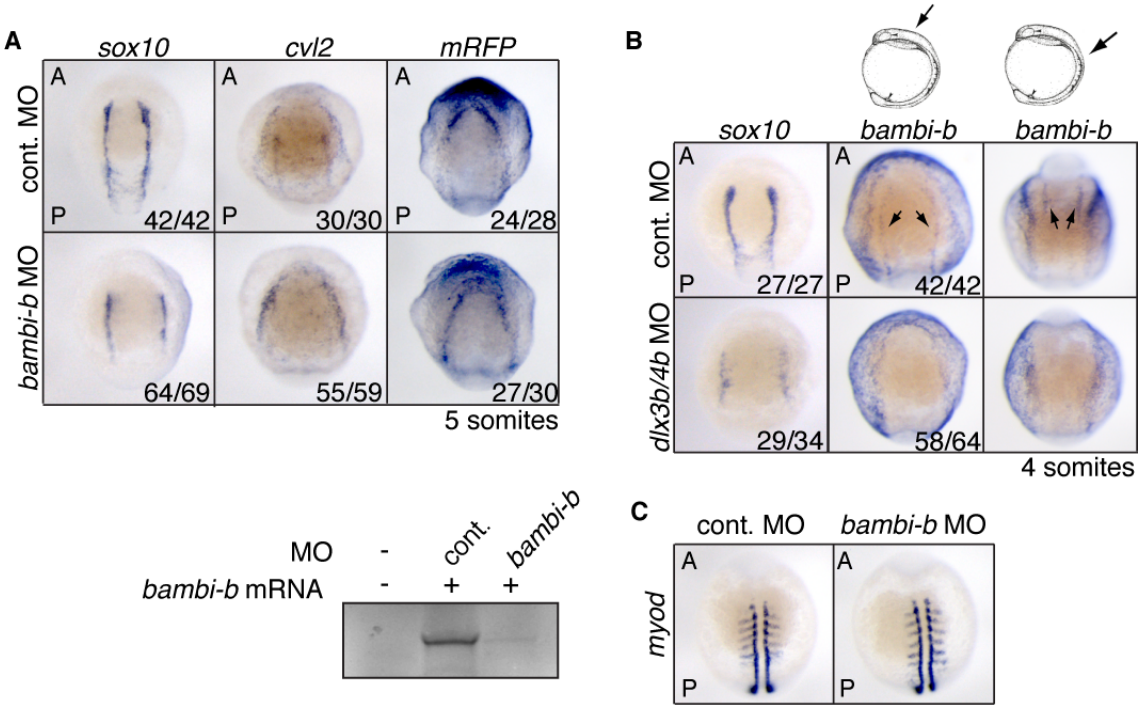

Figure 3.19 *bambi-b* morphants lack inner BMP signalling domain. *bambi-b* expression is dependent on dlx3b/4b

(A) *Upper panel: ISH for sox10, cvl2 and mRFP on bambi-b morphants compared with controls. Embryos were injected with 10 ng bambi-b or control MO. Dorsal anterior view, anterior to the top. Lower panel: synthetic mRNA corresponding to native bambi-b was translated in reticulocyte lysate in the presence of 0.2 mM bambi-b MO and [^{35}S]-methionine. Translation products were separated by SDS-PAGE and visualised by autoradiography.*

(B) *ISH for sox10 and bambi-b on dlx3b/4b morphants compared with control MO-injected embryos. Arrows mark the inner bambi-b expression domain. Views are as in Figure 3.17B*

Numbers indicate embryos with the observed phenotype for a representative experiment.

(C) *myod ISH of bambi-b morphants.*

In conclusion, Bambi-b, which is expressed after bud stage under the control of Dlx3b, is an excellent candidate to inhibit BMP activity in these *dlx3b*-expressing cells and as a result enable them to be specified as PPE. Moreover, it is required for the formation of the NC domain of BMP activity and thus NC development.

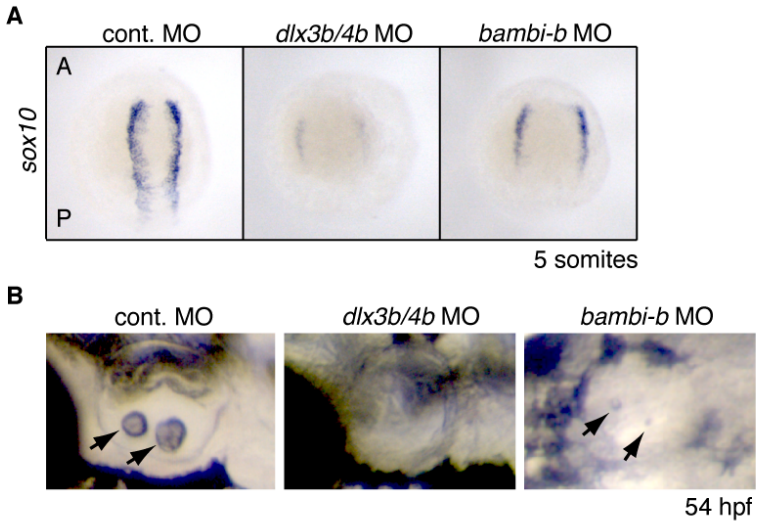

Figure 3.20 *bambi-b* is required for otic placode development

(A) *ISH for sox10 on dlx3b/4b and bambi-b morphants embryos (upper panel).*
(B) *Otoliths are absent in the otic vesicle of dlx3b/4b MO injected and greatly reduced in bambi-b MO injected embryos.*

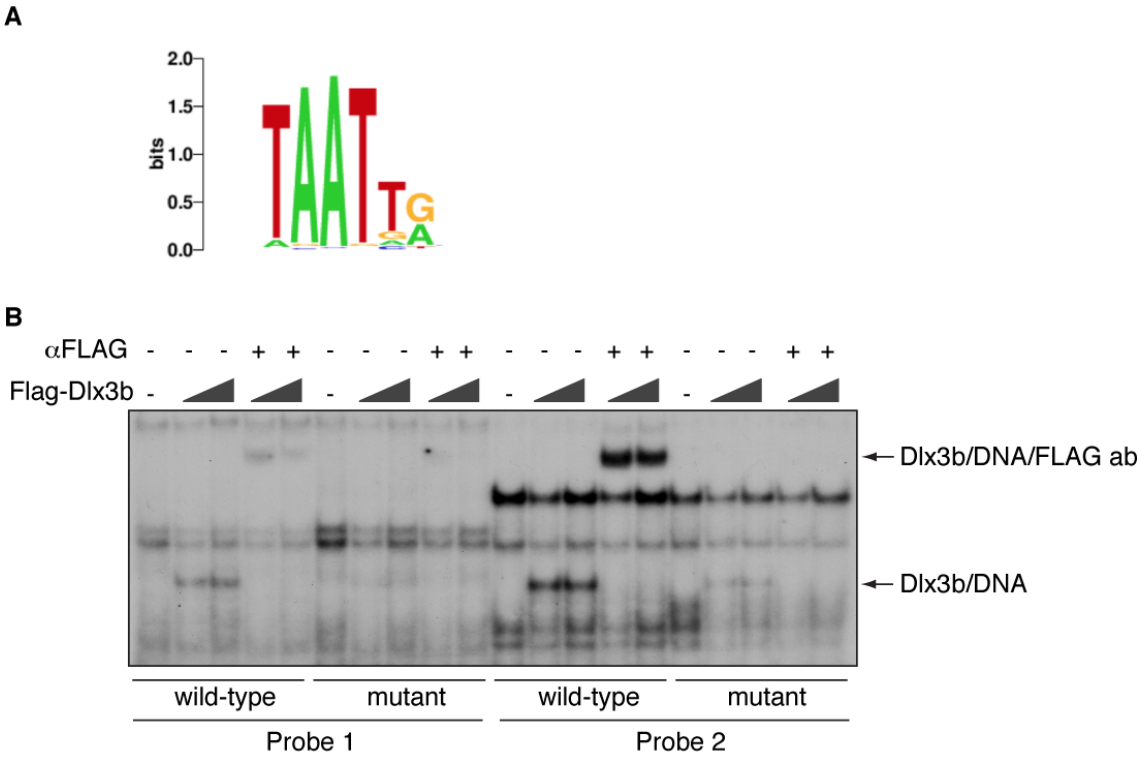

Figure 3.21 *dlx3b* can bind to *bambi-b* gene

(A) *Dlx3b DNA-binding motif predicted using PreMoTF.*
(B) *FLAG-Dlx3b expressed in HEK293T cells was assayed for binding to DNA using a bandshift assay. The wild-type probes correspond to the two putative Dlx3b binding sites in the bambi-b gene and the mutant probes contain point mutations in the binding sites. The Dlx3b–DNA complexes are indicated, as are the supershifted complexes that additionally contain the anti-FLAG antibody.*

3.3 Discussion

3.3.1 Summary of results

- BMP activity is dynamically regulated and two distinct BMP signalling domains arise at the NPB after gastrulation with an inner domain coinciding with the NC
- *cvl2* is expressed in domains of BMP activity
- *cvl2* is a novel regulator of NC development through modulating BMP signalling
- The PPE is devoid of BMP activity and resides between the two domains of BMP signalling
- *dlx3b/4b*, which are expressed in the PPE, are required for formation of the NC BMP activity domain
- The transcription factor *dlx3b* is required for the expression of an BMP inhibitor, Bambi-b, in the PPE, which in turn is necessary for the establishment of the NC domain of BMP signalling

3.3.2 Identification of dynamic BMP signalling domains at the NPB during ectodermal patterning

I have used a transgenic zebrafish BMP reporter line to identify distinct territories of BMP activity at the NPB. I show that at the end of gastrulation, BMP activity concentrates into a horseshoe-shaped domain at the border of the neural plate, which then resolves into two distinct domains: an outer domain abutting the epidermis and an inner domain. DFISH reveals this inner domain corresponds to the NC directly demonstrating on-going BMP activity in the NC cell population. I further show that BMP signalling is absolutely required for the maintenance of NC progenitors, as inhibition of BMP signalling at the onset of neurulation reduced the expression of NC markers. These results give direct proof of a dynamic spatial and temporal regulation of BMP signalling domains during ectodermal patterning. Previous evidence has been rather circumstantial as it has relied on the use of mutants or addition of BMP inhibitors at various developmental stages and furthermore imaging endogenous BMP activity using IF against PSmad1/5 is not very sensitive. This approach has allowed for the detection of strong signals such

as the initial BMP signalling gradient during gastrulation. During somitogenesis, using PSmad1/5 staining, I was also able to visualise the outer horseshoe-shaped domain at the NPB. However, the BMP activity in the NC could not be detected. The transgenic *Tg(BRE:mRFP)* reporter line on the other hand now enables us to reveal weaker signals using ISH against *mRFP* as a readout. A recent publication from our lab provides evidence of a short half-life of *mRFP* mRNA. During the establishment of the early BMP activity gradient at the onset of epiboly *mRFP* transcripts are cleared within 20 min of the gradient detection by PSmad1/5 immunostaining (Ramel and Hill, 2013). Therefore *Tg(BRE:mRFP)* embryos are proving to be a useful tool to assess *in vivo* signalling dynamics. Moreover, larger numbers of embryos can be processed in ISH compared to the time consuming analysis of IF stained embryos with confocal microscopy.

I further went on to determine which ligands contribute to the localised BMP activity. Historically *bmp2b, bmp7a* and *bmp4* have been implicated in NC development. After gastrulation *bmp4* expression differs from the patterns observed for *bmp2b* and *bmp7a* and can be detected in the posterior epidermis and the polster, but not at the NPB (Thisse et al., 2001). Analysis of two zebrafish *bmp4* mutants demonstrates the requirement of Bmp4 for ventroposterior cell fates (Stickney et al., 2007). However, although *X. laevis bmp4* overexpression can rescue *bmp2b* and *bmp7a* mutants (Kishimoto et al., 1997, Nguyen et al., 1998), zebrafish *bmp4* does not seem to be directly involved in NC development. I have also demonstrated that *bmp6* is expressed in the horseshoe-shaped domain of BMP activity that abuts the epidermis. Bmp6 alone, however, is not responsible for formation of this domain, but is likely to reinforce and sharpen the signalling domain in concert with Bmp2b and Bmp7a. Moreover, I have identified Gdf6a as the BMP ligand required for BMP signalling activity in the NC and also for NC cell fate, thus solving the conundrum of how BMP signalling is activated in the NC given the absence of *bmp2b, bmp4* and *bmp7a* expression in this specific domain. How transcription of *gdf6a* is induced in this specific domain remains to be determined. There are several *gdf6a* mutants available, which could be used for further analysis (den Hollander et al., 2010, Gosse and Baier, 2009). I have also reviewed the published expression pattern of other known Bmp and Gdf ligands. However, most of them are either expressed later in development such as *bmp10, bmp15, bmp16, gdf5, gdf9* and *dvr1 (gdf3)* {Thisse, 2004 #430;Laux, 2013 #402;Liu, 2007

#432;Schwend, 2009 #431} or their expression patterns do not suggest a a role in NC and PPE development such as *bmp1a, bmp2a, bmp7b, gdf2, gdf6b, gdf11* and *mstnb (gdf8)* {Bruneau, 1997 #404;Jasuja, 2006 #365;Shawi, 2008 #401;Thisse, 2004 #430}. *bmp3* and *bmp5* are expressed in the pharyngeal arches and have been implicated in cranial development suggesting a role in later stages of NC development for example in the signalling cues leading to correct NC migration {Schoenebeck, 2012 #399;Thisse, 2004 #430}. *gdf10a* can be detected in the epidermis at the anterior at early somitogenesis {Thisse, 2004 #430}. It would be interesting to review its expression pattern and test the requirement for this ligand for BMP activity in a morpholino approach.

3.3.3 Cvl2 focuses BMP activity at the NPB and is required for NC development

The reshaping of BMP activity at the end of gastrulation from a gradient to sharply defined domains at the NPB prompted me to search for spatial regulators of BMP signalling. I identified the secreted BMP-binding protein Cvl2 as playing a critical role in “focusing” BMP activity into the two distinct domains at the NPB. Cvl2 has been described as both an activator and an inhibitor of BMP signalling (Binnerts et al., 2004, Kamimura et al., 2004, Moser et al., 2003, Conley et al., 2000, Ambrosio et al., 2008). Cvl2 is bound to the membrane via glycosylphosphatidylinositol-anchored Heparan-Sulphate Proteoglycans (HSPGs) and thus is thought to act at short range compared to other secreted BMP modulators such as the BMP antagonist Chordin (Serpe et al., 2008). Like many other proteins that interact with BMPs, Chordin amongst them, Cvl2 contains cysteine-rich domains (Conley et al., 2000). Indeed, Cvl2 has been shown to interact with Bmp2, Bmp4 and Bmp7, as well as Chordin and type I BMP receptors (Ambrosio et al., 2008, Rentzsch et al., 2006, Serpe et al., 2008, Zhang et al., 2010). Different mechanisms have been proposed for its activatory effect on BMP signalling. In the posterior crossvein of the *Drosophila* pupal wing it is thought to act at short range by promoting binding of BMPs to receptors (Serpe et al., 2008). In zebrafish, Cvl2 has been shown to act during gastrulation in BMP gradient formation by stabilising BMP signalling territories, at least partly by competing with Chordin for binding to BMPs (Rentzsch

et al., 2006). That study also suggested that proteolytic cleavage converts Cvl2 from an anti- to a pro-BMP factor, with the cleaved form being predominantly present during zebrafish development. The same lab then proposed a ternary complex consisting of Chordin, Cvl2 and Bmp. This leads to a conformational change in the Chordin protein thus releasing Chordin and making Bmp more available for receptor activation (Zhang et al., 2010). During *X. laevis* development, Cvl2 has been suggested to act as a Bmp4-dependent feedback inhibitor (Ambrosio et al., 2008). Other evidence for an inhibitory function of Cvl2 comes from overexpression studies. However, this is likely to result in sequestering Bmp ligands accounting for the inhibitory behaviour (Moser et al., 2003, Binnerts et al., 2004). In contrast, I have not seen evidence of endogenous *cvl2* being expressed in regions devoid of BMP activity at the stages examined. I have shown that at neurula stages *cvl2* expression recapitulates patterns of BMP activity and is also under BMP control. My loss-of-function data using three independent MOs against *cvl2* further demonstrate a pro-BMP function of Cvl2 at these stages and its requirement for BMP domain formation at the NPB. This constitutes a novel role for Cvl2 in NC development. The fact that pigmentation in *cvl2* morphants is not severely affected suggests a specific role for cranial NC rather than trunk NC. My experiments demonstrate that Cvl2 and BMP signalling act in a positive feedback loop, and the non-diffusible nature of the BMP ligands probably contributes to this (Ramel and Hill, 2013). I propose that Cvl2 may focus BMP activity in the discrete domains at the NPB via a mechanism analogous to that suggested to operate at the *Drosophila* posterior crossvein. This would ensure robust levels of BMP activity while the territories of BMP signalling are being reshaped.

3.3.4 The PPE is specified in the region that lacks BMP activity

Previous work has indicated that PPE specification requires full inhibition of BMP signalling at the end of gastrulation (Kwon et al., 2010), and I directly demonstrate this here using DFISH. Using *dlx3b* as a marker for the PPE, I reveal the process of separation of *dlx3b* and *cvl2/mRFP*-positive cells into distinct domains at the NPB. Taking advantage of the high resolution of DFISH, I carefully analysed how *cvl2* and *dlx3b* expression changes from the end of gastrulation to the one-somite stage.

cvl2 and *dlx3b* are expressed in similar domains during gastrulation. However, by the one-somite stage *dlx3b* and *cvl2* are expressed in mutually exclusive domains. This separation occurs as the cells converge dorsally as a result of gastrulation movements (Schier and Talbot, 2005). I could not definitively determine whether *cvl2* and *dlx3b* are co-expressed in the same cells, or are expressed uniquely in intermingled cells. However, the observation that the formation of the distinct *dlx3b* and *cvl2* expression domains is very rapid (around 1 hour) would support a mechanism whereby intermingled cells are separated by cell sorting, with *dlx3b*-expressing cells migrating slightly more dorsally than the *cvl2*-expressing cells. It will be important in the future to determine how this is achieved. There are several examples of cell sorting *in vivo* being regulated by Eph/ephrin signalling and the differential expression of cadherins (Batlle and Wilkinson, 2012). Reciprocal expression of the Eph receptors and the ephrin ligands is sufficient for the segregation of intermingled cells (Tanaka et al., 2003, Cortina et al., 2007, Poliakov et al., 2008). Reviewing the expression patterns of several of the Eph/ephrin pathway components did not yield any plausible candidates. Nevertheless, this pathway poses an intriguing possibility as a mechanism to separate *cvl2/mRFP* and *dlx3b* expression domains.

3.3.5 Expression of *bambi-b* under control of Dlx3b/4b inhibits BMP activity in the PPE

The DFISH analysis demonstrated rapid clearance of BMP activity from *dlx3b* expressing cells by the one-somite stage. This indicates that active inhibition of BMP signalling occurs in the *dlx3b*-positive cells and hence predicted the expression of a cell autonomous BMP inhibitor in the PPE. I have identified Bambi-b as an excellent candidate that would fulfil this role. As mRNA expression levels of *bambi-b* are very low, I was unable to formerly prove that *bambi-b* is indeed expressed in the PPE, but careful visual analysis of the stained embryos strongly suggests that the inner *bambi-b* expression domain coincides with *dlx3b* expression. The data show that Bambi-b is able to inhibit BMP activity in response to a signal in tissue culture cells. I also attempted overexpression of Bambi-b in zebrafish embryos to test the BMP inhibitory function *in vivo*. The mRNA, however,

appears to be highly regulated, as even after injection of high doses of *bambi-b* mRNA I was unable to detect protein expression in the embryos. This is not due to a faulty expression construct, as the mRNA was readily translated in a rabbit reticulocyte *in vitro* translation assay (data not shown) and I used the same expression construct for expression of *bambi-b* in tissue culture (Figure 3.18). I have demonstrated that *bambi-b* morphants lack the inner domain of *cvl2*/BMP activity, and thus they display a similar phenotype to *dlx3b/4b* morphants. This strongly suggested that *bambi-b* expression is regulated by *dlx3b/4b*, which I was able to demonstrate. This is the first transcriptional target described for Dlx3b. To substantiate the data it would be interesting to perform ChIP experiments from zebrafish embryos. The limiting factor, however, is the availability of a suitable antibody. The antibodies tested so far were not able to detect zebrafish Dlx3b. Thus, a tagged version of Dlx3b would be required. In addition, Dlx3b expression alone is not sufficient to induce *bambi-b* transcription, as *bambi-b* mRNA can only be detected from bud stage onwards, whereas *dlx3b* is already expressed during gastrula stages. Moreover, *bambi-b* is not only present in the PPE, but also in the non-neural ectoderm, which does not express *dlx3b*, suggesting that *bambi-b* transcription is subject to a different mode of regulation in these cells.

3.3.6 A two-step model for controlling cells fate decisions during ectodermal patterning

Different tissues require distinct levels of BMP signalling at specific times during ectodermal patterning. NC requires intermediate to low levels of BMP signalling for induction (Schumacher et al., 2011) and as I show here, continues to require BMP activity for its maintenance. PPE in contrast only requires BMP activity during its induction phase, but is devoid of BMP signalling after gastrulation. The classical BMP gradient model fails to explain how these contrasting patterns of BMP signalling in neighbouring cell populations are established in time and space. The data I present here provides direct evidence for a two-step model of ectodermal patterning (Figure 3.22). I show that the early BMP DV gradient, present during gastrulation, is remodelled into distinct BMP signalling domains at the NPB. I further demonstrate active BMP signalling in the NC and at the epidermal border,

whereas BMP activity is completely inhibited in the intervening PPE. The ligand responsible for the inner BMP activity domain is Gdf6a, and the activity is focused in this domain by coincident expression of Cvl2. The ligands responsible for the outer BMP activity are Bmp2b, Bmp7a and Bmp6. Again, I demonstrate a crucial role for Cvl2 acting in a positive feedback loop to concentrate their BMP activity at the epidermal border. I show that the region between these two domains of BMP activity is specified as the PPE, which expresses the homeobox transcription factor Dlx3b. I demonstrate that Dlx3b is responsible for inducing expression of the BMP inhibitor Bambi-b, thereby allowing BMP repression in the presumptive PPE. Thus, rather than a linear gradient of BMP specifying cell fates at the NPB, I propose a model which involves dynamic expression of BMP inhibitors and activators that can explain the differential requirements of NC and PPE for BMP activity at different developmental stages.

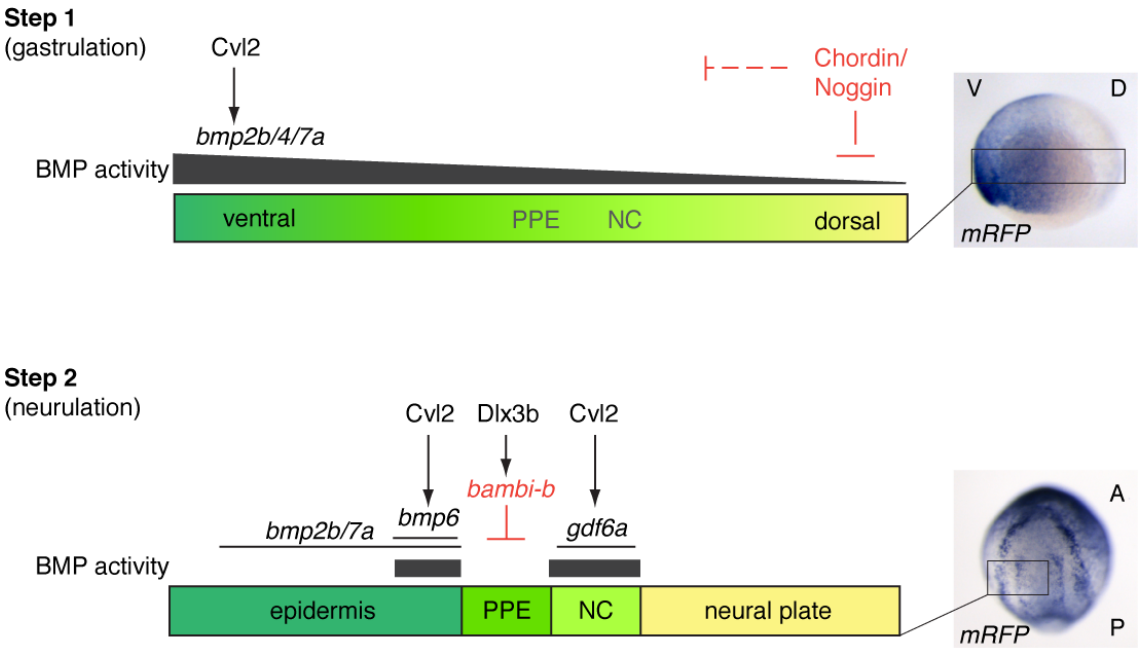

Figure 3.22 A 2-step model for zebrafish ectodermal patterning

Step 1 depicts the DV gradient present during gastrulation. High BMP activity is observed ventrally, generated by bmp2b/4/7 ligand expression and reinforced by Cvl2. BMP activity is inhibited dorsally by expression of the diffusible antagonists Chordin and Noggin. Prospective PPE and NC are formed at intermediate levels of BMP signalling. In step 2 the initial gradient has reshaped into distinct BMP activity domains during neurulation. The regulatory network is depicted. Components in black act positively, whilst those in red act negatively.

Chapter 4.

Chapter 5. The role of Snw1 during vertebrate neural crest development

5.1 Introduction

Snw1 has previously been identified as a regulator of neural crest fate in a large-scale *in vivo* functional screen in *X. laevis* conducted by our lab (Wu et al., 2011). This study identified Snw1 as being required for BMP activity at the NPB. The molecular function of Snw1, however, had not been described. In this chapter I describe the use of *X. laevis* and zebrafish embryos to further investigate Snw1 function during early vertebrate development.

5.2 Results

5.2.1 Snw1 is cell-autonomously required for NC induction in *X. laevis*

As previously described, Snw1 has an important function in NC development (Wu et al., 2011). Both overexpression and depletion of Snw1 resulted in a substantial loss of NC markers such as *slug* and *sox9* in neurula stage (stage 14) *X. laevis* embryos (Figure 5.1). This indicated that expression levels of Snw1 have to be tightly regulated. However, these previous experiments modulate Snw1 globally in the embryo and do not give information regarding the cells in which Snw1 is required for its function.

To address this question, I made use of the fate map that has been produced for 32-cell stage *X. laevis* embryos (Dale and Slack, 1987). This fate map enabled me to specifically manipulate the levels of Snw1 in the blastomere that contributes to the tissues at the NPB (and thus the NC), whereas for example maintaining its wild type expression patterns in the underlying mesoderm. I co-injected fluorescein isothiocyanate–dextran (Fdx) to trace the cells that arise from this blastomere and have received the injected MO. Fdx can be visualised under a fluorescent microscope with an excitation and emission spectrum peak wavelengths of approximately 495 nm/519 nm. Alternatively, I used an anti-FITC

antibody and BCIP for colourimetric detection. The analysis clearly showed that *slug* ISH staining (blue) is lost in the cells that have been injected with the *snw1* MO (marked by turquoise) whereas loss of Snw1 in adjacent cells did not affect the NC (Figure 5.2). This suggests that Snw1 function is required in the NC cell population itself.

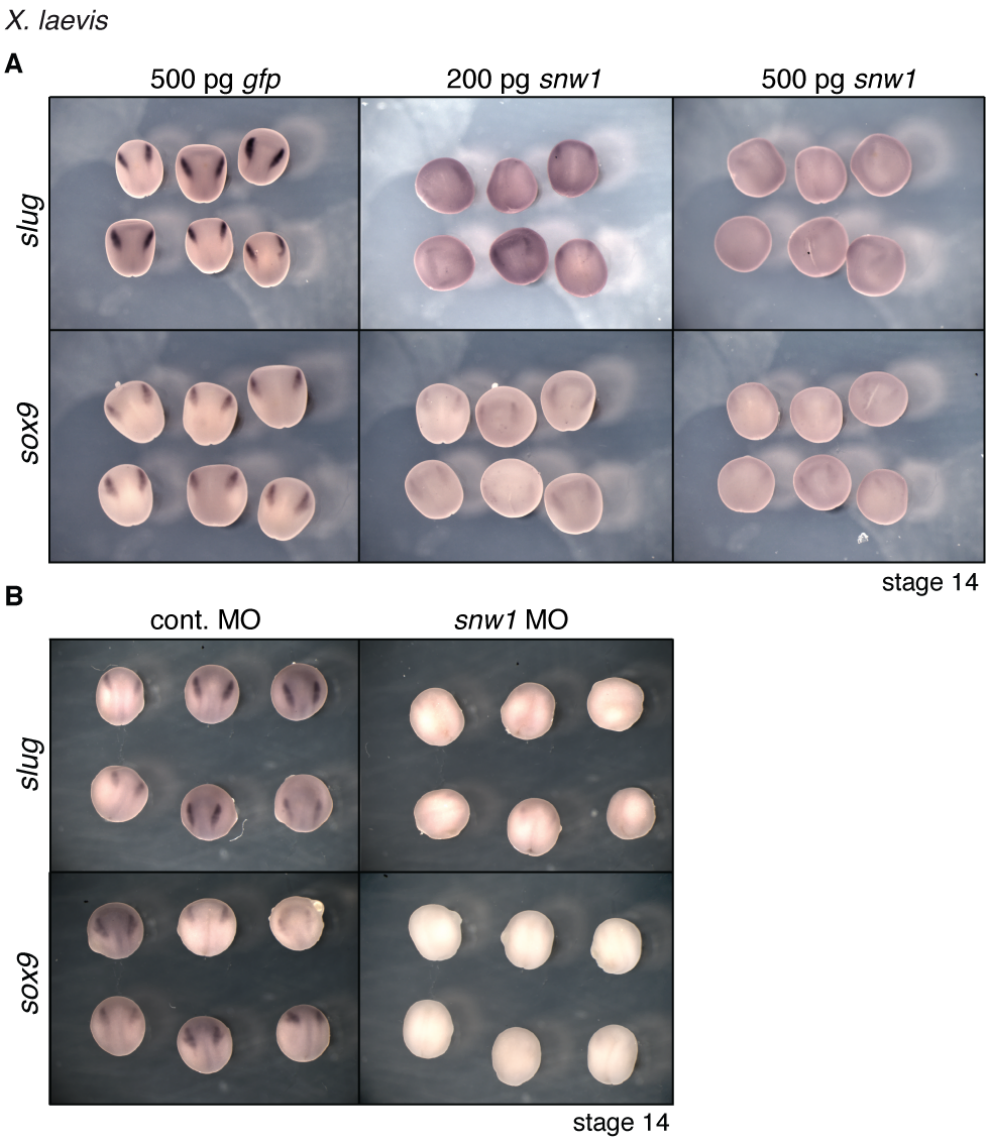

Figure 5.1 Overexpression and knockdown of Snw1 in *X. laevis*
(A) *ISH of X. laevis embryos injected with indicated amounts of gfp or snw1 mRNA using probes against the NC markers slug and sox9.*
(B) *ISH of embryos injected with 20 ng of cont. or snw1 MO, using probes against the NC markers slug and sox9.*
All views show embryos dorsal view with anterior to the top.

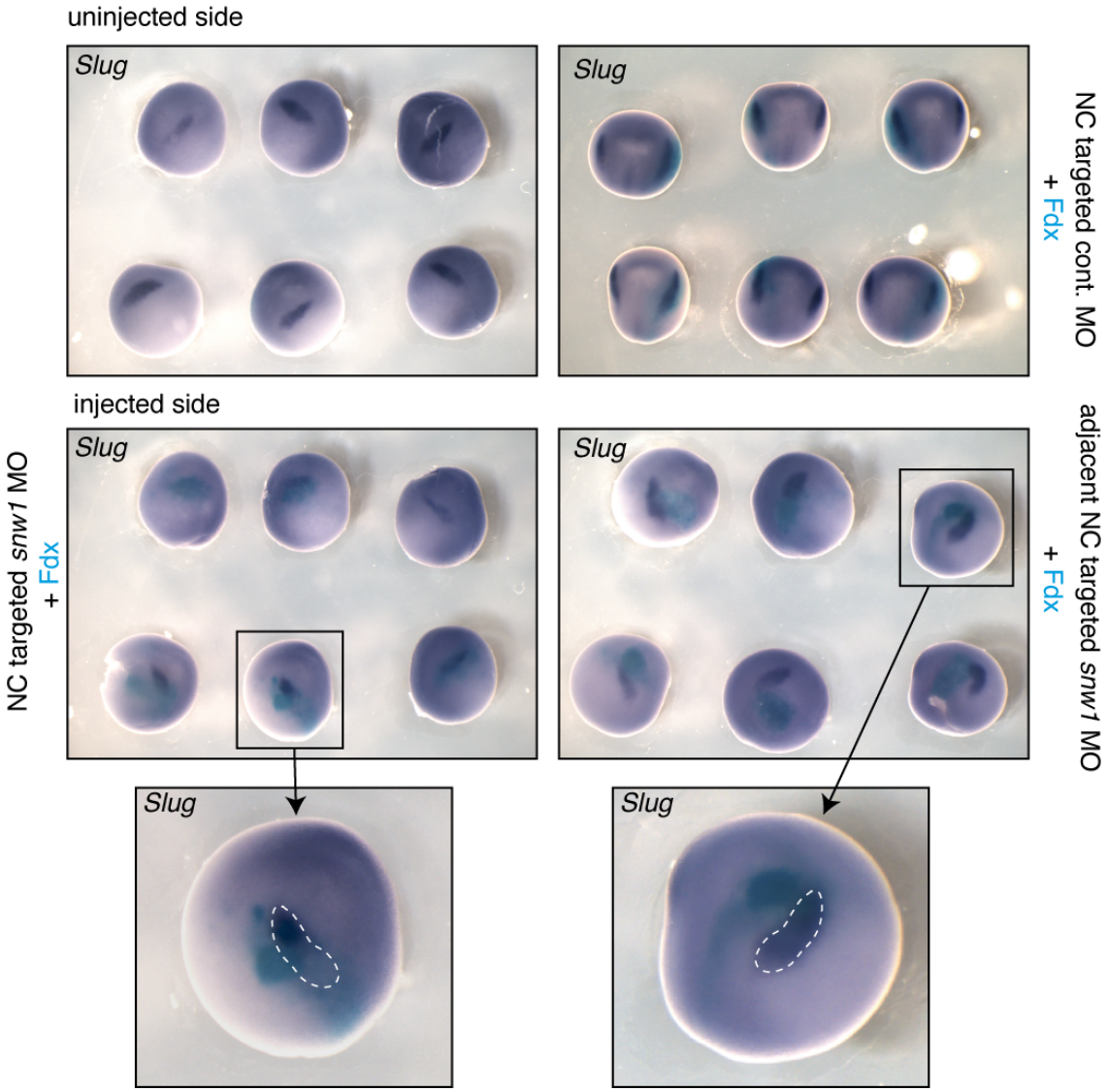

Figure 5.2 Targeting of the snw1 MO to the neural folds (*X. laevis*)
ISH of embryos injected with the indicated MO and Fdx to trace the targeted tissue. slug ISH staining visualises the NC (dark blue) whereas Fdx (turquoise) labels the cells that have received the MO. Upper panel shows embryos with cont. MO targeted to the neural folds. Middle panels show targeted snw1 MO. Left is the uninjected side as a control, on the right is the injected. At the bottom left is a magnification of an example embryo with the snw1 MO targeted to the NC. The lower right panel shows embryos with the snw1 MO targeted adjacent to the NC, as visualised using Fdx. The white dashed line depicts the expected wt territory of slug NC marker expression.

To demonstrate that the NC cell fate in these cells was not merely delayed but permanently abolished, I monitored the NC cell population of injected embryos at a later developmental stage when the NC cells have migrated to populate the four branchial arches (reviewed in (Minoux and Rijli, 2010)).

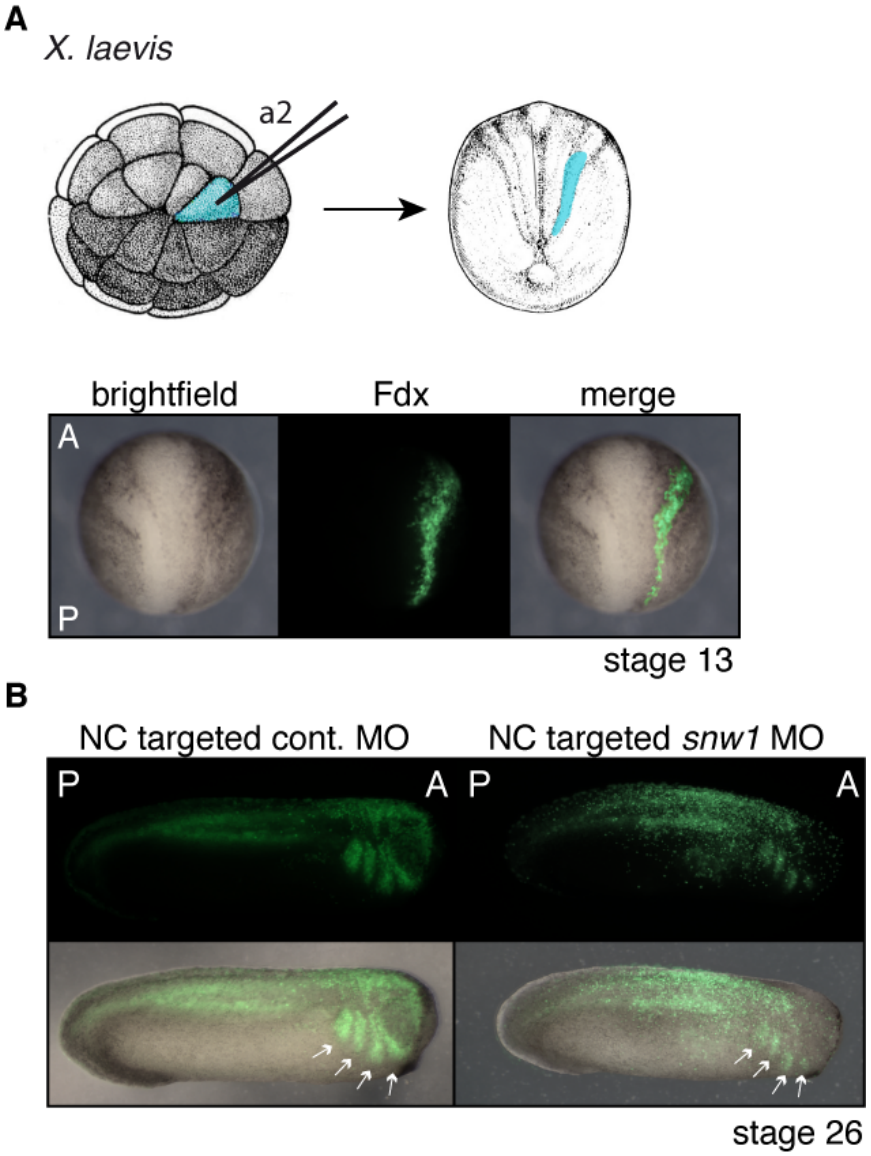

Figure 5.3 NC lacking Snw1 fails to populate the branchial arches (*X. laevis*)
(A) *Schematic indicates the blastomere that contributes to the NC. Successful targeting was monitored by visualising Fdx using a fluorescent microscope (lower panel).*
(B) *Embryos injected with either a control or snw1 MO were analysed for migration of the NC into the branchial arches. The injected cells were visualised using Fdx. The white arrows indicate the four brachial arches.*
Embryos shown are representative for several experiments.

I again injected embryos with a control or *snw1* MO into blastomere a2 and confirmed efficient targeting under a fluorescence microscope (Figure 5.3A). The successfully injected embryos were then further analysed at stage 26. In control embryos I could indeed detect targeted cells in the branchial arches (Figure 5.3B). The number of these cells was drastically reduced in Snw1-depleted embryos (Figure 5.3B). Instead a greater number of "scattered" fluorescent cells were detected in the dorsal ectoderm, visible in the upper panel of Figure 5.3B, indicating that loss of Snw1 does not lead to a depletion of the targeted cell population but a loss of NC identity.

5.2.2 The role of Snw1 is conserved in zebrafish

The Snw1 protein is highly conserved between vertebrates (Wu et al., 2011), suggesting that its function might also be conserved amongst species.

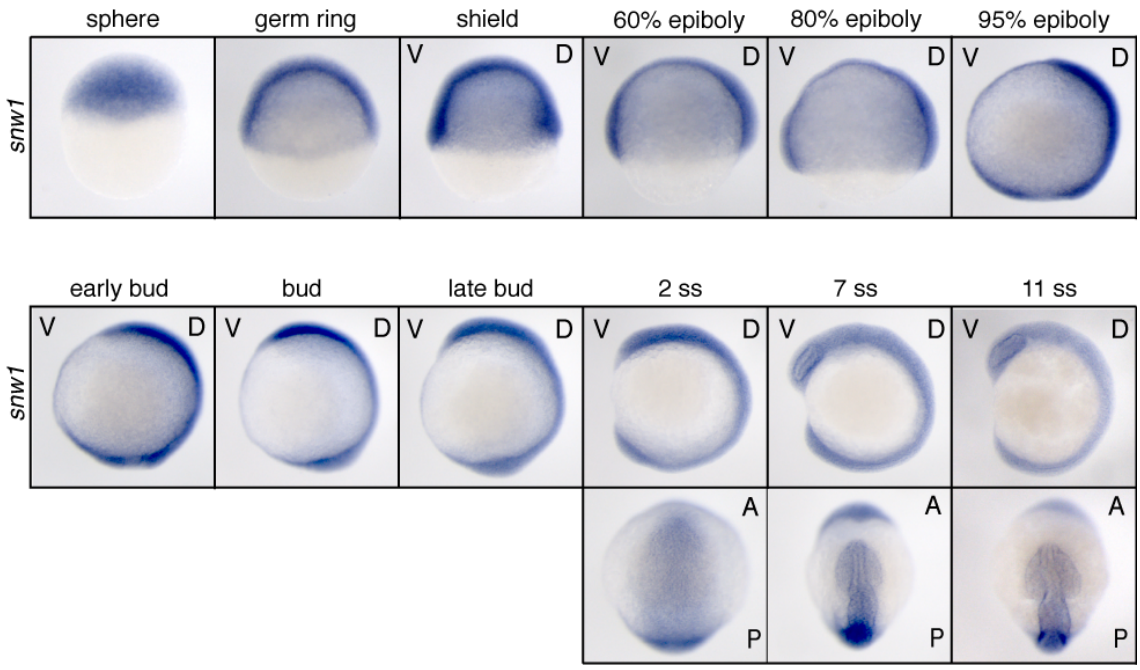

Figure 5.4 Temporal expression pattern of *snw1* during early zebrafish development
ISH for snw1 at the indicated stages. Lateral views; from 2 ss onwards lateral view (upper panel) and dorsal anterior view (lower panel).

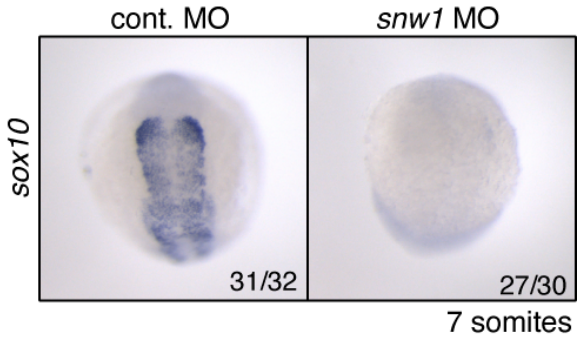

Figure 5.5 SNW1 function is conserved in zebrafish
ISH of embryos injected with 10 ng control or snw1 MO using probes against sox10. Numbers indicate the embryos with the observed phenotype for a representative experiment. Embryos shown in dorsal view with anterior to the top.

As shown in X. laevis, in zebrafish snw1 is ubiquitously expressed from early embryogenesis onwards and becomes then restricted to the NP after gastrulation (**Figure 5.4**, (Wang et al., 2010b, Wu et al., 2011)). Furthermore, depletion of Snw1 in zebrafish embryos resulted in a loss of the NC marker sox10 (**Figure 5.5**, (Wu et al., 2011)).

Taken together, these analyses confirm a conserved expression pattern as well as a requirement for Snw1 in NC induction.

5.2.3 Snw1 is essential for BMP and Wnt signalling in zebrafish

Using the transgenic *Tg(BRE:mRFP)* zebrafish BMP reporter line, our lab had previously demonstrated that Snw1 is required for NPB formation by regulating BMP activity in this domain (Wu et al., 2011). Indeed I could confirm that l.1oss of Snw1 resulted in a global reduction of BMP activity visualised by *mRFP* ISH staining in *Tg(BRE:mRFP)* embryos (Figure 5.6).

In *X. laevis* Snw1 has been shown to modulate Wnt/β-catenin signalling (Wang et al., 2010b)(1.4.2.3), thus giving a possible alternative explanation for the loss of NC in *snw1* morphants. I wanted to test whether this also holds true in zebrafish embryos. For this purpose I used the transgenic *Tg(7xTCF-Xla.Siam:GFP)*^{ia4} Wnt reporter line, which expresses eGFP under the control of seven multimerised TCF responsive elements upstream of the minimal promoter of the *X. laevis* direct β-catenin target gene *siamois* (Moro et al., 2012). At the two

somite stage ISH using probes against *gfp* revealed Wnt activity in the posterior NP, but not in the NC, although BMP activity can be detected in NC derived cells at later stages (Figure 5.7A, (Moro et al., 2012)).

I then went on to test the requirement of Snw1 for Wnt signalling in zebrafish. Indeed, depletion of Snw1 resulted in a loss of Wnt activity in *Tg(7xTCF-Xla.Siam:GFP)*^{ia4} embryos (Figure 5.7B), as had been previously reported in *X. laevis* and in tissue culture cells (Wang et al., 2010b).

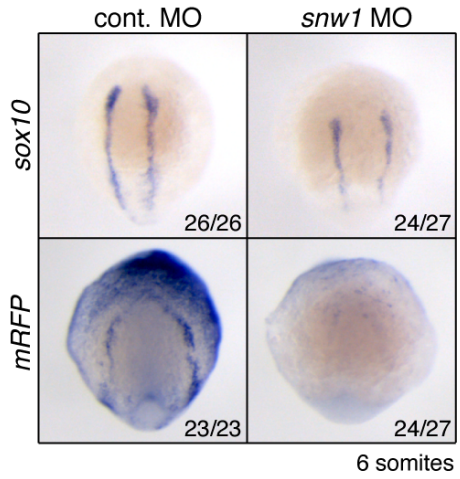

Figure 5.6 Snw1 is required for BMP activity at the NPB during NC development (zebrafish)

ISH on Tg(BRE:mRFP) embryos injected with 10 ng of a control or snw1 MO using probes against the NC marker sox10 or mRFP for detection of BMP activity.
Numbers indicate the embryos with the observed phenotype for a representative experiment. sox10 phenotype is weaker as embryos were injected at the 2-4 cell stage (instead of 1-2 cell stage). All views show embryos dorsal view with anterior to the top.

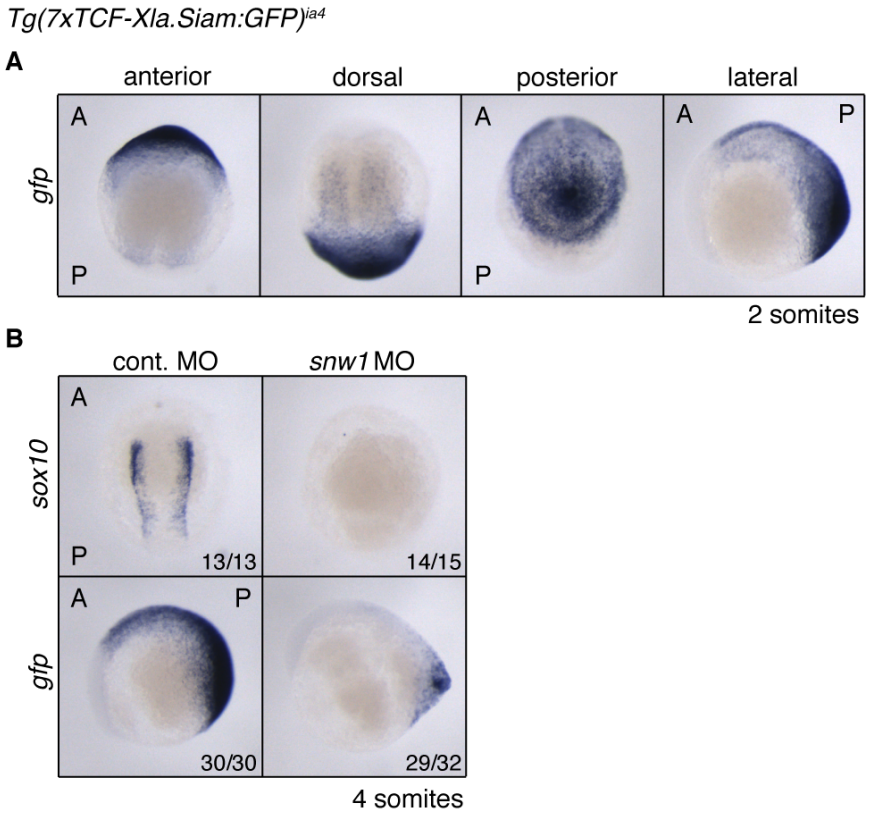

Figure 5.7 Snw1 is required for canonical Wnt signalling in zebrafish embryos
(A) *gfp ISH on 2 somite stage embryos. Orientations are as indicated.*
(B) *ISH on embryos injected with either 10 ng control or snw1 MO using probes against sox10 and gfp. sox10 are displayed in a dorsal anterior view with dorsal to the top, gfp stained embryos are oriented in a lateral view with anterior to the left.*
Numbers indicate the embryos with the observed phenotype for a representative experiment.

5.2.4 The dependence of the NC on BMP and Wnt signalling at different developmental stages

As demonstrated in Chapter 3, BMP signalling is required throughout early development for NC induction and maintenance (Figure 3.3). Similarly Wnt signalling has been implicated at different steps of NC development (Dorsky et al., 1998, Lewis et al., 2004, Steventon et al., 2009). In *X. laevis,* global inhibition of BMP and Wnt signalling by overexpression of the BMP antagonist *noggin* (Zimmerman et al., 1996) or the Wnt antagonist *dickkopf 1* (*dkk1*) (Glinka et al., 1998) prevents the expression of NC markers (Figure 5.8).

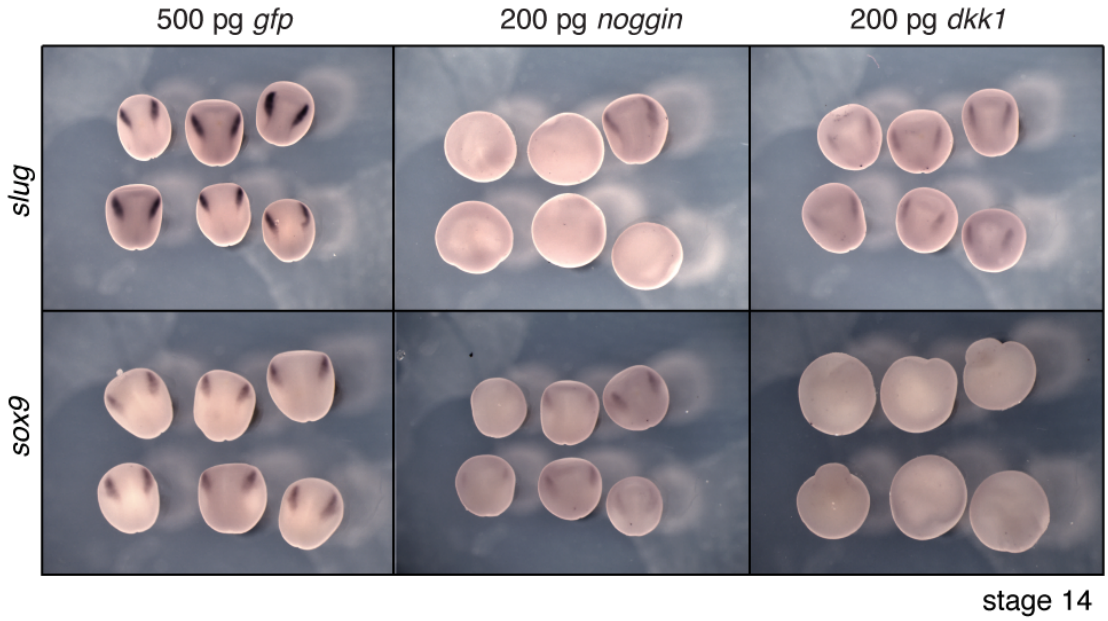

Figure 5.8 Inhibition of BMP and Wnt signalling abolishes NC cell fate in *X. laevis*
ISH on X. laevis embryos injected with the indicated mRNA. Probes against slug and sox9 mark the NC cell population. Dorsal view with anterior to the top.

The previous experiment demonstrated that both BMP and Wnt signalling are important in NC development (Figure 5.8). Loss of Snw1 impaired the activity of both pathways (Figure 5.7). Thus it is not clear whether the NC phenotype in *snw1* morphants is due to an inhibition of BMP or Wnt signalling or a combination of both. It was therefore important to determine what the contribution of either pathway to NC development in the context of this study is at the time of NC induction. For this purpose I made use of chemical modulators that were added to the water of dechorionated developing embryos at early-gastrulation to achieve inhibition when NC is induced. This also recapitulates the timing of effective Snw1 depletion (Wu et al., 2011).

I added Leflunomide (White et al., 2011) to inhibit BMP activity (6.2.7 [1]) and the tankyrase inhibitor XAV939 was added to inhibit Wnt signalling (Huang et al., 2009). I then monitored the expression of the NC marker *sox10* as well as the activity of the signalling pathways using the respective transgenic reporter lines.

[1] I show in Chapter 5 that Leflunomide, a known regulator of NC development, effectively inhibits BMP activity.

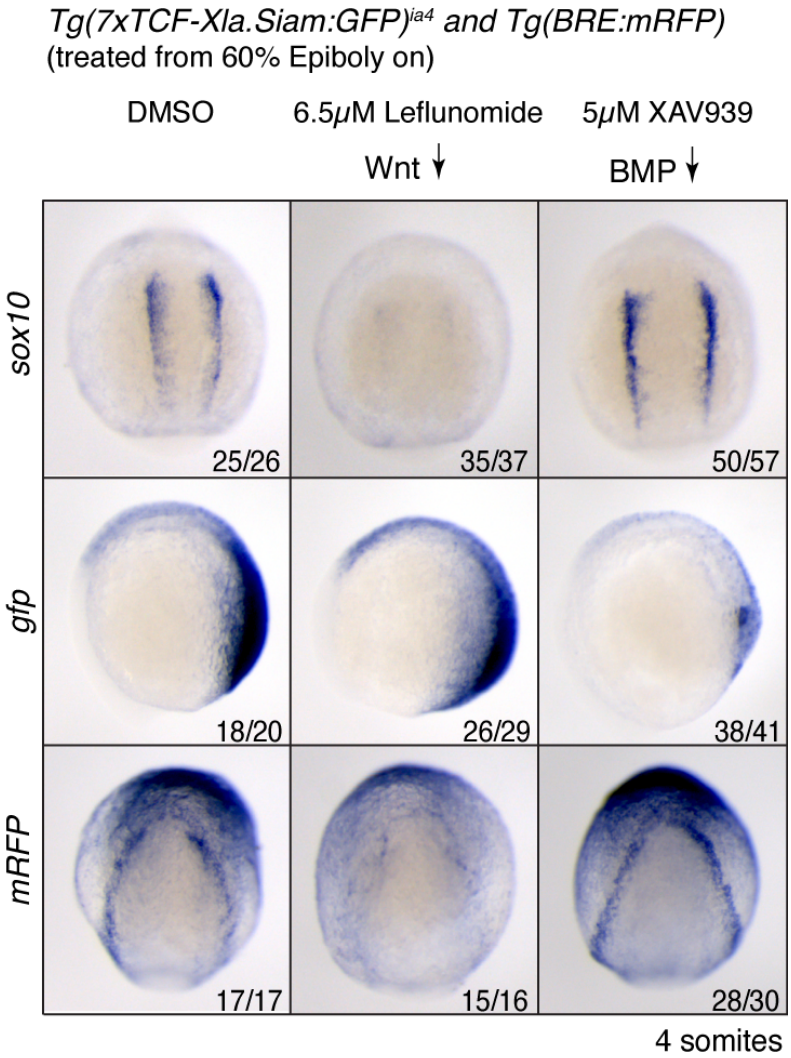

Figure 5.9 Modulation of BMP and Wnt activity during NC induction in zebrafish
ISH using probes against sox10, gfp and mRFP of embryos treated with the indicated chemical modulators from 60% epiboly onwards. Numbers indicate the embryos with the observed phenotype for a representative experiment. All views show embryos in an dorsal view with anterior to the top.

Inhibition of BMP signalling, confirmed by loss of *mRFP* in *Tg(BRE:mRFP)* embryos, efficiently prevented NC induction. In contrast, I did not observe an effect on Wnt signalling activity, indicating that inhibition of BMP activity alone is sufficient to abolish NC cell fate. Furthermore, inhibition of Wnt signalling did not affect BMP activity and did not perturb NC induction.

Taken together, this data indicates that the NC phenotype observed in *snw1* morphants is most likely due to a loss of BMP activity, rather than inhibition of Wnt signalling.

5.2.5 Ectopic expression of Snw1 does not modulate BMP activity in *X. laevis* embryos

Depletion of Snw1 inhibits BMP activity in *Tg(BRE:mRFP)* embryos, which is also demonstrated in a loss of PSmad1/5 levels detected by Western blot analysis, especially in post-gastrulation embryos (Wu et al., 2011). Additionally, overexpression of Snw1 in *X. laevis* resulted in an increase of PSmad1/5 in Western blots (Wu et al., 2011). Knockdown studies in tissue culture, however, indicate that Snw1 does not act downstream of the BMP receptors as depletion in MDA-MB-231 cells does not impair the cellular response to recombinant ligand stimulation (Wu et al., 2011). Moreover, the Snw1 phenotype can be rescued in *X. laevis* by targeted injection of *bmp2b* cDNA, indicating that the cells are competent to respond to a BMP stimulus (Wu et al., 2011).

To further elucidate the prevalent mechanism I cloned a *X. laevis* GFP-tagged Snw1. Snw1 has been described as a nuclear factor (Dahl et al., 1998).

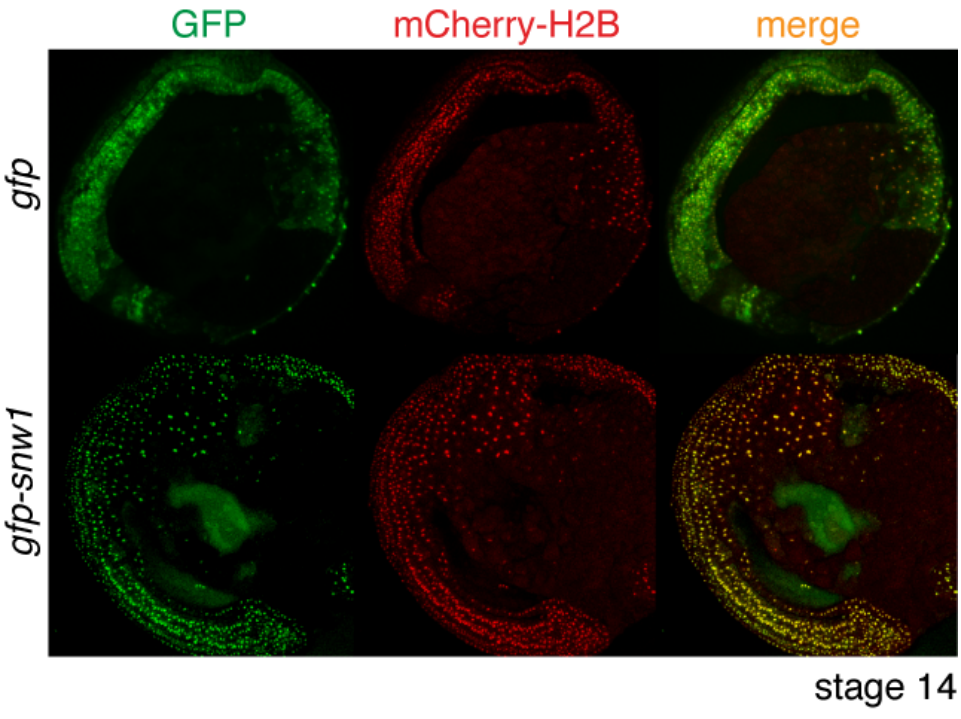

Figure 5.10 Snw1 is localised to the nucleus (*X. laevis*)
X. laevis embryos were injected with 250 pg either gfp or gfp-snw1 mRNA as well as 375 pg mcherry-h2b. Embryos were injected in both cells at the 2-cell stage, fixed at stage 14 and then bisected along the dorsal anterior-posterior axis for imaging under a fluorescent microscope.

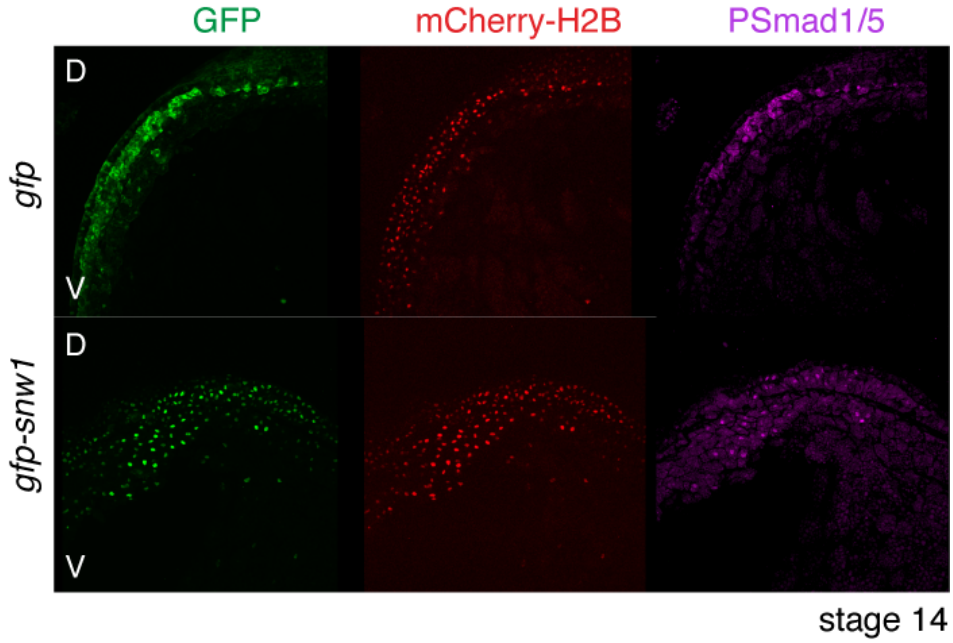

Figure 5.11 Ectopic expression of Snw1 does not increase PSmad1/5 levels (*X. laevis*)
X. laevis embryos were injected as in Figure 5.10. PSmad1/5 staining was performed and neural folds were imaged using a fluorescent microscope.

Indeed, GFP-Snw1, overexpressed in *X. laevis* from injected mRNA, could be detected exclusively in the nucleus, whereas GFP alone was also present in the cytoplasm (Figure 5.10). Coinjection of *mcherry-h2b* marked the nucleus and also indicated injected cells.

I next wanted to test whether overexpression of Snw1 in *X. laevis* was sufficient to increase cellular PSmad1/5 levels. I injected embryos as detailed in the previous experiment and performed PSmad1/5 immunostaining on embryos that where bisected along the dorsal-ventral axis to image the neural folds where the NC is induced. No increase in PSmad1/5 could be detected compared to *gfp*-injected control embryos and there were clearly cells present that expressed high levels of GFP-Snw1, but were low in nuclear PSmad1/5. This indicates that overexpression of Snw1 is not sufficient to activate cellular BMP activity or that Snw1 is not a limiting factor for BMP activity in the neural folds. Please not that I here assume the GFP-Snw1 is active as it is folded well enough to be localised to the nucleus. However, I don't formerly show this.

5.2.6 Loss of Snw1 increases *bmp2b* mRNA levels at the NPB but reduces Bmp2b protein levels

As outlined in the Introduction, Snw1 has been implicated as a transcriptional co-regulator that recruits, depending on the cellular context, activating or repressing complexes to mediate various signalling pathways. Moreover, previous work in our lab indicated, that Snw1 likely acted downstream/at the level of ligand transcription and upstream of receptor activation (Wu et al., 2011) (1.4). It was therefore conceivable that Snw1 acts on the transcriptional regulation of BMP signalling components to regulate pathway activity. To test this I performed ISH using probes against Bmp ligands that are required for BMP activity at the NPB. Surprisingly, I observed a dramatic increase in *bmp2b* mRNA (Figure 5.12). This effect is specific to the NPB where the *bmp2b* expression domain is likely to overlap with *snw1* expression (Wu et al., 2011). In contrast, *bmp7a* levels did not seem to be significantly changed (Figure 5.13).

Thus, I observed an increase in *bmp2b* transcripts despite a loss of BMP activity at the NPB. A possible explanation would be inefficient mRNA processing or subsequent translation.

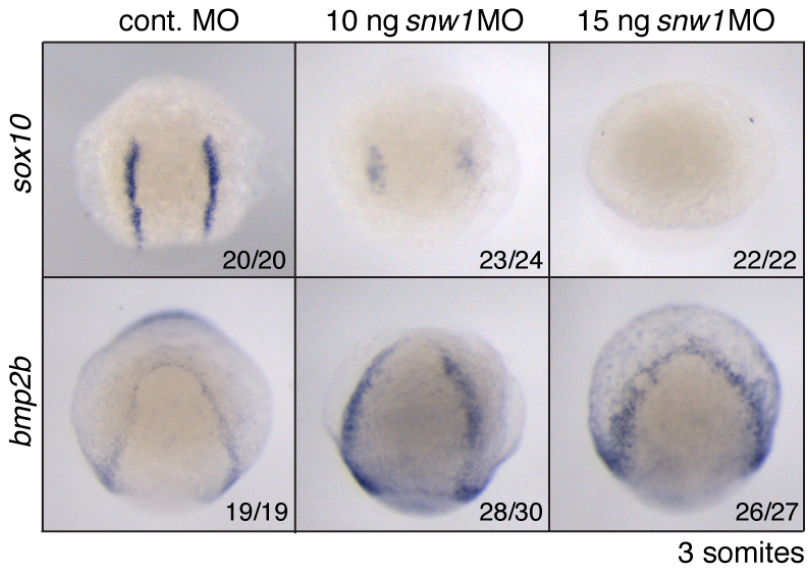

Figure 5.12 *bmp2b* is increased at the NPB in *snw1* zebrafish morphants
ISH using probes against sox10 and bmp2b on embryos injected with the indicated amounts of snw1 MO. All views show embryos in an dorsal view with anterior to the top.

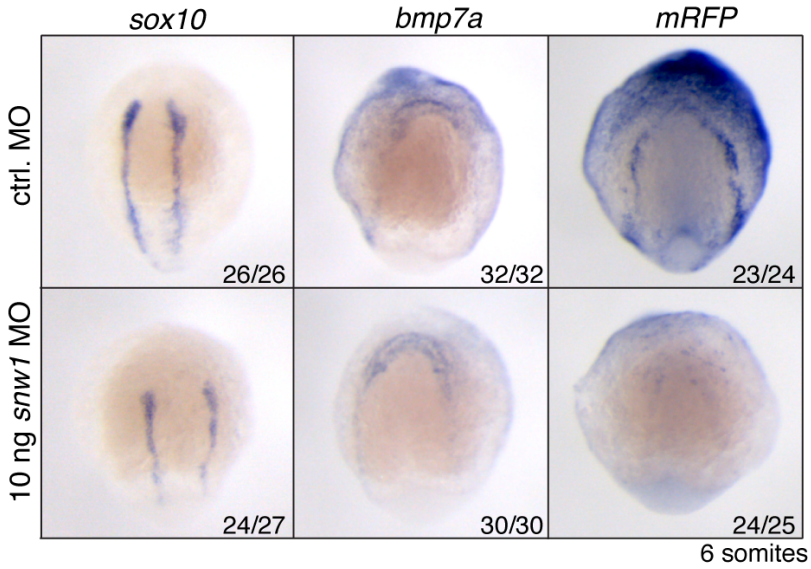

Figure 5.13 Loss of Snw1 in zebrafish does not affect *bmp7a* transcript levels
ISH using probes against sox10, bmp7a and mRFP on snw1 morphants. Numbers indicate the embryos with the observed phenotype for a representative experiment. . All views show embryos in an dorsal view with anterior to the top.

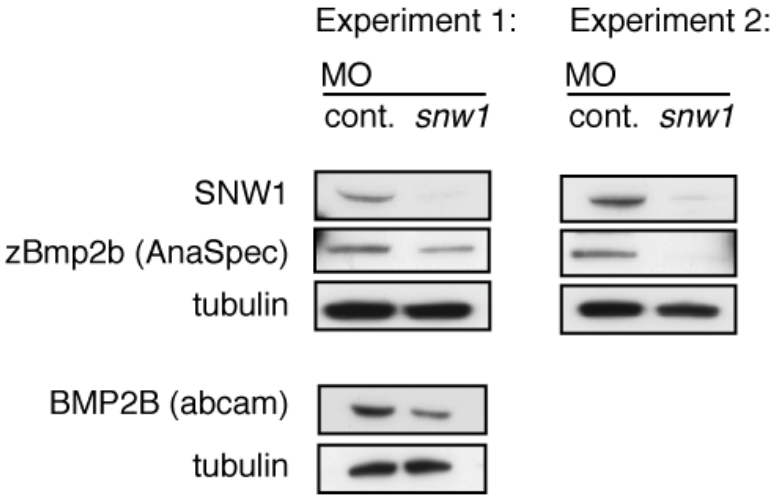

Figure 5.14 Bmp2b expression is decreased in *snw1* morphants
Western blot analysis of Snw1-depleted embryos using the indicated antibodies. Lysates of 3 somite stage embryos from two independent experiments were analysed.

I investigated this using two antibodies against the Bmp2b protein. A zebrafish specific antibody, that recognises the pro-protein, but not the mature form (AnaSpec) and an antibody against the human, processed Bmp2 (abcam). In two independent experiments I could show decreased levels of Bmp2b in 3 somite stage *snw1* morphant embryos (Figure 5.14).

5.2.7 Gene expression at the NPB does not seem to be global changes

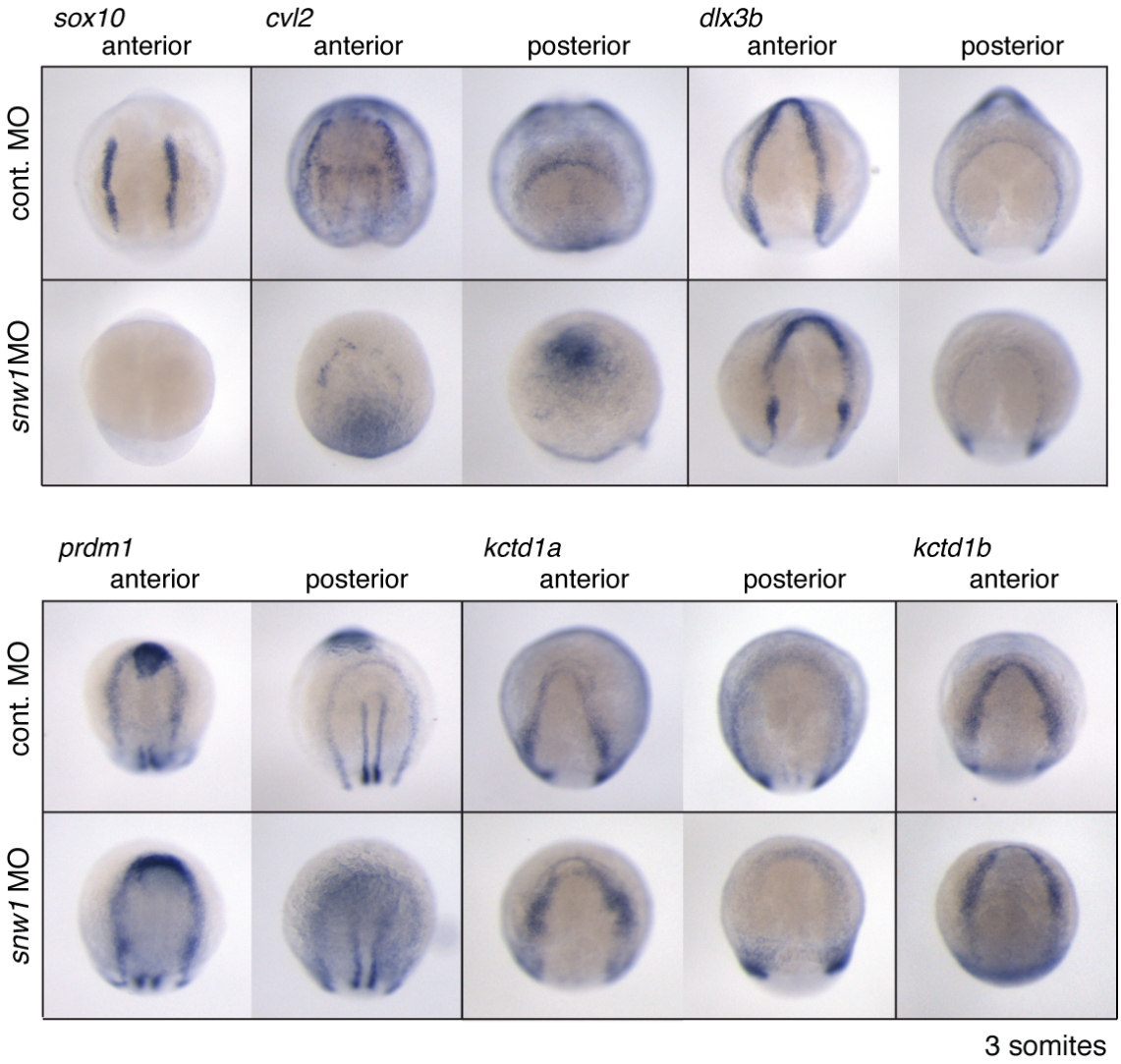

Figure 5.15 Expression of NPB markers in *snw1* morphants
ISH using probes against sox10, cvl2 and the NPB markers dlx3b, prdm1, kctda15a and kctd15b on snw1 morphants. Orientation is as labelled above. . All views show dorsal view with anterior or posterior to the top as indicated.

To investigate how general the change of gene expression at the NPB was in *snw1* morphants and whether tissue patterning *per se* was changed I performed ISH using probes against several NPB markers. Consistent with a requirement of Snw1 for BMP signalling, expression of *cvl2* was significantly decreased in Snw1-depleted embryos. However, expression of none of the other NPB markers was changed (Figure 5.15). Note also that the NP does not seem to be extensively broader, indicating that Snw1 is not required for early BMP activity during dorsal-ventral axis formation. This is consistent with experiments that showed a significant reduction in PSmad1/5 only after gastrulation in *snw1* morphants ((Wu et al., 2011).

Taken together, I demonstrated that the defect in NC development in *snw1* morphants is likely to result from an inhibition of BMP activity rather than Wnt signalling. Surprisingly, BMP signalling is inhibited upon loss of Snw1 despite an increase in *bmp2b* transcripts at the NPB.

5.3 Discussion

5.3.1 Summary of results

- As previously shown, overexpression and knockdown of Snw1 inhibits NC development in *X. laevis.*
- This function is conserved in zebrafish.
- Snw1 is required in the NC cells for its function.
- Loss of Snw1 inhibits BMP activity and Wnt signalling in neurula stage embryos.
- The *snw1* morphant phenotype is likely to be conferred by a loss of BMP signalling and not inhibition of Wnt signalling.
- Snw1 depletion leads to a loss of Bmp2b protein expression despite an increase in *bmp2b* transcripts at the NPB.
- The expression of *bmp7a* and several NPB markers is unchanged after Snw1-depletion.

5.3.2 Snw1 functions in NC development

A previous study in our lab provided evidence for a role for Snw1 in vertebrate development (Wu et al., 2011). In both *X.laevis* and zebrafish, depletion of Snw1 abolishes NC cell fate. RNAi-mediated loss of Snw1 causes gastrulation defects in *C. elegans* and leads to post-gastrulation lethality in *Drosophila* (Kostrouchova et al., 2002, Negeri et al., 2002). Similarly, in vertebrates Snw1 is likely to be required for gastrulation. However, maternally deposited protein appears to be stable enough to provide Snw1 protein that is sufficient for normal gastrulation. Depletion of Snw1 using a morpholino approach seems only to be efficient from mid-late gastrulation as measured by Snw1 protein and Smad1/5 phosphorylation levels using western blot (Wu et al., 2011). This meant we were able to circumvent defects in early embryonic development and determine Snw1 function at later developmental stages.

Combined signals from the NNE and the NP, both abutting the NC, and the underlying mesoderm are thought to contribute to NC induction (reviewed in (Stuhlmiller and Garcia-Castro, 2012a). I therefore wanted to ask in which cells was Snw1 specifically required for its function by using targeted injections of the *snw1*

MO in *X. laevis*. Only targeting the *snw1* MO directly to the prospective NC abolished expression of the NC marker *slug*, whereas loss of Snw1 in adjacent cells yielded no effect. This suggests that Snw1 is not required for the expression of a secreted factor in the surrounding tissue, but for signals in the NC cell population itself as I will further discuss later.

5.3.3 The Snw1 NC phenotype is likely a result of BMP activity inhibition and not lack of canonical Wnt signalling

Snw1 is required for BMP activity at the NPB (Wu et al., 2011) and has also been implicated in inhibiting Wnt signalling during NC induction as part of the LEF1/TCF transcriptional complex (1.4.2.3) (Wang et al., 2010b).

During early embryonic development, BMP signalling is indispensable for the establishment of the DV axis. BMP pathway mutants display ectodermal patterning defects including an expansion of neural tissues at the expense of ventral tissues (Schumacher et al., 2011, Tucker et al., 2008). Strong inhibition of BMP activity, such as in the zebrafish *swirl/bmp2b* mutant, results in a loss of NC progenitors whereas reduction of BMP activity to intermediate levels as in *somitabun/smad5* and *snailhouse/bmp7a* mutants expands the population of NC marker positive cells. This suggests that intermediate levels of BMP signalling are required to create a NC “competency” zone for initial NC induction. Similarly, I have previously shown that inhibition of BMP activity during mid-gastrulation, when the NC is induced, abolished expression of NC markers (Figure 3.3). Moreover, BMP signalling is essential for NC maintenance during early somitogenesis (Figure 3.3) (Steventon et al., 2009).

The importance for Wnt signalling in the patterning of the vertebrate anterior-posterior axis has been extensively studied (Kiecker and Niehrs, 2001, Yamaguchi, 2001). Moreover, maternally deposited Wnt8b contributes to DV patterning (Pandur et al., 2002). Thus, disturbing Wnt signalling prior to stages when NC induction occurs might have indirect effects on NC due to early ectodermal patterning defects, similar to early inhibition of BMP activity. This likely explains the lack of NC in *X. laevis* embryos injected with *noggin* (BMP inhibition) or *dkk1* (Wnt inhibition) mRNA (Figure 5.8). At later stages, evidence from the

ectopic expression of several Wnt ligands argues that Wnt activity is a positive regulator of NC induction (Bang et al., 1999, Saint-Jeannet et al., 1997). Also, inhibition of Wnt signalling by expressing a truncated version of the tcf3 gene *headless* in response to heat shock at bud stage, but not after 3 somite stage, led to a loss of NC, indicating a stage-specific requirement for Wnt activity during NC development (Lewis et al., 2004). Lewis et al. went on to identify *wnt8a* as the ligand expressed during NC induction at 80% epiboly. However, *wnt8a* is not expressed in the NC at stages when the authors perform the heat shock experiments and show Wnt signals to be important. Moreover, loss of Wnt8 only delays the onset of NC marker expression but does not abolish it. In my experimental setup, Wnt signalling seemed not to be required for NC induction. Abolition of Wnt activity by the use of a chemical inhibitor from gastrulation onwards did not affect the NC cell population, in contrast to inhibition of BMP signalling. I cannot exclude the possibility that Wnt signals were not sufficiently blocked to impair NC induction. Nevertheless, from currently available studies, it is still not clear whether Wnt-mediated effects on NC induction are direct or indirect.

My analysis suggests, that even if loss of Snw1 impairs Wnt as well as BMP activity, the effect on NC at the investigated stages is likely a BMP-dependent phenotype. Further investigations, for example using heat-shock inducible zebrafish models, will be required to further delineate the involvement of both signalling pathways in NC development. Moreover, as Wnt is anterior-posterior axis formation, it would be interesting to test whether anterior-posterior patterning is affected in Snw1 morphants.

5.3.4 Bmp2b can rescue the Snw1 phenotype

Snw1 plays an essential role in regulating BMP activity post gastrulation. Analyses in tissue culture cells have indicated it is not part of the core-signalling pathway, as cells depleted of Snw1 show a wild-type response to recombinant Bmp ligand exposure (Wu et al., 2011). This is in contrast with previous studies, which reported overexpressed Snw1 interacting with Smad proteins to enhance TGF-β-and Bmp-dependent signalling (Figueroa and Hayman, 2004, Leong et al., 2001). Moreover, data from our lab has provided evidence that targeted expression of *bmp2b* cDNA

can rescue the NC phenotype in *snw1 X. laevis* morphants, demonstrating the sustained ability of cells to respond to Bmp ligand stimulation. The injection of cDNA also circumvents the regulation via the 5'UTR or 3'UTR and the requirement for splicing. It would be interesting to test whether in zebrafish Bmp2b expressed in response to a heat shock can also rescue the NC phenotype. Importantly, this experiment argues against a Wnt-dependent Snw1 phenotype on NC as re-expression of Bmp2b alone is sufficient for rescue. Taken together, our evidence places Snw1 upstream of receptor activation and at the level/downstream of ligand transcription.

To further elucidate the function of Snw1 I investigated Bmp ligand transcription at the NPB of zebrafish embryos. Previous research in had indicated that bmp2b transcript levels might not be changed but the expression domain sharpened to the NPB {Wu, 2011 #33}. I revisited this observation and could show that whereas the expression of *bmp7a* in *snw1* morphants was not altered, the abundance of *bmp2b* transcripts was strongly increased. This effect was limited to the neural plate border, where Bmp activity and *snw1* expression overlap, arguing for a direct effect on *bmp2b* ligand levels. Importantly, despite increased *bmp2b* transcript levels, Bmp2b protein appears to be reduced in *snw1*-depleted embryos. This indicates a role for Snw1 in co- or post-transcriptional processing of *bmp2b* ligands. Given the broad expression pattern of Snw1, *bmp2b* is unlikely to be the sole target. Therefore it was important to determine how specific the effect of Snw1 depletion on *bmp2b* was and whether levels of other transcripts were similarly changed, as I will address in the following chapter.

5.3.5 Possible functions of Snw1

The function of Snw1 in NC is conserved between *X. laevis* and zebrafish. The NC phenotype observed in Snw1-depleted embryos is most likely due to impaired BMP activity at the NPB as demonstrated in zebrafish embryos. Importantly, despite of inhibition of BMP signalling, *bmp2b* transcripts can still be detected and are actually increased at the NPB where *snw1* and *bmp2b* expression overlap. This phenotype can be explained by the loss of Bmp2b protein expression. Moreover, it is clear that the cells at the NPB can still respond to a BMP stimulus as

targeted injection of *bmp2b* cDNA can rescue the NC phenotype in *X. laevis*. This approach circumvents the necessity of splicing as well as any regulation conferred by the 5'- or 3' UTR. In summary, the data so far suggests that Snw1 function at the level of ligand transcription or co-/post-transcriptional processes.

Snw1 has been implicated in a range of such processes as described in the Introduction. For example, Snw1 was described as a component of the activated spliceosome in *S.cerevisiae, S.pombe* and *H.sapiens* in several independent screens (Ajuh et al., 2000, Gavin et al., 2002, Neubauer et al., 1998, Ohi et al., 2002, Zhou et al., 2002). The exact function of Snw1 in splicing is yet to be revealed, however, a recent publication reports Snw1 contributing to the splicing efficiency of substrates not conforming to the consensus (Gahura et al., 2009). It is not clear whether *snw1* belongs to this class of transcripts.

Apart from its role in splicing, Snw1 has been implicated as a transcriptional co-regulator that recruits, depending on the cellular context, activating or repressing complexes to mediate various signalling pathways such as Wnt, VDR, Notch and TGF-β signalling (1.4). As explained earlier, we exclude a role for Snw1 downstream of TGF-β/BMP receptor activation, as Snw1-depleted cells are still responsive to BMP signalling *in vivo* as well as in tissue culture.

Recent work by the Katherine A. Jones lab suggested a different role for Snw1 (Bres et al., 2005, Bres et al., 2009, Chen et al., 2011). As explained in more detail in 1.4.3, their work suggests that SNW1 is associated with the P-TEFb transcriptional elongation complex and is required for HIV-1 Tat transactivation. Moreover, SNW1 binds the U5snRNP and can facilitate the recognition of alternative HIV-1 Tat splice sites. Under DNA damage stress, SNW1 and P-TEFb become dispensable for HIV1 Tat transactivation. However, SNW1 is then required for gene-specific splicing of *p21.*

Taken together, Snw1 is an important regulator of BMP activity at the NPB and required in the NC cell population for NC development. Interestingly, despite inhibition of BMP activity and loss of Bmp2b protein expression in snw1 morphants, *bmp2b* transcript levels are significantly increased. This holds not true for other transcripts at the NPB. It is an intriguing possibility that Snw1 is necessary for gene-specific splicing during developmental processes. Impaired splicing of the bmp2b transcript might then lead to the accumulation of unspliced pre-mRNA and would explain the increased transcript levels at the NPB.

Chapter 6.

6.1 Introduction

As described in the previous chapter, Snw1 is a regulator of NC development and BMP activity. Loss of Snw1 inhibits BMP signalling and Bmp2b expression despite an increase of *bmp2b* transcript levels at the NPB.

Snw1 was first described in *Drosophila,* where it is called Bx42 and was found to be specifically expressed in a series of developmentally-active puffs on salivary gland chromosomes (Saumweber et al., 1990). Snw1 has a diverse, highly conserved protein structure and has been suggested to act as a scaffold in large protein complexes (Figure 1.6). Indeed, Snw1 has been then reported to interact with an extensive list of binding partners and has been implicated in a range of processes, such as splicing and transcriptional co-regulation (1.4) (Bres et al., 2005, Luo et al., 1999, Zhou et al., 2000). The molecular mechanism that leads to the embryonic *snw1* morphant phenotype and inhibition of BMP activity has not been described. In this chapter, I will further investigate Snw1's mechanism of action using global approaches such as mass spectrometry and RNA sequencing.

6.2 Results

6.2.1 Mass spectrometry analysis of SNW1 interaction partners

Previous analysis has yielded a plethora of Snw1 interaction partners, many of which were identified in yeast-2-hybrid screens and overexpression studies (Barry et al., 2003, Bres et al., 2009, Zhou et al., 2000). In an unbiased approach, I aimed to confirm and identify SNW1 interaction partners by performing an SNW1 pull-down and analysing associated proteins by mass spectrometry. This assay was aimed to clarify the processes SNW1 is involved in. To this end I generated HEK293T cell lines expressing stably Flag-tagged human SNW1 (Figure 6.1A). For the further analysis I selected a cell line expressing endogenous levels of Flag-SNW1. I performed several repeats of the experiment detailed below to ensure the accuracy the results. First, a large scale Flag-IP was performed. After initial experiments I included a benzonase endonuclease step to minimise indirect

interactions mediated by DNA/RNA. A cell line expressing just the Flag-tag was used as a control. The protein complexes were then eluted in five fractions using a 3xFlag peptide. An aliquot of each of the different elution fractions was analysed by western blot to determine which elution steps should be pooled and to ensure that the samples had not degraded (Figure 6.2). Elutions 2-4 were combined and the samples concentrated to a suitable volume.

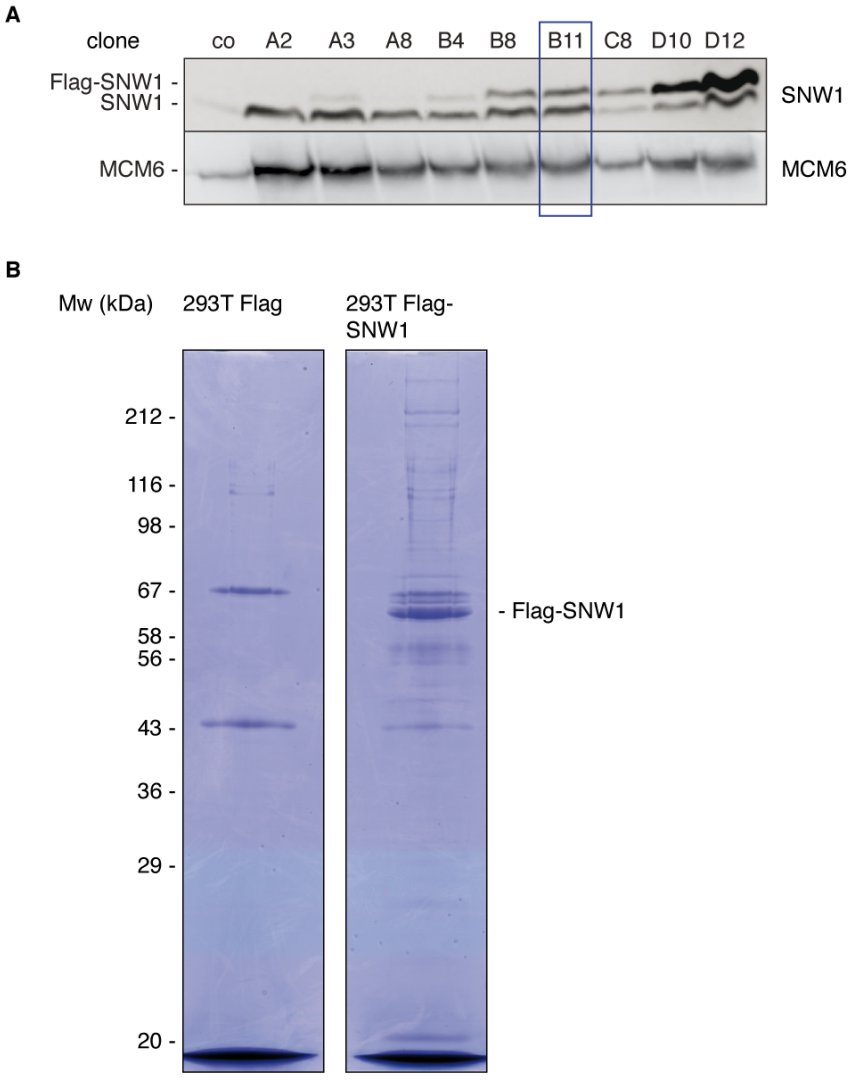

Figure 6.1 The Flag-Snw1 expressing cell line

A *HEK393T cells were stably transfected with a plasmid expressing Flag-SNW1 and clones were analysed by western blotting. Cell line B11 was selected for further experiments.*

B *A representative example of a coomassie stained 12.5% SDS-PAGE of Flag-IP samples submitted for mass spectrometry analysis. A Flag expressing cell line was used as a control.*

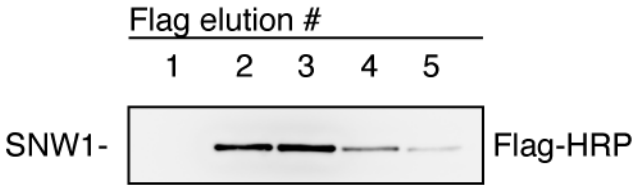

Figure 6.2 Western blot analysis of Flag elutions
Western blot analysis of the different Flag elutions using a Flag-HRP antibody to determine which elutions should be pooled.

The samples were then run on a 12.5% SDS-PAGE and Coomassie stained (Figure 6.1B). The relevant lanes were cut into 1 mm thick stripes and submitted for analysis by mass spectrometry. To determine SNW1 interaction partners, proteins were selected that were only present or significantly more abundant in the Flag-SNW1-IP compared to the IP from the Flag only expressing cell line (Appendix 4). This was subsequently confirmed by intensity-based absolute quantification (iBAQ), which normalises peak intensities to the theoretically observable peptides and thus provides an accurate estimation of protein levels ((Schwanhausser et al., 2011), Appendix 5). Moreover, I considered a published list of common background contaminants from the Flag-IP procedure in HEK293 cells (Chen and Gingras, 2007).

Snw1 has been described as a component of the spliceosome in *S.cerevisiae, S.pombe* and *H.sapiens* in several independent screens (Neubauer et al., 1998, Ajuh et al., 2000, Gavin et al., 2002, Ohi et al., 2002, Zhou et al., 2002). Similarly, I found SNW1 to be associated with splicosomal proteins, especially components of the Cdc5/Prp19 subcomplex, which is part of the B* and C complexes and the post-spliceosomal species (Albers et al., 2003, Makarov et al., 2002) Figure 6.3, Appendix 1).

My analysis also identified interactions with many chromatin-associated proteins such as SWI/SNF complex components and histone modifiers such as SETD2, RUVBL1 and RUVBL2 (Appendix 2). This is in agreement with the concept of a tight coupling of transcriptional processes, chromatin modifications and splicing (Montes et al., 2012).

To validate the results obtained using mass spectrometry analysis, I performed co-IPs of SNW1 using the Flag-SNW1 expressing cell line (Figure 6.4A) as well endogenous IPs when possible (Figure 6.4B). I corroborated the specific interaction of SNW1 with several spliceosome-associated proteins. As described in the previous chapter, SNW1 was proposed to interact with the transcriptional repressor SKI, which is a negative regulator of the BMP signalling pathway (Wang et al., 2000)(1.4.2.4). Hence the alternative name for SNW1, SKIP (SKI-interacting protein). However, I could not detect such an interaction either by mass spectrometry or co-IP, consistent with previous results from our lab (Wu et al., 2011).

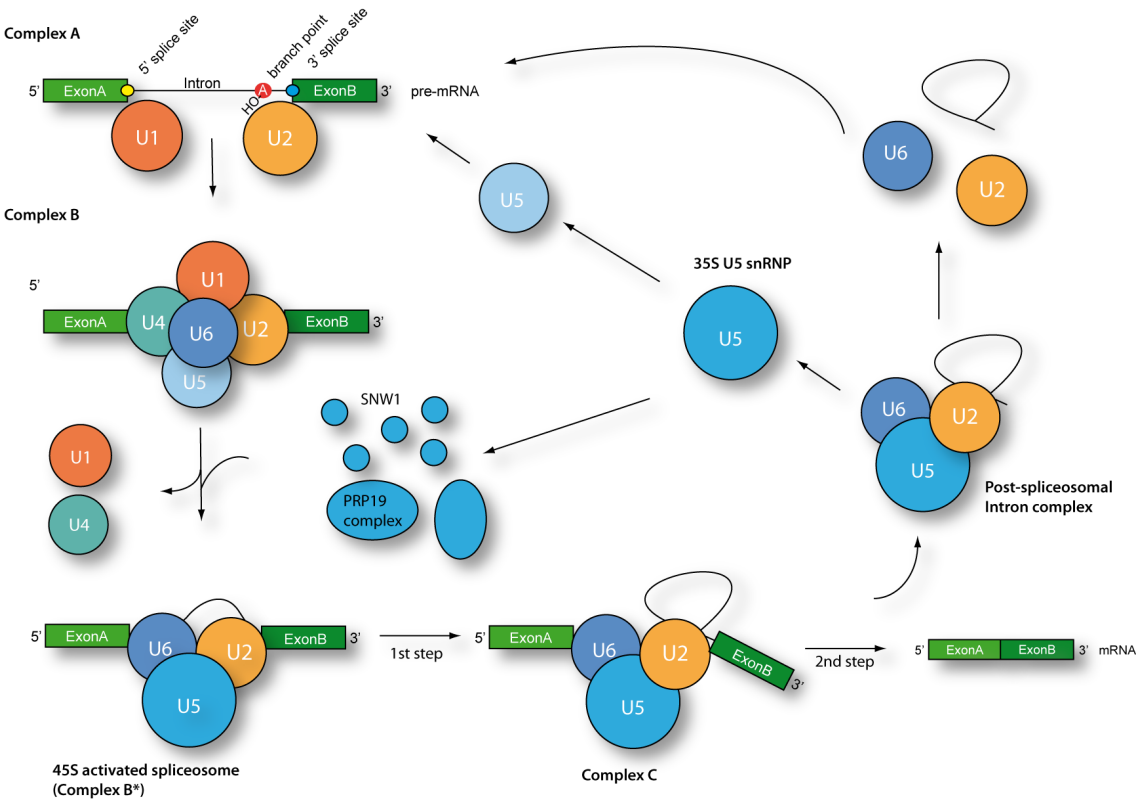

Figure 6.3 Schematic diagram of spliceosomal and snRNP remodelling events (adapted from (Makarov et al., 2002))
Complexes in dark blue contain SNW1.

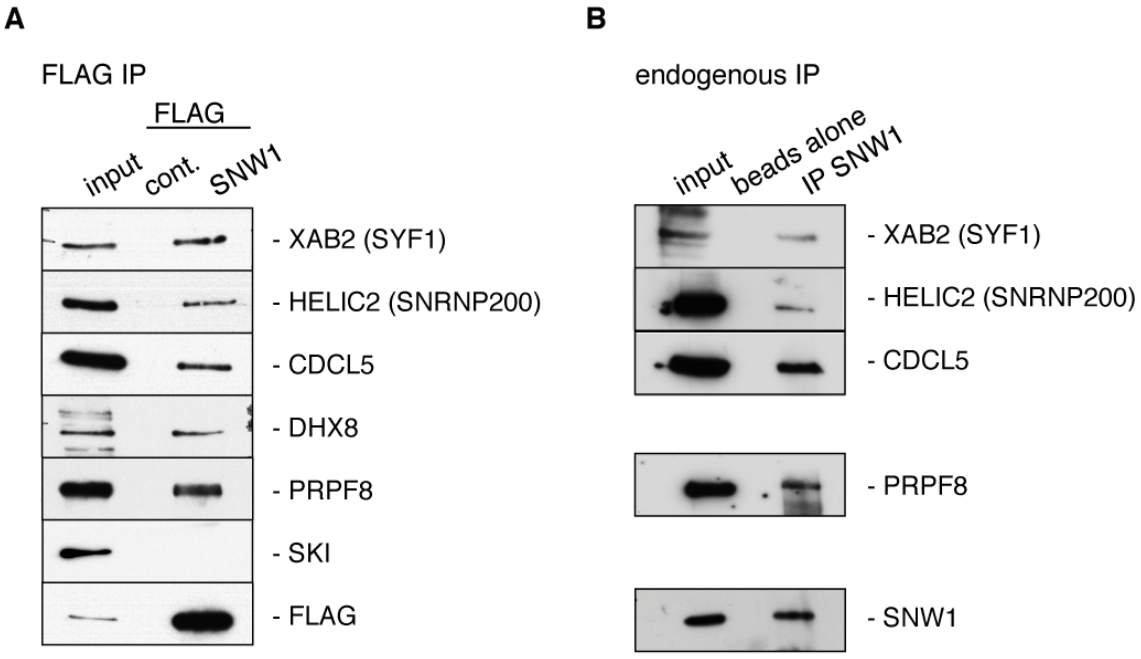

Figure 6.4 Validation of SNW1 interaction partners using IP
(A) *Flag-IP from whole cell extracts of HEK293T cells expressing FLAG-SNW1.*
(B) *Endogenous IP for SNW1 from HEK293T whole cell extracts.*
Western blotting was performed using the indicated antibodies.

Taken together, my analyses confirmed that SNW1 is associated with the splicing machinery. It was therefore important to analyse transcripts isolated from *snw1* morphants for splicing defects. I also identified interactions with factors involved in chromatin remodelling and transcriptional processes, thus confirming known and identifying new Snw1 binding proteins.

6.2.2 SNW1 is phosphorylated

Analysis by mass spectrometry not only provides information about the peptide sequences present in a specific sample but also about certain posttranslational modifications such as phosphorylation, acetylation and ubiquitination (Witze et al., 2007). I found that SNW1 is phosphorylated at serine 224 (S224) close to the central SNW motif (Figure 6.5A). Treatment of 293T cell lysates with calf intestinal phosphatase (CIP) led to a shift in the migration of SNW1 on a SDS-PAGE (Figure 6.5B). This shift is specific to phosphorylation at S224 as mutation of this site to

alanine (S224A) resulted in a loss of the SNW1 shift upon addition of CIP (the mutation of S224 was introduced by Becky Randall). The efficiency of the CIP treatment was demonstrated by monitoring the loss of PSmad1/5 in the treated lysates (Figure 6.5C).

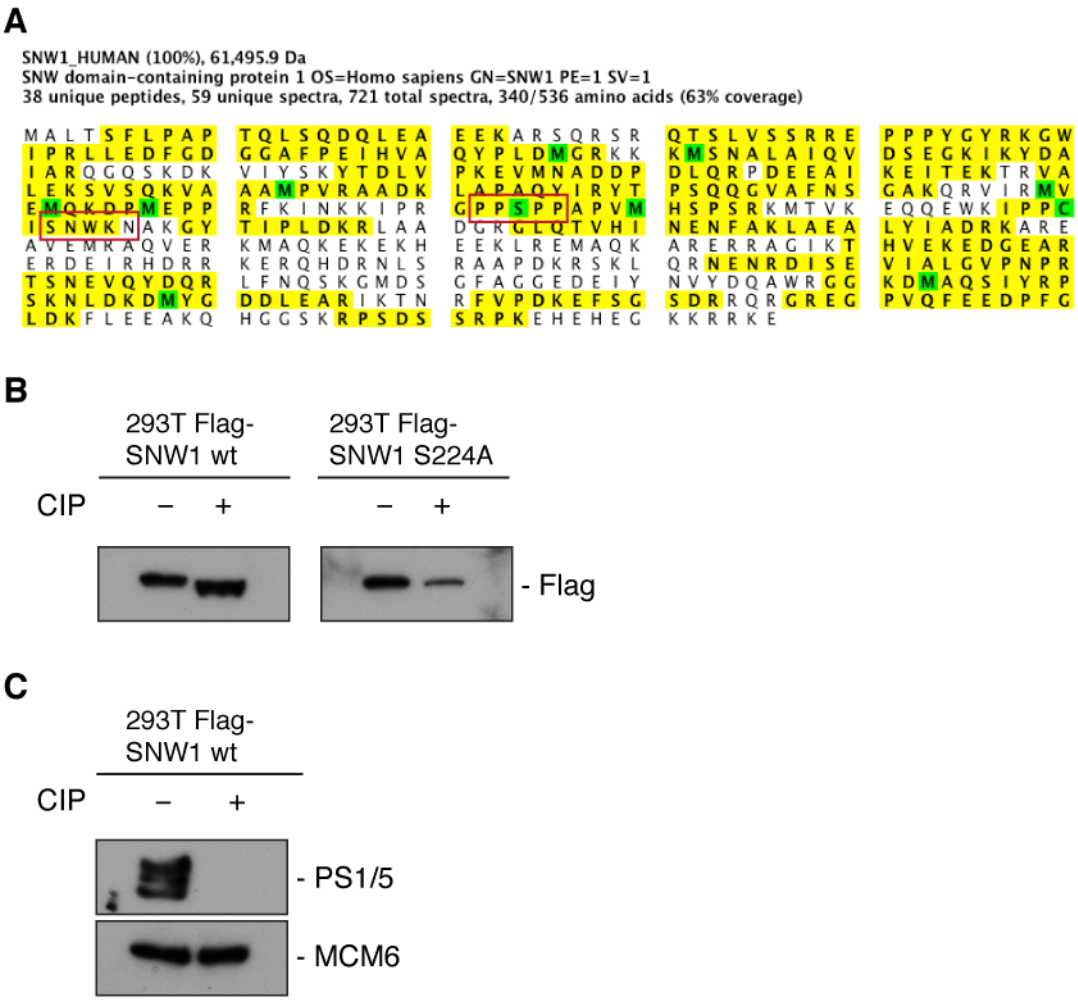

Figure 6.5 SNW1 is phosphorylated at serine 224 (S224)

(A) *SNW1 protein detected by mass spectrometry and visualised using Scaffold software. The sequence coverage is highlighted in yellow. Green marks the amino acids oxidised methionine (M) and carbamidomethyl cysteine (C). Red Boxes indicate the motif surrounding the phosphorylated S224 and the central SNW motif.*

(B) *Whole cell extract from HEK293T cells expressing either wild-type (wt) Flag-SNW1 or Flag-SNW1 S224 were treated with CIP and analysed by western blotting using an antibody against Flag.*

(C) *Whole cell extracts were treated with CIP and analysed by western blotting using an antibody against PSmad1/5. MCM6 is a loading control.*

This PPSPP motif containing the S224 phosphorylation site is conserved across species, indicating an important role in regulating SNW1 function (Wu et al., 2011). It will be necessary to determine the function of the phosphorylation for example regarding whether it is required for the interaction with other proteins.

6.2.3 Analysis of *bmp2b* transcripts in *snw1* morphant zebrafish embryos

As described in the previous chapter, zebrafish *snw1* morphants lack BMP activity and Bmp2b protein despite an increase in *bmp2b* transcript levels at the NPB. This strongly suggests a possible defect in mRNA processing. My mass spectrometry as well as analysis of the spliceosome in other studies implicated Snw1 in pre-mRNA splicing. Therefore I asked whether I could observe an increase in unspliced *bmp2b* in embryos lacking Snw1. For this purpose I designed various primer pairs along the *bmp2b* transcript covering exon/exon and exon/intron boundaries (Figure 6.6).

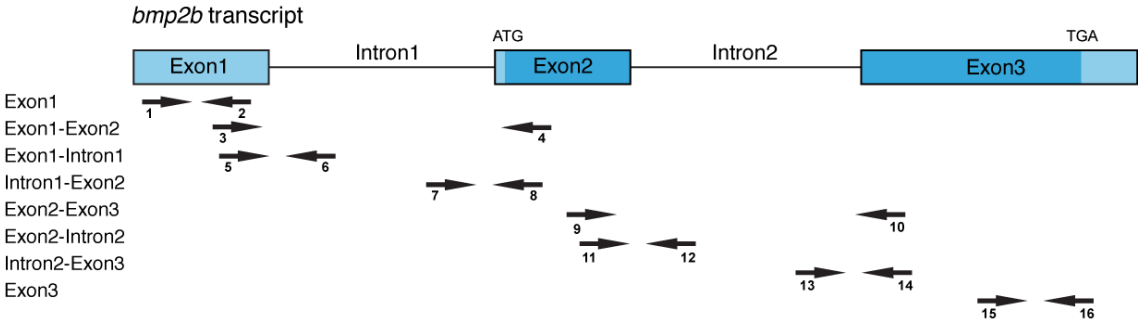

Figure 6.6 Primers designed for qRT-PCR along the *bmp2b* transcript
Primer pairs were designed to cover the bmp2b transcript and evaluate relative amounts of spliced and unspliced mRNA present in a sample. Arrows indicate the location of the primer pair along the transcript.

I then isolated total RNA from *snw1* morphants and generated cDNA. As it was not clear whether potentially unspliced mRNA is polyadenylated or is rapidly degraded, I tested oligodT versus random primers for the cDNA reaction but did not find any significant difference in the subsequent analysis (data not shown). For each primer pair the data is depicted relative to the transcript levels present in control MO injected embryos (set as 1). This allows for the comparison of transcript levels amplified by a specific primer pair but not between primer pairs. Injection of

an increasing amount of *snw1* MO resulted in higher levels of *bmp2b* as observed in ISH (Figure 6.7A, Figure 5.12). However, there did not appear to be a bias towards unspliced versus spliced *bmp2b* mRNA, but a general, partially dose-dependent, increase in transcript abundance. This was not a general effect on transcripts at the NPB, as for example *dlx3b* expression was not changed (Figure 6.7B). A previous study had shown that the effect of Snw1 depletion on BMP activity monitored by PSmad1/5 levels can only be observed after the end of gastrulation/early somitogenesis (Wu et al., 2011).

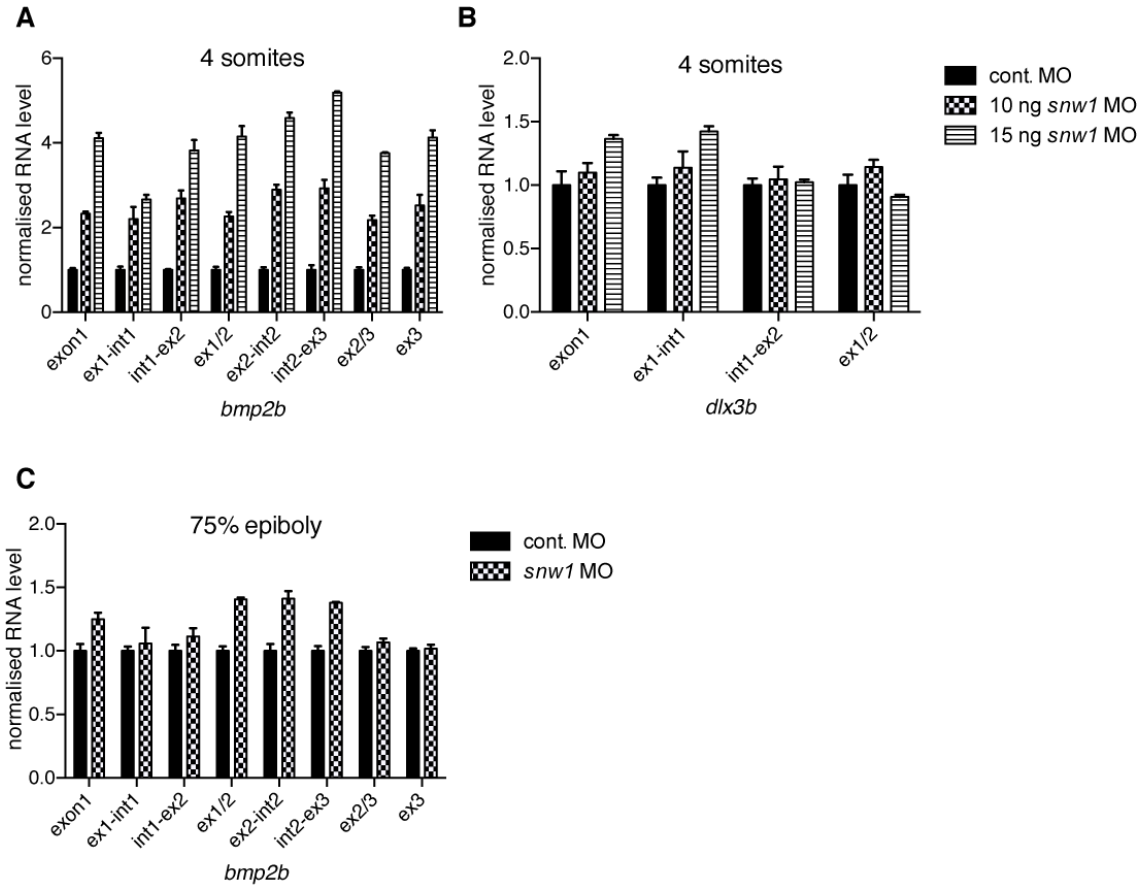

Figure 6.7 qRT-PCR analysis of *bmp2b* and *dlx3b* mRNA in zebrafish *snw1* morphants

(A) *qRT-PCR analysis of bmp2b mRNA from 4 somite stage embryos injected with the indicated MO. Primers used cover the exon/intron and exon/exon boundaries as indicated on the x-axis.*

(B) *Analysis on embryos as above using primers against dlx3b.*

(C) *bmp2b qRT-PCR analysis from 75% epiboly stage embryos.*

All RNA levels were normalised to ef1α. Shown are representative experiments. Error bars are standard deviations from technical replicates.

Similarly there is no effect of loss of Snw1 on the *bmp2b* transcript at 75% epiboly (Figure 6.7C), presumably as maternally deposited protein is still present at this stage (Wu et al., 2011).

In summary, qRT-PCR confirmed a specific increase in *bmp2b* mRNA levels during early somite stages as observed with ISH. However, this did not seem to be due to an accumulation of unspliced versus spliced transcripts.

6.2.4 **RNA sequencing to identify Snw1 targets**

Snw1 is broadly expressed during development (
Figure 5.4) and interacts with components of ubiquitously used protein complexes, suggesting that very likely additional Snw1 targets exist. I therefore wanted to perform RNA sequencing to monitor global changes in the RNA expression pattern in *snw1* morphants. The initial approach was to perform total RNA sequencing as I was concerned I might miss crucial effects if I was enriching for polyadenylated mRNA. The caveat of this approach, however, is that approximately 80% of the total RNA is comprised of rRNA, which can complicate the noise/signal detection by RNA sequencing. I therefore tested a rRNA removal kit that was predicted to work for zebrafish total RNA (Ribo-Zero^{TM}). The technical difficulties of "accumulating" sufficient purified RNA for efficient RNA sequencing, however, were such that I decided to perform conventional mRNA sequencing, especially as qRT-PCR analysis suggested that data acquired using polyadenylated RNA yielded similar results to using total RNA (6.2.3).

NGS	MO	Reads	Alignments	Unique Alignments
NGS-1406	cont.	44600082	42857846	10620088
NGS-1407	15 ng *snw1*	42471691	41539904	9440902
NGS-1408	20 ng *snw1*	44216231	34498353	4340922
NGS-1409	cont.	40758884	36528173	4114581
NGS-1410	10 ng *snw1*	27233645	29286162	4463890
NGS-1411	15 ng *snw1*	27928944	25086140	4288667

Table 6.1 RNA sequencing raw data

	NGS-1406	NGS-1407	NGS-1408	NGS-1409	NGS-1410	NGS-1411
	cont.	15 ng *snw1*	20 ng *snw1*	cont.	10 ng *snw1*	15 ng *snw1*
bmp2b	638	1673	1888	693	1357	2334
dlx3b	2204	2440	1839	1651	2124	2223

Table 6.2 *bmp2b* and *dlx3b* raw reads

RNA sequencing was performed on RNA extracts from embryos injected with either control or *snw1* MO. Two independent experiments were analysed. For each experiment a different batch of *snw1* MO was used. Please note that the second batch of *snw1* MO was more active compared to the one used for the first set of experiments. Therefore, I lowered the amount of MO injected from 15 and 20 ng to 10 and 15 ng. For subsequent statistical analysis the data was grouped in lower and higher MO dose.

The analysis of the RNA sequencing data was performed in collaboration with Richard Mitter (LRI Bioinformatics Department). The library size slightly varied for the different samples (Table 6.1) but encouragingly the read counts for *bmp2b* followed the expected pattern (Table 6.2). We therefore decided to go ahead with the analysis using the following parameters: A false discovery rate (FDR) ≤ 0.05 and an absolute fold change between control and the lower amount of *snw1* MO of at least 2 fold. I also included only genes with a raw read count of 200 or more in either the control sample or the sample injected with the lower dose of *snw1* MO (heatmap in Appendix 3). For comparison of samples from the different libraries, the count numbers were normalised to counts per million reads (CPM). Thus we identified 418 gene transcripts that were significantly changed upon loss of Snw1 in the cont. versus lower dose of *snw1* MO samples. Around two/thirds of these genes were significantly increased, where 130 were decreased. The complete lists of the datasets with the cut off can be found on a disc as Appendix 6 and 7: (FDR) ≤ 0.05, fold change > 2 between cont. MO and lower/higher amount of *snw1* MO, read count ≥ 200 in one of the samples.

I also wanted to test whether intronic reads are overrepresented in Snw1-depleted samples. For a crude analysis it was assumed that all reads that map within a transcript but were not overlapping with an exon must be intronic. The cut off criteria were as above but a read number of ≥ 30 was accepted. Although statistical

analysis yielded some significantly changed targets, the read number in introns overall was low, so no general trend could be identified (Appendix 8). Visual analysis of the data using IGV software indicated that there might be a 3'-UTR bias present in *snw1* morphants. Therefore the average RNA sequencing read coverage along the transcripts of significantly changed genes was analysed to identify whether there is a general 3' bias as an artefact of the RNA sequencing or a significant Snw1-dependent change. However, the read coverage seemed even along the transcripts with the exception of NGS-1409, which is a control sample, and thus the effect is most likely an artefact of the library preparation (Figure 6.8).

Taken together, embryonic loss of Snw1 effects the transcript levels of many genes and mostly leads to an increase rather than a reduction in transcript abundance. However, no obvious defect in splicing could be detected nor a bias in read numbers along transcripts. This reflects what I had observed analysing *bmp2b* transcript by qRT-PCR (Figure 6.7). I next validated selected targets by qRT-PCR.

6.2.5 RNA sequencing validation

I next went on to validate possible targets identified in the RNA sequence analysis and designed primers for qRT-PCR along the transcripts (Table 6.3). I chose targets that were expressed at the right developmental stage and domain to be *snw1* dependent (Thisse et al., 2001). More than one primer pair was designed if there were interesting features regarding reads along the transcripts observed, such as high read density in an intron.

All the differentially expressed transcripts selected validated in qRT-PCR, giving me confidence in the general RNA sequencing setup and analysis (Figure 6.9). In general, when several primer pairs per transcript were chosen, there did not seem to be strong differences in the expression levels, confirming the previous analyses that loss of Snw1 does not result in a significant change in pre-mRNA processing.

NGS-1406

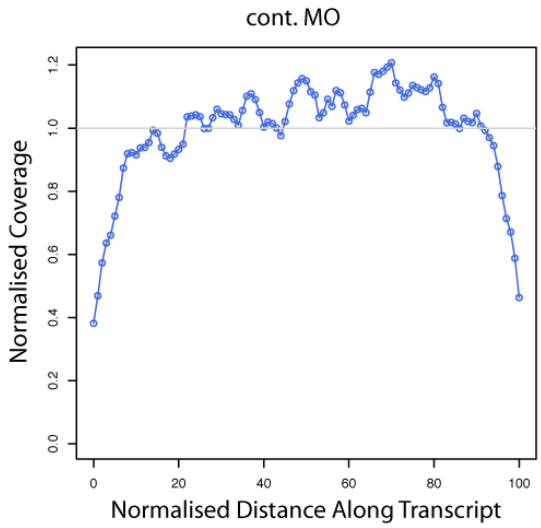

NGS-1409

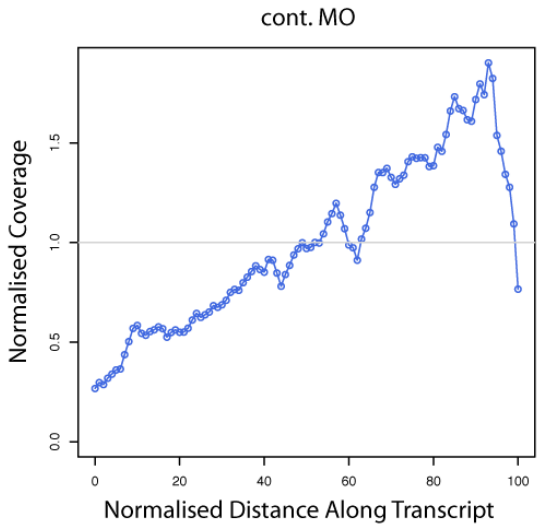

NGS-1407

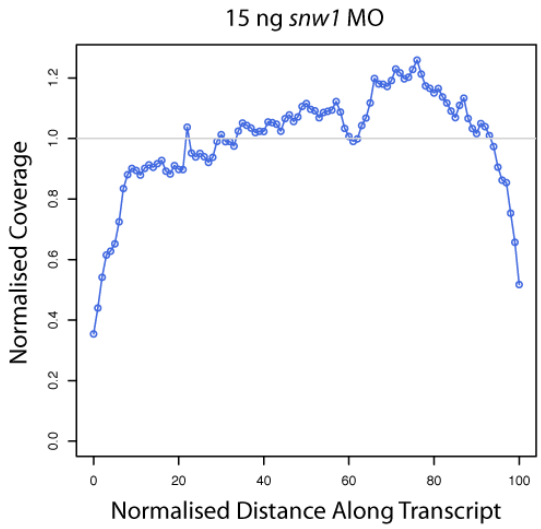

NGS-1410

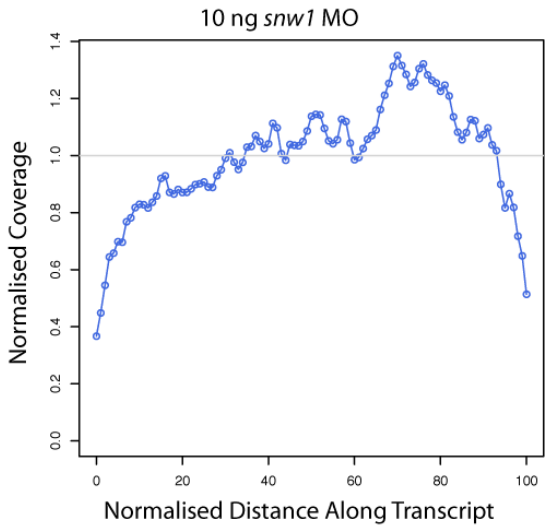

NGS-1408

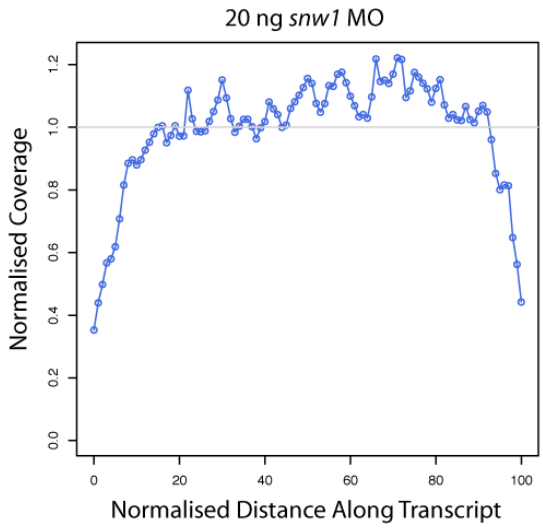

NGS-1411

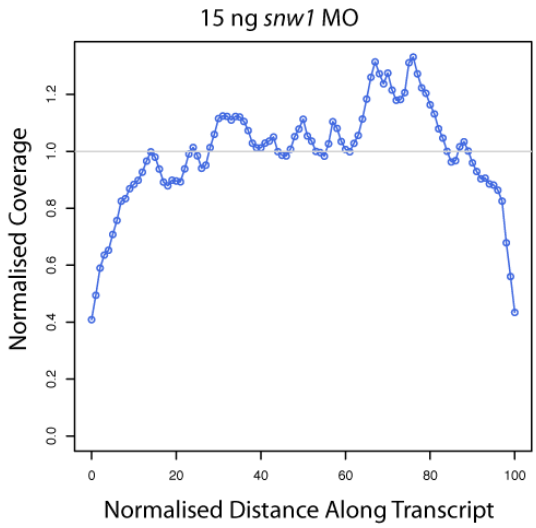

Figure 6.8 RNA sequencing coverage along the transcript

Read density along the transcript depicts the normalised coverage (with regard to library size) over the normalised distance along the transcript to identify a possible accumulation of reads in a specific region of the transcript.

Symbol	15ng_Vs_ Ctrl.FDR	20ng_Vs_ Ctrl.FDR	Description	NGS-1406.CPM	NGS-1409.CPM	NGS-1407.CPM	NGS-1410.CPM	NGS-1408.CPM	NGS-1411.CPM
				cont.	cont.	15 ng *snw1*	20 ng *snw1*	10 ng *snw1*	15 ng *snw1*
gadd45aa	1.87E-16	4.16E-20	growth arrest and DNA-damage-inducible, alpha, a	4	2	139	202	141	434
RBL2	1.69E-12	2.20E-13	retinoblastoma-like 2 (p130)	11	2	241	253	212	348
foxo3b	1.36E-08	5.31E-09	forkhead box O3b	26	7	294	359	223	488
sesn3	1.36E-08	1.71E-09	sestrin 3	87	37	1042	863	841	1414
mdm2	7.69E-09	7.66E-10	transformed 3T3 cell double minute 2 homolog	105	59	1111	1186	1000	1687
mat2al	5.65E-09	3.64E-12	methionine adenosyltransferase II, alpha-like	20	19	201	173	243	321
phlda2	5.89E-06	1.33E-08	pleckstrin homology-like domain, family A, member 2	12	6	75	65	64	154
lnx1	2.87E-08	1.31E-08	ligand of numb-protein X 1	16	8	150	99	119	141
rasl11b	0.00271	4.89E-06	RAS-like, family 11, member B	25	47	123	263	177	513
DEM1	4.45E-10	2.28E-09	defects in morphology 1 homolog (S. cerevisiae)	17	18	179	145	129	166
rps6ka3a	9.49E-05	9.21E-06	ribosomal protein S6 kinase, polypeptide 3a	56	36	306	204	275	329
foxi1	0.00015	1.05E-05	forkhead box i1	18	16	73	104	71	143
cdkn1a (p21)	6.80E-05	7.76E-06	cyclin-dependent kinase inhibitor 1A	10	9	47	56	55	65

Table 6.3 List of RNA sequencing targets for validation

List of selected targets for validation. Read numbers were normalised to counts per million (CPM). Control MO (NGS-1406; NGS-1409), 10 ng (NGS-1407; NGS-1410) snw1 MO, 15 ng (NGS-1408; NGS-1411) snw1 MO.

Taken together, global analysis of mRNA transcripts in zebrafish *snw1* morphants does not suggest an accumulation of unspliced mRNA upon Snw1 depletion. However, transcript levels are significantly increased for specific genes suggesting that Snw1 indeed is important for the regulation of transcriptional processes.

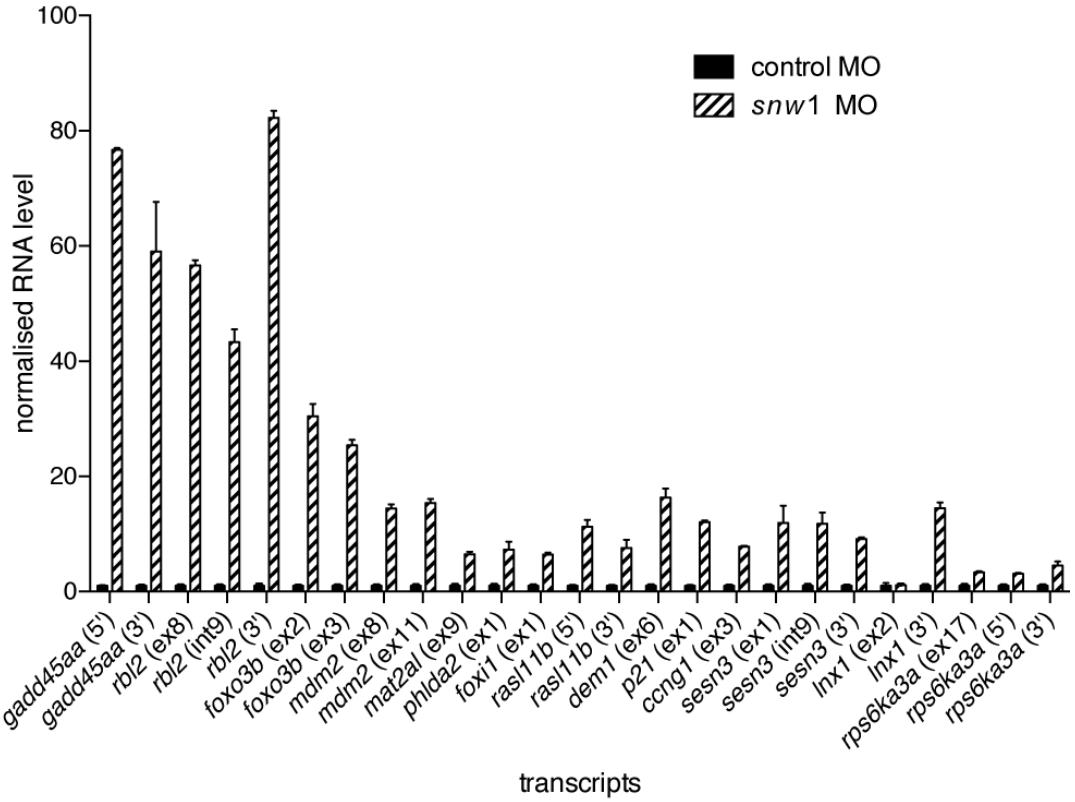

Figure 6.9 qRT-PCR for RNA sequencing validation

All RNA levels were normalised to ef1α. The values detected for the control situation were set to 1 and morphants adjusted accordingly to measure the fold-induction.

6.2.6 Function of SNW1 interaction partner

I and others have demonstrated that Snw1 is associated with components of the splicing machinery (6.2.1, (Zhou et al., 2002)). I therefore asked next, whether loss of spliceosomal interaction partners recapitulates the phenotype as depletion of Snw1. I chose spliceosome-associated proteins that were either U5 specific (Prp8), part of the Prp19 complex, which is involved U5 remodelling, (Prp19) and an RNA helicase, required for release of the RNA from the spliceosome, (Dhx8). Using a morpholino approach I knocked down *prp8, prp19* and *dhx8,* which all display a similar expression pattern to *snw1* (Thisse et al., 2001), and monitored levels of the NC marker *sox10*. Loss of Prp8 and Prp19 reduced expression of *sox10*, whereas depletion of Dhx8 did not have any effect on NC (Figure 6.10).

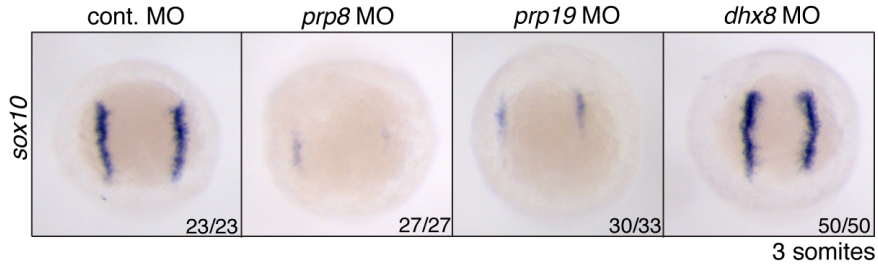

Figure 6.10 NC development in Snw1 interaction partner morphants
ISH against sox10 on embryos injected with 10 ng of cont. MO, prp8 Mo, prp19 MO or dhx8 MO. Numbers indicate the embryos with the observed phenotype for a representative experiment. Dorsal view with anterior to the top.

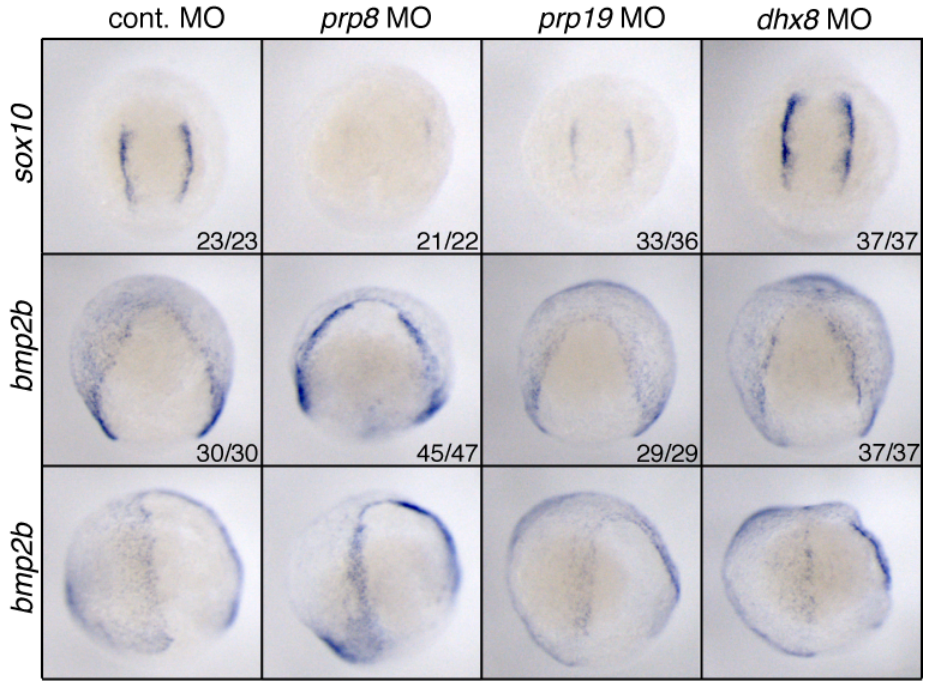

Figure 6.11 *bmp2b* transcript levels in Snw1 interaction partner morphants
ISH against sox10 and bmp2b on embryos injected with 10 ng of the indicated MO. All views are dorsal anterior, anterior to the op. The embryos in the bottom panel correspond to embryos above but are laterally tilted to allow for a better view of the NPB. Numbers indicate the embryos with the observed phenotype for a representative experiment. Dorsal view with anterior to the top.
Embryos were fixed at 3 somites.

As I previously demonstrated *snw1* morphants have increased *bmp2b* transcript levels at the neural plate border (Figure 5.12). I therefore tested whether this can be observed in other "splicing" morphants as well. Although, both loss of Prp8 and Prp19 resulted in a NC phenotype, only *prp8* morphants displayed increased levels of *bmp2b* specifically at the NPB (Figure 6.11). This observation could be confirmed in qRT-PCR (Figure 6.12).

To test whether targets identified in the RNA sequencing are dependent on other splicing factors similar to Snw1, I performed qRT-PCR analysis for *bmp2b* and some of the validated targets. Interestingly, loss of Prp8 had a similar effect on the transcript levels as *snw1* depletion, indicating that both proteins must function using a similar mechanism (Figure 6.12, Figure 6.7). Similarly, the abundance of Snw1 targets identified by RNAseq increased in *prp8* morphants (Figure 6.13). Also the fold-increase for the specific transcripts was very similar in *snw1* and *prp8* morphants (Figure 6.9). Loss of *prp19* or *dhx8* only had a mild effect on transcript levels, however it was significant in the cases of the more strongly induced targets such as *gadd45aa* and *rbl2*. This indicated, that loss of these proteins has similar effects to loss of Snw1 and Prp8, however, less pronounced. I can not exclude that the knockdown of the splicing components Prp19 and Dhx8 did not yield the same phenotype because their function could partly be rescued by redundant factors as opposed to both proteins being involved in a different mechanism.

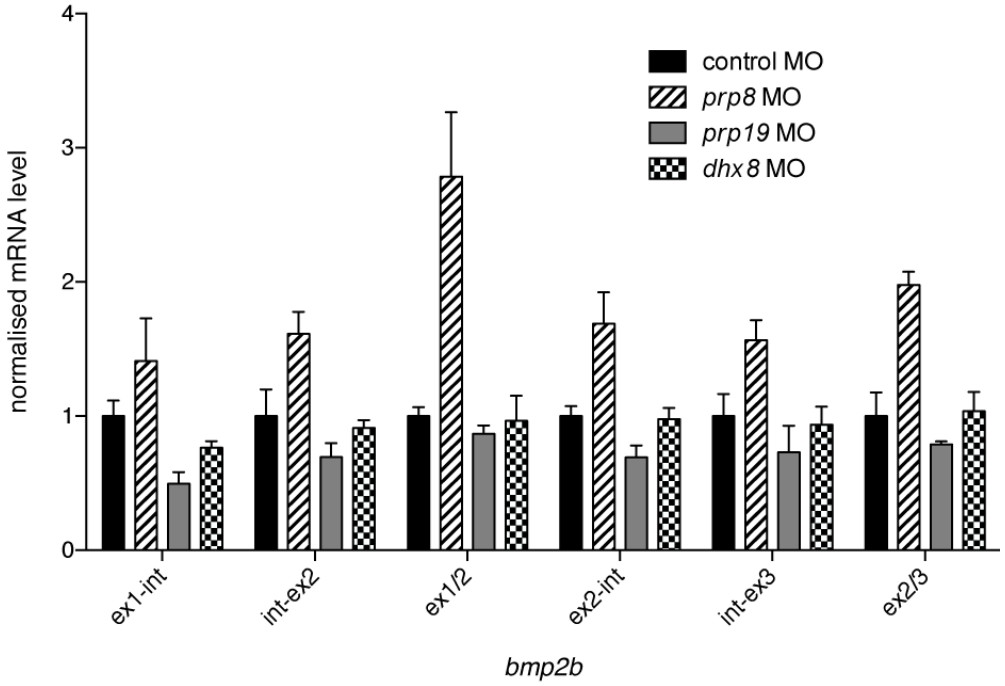

Figure 6.12 qRT-PCR for *bmp2b*

qRT-PCR on RNA isolated from embryos injected with 10 ng of the indicated MO. RNA levels were normalised to ODC. The values detected for the control situation were set to 1 and morphants adjusted accordingly to measure the fold-induction.

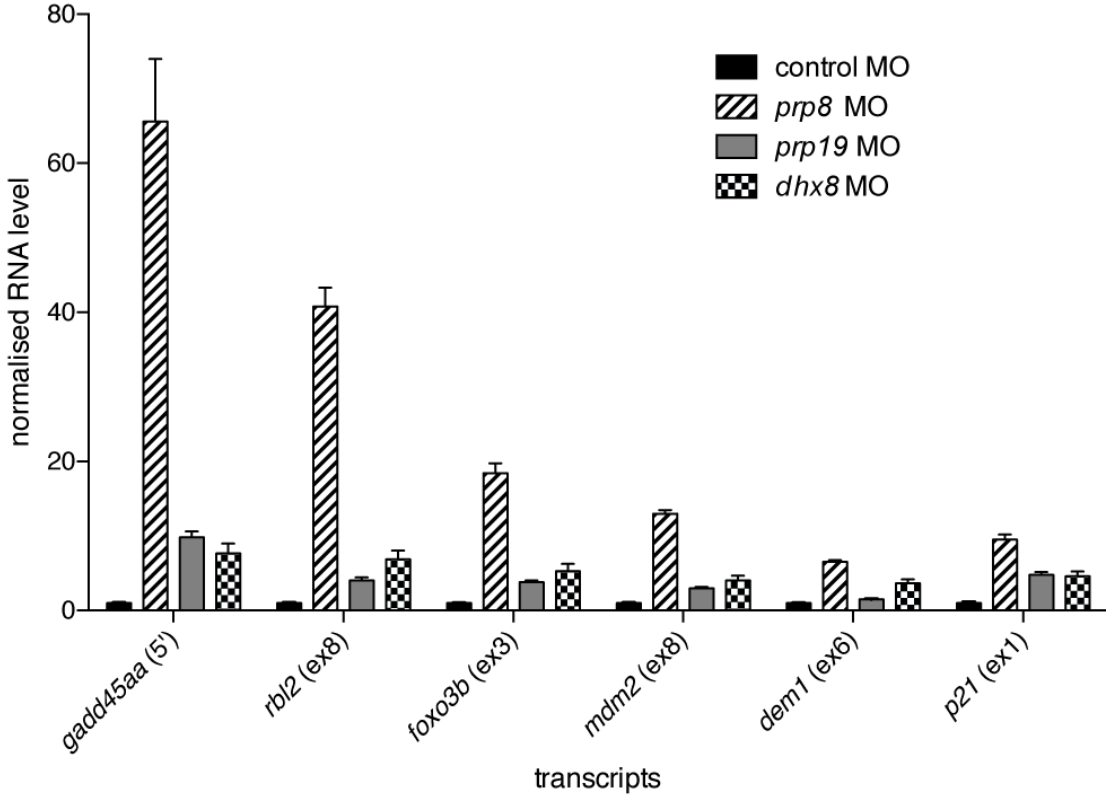

Figure 6.13 qRT-PCR on RNA sequencing targets
qRT-PCR on RNA isolated from embryos injected with 10 ng of the indicated MO. RNA levels were normalised to ODC. The values detected for the control situation were set to 1 and morphants adjusted accordingly to measure the fold-induction.

6.2.7 The NC/BMP activity are sensitive to defects in the transcriptional machinery

A recent study identified a small molecule suppressor of NC development in zebrafish (White et al., 2011). Leflunomide belongs to a class of compounds that inhibit dihydroorotate dehydrogenase (DHODH), an enzyme required for pyrimidine synthesis. Inhibition of DHODH thus results in an impairment of transcriptional elongation.

As the phenotype and the processes involved are similar to what I observed in *snw1* morphants, I asked whether inhibition of transcriptional elongation could have an effect on BMP activity as well and might thus explain the NC phenotype in leflunomide-treated embryos. Indeed, embryos exposed to leflunomide displayed a defect in NC development and reduced *sox10* expression. Interestingly, BMP activity was inhibited in treated *Tg(BRE:mRFP)* embryos and consistent with a loss of BMP signalling phenotype the *krox20* expression domain, marking the hindbrain, was slightly expanded. Expression of *ncad* in the NP and *hgg* in the hatching glad was not altered. Preliminary data indicates that there is no increase in *bmp2b* transcript levels detected by ISH and qRT-PCR (data not shown).

In summary this result suggests that BMP signalling is sensitive to alterations in transcriptional elongation/splicing processes but that Leflunomide and Snw1 perturb BMP activity by different mechanisms.

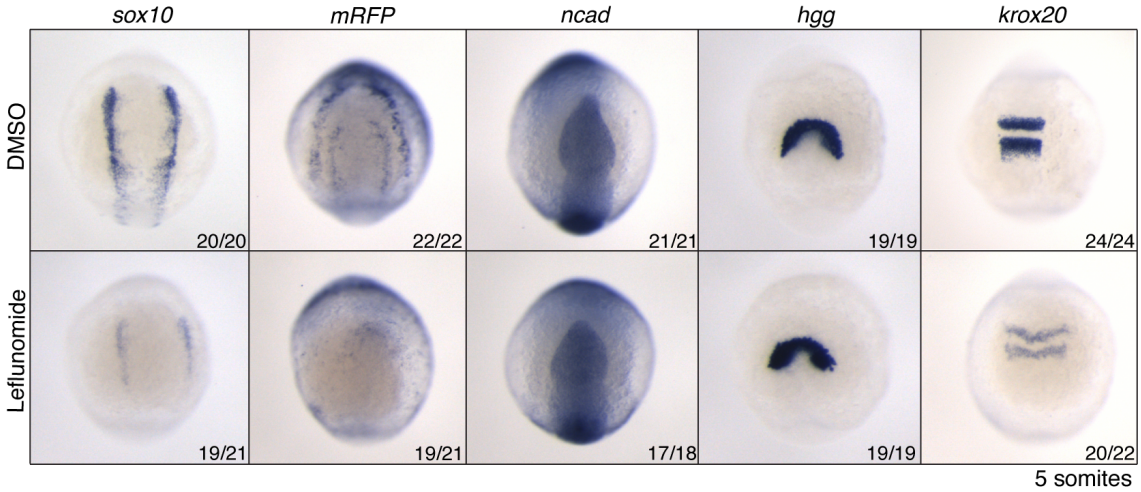

Figure 6.14 Leflunomide inhibits BMP activity

ISH using the indicated probes on embryos treated from 4 hpf onwards with DMSO or 6.5 µM Leflunomide. Numbers indicate the embryos with the observed phenotype for a representative experiment. Dorsal view with anterior to the top.

6.3 Discussion

6.3.1 Summary of results

- Snw1 is part of the protein machinery that regulates splicing and transcriptional processes.
- Snw1 is phosphorylated at serine 224.
- *bmp2b* mRNA levels are increased in *snw1* morphants, but there is no accumulation of unspliced transcripts.
- RNA sequencing identified more than 400 transcript that were significantly changed upon depletion of Snw1.
- The read-density was equally distributed along transcripts and there was no apparent bias towards unspliced pre-mRNAs.
- Depletion of Snw1 interaction partners partly recapitulates the Snw1 morphant phenotype.
- Chemical inhibition of transcriptional elongation also affects NC development and BMP activity.

6.3.2 SNW1 interaction partners

As discussed in the previous chapter, Snw1 has been identified as part of the active spliceosome in several independent analyses. Using mass spectrometry I confirmed many of the reported interactions, predominantly with U5snRNP specific proteins such as PRP8 and SNRNP200, and catalytic step II and late acting proteins such as DHX8 and DHX38 (Figure 6.3). In addition, SNW1 associates with non-snRNP spliceosome assembly proteins, for example CDC5L, CRNKL1 and PRP19.

Interestingly SNW1 also interacts with many histone modifiers that might act to control transcriptional and co-/post-transcriptional processes such as components of the SWI/SNF complex (Tyagi et al., 2009) and SETD2 (Carvalho et al., 2013). There has been accumulating evidence for a functional connection between transcription and splicing, with these processes co-regulating each other (Montes et al., 2012). Splicing is now thought to occur co-transcriptionally and that

this is important for the regulation of gene expression such as through alternative splicing. How this is thought to be regulated I will discuss in the following section.
Although I could confirm some of the reported interactions, I failed to detect many other binding partners. In fission yeast the Snw1 homologue spSNW1 has previously been shown to interact with the 3' recognition complex subunit U2AF35 (Ambrozkova et al., 2001) and recombinant SNW1 has been reported to bind U2AF65 from HCT116 nuclear extracts (Chen et al., 2011). As already mentioned in the introduction, this interaction is proposed to be required for loading of U2AF65 onto the unspliced *p21* pre-mRNA in a gene specific manner. In my analysis I only identified very low numbers of peptides for these U2snRNP specific proteins. In general, components of the U2snRNP particle were underrepresented and appeared more nonspecific/indirect compared to, for example, proteins of the activated spliceosome and the U5snRNP. Thus, my data suggest an involvement of SNW1 in the splicing process after splice site recognition.

In addition to splicing, Snw1 has been implicated in many cellular processes and pathways as outline in Chapter I (1.4.2). Snw1 was reported to interact with and enhance the activity of transcription factors such as Smad2/3, vitamin D receptor and the Notch intracellular domain (NotchICD) amongst others (for review (Folk et al., 2004)). Also, Snw1 has also been demonstrated to interact with components of the Wnt signaling pathway, such as β-catenin, thereby regulating Wnt signaling activity during NC development (Wang et al., 2010b). I could not detect binding with any of these suggested partners. The reason for this could be varying stringencies in the experimental setup. In addition, some of the interactions might be cell type/tissue specific. However, many of the proposed binding partners have been identified using yeast two-hybrid, recombinant proteins and immunoprecipitation with high overexpression of at least one of the components. In my analysis I used Flag-SNW1 expressed at endogenous levels and validated interaction partners by endogenous IPs. Overall, I detected traces of many proteins at low number in mass spectrometry that appeared to be nonspecific contaminants. It is conceivable that when hugely overexpressed, the system is forced into false-positive interactions. Interestingly, stretches of the Snw1 protein are suggested to be present as partially unfolded in a native state and undergo refolding upon binding of an interaction partner (Folk et al., 2004). It thus presents a structure, which is ideal to flexibly interact with many proteins. However, this fact might also

render Snw1 prone to nonspecific binding under the above-mentioned conditions. Thus my analysis shows the difficulties in genuinely validating *in vivo* protein interactions and indicates that some of the reported Snw1 interactions may have to be reevaluated. However, the association of Snw1 with the spliceosome has been sufficiently proven. Given the array of additional binding partners it is possible that Snw1 plays a role in the coupling of transcription and splicing. I will discuss this further below. It will also be important to assess the function of Snw1 S224 phosphorylation revealed by mass spectrometry.

6.3.3 The role of Snw1 in co-transcriptional processes

RNA polymerase II (RNAPII) binding to the core promoter of genes depends on the promoter sequence and the surrounding chromatin landscape and requires a wide range of transcription factors. During the transcriptional process, modification of the carboxyl terminal domain (CTD) of the large RNAPII subunit is important for the control of transcriptional and co-transcriptional processes such as pre-mRNA capping, 3' end-processing and splicing (Hsin and Manley, 2012). The different modification patterns lead to the timely recruitment of factors to the CTD and thus the nascent transcript, which are required at various specific transcriptional stages for correct processing of the transcript (Figure 6.15A). Phosphorylation of the CTD at Ser5 triggers release of RNAPII from the promoter and the recruitment of histone modifying complexes for the trimethylation of histone H3 at Lys4 (H3K4me3) at proximal nucleosomes. H3K4me3 is required for transcription initiation (Vermeulen et al., 2007) and recruitment of splicing machinery (Sims et al., 2007). After initiation the RNAPII is temporally paused through the negative elongation factor complex (NELF) possibly to give time for recruitment of necessary factors. Pausing is reversed by the positive transcription elongation factor P-TEFb (Cyclin T1:CDK9), which phosphorylates Ser2 in the CTD of RNAPII. This in turn facilitates the recruitment of the SETD2 histone modification complex and H3K36me3 during transcriptional elongation. H3K36me3 marks are not evenly distributed along the gene, but are, for example, enriched in exons over introns (Kolasinska-Zwierz et al., 2009, Wilhelm et al., 2011) and towards the 3' end of a gene (Bannister et al., 2005). This might influence the pausing and elongation rate of RNAPII.

Interestingly, splicing increases the recruitment of SETD2 and subsequently trimethylation of H3K36 (de Almeida et al., 2011).

So far it is clear that Snw1-depletion in zebrafish does not lead to the general repression of *bmp2b* transcription, which might have explained the loss of BMP activity at the neural plate border. In contrast, *bmp2b* transcript levels are locally increased at the NPB, where Snw1 is no longer expressed. However, these accumulated transcripts do not appear to be translated into Bmp2b protein indicating defects in correct pre-mRNA processing.

Snw1 binds to promoters as well as transcribed regions, and has been implicated in both, transcriptional elongation and co-transcriptional splicing as already described in the introduction (Bres et al., 2005, Bres et al., 2009, Chen et al., 2011). SNW1 associates with PTEFb and is required for Tat-dependent HIV-1 transactivation (Bres et al., 2005, Bres et al., 2009). This step is dispensable under stress such as UV-treatment. However, SNW1 is necessary for p53 stress-induced p21 protein expression by gene specifically controlling *p21* splicing (Chen et al., 2011). Interestingly, CDK9 was one of the interaction partners I detected using mass spectrometry, albeit in comparably small amounts. I therefore tested whether similar effects as described in Chen *et al.* can be observed in zebrafish *snw1* morphants. Indeed, *p21* is a possible target of zebrafish Snw1 as identified by RNAseq. However, in contrast to my observations, Chen *et al*. did not detect elevated but reduced levels of *p21* mRNA. I confirmed the reduction in *p21* mRNA in MDA-MB-231 cells upon loss of SNW1, thus there seems to be an opposite effect in embryos and tissue culture cells. Due to the lack of a specific antibody I could not test p21 protein expression in Snw1-depleted zebrafish embryos. I did not observe differences in the splicing efficiency between wild-type and morphant embryos. It is not clear how exactly the authors calculated the ratio of spliced/unspliced transcripts and to what extent, for example, primer efficiencies were taken into account. It will be interesting to test whether in addition to *p21* there is an overlap of targets affected in tissue culture cells and in embryos when Snw1 is lost. However, my data do not indicate a general defect of *bmp2b* pre-mRNA splicing nor did I find evidence for other transcripts not being spliced.

An explanation for the observed discrepancies might be that differences in the regulation of co-transcriptional processes during development and mammalian cells, as used by Chen *et al*., exist. The cell cycle rate is much higher in the

developing embryo and the timing and pattern of transcriptional processes are critical. This may account for mechanistic differences in ensuring robust, coordinated gene expression. The stability of unspliced pre-mRNA and RNA turnover processes in general, for example, could differ. Work in yeast shows that unspliced pre-mRNA is usually rapidly degraded. Depending on which splicing step is disturbed, this occurs by a nuclear or a cytoplasmic decay pathway or nonsense-mediated decay (Bousquet-Antonelli et al., 2000, Hilleren and Parker, 2003, Sayani et al., 2008). These pathways could be leveraged differentially in different biological setups. Moreover, it has been suggested that RNA surveillance mechanisms can mask the effects of mutations in spliceosomal components (Kawashima et al., 2009). Snw1 has also been implicated in the nuclear export of mRNA (Farny et al., 2008). Impaired transport of mRNA into the cytoplasm might account for the transcript accumulation I observe and prevent protein translation. It will be important to test whether mRNA decay and/or cellular localisation is changed upon loss of Snw1. In SNW1 depleted mammalian cells, the nuclear export of mRNAs under DNA damage conditions was not changed (Chen et al., 2011). However, this may differ during vertebrate development.

Another possible explanation for the accumulation of transcripts in *snw1* morphants, is a change in RNAPII occupancy/elongation rate, assuming that none of the required factors is limiting (Figure 6.15B). Interestingly, a change in the elongation rate has been linked to the use of cryptic splice sites as well as alternative splicing (de la Mata et al., 2003) and there is data suggesting that this can be influenced by histone deacetylation (Hnilicova et al., 2011, Allo et al., 2009). Loss of SETD2, and thus H3K36me3, results in an increased occupancy at internal exons and intragenic transcription initiation in a subset of active genes (Carvalho et al., 2013). Data also suggests that H3K36 methyl groups is required to dampen the activity potential of just transcribed regions thus regulating transcription levels {Carrozza, 2005 #434;Keogh, 2005 #435}. It is possible that Snw1 is required to recruit factors such as SETD2 that modulate RNAPII travelling speed and pausing thus altering the abundance of the wild-type ‘mature” transcript. Indeed, unpublished data from yeast suggests that in temperature sensitive Snw1 mutants the RNAPII elongation rate as well as transcript levels are increased (Prof. Jean Beggs, personal communication).

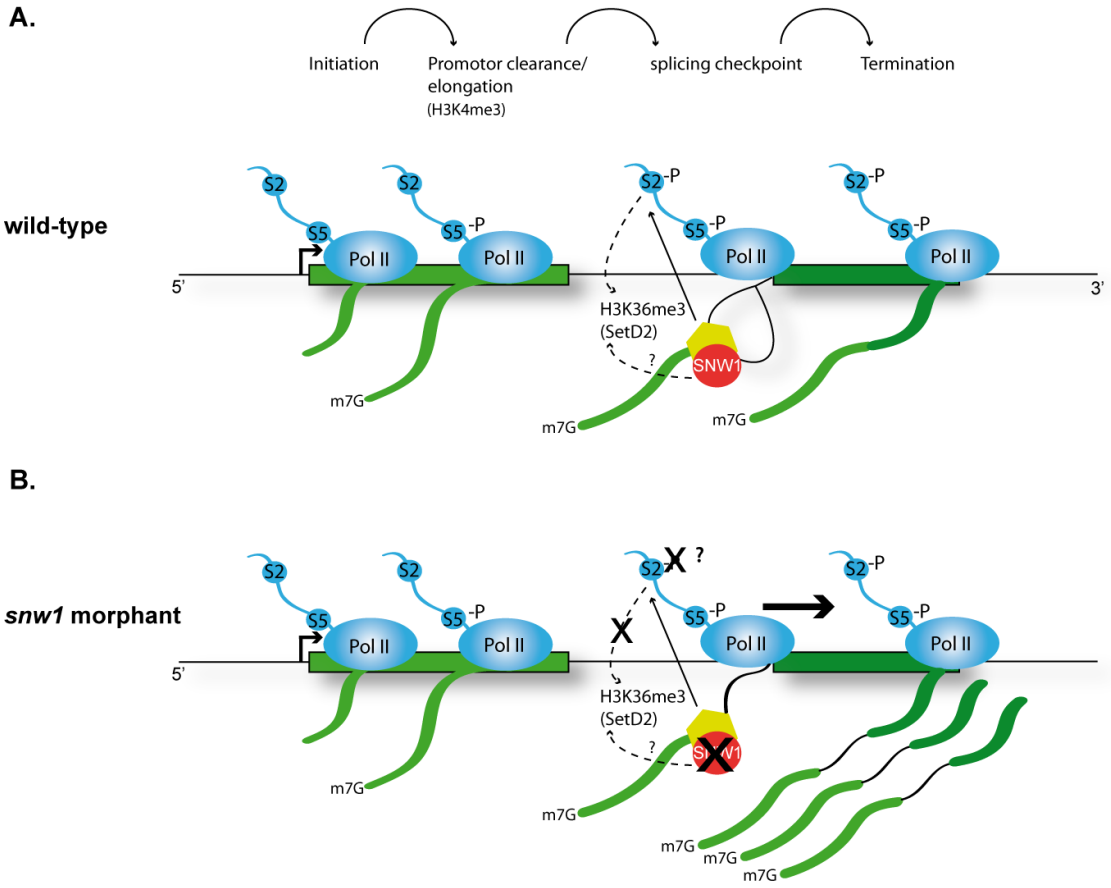

Figure 6.15 Possible role of SNW1 in co-transcriptional processes

(A) *Transcription by RNAPII is regulated at various steps. After initiation Ser5 (S5) phosphorylation of the CTD leads to the release of RNAPII from the promoter whereas subsequent Ser2 (S2) phosphorylation results in the elongating form RNAPII. This is accompanied my modification of the surrounding chromatin. SNW1 can be found in complexes containing PTEFb (yellow), which is required for Ser2 phosphorylation. It might also interact with SETD2 a factor important for H3K36me3.*
(B) *Loss of SNW1 could possibly interfere with RNAPII Ser2 phosphorylation as well as directly or indirectly with H3K36me3 thus leading to an accumulation of un- or alternatively spliced transcript.*

It will be important to further analyse the RNAseq data also using newly available custom-built libraries to accurately analyse for example the use of cryptic splice sites {Markmiller, 2014 #433}

As previously described, Snw1 is part of the PRP19 splicing complex (6.2.1). A recent study has identified that in yeast this complex is absolutely required for the recruitment of the TREX complex, which couples transcription to mRNP export, to actively transcribed genes (Jimeno et al., 2010, Chanarat et al., 2011). This complex is conserved in higher eukaryotes. Depletion of the PRP19 complex component Syf1 (the yeast homologue of XAB2, another Snw1 binding partner,

Appendix 1) and the resulting loss of TREX recruitment decreases transcriptional activity (Chanarat et al., 2011). The lower mRNA level observed in this experimental setup more resembles the phenotype observed in mammalian cells lacking SNW1 and does not reflect the observations in zebrafish *snw1* morphants. However, I have shown that depletion of Prp19 in zebrafish embryos results in an impaired NC development and an increase in mRNA levels of specific targets, although the phenotype on transcripts is not as pronounced as upon loss of Snw1. This may again indicate that disruption of similar processes can have different outcomes during development versus cell maintenance.

Taken together, Snw1 possibly is another player in the functional coupling of transcription and co-transcriptional processes. It will be important to assess transcriptional elongation rates in Snw1 depleted cells as well as modifications to the histone landscape. Moreover, Snw1 ChIPs on DNA from zebrafish embryos for targets identified by RNAseq will answer whether Snw1 directly binds to these genes or whether the increase in some transcript levels is an indirect effect of Snw1 depletion. I am also testing antibodies to determine whether protein expression is abolished even if certain mRNAs are more abundant in *snw1* morphants, similar to *bmp2b*. This is currently hampered by a lack of suitable antibodies against many zebrafish proteins. In addition, I will perform RNAPII ChIPs or global analysis like global run-on sequencing (GRO-seq) to identify whether presence of RNAPII is augmented in Snw1 depleted embryos and whether there are differences in RNAPII dynamics.

Although I did not observe an increase in unspliced transcript in *snw1* morphants it is still a possibility that alternative splicing through for example RNAPII elongation rate results in a non-functional mRNA. This would explain the loss of Bmp2b proteins despite the presence of bmp2b.

6.3.4 RNAseq reveals differential transcript levels in Snw1 zebrafish morphants

Global analysis of the altered transcripts identified in RNAseq using the **D**atabase for **A**nnotation, **V**isualization and **I**ntegrated **D**iscovery (**DAVID**) suggests an overrepresentation of genes involved in DNA replication, DNA metabolic processes, the p53 signalling pathway and the regulation of apoptosis (data not shown). This is

in line with Fluorescence-activated cell sorting (FACS) experiments showing that tissue culture cells undergo G1 cell cycle arrest upon loss of SNW1 (data not shown). However, it is difficult to distinguish between direct and indirect effects of Snw1 loss in zebrafish as the RNA was isolated from around 13 hour old embryos. This means that the upregulation of genes related to cellular stress responses could be a result of the loss of crucial survival factors, which in turn leads to the induction cell cycle arrest and apoptosis by the time the analysis of the transcriptome was conducted. Gadd45aa for example is a growth arrest and DNA-damage-inducible factor playing a role in this process. Similarly, Rbl2 and p21 function as regulators of cell cycle progression and can mediate cell cycle arrest. As previously mentioned p21 has been identified as a SNW1 target in tissue culture cells {Chen, 2011 #161}. According to this Snw1 would be required for p21 protein expression thus higher transcript levels of *p21* might not result in higher protein levels similar to our obervations regarding *bmp2b*. This example highlights another level of complication in the RNAseq data analysis. As mentioned in the previous chapter it will be crucial to identify if higher mRNA levels translate in higher protein abundance in order to speculate on a possible role of the identified targets. I will thus conduct more experiments using the tissue culture system as this will allow me to more easily distinguish between direct and indirect effects and give me access to a larger panel of antibodies to test protein expression levels of potential SNW1 targets. Moreover, my phenotypical analysis of Snw1 morphants has so far be restricted to ectodermal patterning. It is very likely that loss of Snw1 results in other developmental defects and it will be interesting to identify these and possibly correlate them with genes identified in the RNAseq.

6.3.5 Depletion of Snw1 binding partners leads to gene specific effects

As mentioned in the previous section, depletion of Prp19 resulted in a moderate increase of certain mRNA transcript levels and interfered with NC development. Loss of Prp8, another U5 snRNP specific protein, also abolished expression of NC cell markers. Interestingly, qRT-PCR revealed a similarly strong effect of Prp8 depletion on, for example, *gadd45aa* and *rbl2* as loss of Snw1, indicating that both are part of the same mechanistic network. In contrast, loss of

Dxh8 did not have an effect on NC, although levels of some transcripts were elevated.

Overall, it is astonishing that the depletion of general, and in yeast essential, splicing factors affects selective tissues such as the NC. However, this has been observed in several other contexts. Mutations in PRP8 cause the retina-specific disease retinitis pigmentosa, the most common form of inherited blindness (McKie et al., 2001). Similarly, zebrafish Dhx8 mutants display defects in early haematopoiesis (English et al., 2012). There are several possible explanations for these selective phenotypes. It is conceivable that some tissues are more sensitive to splicing/transcription defects than others. The retina is among the biosynthetically most active tissues in the body (Graziotto et al., 2011). Similarly, hematopoietic progenitors are highly proliferative. This might render these tissues more susceptible to suboptimal levels of pre-mRNA processing factors. However, other cell types are probably affected as well to a lesser extent and *dhx8* and *snw1* mutant fish die within several days of development (Amsterdam et al., 2004, English et al., 2012). Another possibility is that splicing factors display gene specificity depending on the cellular context or different signalling inputs. This has been demonstrated for *p21* pre-mRNA in the case of SNW1 (Chen et al., 2011). A microarray based approach in yeast also revealed transcript specific splicing of pre-mRNAs for several core components of the splicing machinery (Pleiss et al., 2007). Thus, it is possible that some cell-specific pre-mRNAs are more affected by perturbation of co-/transcriptional processes leading to tissue-specific phenotypes. It would be interesting to determine whether Snw1 interacts gene specifically with a subset of binding partners.

6.3.6 The neural crest is sensitive to defects in transcription elongation

As discussed earlier, the rate of transcription elongation i.e. the speed RNAPII travels along a gene is an important regulatory mechanism for gene expression. Thus organisms should be sensitive to perturbation of transcription elongation rates. Indeed, in zebrafish mutants for the elongation factors Spt5 (*foggy*) and Spt6 (*pandora*) show defects in heart and neuronal development (Cooper et al., 2005, Guo et al., 2000, Keegan et al., 2002). The specificity of the phenotypes is further

evidence supporting the idea that controlling processes such as transcription elongation and splicing is more critical in particular cell types and tissues. That this can have therapeutic implications has been demonstrated recently in zebrafish. A large-scale chemical screen identified a regulator for NC development that also inhibits melanoma growth (White et al., 2011). Leflunomide is an inhibitor of dihydroorotate dehydrogenase (DHODH), required for pyrimidine synthesis. Inhibition of DHODH thus impairs transcriptional elongation. I reasoned that if *bmp2b* is vulnerable to disruption of co-transcriptional/transcriptional processes, the NC phenotype observed in embryos treated with leflunomide might be due to an inhibition of BMP activity. Indeed, BMP activity, but not Wnt activity, was strongly reduced, underlining the sensitivity of particular transcripts to disruptions in transcriptional kinetics.

Taken together, SNW1 appears to have functional roles outside of simply disrupting splicing, possibly in linking splicing to transcript elongation or nuclear export. There is accumulating evidence that changing levels of general factors of the transcriptional machinery can have gene specific as opposed to global effects thus affected particular tissues. How this is accomplished on a mechanistic level will be important to determine.

Chapter 7. Concluding Remarks and Future Perspectives

The temporal and spatial control of signalling pathways is essential for tissue and organ formation during embryonic development. Elucidating the underlying mechanism has important implications for understanding diseases, as many of the embryonic circuits are redeployed in pathological contexts, for example in cancer.

For my PhD thesis project I wanted to understand how the BMP signalling pathway is regulated to allow for the induction and specification of the NC and other progenitor cells at the NPB. I identified a novel network of BMP regulators that explains how cell types with different requirements for BMP activity can be specified in close proximity. My work expands on the current gradient model and gives evidence for a two-step model, with distinct domains of BMP activity after gastrulation. Moreover, I investigated the function of the nuclear factor Snw1 in regulating BMP activity at the NPB during neural crest development. Interestingly, Snw1 is not directly involved in pathway activity downstream of the receptors, but appears to regulate gene-specific co-transcriptional processes with *bmp2b* being one of the targets.

Thus my work gives novel insight into processes regulating ectodermal patterning. I provide direct evidence for the existence of distinct BMP signalling domains at the NPB and suggest mechanisms by which they are established. I will discuss the implications of my studies in the following sections

7.1 The use of transgenic zebrafish reporter lines

With the emergence of different genetic and imaging tools, the zebrafish has increasingly proven to be an excellent model organism with which to study early vertebrate development and signalling dynamics. Transgenic lines, expressing fluorescent reporters under the control of tissue-specific promoters, have been used to analyses cell fate decisions and tissue interactions. Sox10:eGFP lines for example have been exploited extensively to identify and analyse NC derivatives (Carney et al., 2006, Kwak et al., 2013, Saxena et al., 2013). In order to fully understand tissue specification during development, as well as tissue homeostasis

and tumour growth, it is crucial to study the signalling pathways that regulate these processes. Many of the important pathways have been dissected at the cellular level and considerable effort has been made to understand how different pathways influence each other. Although this approach provides important information on the signal transduction cascades themselves, it lacks *in vivo* relevance. The identification of signalling pathway responsive *cis*-elements from relevant target genes has allowed for the generation of transgenic zebrafish lines suitable for studying *in vivo* signalling dynamics.

For the BMP/GDF signalling pathway such a reporter line was generated in our lab using a well-characterised, specific BMP-responsive element (BRE) from the mouse *Id1* enhancer, which binds phosphorylated Smad1/5–Smad4 complexes (Ramel and Hill, 2013, Wu et al., 2011). This line proved to be crucial for my studies of the BMP signalling dynamics at the NPB during ectodermal patterning, as it is more sensitive than immunostaining for PSmad1/5. To rely on transgenic reporter lines as a genuine read-out for pathway activity, several points have to be taken into account, such as the nature of the pathway responsive element and the selection of an appropriate reporter protein. The sensitivity of a reporter line can depend on the number of tandem repeats of the *cis*-elements used. Increasing this number can lead to an enhanced responsiveness, as seen for two independent Wnt reporter lines with 4 or 7 TCF/Lef elements upstream of a minimal promoter (Dorsky et al., 2002, Moro et al., 2012). The TCFsiam line, which contains 7 elements, displays higher levels of mRNA and fluorescence as well as broader expression domains compared to the TOPdGFP line, which contains only 4. However, the two lines also make use of different minimal promoters (c-fos in case of TOPdGFP, siamois for TCFsiam), which could account for these differences. Moreover, the TOPdGFP transgenic line uses a destabilised version of GFP and thus fluorescent protein accumulation is inherently lower than would be expected in the TCFsiam line, which uses eGFP or mCHERRY. Thus in the TCFsiam line some of the domains where fluorescence is detected might indicate areas where Wnt signalling is no longer active. As mRNA is usually less stable than proteins, using mRNA expression as a readout can aid to give a more dynamic picture of the signalling events. This is also the case for the *Tg(BRE:mRFP)*. I was using. The mRNA half-life of mRFP is less than 20 min compared to more than 12 hours for the protein. This is not only of importance with regard to the reporter protein but

also the mRNA. Whilst *mRFP* mRNA has a short half-life, for example, the half-life of *eGFP* is around 5 hours. This reflects the importance of choosing the right fluorescent protein for the intended purpose, as well stringent validation of transgenic reporter lines. To study dynamic signalling a short half-life of the reporter is desirable, whereas for cell linage tracking for example, a long half-life fluorophore is more useful. Generating reporter lines for different signalling pathways using distinct fluorophores enables simultaneous study of multiple pathways.

Transgenic reporter lines have to be rigorously validated as genuine pathway read-out. There are different methods to validate ranging from genetic analysis to validation using pharmacological compounds. Thus modulating the targeted signalling pathways gives crucial information on the dynamic nature of the readout as well as signal specificity. This is important, as random multiple integration events of the transgene, as it occurs for example using Tol2 transgenesis, can result in a reporter being under the influence of their genomic environment e.g. enhancer elements. In order to eliminate false readouts by such positional effects, it is important to screen the progeny of several independent founder fish. Current literature can also give information on the expected reporter expression. The *Tg(BRE:mRFP)* has been validated in such a manner as outlined in the Introduction (1.3).

Taken together, zebrafish transgenic reporter lines are proving to be a crucial tool to study signalling dynamics in living vertebrates as zebrafish are easy to manipulate and optically accessible. Already, pharmacological screens have identified novel pathway regulators (Gorelick and Halpern, 2011, Molina et al., 2009, Sanvitale et al., 2013). Moreover, pathway reporter lines will be very useful in combination with the emerging zebrafish disease models, for example for studying the signalling environment during tumour progression. Recent advances in developing direct tools for gene manipulation, such as zinc finger nucleases (Meng et al., 2008, Sander et al., 2011), TALEN mutagenesis (Bedell et al., 2012, Doyon et al., 2008, Huang et al., 2011) and the CRISPR/Cas system (Hwang et al., 2013), will open up a range new possibilities to target specific genes and create mutants with high efficiency.

7.2 Integrating Snw1 function into the two-step model of BMP activity

As discussed earlier, previous studies in our lab identified Snw1 as a regulator of BMP activity during vertebrate neural crest development (Wu et al., 2011). I could demonstrate that loss of Snw1 led to increased *bmp2b* transcript levels. This effect, however, is confined to the NPB although *bmp2b* transcripts are present in the entire NNE. Snw1 is expressed only dorsally, in the NP region, during somitogenesis, thus overlapping with *bmp2b* expression only where the horseshoe-shaped domain of BMP activity is initially detected. This suggests a tissue specific requirement for the control of *bmp2b* transcription and thus BMP activity at the NPB.

Interestingly, Snw1 is only essential for BMP activity after gastrulation. Partly, this could be due to maternally deposited Snw1. However, depletion of Snw1 using morpholinos in zebrafish indicated a loss of Snw1 protein during gastrulation without affecting BMP activity during gastrulation as measured by PSmad1/5 western blotting (Wu et al., 2011). It is an intriguing possibility that Snw1 contributes to the switch from a gradient of BMP activity to distinct domains at the neural plate border. Interestingly, BMP activity is initially restricted to the NPB after gastrulation although transcripts can be detected I the entire NNE. This could be due to the requirement for Cvl2 to focus BMP activity or a BMP repressor such as Bambi-b might inhibit BMP activity in the lateral and ventral ectoderm. There is also the possibility that Snw1 is required for proper *bmp2b* processing after gastrulation, which is why active Bmp2b proteins would only be synthesised at the NPB. This hypothesis will have to be tested in the future possibly by the use of photo-cleavable morpholinos that give temporal control over gene expression.

7.3 Implications for cancer

Studying signalling during early development and organogenesis also has implications outside of understanding developmental processes. Many of the underlying signalling pathways are redeployed in diseases such as cancer. Thus identifying pathway regulators might provide novel therapeutic targets. An example for this is leflunomide, which was identified in a chemical screen for regulators of

NC development (White et al., 2011). Leflunomide not only inhibits NC cell fate, but also melanoma growth in tissue culture and a transgenic zebrafish melanoma model. I have demonstrated that leflunomide possibly acts by inhibiting BMP activity after gastrulation. It is not clear yet whether this is due to defects at the level of *bmp2b* regulation. Currently, leflunomide is being tested in a phase I clinical trial (Prof. Leonard Zon, personal communication).

Many of the components I have identified to be part of the BMP gene regulatory network have been implicated in disease. Mutations of DLX3 in humans result in defects in tooth development (Dong et al., 2005, Nieminen et al., 2011), which is likely to be a result of impaired NC development. In contrast, increased levels of Cvl2/BMPER have been reported in malignant tumours of several tissues (Heinke et al., 2012). Similarly, the BMP inhibitor BAMBI is linked to cancer development. BAMBI is present at high levels in ovarian cancer (Pils et al., 2010) and overexpression of BAMBI in colorectal cancer increases the metastatic potential (Fritzmann et al., 2009, Togo et al., 2008), whereas BAMBI expression is silenced in a subset of high-grade bladder cancer (Khin et al., 2009). This discrepancy might reflect the dual role, as a tumour promoting and inhibiting factor, of BMP/TGF-β signalling (Connolly et al., 2012, Thawani et al., 2010, Wakefield and Hill, 2013).

Snw1 has not yet been directly implicated in tumourigenesis. However, there are indications that Snw1 might play a role in some cancers. The catalogue of somatic mutations (COSMIC) is a database that collects mutation data from primary literature (http://cancer.sanger.ac.uk/cosmic). According to the collected data 42 unique mutations have been identified for Snw1, 29 of which are missense and 7 are silent mutation and whereas 3 mutation lead to a frameshift. There are no obvious clusters and the mutations are distributed along the whole length of the transcript. Also it is not clear whether any of the mutations are driving mutations but several amino acids are mutated in different tissues. No mutation of the S224 phosphorylation site has so far been identified.

Snw1 is an essential survival factor and in my analysis, loss of Snw1 leads to cell cycle arrest in G2 (data not shown). However, during development, NC is most sensitive to Snw1 depletion, indicating a increased dependency on Snw1 function compared to other tissues. Since melanocytes are a derivative of NC, I tested Snw1 expression in commonly used melanoma cell lines compared to

melanocytes. I identified several melanoma cells lines with dramatically increased Snw1 protein levels (data not shown). Interestingly, this correlated with activation of BMP signalling and growth rate. It will be exciting to further test a possible role of Snw1 by for example overexpression of Snw1 in melanocytes to induce tumourigenic properties. As genetic tools become more readily available it will be interesting to study some of the factors I identified in this study in zebrafish tumours models. For example, it would be exciting to test the function of Snw1 in skin cancer using an established zebrafish model for melanoma formation (White et al., 2011). Using such disease models in combination with the *Tg(BRE:mRFP)* reporter will also give novel insight into the regulation of BMP activity at different stages of tumour progression and metastasis.

Taken together, my research demonstrates the relevance of studying *in vivo* regulators of signalling pathways. I hope that my results will contribute not only to the understanding of the regulation and contribution of BMP signalling during ectodermal patterning, but will also help to decipher the processes underlying diseases.

Chapter 8. Appendix

Appendix 1: Selected list of spliceosome-associated proteins identified using mass spectrometry with Flag-SNW1 as a bait.

Appendix 2: Selected list of non-spliceosome associated proteins identified using mass spectrometry with Flag-SNW1 as a bait.

Appendix 3: Heat map for following data set: (FDR) ≤ 0.05, fold change > 2 between cont. MO and lower amount of *snw1* MO, read count ≥ 200 in one of the samples.

On CD:

Appendix 4: Original data file of a representative experiment (including benzonase step) containing proteins identified using mass spectrometry. To be opened using scaffold.

Appendix 5: iBAQ analysis of the above mentioned experiment.

Appendix 6: complete list of Snw1 targets identified in the RNA sequencing with following cut off criteria: (FDR) ≤ 0.05, fold change > 2 between cont. MO and lower amount of *snw1* MO, read count ≥ 200 in one of the samples.

Appendix 7: complete list of Snw1 targets with following cut off criteria: (FDR) ≤ 0.05, fold change > 2 between cont. MO and higher amount of *snw1* MO, read count ≥ 200 in one of the samples.

Appendix 8: Intronic reads: (FDR) ≤ 0.05, fold change > 2 between cont. MO and higher amount of *snw1* MO, read count ≥ 30 in one of the samples.

Reference List

ABU-ELMAGD, M., GARCIA-MORALES, C. & WHEELER, G. N. 2006. Frizzled7 mediates canonical Wnt signaling in neural crest induction. *Dev Biol,* 298**,** 285-98.

AHRENS, K. & SCHLOSSER, G. 2005. Tissues and signals involved in the induction of placodal Six1 expression in Xenopus laevis. *Dev Biol,* 288**,** 40-59.

AJUH, P., KUSTER, B., PANOV, K., ZOMERDIJK, J. C., MANN, M. & LAMOND, A. I. 2000. Functional analysis of the human CDC5L complex and identification of its components by mass spectrometry. *EMBO J,* 19**,** 6569-81.

AKIMENKO, M. A., EKKER, M., WEGNER, J., LIN, W. & WESTERFIELD, M. 1994. Combinatorial expression of three zebrafish genes related to distal-less: part of a homeobox gene code for the head. *J Neurosci,* 14**,** 3475-86.

AKIYOSHI, S., INOUE, H., HANAI, J., KUSANAGI, K., NEMOTO, N., MIYAZONO, K. & KAWABATA, M. 1999. c-Ski acts as a transcriptional co-repressor in transforming growth factor-beta signaling through interaction with smads. *J Biol Chem,* 274**,** 35269-77.

ALARCON, C., ZAROMYTIDOU, A. I., XI, Q., GAO, S., YU, J., FUJISAWA, S., BARLAS, A., MILLER, A. N., MANOVA-TODOROVA, K., MACIAS, M. J., SAPKOTA, G., PAN, D. & MASSAGUE, J. 2009. Nuclear CDKs drive Smad transcriptional activation and turnover in BMP and TGF-beta pathways. *Cell,* 139**,** 757-69.

ALBERS, M., DIMENT, A., MURARU, M., RUSSELL, C. S. & BEGGS, J. D. 2003. Identification and characterization of Prp45p and Prp46p, essential pre-mRNA splicing factors. *RNA,* 9**,** 138-50.

ALLO, M., BUGGIANO, V., FEDEDA, J. P., PETRILLO, E., SCHOR, I., DE LA MATA, M., AGIRRE, E., PLASS, M., EYRAS, E., ELELA, S. A., KLINCK, R., CHABOT, B. & KORNBLIHTT, A. R. 2009. Control of alternative splicing through siRNA-mediated transcriptional gene silencing. *Nat Struct Mol Biol,* 16**,** 717-24.

ALONSO, L. G., GARCIA-ALAI, M. M., NADRA, A. D., LAPENA, A. N., ALMEIDA, F. L., GUALFETTI, P. & PRAT-GAY, G. D. 2002. High-risk (HPV16) human papillomavirus E7 oncoprotein is highly stable and extended, with conformational transitions that could explain its multiple cellular binding partners. *Biochemistry,* 41**,** 10510-8.

AMBROSIO, A. L., TAELMAN, V. F., LEE, H. X., METZINGER, C. A., COFFINIER, C. & DE ROBERTIS, E. M. 2008. Crossveinless-2 Is a BMP feedback inhibitor that binds Chordin/BMP to regulate Xenopus embryonic patterning. *Dev Cell,* 15**,** 248-60.

AMBROZKOVA, M., PUTA, F., FUKOVA, I., SKRUZNY, M., BRABEK, J. & FOLK, P. 2001. The fission yeast ortholog of the coregulator SKIP interacts with the small subunit of U2AF. *Biochem Biophys Res Commun,* 284**,** 1148-54.

AMSTERDAM, A., NISSEN, R. M., SUN, Z., SWINDELL, E. C., FARRINGTON, S. & HOPKINS, N. 2004. Identification of 315 genes essential for early zebrafish development. *Proc Natl Acad Sci U S A,* 101**,** 12792-7.

ANDERSSON, E. R., SANDBERG, R. & LENDAHL, U. 2011. Notch signaling: simplicity in design, versatility in function. *Development,* 138**,** 3593-612.

ARAGON, E., GOERNER, N., ZAROMYTIDOU, A. I., XI, Q., ESCOBEDO, A., MASSAGUE, J. & MACIAS, M. J. 2011. A Smad action turnover switch

operated by WW domain readers of a phosphoserine code. *Genes Dev,* 25**,** 1275-88.

ATTISANO, L. & LEE-HOEFLICH, S. T. 2001. The Smads. *Genome Biol,* 2**,** REVIEWS3010.

BANG, A. G., PAPALOPULU, N., GOULDING, M. D. & KINTNER, C. 1999. Expression of Pax-3 in the lateral neural plate is dependent on a Wnt-mediated signal from posterior nonaxial mesoderm. *Dev Biol,* 212**,** 366-80.

BANNISTER, A. J., SCHNEIDER, R., MYERS, F. A., THORNE, A. W., CRANE-ROBINSON, C. & KOUZARIDES, T. 2005. Spatial distribution of di- and tri-methyl lysine 36 of histone H3 at active genes. *J Biol Chem,* 280**,** 17732-6.

BARRY, J. B., LEONG, G. M., CHURCH, W. B., ISSA, L. L., EISMAN, J. A. & GARDINER, E. M. 2003. Interactions of SKIP/NCoA-62, TFIIB, and retinoid X receptor with vitamin D receptor helix H10 residues. *J Biol Chem,* 278**,** 8224-8.

BATLLE, E. & WILKINSON, D. G. 2012. Molecular mechanisms of cell segregation and boundary formation in development and tumorigenesis. *Cold Spring Harb Perspect Biol,* 4**,** a008227.

BAUDINO, T. A., KRAICHELY, D. M., JEFCOAT, S. C., JR., WINCHESTER, S. K., PARTRIDGE, N. C. & MACDONALD, P. N. 1998. Isolation and characterization of a novel coactivator protein, NCoA-62, involved in vitamin D-mediated transcription. *J Biol Chem,* 273**,** 16434-41.

BEDELL, V. M., WANG, Y., CAMPBELL, J. M., POSHUSTA, T. L., STARKER, C. G., KRUG, R. G., 2ND, TAN, W., PENHEITER, S. G., MA, A. C., LEUNG, A. Y., FAHRENKRUG, S. C., CARLSON, D. F., VOYTAS, D. F., CLARK, K. J., ESSNER, J. J. & EKKER, S. C. 2012. In vivo genome editing using a high-efficiency TALEN system. *Nature,* 491**,** 114-8.

BEPPU, H., KAWABATA, M., HAMAMOTO, T., CHYTIL, A., MINOWA, O., NODA, T. & MIYAZONO, K. 2000. BMP type II receptor is required for gastrulation and early development of mouse embryos. *Dev Biol,* 221**,** 249-58.

BILLIN, A. N., THIRLWELL, H. & AYER, D. E. 2000. Beta-catenin-histone deacetylase interactions regulate the transition of LEF1 from a transcriptional repressor to an activator. *Mol Cell Biol,* 20**,** 6882-90.

BINNERTS, M. E., WEN, X., CANTE-BARRETT, K., BRIGHT, J., CHEN, H. T., ASUNDI, V., SATTARI, P., TANG, T., BOYLE, B., FUNK, W. & RUPP, F. 2004. Human Crossveinless-2 is a novel inhibitor of bone morphogenetic proteins. *Biochem Biophys Res Commun,* 315**,** 272-80.

BIRNBOIM, H. C. & DOLY, J. 1979. A rapid alkaline extraction procedure for screening recombinant plasmid DNA. *Nucleic Acids Res,* 7**,** 1513-23.

BLANCO CALVO, M., BOLOS FERNANDEZ, V., MEDINA VILLAAMIL, V., APARICIO GALLEGO, G., DIAZ PRADO, S. & GRANDE PULIDO, E. 2009. Biology of BMP signalling and cancer. *Clin Transl Oncol,* 11**,** 126-37.

BOUSQUET-ANTONELLI, C., PRESUTTI, C. & TOLLERVEY, D. 2000. Identification of a regulated pathway for nuclear pre-mRNA turnover. *Cell,* 102**,** 765-75.

BRAULT, V., MOORE, R., KUTSCH, S., ISHIBASHI, M., ROWITCH, D. H., MCMAHON, A. P., SOMMER, L., BOUSSADIA, O. & KEMLER, R. 2001. Inactivation of the beta-catenin gene by Wnt1-Cre-mediated deletion results in dramatic brain malformation and failure of craniofacial development. *Development,* 128**,** 1253-64.

BRAY, S. & FURRIOLS, M. 2001. Notch pathway: making sense of suppressor of hairless. *Curr Biol,* 11**,** R217-21.

BRES, V., GOMES, N., PICKLE, L. & JONES, K. A. 2005. A human splicing factor, SKIP, associates with P-TEFb and enhances transcription elongation by HIV-1 Tat. *Genes Dev,* 19**,** 1211-26.

BRES, V., YOSHIDA, T., PICKLE, L. & JONES, K. A. 2009. SKIP interacts with c-Myc and Menin to promote HIV-1 Tat transactivation. *Mol Cell,* 36**,** 75-87.

BRESNICK, E. H., CHU, J., CHRISTENSEN, H. M., LIN, B. & NORTON, J. 2000. Linking Notch signaling, chromatin remodeling, and T-cell leukemogenesis. *J Cell Biochem Suppl,* Suppl 35**,** 46-53.

BRIDGES, C. B. 1920. The Mutant Crossveinless in Drosophila Melanogaster. *Proc Natl Acad Sci U S A,* 6**,** 660-3.

BRUGMANN, S. A., PANDUR, P. D., KENYON, K. L., PIGNONI, F. & MOODY, S. A. 2004. Six1 promotes a placodal fate within the lateral neurogenic ectoderm by functioning as both a transcriptional activator and repressor. *Development,* 131**,** 5871-81.

BRUNEAU, S., MOURRAIN, P. & ROSA, F. M. 1997. Expression of contact, a new zebrafish DVR member, marks mesenchymal cell lineages in the developing pectoral fins and head and is regulated by retinoic acid. *Mech Dev,* 65**,** 163-73.

BUTLER, S. J. & DODD, J. 2003. A role for BMP heterodimers in roof plate-mediated repulsion of commissural axons. *Neuron,* 38**,** 389-401.

CALADO, A., KUTAY, U., KUHN, U., WAHLE, E. & CARMO-FONSECA, M. 2000. Deciphering the cellular pathway for transport of poly(A)-binding protein II. *RNA,* 6**,** 245-56.

CARNEY, T. J., DUTTON, K. A., GREENHILL, E., DELFINO-MACHIN, M., DUFOURCQ, P., BLADER, P. & KELSH, R. N. 2006. A direct role for Sox10 in specification of neural crest-derived sensory neurons. *Development,* 133**,** 4619-30.

CARVALHO, S., RAPOSO, A. C., MARTINS, F. B., GROSSO, A. R., SRIDHARA, S. C., RINO, J., CARMO-FONSECA, M. & DE ALMEIDA, S. F. 2013. Histone methyltransferase SETD2 coordinates FACT recruitment with nucleosome dynamics during transcription. *Nucleic Acids Res,* 41**,** 2881-93.

CHANARAT, S., SEIZL, M. & STRASSER, K. 2011. The Prp19 complex is a novel transcription elongation factor required for TREX occupancy at transcribed genes. *Genes Dev,* 25**,** 1147-58.

CHEN, G. I. & GINGRAS, A. C. 2007. Affinity-purification mass spectrometry (AP-MS) of serine/threonine phosphatases. *Methods,* 42**,** 298-305.

CHEN, Y., ZHANG, L. & JONES, K. A. 2011. SKIP counteracts p53-mediated apoptosis via selective regulation of p21Cip1 mRNA splicing. *Genes Dev,* 25**,** 701-16.

CHRISTENSEN, R. G., ENUAMEH, M. S., NOYES, M. B., BRODSKY, M. H., WOLFE, S. A. & STORMO, G. D. 2012. Recognition models to predict DNA-binding specificities of homeodomain proteins. *Bioinformatics,* 28**,** i84-9.

CONLEY, C. A., SILBURN, R., SINGER, M. A., RALSTON, A., ROHWER-NUTTER, D., OLSON, D. J., GELBART, W. & BLAIR, S. S. 2000. Crossveinless 2 contains cysteine-rich domains and is required for high levels of BMP-like activity during the formation of the cross veins in Drosophila. *Development,* 127**,** 3947-59.

CONNOLLY, E. C., FREIMUTH, J. & AKHURST, R. J. 2012. Complexities of TGF-beta targeted cancer therapy. *Int J Biol Sci,* 8**,** 964-78.

COOPER, K. L., ARMSTRONG, J. & MOENS, C. B. 2005. Zebrafish foggy/spt 5 is required for migration of facial branchiomotor neurons but not for their survival. *Dev Dyn,* 234**,** 651-8.

CORTINA, C., PALOMO-PONCE, S., IGLESIAS, M., FERNANDEZ-MASIP, J. L., VIVANCOS, A., WHISSELL, G., HUMA, M., PEIRO, N., GALLEGO, L., JONKHEER, S., DAVY, A., LLORETA, J., SANCHO, E. & BATLLE, E. 2007. EphB-ephrin-B interactions suppress colorectal cancer progression by compartmentalizing tumor cells. *Nat Genet,* 39**,** 1376-83.

CUI, Y., HACKENMILLER, R., BERG, L., JEAN, F., NAKAYAMA, T., THOMAS, G. & CHRISTIAN, J. L. 2001. The activity and signaling range of mature BMP-4 is regulated by sequential cleavage at two sites within the prodomain of the precursor. *Genes Dev,* 15**,** 2797-802.

DAHL, R., WANI, B. & HAYMAN, M. J. 1998. The Ski oncoprotein interacts with Skip, the human homolog of Drosophila Bx42. *Oncogene,* 16**,** 1579-86.

DAI, H., HOGAN, C., GOPALAKRISHNAN, B., TORRES-VAZQUEZ, J., NGUYEN, M., PARK, S., RAFTERY, L. A., WARRIOR, R. & ARORA, K. 2000. The zinc finger protein schnurri acts as a Smad partner in mediating the transcriptional response to decapentaplegic. *Dev Biol,* 227**,** 373-87.

DAL-PRA, S., FURTHAUER, M., VAN-CELST, J., THISSE, B. & THISSE, C. 2006. Noggin1 and Follistatin-like2 function redundantly to Chordin to antagonize BMP activity. *Dev Biol,* 298**,** 514-26.

DALE, L. & SLACK, J. M. 1987. Fate map for the 32-cell stage of Xenopus laevis. *Development,* 99**,** 527-51.

DANIELIAN, P. S., MUCCINO, D., ROWITCH, D. H., MICHAEL, S. K. & MCMAHON, A. P. 1998. Modification of gene activity in mouse embryos in utero by a tamoxifen-inducible form of Cre recombinase. *Curr Biol,* 8**,** 1323-6.

DE ALMEIDA, S. F., GROSSO, A. R., KOCH, F., FENOUIL, R., CARVALHO, S., ANDRADE, J., LEVEZINHO, H., GUT, M., EICK, D., GUT, I., ANDRAU, J. C., FERRIER, P. & CARMO-FONSECA, M. 2011. Splicing enhances recruitment of methyltransferase HYPB/Setd2 and methylation of histone H3 Lys36. *Nat Struct Mol Biol,* 18**,** 977-83.

DE BELLARD, M. E., CHING, W., GOSSLER, A. & BRONNER-FRASER, M. 2002. Disruption of segmental neural crest migration and ephrin expression in delta-1 null mice. *Dev Biol,* 249**,** 121-30.

DE LA MATA, M., ALONSO, C. R., KADENER, S., FEDEDA, J. P., BLAUSTEIN, M., PELISCH, F., CRAMER, P., BENTLEY, D. & KORNBLIHTT, A. R. 2003. A slow RNA polymerase II affects alternative splicing in vivo. *Mol Cell,* 12**,** 525-32.

DEARDORFF, M. A., TAN, C., SAINT-JEANNET, J. P. & KLEIN, P. S. 2001. A role for frizzled 3 in neural crest development. *Development,* 128**,** 3655-63.

DEN HOLLANDER, A. I., BIYANWILA, J., KOVACH, P., BARDAKJIAN, T., TRABOULSI, E. I., RAGGE, N. K., SCHNEIDER, A. & MALICKI, J. 2010. Genetic defects of GDF6 in the zebrafish out of sight mutant and in human eye developmental anomalies. *BMC Genet,* 11**,** 102.

DENG, C. X., WYNSHAW-BORIS, A., SHEN, M. M., DAUGHERTY, C., ORNITZ, D. M. & LEDER, P. 1994. Murine FGFR-1 is required for early postimplantation growth and axial organization. *Genes Dev,* 8**,** 3045-57.

DONG, J., AMOR, D., ALDRED, M. J., GU, T., ESCAMILLA, M. & MACDOUGALL, M. 2005. DLX3 mutation associated with autosomal dominant amelogenesis imperfecta with taurodontism. *Am J Med Genet A,* 133A**,** 138-41.

DOREY, K. & AMAYA, E. 2010. FGF signalling: diverse roles during early vertebrate embryogenesis. *Development,* 137**,** 3731-42.

DORSKY, R. I., MOON, R. T. & RAIBLE, D. W. 1998. Control of neural crest cell fate by the Wnt signalling pathway. *Nature,* 396**,** 370-3.

DORSKY, R. I., SHELDAHL, L. C. & MOON, R. T. 2002. A transgenic Lef1/beta-catenin-dependent reporter is expressed in spatially restricted domains throughout zebrafish development. *Dev Biol,* 241**,** 229-37.

DOYON, Y., MCCAMMON, J. M., MILLER, J. C., FARAJI, F., NGO, C., KATIBAH, G. E., AMORA, R., HOCKING, T. D., ZHANG, L., REBAR, E. J., GREGORY, P. D., URNOV, F. D. & AMACHER, S. L. 2008. Heritable targeted gene disruption in zebrafish using designed zinc-finger nucleases. *Nat Biotechnol,* 26**,** 702-8.

DREESEN, O. & BRIVANLOU, A. H. 2007. Signaling pathways in cancer and embryonic stem cells. *Stem Cell Rev,* 3**,** 7-17.

DUDAS, M., SRIDURONGRIT, S., NAGY, A., OKAZAKI, K. & KAARTINEN, V. 2004. Craniofacial defects in mice lacking BMP type I receptor Alk2 in neural crest cells. *Mech Dev,* 121**,** 173-82.

DUNN, N. R., WINNIER, G. E., HARGETT, L. K., SCHRICK, J. J., FOGO, A. B. & HOGAN, B. L. 1997. Haploinsufficient phenotypes in Bmp4 heterozygous null mice and modification by mutations in Gli3 and Alx4. *Dev Biol,* 188**,** 235-47.

DUPIN, E., CREUZET, S. & LE DOUARIN, N. M. 2006. The contribution of the neural crest to the vertebrate body. *Adv Exp Med Biol,* 589**,** 96-119.

DUTTON, K. A., PAULINY, A., LOPES, S. S., ELWORTHY, S., CARNEY, T. J., RAUCH, J., GEISLER, R., HAFFTER, P. & KELSH, R. N. 2001. Zebrafish colourless encodes sox10 and specifies non-ectomesenchymal neural crest fates. *Development,* 128**,** 4113-25.

EIVERS, E., DEMAGNY, H., CHOI, R. H. & DE ROBERTIS, E. M. 2011. Phosphorylation of Mad controls competition between wingless and BMP signaling. *Sci Signal,* 4**,** ra68.

ELKOUBY, Y. M., ELIAS, S., CASEY, E. S., BLYTHE, S. A., TSABAR, N., KLEIN, P. S., ROOT, H., LIU, K. J. & FRANK, D. 2010. Mesodermal Wnt signaling organizes the neural plate via Meis3. *Development,* 137**,** 1531-41.

ENDO, Y., OSUMI, N. & WAKAMATSU, Y. 2002. Bimodal functions of Notch-mediated signaling are involved in neural crest formation during avian ectoderm development. *Development,* 129**,** 863-73.

ENGERT, J. C., SERVAES, S., SUTRAVE, P., HUGHES, S. H. & ROSENTHAL, N. 1995. Activation of a muscle-specific enhancer by the Ski proto-oncogene. *Nucleic Acids Res,* 23**,** 2988-94.

ENGLISH, M. A., LEI, L., BLAKE, T., WINCOVITCH, S. M., SR., SOOD, R., AZUMA, M., HICKSTEIN, D. & LIU, P. P. 2012. Incomplete splicing, cell division defects, and hematopoietic blockage in dhx8 mutant zebrafish. *Dev Dyn,* 241**,** 879-89.

ESTERBERG, R., DELALANDE, J. M. & FRITZ, A. 2008. Tailbud-derived Bmp4 drives proliferation and inhibits maturation of zebrafish chordamesoderm. *Development,* 135**,** 3891-901.

ESTERBERG, R. & FRITZ, A. 2009. dlx3b/4b are required for the formation of the preplacodal region and otic placode through local modulation of BMP activity. *Dev Biol,* 325**,** 189-99.

FARNY, N. G., HURT, J. A. & SILVER, P. A. 2008. Definition of global and transcript-specific mRNA export pathways in metazoans. *Genes Dev,* 22**,** 66-78.

FIGUEROA, J. D. & HAYMAN, M. J. 2004. Differential effects of the Ski-interacting protein (SKIP) on differentiation induced by transforming growth factor-beta1 and bone morphogenetic protein-2 in C2C12 cells. *Exp Cell Res,* 296**,** 163-72.

FIUZA, U. M. & ARIAS, A. M. 2007. Cell and molecular biology of Notch. *J Endocrinol,* 194**,** 459-74.

FOLK, P., PUTA, F., KRPEJSOVA, L., BLAHUSKOVA, A., MARKOS, A., RABINO, M. & DOTTIN, R. P. 1996. The homolog of chromatin binding protein Bx42 identified in Dictyostelium. *Gene,* 181**,** 229-31.

FOLK, P., PUTA, F. & SKRUZNY, M. 2004. Transcriptional coregulator SNW/SKIP: the concealed tie of dissimilar pathways. *Cell Mol Life Sci,* 61**,** 629-40.

FORD-PERRISS, M., ABUD, H. & MURPHY, M. 2001. Fibroblast growth factors in the developing central nervous system. *Clin Exp Pharmacol Physiol,* 28**,** 493-503.

FRENCH, C. R., ERICKSON, T., FRENCH, D. V., PILGRIM, D. B. & WASKIEWICZ, A. J. 2009. Gdf6a is required for the initiation of dorsal-ventral retinal patterning and lens development. *Dev Biol,* 333**,** 37-47.

FRITZMANN, J., MORKEL, M., BESSER, D., BUDCZIES, J., KOSEL, F., BREMBECK, F. H., STEIN, U., FICHTNER, I., SCHLAG, P. M. & BIRCHMEIER, W. 2009. A colorectal cancer expression profile that includes transforming growth factor beta inhibitor BAMBI predicts metastatic potential. *Gastroenterology,* 137**,** 165-75.

FUENTEALBA, L. C., EIVERS, E., IKEDA, A., HURTADO, C., KURODA, H., PERA, E. M. & DE ROBERTIS, E. M. 2007. Integrating patterning signals: Wnt/GSK3 regulates the duration of the BMP/Smad1 signal. *Cell,* 131**,** 980-93.

FUJISE, M., TAKEO, S., KAMIMURA, K., MATSUO, T., AIGAKI, T., IZUMI, S. & NAKATO, H. 2003. Dally regulates Dpp morphogen gradient formation in the Drosophila wing. *Development,* 130**,** 1515-22.

FUJIWARA, T., DEHART, D. B., SULIK, K. K. & HOGAN, B. L. 2002. Distinct requirements for extra-embryonic and embryonic bone morphogenetic protein 4 in the formation of the node and primitive streak and coordination of left-right asymmetry in the mouse. *Development,* 129**,** 4685-96.

FURRIOLS, M. & BRAY, S. 2000. Dissecting the mechanisms of suppressor of hairless function. *Dev Biol,* 227**,** 520-32.

FURTHAUER, M., THISSE, C. & THISSE, B. 1997. A role for FGF-8 in the dorsoventral patterning of the zebrafish gastrula. *Development,* 124**,** 4253-64.

FURTHAUER, M., VAN CELST, J., THISSE, C. & THISSE, B. 2004. Fgf signalling controls the dorsoventral patterning of the zebrafish embryo. *Development,* 131**,** 2853-64.

GAHURA, O., ABRHAMOVA, K., SKRUZNY, M., VALENTOVA, A., MUNZAROVA, V., FOLK, P. & PUTA, F. 2009. Prp45 affects Prp22 partition in spliceosomal complexes and splicing efficiency of non-consensus substrates. *J Cell Biochem,* 106**,** 139-51.

GAJAVELLI, S., WOOD, P. M., PENNICA, D., WHITTEMORE, S. R. & TSOULFAS, P. 2004. BMP signaling initiates a neural crest differentiation program in embryonic rat CNS stem cells. *Exp Neurol,* 188**,** 205-23.

GARNETT, A. T., SQUARE, T. A. & MEDEIROS, D. M. 2012. BMP, Wnt and FGF signals are integrated through evolutionarily conserved enhancers to achieve robust expression of Pax3 and Zic genes at the zebrafish neural plate border. *Development,* 139**,** 4220-31.

GAVIN, A. C., BOSCHE, M., KRAUSE, R., GRANDI, P., MARZIOCH, M., BAUER, A., SCHULTZ, J., RICK, J. M., MICHON, A. M., CRUCIAT, C. M., REMOR, M., HOFERT, C., SCHELDER, M., BRAJENOVIC, M., RUFFNER, H., MERINO, A., KLEIN, K., HUDAK, M., DICKSON, D., RUDI, T., GNAU, V., BAUCH, A., BASTUCK, S., HUHSE, B., LEUTWEIN, C., HEURTIER, M. A., COPLEY, R. R., EDELMANN, A., QUERFURTH, E., RYBIN, V., DREWES, G., RAIDA, M., BOUWMEESTER, T., BORK, P., SERAPHIN, B., KUSTER, B., NEUBAUER, G. & SUPERTI-FURGA, G. 2002. Functional organization of the yeast proteome by systematic analysis of protein complexes. *Nature,* 415**,** 141-7.

GEISS-FRIEDLANDER, R. & MELCHIOR, F. 2007. Concepts in sumoylation: a decade on. *Nat Rev Mol Cell Biol,* 8**,** 947-56.

GLAVIC, A., MARIS HONORE, S., GLORIA FEIJOO, C., BASTIDAS, F., ALLENDE, M. L. & MAYOR, R. 2004a. Role of BMP signaling and the homeoprotein Iroquois in the specification of the cranial placodal field. *Dev Biol,* 272**,** 89-103.

GLAVIC, A., SILVA, F., AYBAR, M. J., BASTIDAS, F. & MAYOR, R. 2004b. Interplay between Notch signaling and the homeoprotein Xiro1 is required for neural crest induction in Xenopus embryos. *Development,* 131**,** 347-59.

GLINKA, A., WU, W., DELIUS, H., MONAGHAN, A. P., BLUMENSTOCK, C. & NIEHRS, C. 1998. Dickkopf-1 is a member of a new family of secreted proteins and functions in head induction. *Nature,* 391**,** 357-62.

GOLDMAN, D. C., HACKENMILLER, R., NAKAYAMA, T., SOPORY, S., WONG, C., KULESSA, H. & CHRISTIAN, J. L. 2006. Mutation of an upstream cleavage site in the BMP4 prodomain leads to tissue-specific loss of activity. *Development,* 133**,** 1933-42.

GORELICK, D. A. & HALPERN, M. E. 2011. Visualization of estrogen receptor transcriptional activation in zebrafish. *Endocrinology,* 152**,** 2690-703.

GOSSE, N. J. & BAIER, H. 2009. An essential role for Radar (Gdf6a) in inducing dorsal fate in the zebrafish retina. *Proc Natl Acad Sci U S A,* 106**,** 2236-41.

GOUMANS, M. J., VALDIMARSDOTTIR, G., ITOH, S., ROSENDAHL, A., SIDERAS, P. & TEN DIJKE, P. 2002. Balancing the activation state of the endothelium via two distinct TGF-beta type I receptors. *EMBO J,* 21**,** 1743-53.

GOUTEL, C., KISHIMOTO, Y., SCHULTE-MERKER, S. & ROSA, F. 2000. The ventralizing activity of Radar, a maternally expressed bone morphogenetic protein, reveals complex bone morphogenetic protein interactions controlling dorso-ventral patterning in zebrafish. *Mech Dev,* 99**,** 15-27.

GRAY, R. S., BAYLY, R. D., GREEN, S. A., AGARWALA, S., LOWE, C. J. & WALLINGFORD, J. B. 2009. Diversification of the expression patterns and developmental functions of the dishevelled gene family during chordate evolution. *Dev Dyn,* 238**,** 2044-57.

GRAZIOTTO, J. J., FARKAS, M. H., BUJAKOWSKA, K., DERAMAUDT, B. M., ZHANG, Q., NANDROT, E. F., INGLEHEARN, C. F., BHATTACHARYA, S. S. & PIERCE, E. A. 2011. Three gene-targeted mouse models of RNA splicing factor RP show late-onset RPE and retinal degeneration. *Invest Ophthalmol Vis Sci,* 52**,** 190-8.

GRIGORYAN, T., WEND, P., KLAUS, A. & BIRCHMEIER, W. 2008. Deciphering the function of canonical Wnt signals in development and disease: conditional loss- and gain-of-function mutations of beta-catenin in mice. *Genes Dev,* 22**,** 2308-41.

GU, Z., REYNOLDS, E. M., SONG, J., LEI, H., FEIJEN, A., YU, L., HE, W., MACLAUGHLIN, D. T., VAN DEN EIJNDEN-VAN RAAIJ, J., DONAHOE, P. K. & LI, E. 1999. The type I serine/threonine kinase receptor ActRIA (ALK2) is required for gastrulation of the mouse embryo. *Development,* 126**,** 2551-61.

GUILLOT, N., KOLLINS, D., GILBERT, V., XAVIER, S., CHEN, J., GENTLE, M., REDDY, A., BOTTINGER, E., JIANG, R., RASTALDI, M. P., CORBELLI, A. & SCHLONDORFF, D. 2012. BAMBI regulates angiogenesis and endothelial homeostasis through modulation of alternative TGFbeta signaling. *PLoS One,* 7**,** e39406.

GUO, S., YAMAGUCHI, Y., SCHILBACH, S., WADA, T., LEE, J., GODDARD, A., FRENCH, D., HANDA, H. & ROSENTHAL, A. 2000. A regulator of transcriptional elongation controls vertebrate neuronal development. *Nature,* 408**,** 366-9.

HAMMERSCHMIDT, M. & MULLINS, M. C. 2002. Dorsoventral patterning in the zebrafish: bone morphogenetic proteins and beyond. *Results Probl Cell Differ,* 40**,** 72-95.

HARRISON, C. A., AL-MUSAWI, S. L. & WALTON, K. L. 2011. Prodomains regulate the synthesis, extracellular localisation and activity of TGF-beta superfamily ligands. *Growth Factors,* 29**,** 174-86.

HARVEY, K. & TAPON, N. 2007. The Salvador-Warts-Hippo pathway - an emerging tumour-suppressor network. *Nat Rev Cancer,* 7**,** 182-91.

HASHIGUCHI, M. & MULLINS, M. C. 2013. Anteroposterior and dorsoventral patterning are coordinated by an identical patterning clock. *Development,* 140**,** 1970-80.

HEINKE, J., KERBER, M., RAHNER, S., MNICH, L., LASSMANN, S., HELBING, T., WERNER, M., PATTERSON, C., BODE, C. & MOSER, M. 2012. Bone

morphogenetic protein modulator BMPER is highly expressed in malignant tumors and controls invasive cell behavior. *Oncogene,* 31**,** 2919-30.

HERNANDEZ-LAGUNAS, L., POWELL, D. R., LAW, J., GRANT, K. A. & ARTINGER, K. B. 2011. prdm1a and olig4 act downstream of Notch signaling to regulate cell fate at the neural plate border. *Dev Biol,* 356**,** 496-505.

HILLEREN, P. J. & PARKER, R. 2003. Cytoplasmic degradation of splice-defective pre-mRNAs and intermediates. *Mol Cell,* 12**,** 1453-65.

HNILICOVA, J., HOZEIFI, S., DUSKOVA, E., ICHA, J., TOMANKOVA, T. & STANEK, D. 2011. Histone deacetylase activity modulates alternative splicing. *PLoS One,* 6**,** e16727.

HONG, C. S., PARK, B. Y. & SAINT-JEANNET, J. P. 2008. Fgf8a induces neural crest indirectly through the activation of Wnt8 in the paraxial mesoderm. *Development,* 135**,** 3903-10.

HONG, C. S. & SAINT-JEANNET, J. P. 2007. The activity of Pax3 and Zic1 regulates three distinct cell fates at the neural plate border. *Mol Biol Cell,* 18**,** 2192-202.

HSIN, J. P. & MANLEY, J. L. 2012. The RNA polymerase II CTD coordinates transcription and RNA processing. *Genes Dev,* 26**,** 2119-37.

HUANG, P., XIAO, A., ZHOU, M., ZHU, Z., LIN, S. & ZHANG, B. 2011. Heritable gene targeting in zebrafish using customized TALENs. *Nat Biotechnol,* 29**,** 699-700.

HUANG, S. M., MISHINA, Y. M., LIU, S., CHEUNG, A., STEGMEIER, F., MICHAUD, G. A., CHARLAT, O., WIELLETTE, E., ZHANG, Y., WIESSNER, S., HILD, M., SHI, X., WILSON, C. J., MICKANIN, C., MYER, V., FAZAL, A., TOMLINSON, R., SERLUCA, F., SHAO, W., CHENG, H., SHULTZ, M., RAU, C., SCHIRLE, M., SCHLEGL, J., GHIDELLI, S., FAWELL, S., LU, C., CURTIS, D., KIRSCHNER, M. W., LENGAUER, C., FINAN, P. M., TALLARICO, J. A., BOUWMEESTER, T., PORTER, J. A., BAUER, A. & CONG, F. 2009. Tankyrase inhibition stabilizes axin and antagonizes Wnt signalling. *Nature,* 461**,** 614-20.

HWANG, W. Y., FU, Y., REYON, D., MAEDER, M. L., TSAI, S. Q., SANDER, J. D., PETERSON, R. T., YEH, J. R. & JOUNG, J. K. 2013. Efficient genome editing in zebrafish using a CRISPR-Cas system. *Nat Biotechnol,* 31**,** 227-9.

IKEYA, M., KAWADA, M., KIYONARI, H., SASAI, N., NAKAO, K., FURUTA, Y. & SASAI, Y. 2006. Essential pro-Bmp roles of crossveinless 2 in mouse organogenesis. *Development,* 133**,** 4463-73.

IKEYA, M., LEE, S. M., JOHNSON, J. E., MCMAHON, A. P. & TAKADA, S. 1997. Wnt signalling required for expansion of neural crest and CNS progenitors. *Nature,* 389**,** 966-70.

ITOH, N. 2007. The Fgf families in humans, mice, and zebrafish: their evolutional processes and roles in development, metabolism, and disease. *Biol Pharm Bull,* 30**,** 1819-25.

JASUJA, R., VOSS, N., GE, G., HOFFMAN, G. G., LYMAN-GINGERICH, J., PELEGRI, F. & GREENSPAN, D. S. 2006. bmp1 and mini fin are functionally redundant in regulating formation of the zebrafish dorsoventral axis. *Mech Dev,* 123**,** 548-58.

JIA, Q., MCDILL, B. W., LI, S. Z., DENG, C., CHANG, C. P. & CHEN, F. 2007. Smad signaling in the neural crest regulates cardiac outflow tract remodeling through cell autonomous and non-cell autonomous effects. *Dev Biol,* 311**,** 172-84.

JIANG, Y. J., BRAND, M., HEISENBERG, C. P., BEUCHLE, D., FURUTANI-SEIKI, M., KELSH, R. N., WARGA, R. M., GRANATO, M., HAFFTER, P., HAMMERSCHMIDT, M., KANE, D. A., MULLINS, M. C., ODENTHAL, J., VAN EEDEN, F. J. & NUSSLEIN-VOLHARD, C. 1996. Mutations affecting neurogenesis and brain morphology in the zebrafish, Danio rerio. *Development,* 123**,** 205-16.

JIMENO, R., GOMARIZ, R. P., GUTIERREZ-CANAS, I., MARTINEZ, C., JUARRANZ, Y. & LECETA, J. 2010. New insights into the role of VIP on the ratio of T-cell

subsets during the development of autoimmune diabetes. *Immunol Cell Biol,* 88**,** 734-45.

JONES, C. M., ARMES, N. & SMITH, J. C. 1996. Signalling by TGF-beta family members: short-range effects of Xnr-2 and BMP-4 contrast with the long-range effects of activin. *Curr Biol,* 6**,** 1468-75.

KAARTINEN, V., DUDAS, M., NAGY, A., SRIDURONGRIT, S., LU, M. M. & EPSTEIN, J. A. 2004. Cardiac outflow tract defects in mice lacking ALK2 in neural crest cells. *Development,* 131**,** 3481-90.

KAMATO, D., BURCH, M. L., PIVA, T. J., REZAEI, H. B., ROSTAM, M. A., XU, S., ZHENG, W., LITTLE, P. J. & OSMAN, N. 2013. Transforming growth factor-beta signalling: Role and consequences of Smad linker region phosphorylation. *Cell Signal,* 25**,** 2017-24.

KAMIMURA, M., MATSUMOTO, K., KOSHIBA-TAKEUCHI, K. & OGURA, T. 2004. Vertebrate crossveinless 2 is secreted and acts as an extracellular modulator of the BMP signaling cascade. *Dev Dyn,* 230**,** 434-45.

KANG, M. R., LEE, S. W., UM, E., KANG, H. T., HWANG, E. S., KIM, E. J. & UM, S. J. 2010. Reciprocal roles of SIRT1 and SKIP in the regulation of RAR activity: implication in the retinoic acid-induced neuronal differentiation of P19 cells. *Nucleic Acids Res,* 38**,** 822-31.

KAWASHIMA, T., PELLEGRINI, M. & CHANFREAU, G. F. 2009. Nonsense-mediated mRNA decay mutes the splicing defects of spliceosome component mutations. *RNA,* 15**,** 2236-47.

KEEGAN, B. R., FELDMAN, J. L., LEE, D. H., KOOS, D. S., HO, R. K., STAINIER, D. Y. & YELON, D. 2002. The elongation factors Pandora/Spt6 and Foggy/Spt5 promote transcription in the zebrafish embryo. *Development,* 129**,** 1623-32.

KHIN, S. S., KITAZAWA, R., WIN, N., AYE, T. T., MORI, K., KONDO, T. & KITAZAWA, S. 2009. BAMBI gene is epigenetically silenced in subset of high-grade bladder cancer. *Int J Cancer,* 125**,** 328-38.

KHO, A. T., ZHAO, Q., CAI, Z., BUTTE, A. J., KIM, J. Y., POMEROY, S. L., ROWITCH, D. H. & KOHANE, I. S. 2004. Conserved mechanisms across development and tumorigenesis revealed by a mouse development perspective of human cancers. *Genes Dev,* 18**,** 629-40.

KIECKER, C. & NIEHRS, C. 2001. A morphogen gradient of Wnt/beta-catenin signalling regulates anteroposterior neural patterning in Xenopus. *Development,* 128**,** 4189-201.

KIM, W., KIM, M. & JHO, E. H. 2013. Wnt/beta-catenin signalling: from plasma membrane to nucleus. *Biochem J,* 450**,** 9-21.

KIM, Y. J., NOGUCHI, S., HAYASHI, Y. K., TSUKAHARA, T., SHIMIZU, T. & ARAHATA, K. 2001. The product of an oculopharyngeal muscular dystrophy gene, poly(A)-binding protein 2, interacts with SKIP and stimulates muscle-specific gene expression. *Hum Mol Genet,* 10**,** 1129-39.

KIMMEL, C. B., BALLARD, W. W., KIMMEL, S. R., ULLMANN, B. & SCHILLING, T. F. 1995. Stages of embryonic development of the zebrafish. *Dev Dyn,* 203**,** 253-310.

KISHIMOTO, Y., LEE, K. H., ZON, L., HAMMERSCHMIDT, M. & SCHULTE-MERKER, S. 1997. The molecular nature of zebrafish swirl: BMP2 function is essential during early dorsoventral patterning. *Development,* 124**,** 4457-66.

KO, S. O., CHUNG, I. H., XU, X., OKA, S., ZHAO, H., CHO, E. S., DENG, C. & CHAI, Y. 2007. Smad4 is required to regulate the fate of cranial neural crest cells. *Dev Biol,* 312**,** 435-47.

KOISHI, K., ZHANG, M., MCLENNAN, I. S. & HARRIS, A. J. 1995. MyoD protein accumulates in satellite cells and is neurally regulated in regenerating myotubes and skeletal muscle fibers. *Dev Dyn,* 202**,** 244-54.

KOLASINSKA-ZWIERZ, P., DOWN, T., LATORRE, I., LIU, T., LIU, X. S. & AHRINGER, J. 2009. Differential chromatin marking of introns and expressed exons by H3K36me3. *Nat Genet,* 41**,** 376-81.

KONDO, M. 2007. Bone morphogenetic proteins in the early development of zebrafish. *FEBS J,* 274**,** 2960-7.

KOOS, D. S. & HO, R. K. 1999. The nieuwkoid/dharma homeobox gene is essential for bmp2b repression in the zebrafish pregastrula. *Dev Biol,* 215**,** 190-207.

KORCHYNSKYI, O. & TEN DIJKE, P. 2002. Identification and functional characterization of distinct critically important bone morphogenetic protein-specific response elements in the Id1 promoter. *J Biol Chem,* 277**,** 4883-91.

KOSTROUCHOVA, M., HOUSA, D., KOSTROUCH, Z., SAUDEK, V. & RALL, J. E. 2002. SKIP is an indispensable factor for Caenorhabditis elegans development. *Proc Natl Acad Sci U S A,* 99**,** 9254-9.

KRETZSCHMAR, M., DOODY, J. & MASSAGUE, J. 1997. Opposing BMP and EGF signalling pathways converge on the TGF-beta family mediator Smad1. *Nature,* 389**,** 618-22.

KRUPNIK, V. E., SHARP, J. D., JIANG, C., ROBISON, K., CHICKERING, T. W., AMARAVADI, L., BROWN, D. E., GUYOT, D., MAYS, G., LEIBY, K., CHANG, B., DUONG, T., GOODEARL, A. D., GEARING, D. P., SOKOL, S. Y. & MCCARTHY, S. A. 1999. Functional and structural diversity of the human Dickkopf gene family. *Gene,* 238**,** 301-13.

KWAK, J., PARK, O. K., JUNG, Y. J., HWANG, B. J., KWON, S. H. & KEE, Y. 2013. Live image profiling of neural crest lineages in zebrafish transgenic lines. *Mol Cells,* 35**,** 255-60.

KWON, H. J., BHAT, N., SWEET, E. M., CORNELL, R. A. & RILEY, B. B. 2010. Identification of early requirements for preplacodal ectoderm and sensory organ development. *PLoS Genet,* 6.

LABONNE, C. & BRONNER-FRASER, M. 1998. Neural crest induction in Xenopus: evidence for a two-signal model. *Development,* 125**,** 2403-14.

LARRAIN, J., OELGESCHLAGER, M., KETPURA, N. I., REVERSADE, B., ZAKIN, L. & DE ROBERTIS, E. M. 2001. Proteolytic cleavage of Chordin as a switch for the dual activities of Twisted gastrulation in BMP signaling. *Development,* 128**,** 4439-47.

LEONG, G. M., SUBRAMANIAM, N., FIGUEROA, J., FLANAGAN, J. L., HAYMAN, M. J., EISMAN, J. A. & KOUZMENKO, A. P. 2001. Ski-interacting protein interacts with Smad proteins to augment transforming growth factor-beta-dependent transcription. *J Biol Chem,* 276**,** 18243-8.

LEONG, G. M., SUBRAMANIAM, N., ISSA, L. L., BARRY, J. B., KINO, T., DRIGGERS, P. H., HAYMAN, M. J., EISMAN, J. A. & GARDINER, E. M. 2004. Ski-interacting protein, a bifunctional nuclear receptor coregulator that interacts with N-CoR/SMRT and p300. *Biochem Biophys Res Commun,* 315**,** 1070-6.

LEUNG, T., BISCHOF, J., SOLL, I., NIESSING, D., ZHANG, D., MA, J., JACKLE, H. & DRIEVER, W. 2003. bozozok directly represses bmp2b transcription and mediates the earliest dorsoventral asymmetry of bmp2b expression in zebrafish. *Development,* 130**,** 3639-49.

LEWIS, J. L., BONNER, J., MODRELL, M., RAGLAND, J. W., MOON, R. T., DORSKY, R. I. & RAIBLE, D. W. 2004. Reiterated Wnt signaling during zebrafish neural crest development. *Development,* 131**,** 1299-308.

LIANG, J., LINTS, R., FOEHR, M. L., TOKARZ, R., YU, L., EMMONS, S. W., LIU, J. & SAVAGE-DUNN, C. 2003. The Caenorhabditis elegans schnurri homolog sma-9 mediates stage- and cell type-specific responses to DBL-1 BMP-related signaling. *Development,* 130**,** 6453-64.

LITSIOU, A., HANSON, S. & STREIT, A. 2005. A balance of FGF, BMP and WNT signalling positions the future placode territory in the head. *Development,* 132**,** 4051-62.

LITTLE, S. C. & MULLINS, M. C. 2009. Bone morphogenetic protein heterodimers assemble heteromeric type I receptor complexes to pattern the dorsoventral axis. *Nat Cell Biol,* 11**,** 637-43.

LIU, D., BLACK, B. L. & DERYNCK, R. 2001. TGF-beta inhibits muscle differentiation through functional repression of myogenic transcription factors by Smad3. *Genes Dev,* 15**,** 2950-66.

LOGAN, C. Y. & NUSSE, R. 2004. The Wnt signaling pathway in development and disease. *Annu Rev Cell Dev Biol,* 20**,** 781-810.

LOWERY, J. W. & DE CAESTECKER, M. P. 2010. BMP signaling in vascular development and disease. *Cytokine Growth Factor Rev,* 21**,** 287-98.

LUNN, J. S., FISHWICK, K. J., HALLEY, P. A. & STOREY, K. G. 2007. A spatial and temporal map of FGF/Erk1/2 activity and response repertoires in the early chick embryo. *Dev Biol,* 302**,** 536-52.

LUO, K., STROSCHEIN, S. L., WANG, W., CHEN, D., MARTENS, E., ZHOU, S. & ZHOU, Q. 1999. The Ski oncoprotein interacts with the Smad proteins to repress TGFbeta signaling. *Genes Dev,* 13**,** 2196-206.

MAKAROV, E. M., MAKAROVA, O. V., URLAUB, H., GENTZEL, M., WILL, C. L., WILM, M. & LUHRMANN, R. 2002. Small nuclear ribonucleoprotein remodeling during catalytic activation of the spliceosome. *Science,* 298**,** 2205-8.

MARCHANT, L., LINKER, C., RUIZ, P., GUERRERO, N. & MAYOR, R. 1998. The inductive properties of mesoderm suggest that the neural crest cells are specified by a BMP gradient. *Dev Biol,* 198**,** 319-29.

MATSUDA, S. & SHIMMI, O. 2012. Directional transport and active retention of Dpp/BMP create wing vein patterns in Drosophila. *Dev Biol,* 366**,** 153-62.

MAYOR, R., MORGAN, R. & SARGENT, M. G. 1995. Induction of the prospective neural crest of Xenopus. *Development,* 121**,** 767-77.

MCKEEHAN, W. L., WANG, F. & KAN, M. 1998. The heparan sulfate-fibroblast growth factor family: diversity of structure and function. *Prog Nucleic Acid Res Mol Biol,* 59**,** 135-76.

MCKIE, A. B., MCHALE, J. C., KEEN, T. J., TARTTELIN, E. E., GOLIATH, R., VAN LITH-VERHOEVEN, J. J., GREENBERG, J., RAMESAR, R. S., HOYNG, C. B., CREMERS, F. P., MACKEY, D. A., BHATTACHARYA, S. S., BIRD, A. C., MARKHAM, A. F. & INGLEHEARN, C. F. 2001. Mutations in the pre-mRNA splicing factor gene PRPC8 in autosomal dominant retinitis pigmentosa (RP13). *Hum Mol Genet,* 10**,** 1555-62.

MCMILLAN, R. & MATSUI, W. 2012. Molecular pathways: the hedgehog signaling pathway in cancer. *Clin Cancer Res,* 18**,** 4883-8.

MENG, X., NOYES, M. B., ZHU, L. J., LAWSON, N. D. & WOLFE, S. A. 2008. Targeted gene inactivation in zebrafish using engineered zinc-finger nucleases. *Nat Biotechnol,* 26**,** 695-701.

MEULEMANS, D. & BRONNER-FRASER, M. 2004. Gene-regulatory interactions in neural crest evolution and development. *Dev Cell,* 7**,** 291-9.

MEYERS, E. N., LEWANDOSKI, M. & MARTIN, G. R. 1998. An Fgf8 mutant allelic series generated by Cre- and Flp-mediated recombination. *Nat Genet,* 18**,** 136-41.

MILES, W. O., JAFFRAY, E., CAMPBELL, S. G., TAKEDA, S., BAYSTON, L. J., BASU, S. P., LI, M., RAFTERY, L. A., ASHE, M. P., HAY, R. T. & ASHE, H. L. 2008. Medea SUMOylation restricts the signaling range of the Dpp morphogen in the Drosophila embryo. *Genes Dev,* 22**,** 2578-90.

MINOUX, M. & RIJLI, F. M. 2010. Molecular mechanisms of cranial neural crest cell migration and patterning in craniofacial development. *Development,* 137**,** 2605-21.

MISHINA, Y., CROMBIE, R., BRADLEY, A. & BEHRINGER, R. R. 1999. Multiple roles for activin-like kinase-2 signaling during mouse embryogenesis. *Dev Biol,* 213**,** 314-26.

MISHINA, Y., SUZUKI, A., UENO, N. & BEHRINGER, R. R. 1995. Bmpr encodes a type I bone morphogenetic protein receptor that is essential for gastrulation during mouse embryogenesis. *Genes Dev,* 9**,** 3027-37.

MOLINA, G., VOGT, A., BAKAN, A., DAI, W., QUEIROZ DE OLIVEIRA, P., ZNOSKO, W., SMITHGALL, T. E., BAHAR, I., LAZO, J. S., DAY, B. W. & TSANG, M. 2009. Zebrafish chemical screening reveals an inhibitor of Dusp6 that expands cardiac cell lineages. *Nat Chem Biol,* 5**,** 680-7.

MONSORO-BURQ, A. H., FLETCHER, R. B. & HARLAND, R. M. 2003. Neural crest induction by paraxial mesoderm in Xenopus embryos requires FGF signals. *Development,* 130**,** 3111-24.

MONSORO-BURQ, A. H., WANG, E. & HARLAND, R. 2005. Msx1 and Pax3 cooperate to mediate FGF8 and WNT signals during Xenopus neural crest induction. *Dev Cell,* 8**,** 167-78.

MONTES, M., BECERRA, S., SANCHEZ-ALVAREZ, M. & SUNE, C. 2012. Functional coupling of transcription and splicing. *Gene,* 501**,** 104-17.

MORO, E., OZHAN-KIZIL, G., MONGERA, A., BEIS, D., WIERZBICKI, C., YOUNG, R. M., BOURNELE, D., DOMENICHINI, A., VALDIVIA, L. E., LUM, L., CHEN, C., AMATRUDA, J. F., TISO, N., WEIDINGER, G. & ARGENTON, F. 2012. In vivo Wnt signaling tracing through a transgenic biosensor fish reveals novel activity domains. *Dev Biol,* 366**,** 327-40.

MOSER, M., BINDER, O., WU, Y., AITSEBAOMO, J., REN, R., BODE, C., BAUTCH, V. L., CONLON, F. L. & PATTERSON, C. 2003. BMPER, a novel endothelial cell precursor-derived protein, antagonizes bone morphogenetic protein signaling and endothelial cell differentiation. *Mol Cell Biol,* 23**,** 5664-79.

MOSER, M., YU, Q., BODE, C., XIONG, J. W. & PATTERSON, C. 2007. BMPER is a conserved regulator of hematopoietic and vascular development in zebrafish. *J Mol Cell Cardiol,* 43**,** 243-53.

MULLINS, M. C., HAMMERSCHMIDT, M., KANE, D. A., ODENTHAL, J., BRAND, M., VAN EEDEN, F. J., FURUTANI-SEIKI, M., GRANATO, M., HAFFTER, P., HEISENBERG, C. P., JIANG, Y. J., KELSH, R. N. & NUSSLEIN-VOLHARD, C. 1996. Genes establishing dorsoventral pattern formation in the zebrafish embryo: the ventral specifying genes. *Development,* 123**,** 81-93.

NEGERI, D., EGGERT, H., GIENAPP, R. & SAUMWEBER, H. 2002. Inducible RNA interference uncovers the Drosophila protein Bx42 as an essential nuclear cofactor involved in Notch signal transduction. *Mech Dev,* 117**,** 151-62.

NELLEN, D., BURKE, R., STRUHL, G. & BASLER, K. 1996. Direct and long-range action of a DPP morphogen gradient. *Cell,* 85**,** 357-68.

NEUBAUER, G., KING, A., RAPPSILBER, J., CALVIO, C., WATSON, M., AJUH, P., SLEEMAN, J., LAMOND, A. & MANN, M. 1998. Mass spectrometry and EST-database searching allows characterization of the multi-protein spliceosome complex. *Nat Genet,* 20**,** 46-50.

NGUYEN, V. H., SCHMID, B., TROUT, J., CONNORS, S. A., EKKER, M. & MULLINS, M. C. 1998. Ventral and lateral regions of the zebrafish gastrula, including the neural crest progenitors, are established by a bmp2b/swirl pathway of genes. *Dev Biol,* 199**,** 93-110.

NICHANE, M., DE CROZE, N., REN, X., SOUOPGUI, J., MONSORO-BURQ, A. H. & BELLEFROID, E. J. 2008a. Hairy2-Id3 interactions play an essential role in Xenopus neural crest progenitor specification. *Dev Biol,* 322**,** 355-67.

NICHANE, M., REN, X., SOUOPGUI, J. & BELLEFROID, E. J. 2008b. Hairy2 functions through both DNA-binding and non DNA-binding mechanisms at the neural plate border in Xenopus. *Dev Biol,* 322**,** 368-80.

NIE, X., DENG, C. X., WANG, Q. & JIAO, K. 2008. Disruption of Smad4 in neural crest cells leads to mid-gestation death with pharyngeal arch, craniofacial and cardiac defects. *Dev Biol,* 316**,** 417-30.

NIEMINEN, P., LUKINMAA, P. L., ALAPULLI, H., METHUEN, M., SUOJARVI, T., KIVIRIKKO, S., PELTOLA, J., ASIKAINEN, M. & ALALUUSUA, S. 2011. DLX3 homeodomain mutations cause tricho-dento-osseous syndrome with novel phenotypes. *Cells Tissues Organs,* 194**,** 49-59.

NIKAIDO, M., TADA, M., TAKEDA, H., KUROIWA, A. & UENO, N. 1999. In vivo analysis using variants of zebrafish BMPR-IA: range of action and involvement of BMP in ectoderm patterning. *Development,* 126**,** 181-90.

NISHIMATSU, S. & THOMSEN, G. H. 1998. Ventral mesoderm induction and patterning by bone morphogenetic protein heterodimers in Xenopus embryos. *Mech Dev,* 74**,** 75-88.

NUSSLEIN-VOLHARD, C. & WIESCHAUS, E. 1980. Mutations affecting segment number and polarity in Drosophila. *Nature,* 287**,** 795-801.

OHI, M. D., LINK, A. J., REN, L., JENNINGS, J. L., MCDONALD, W. H. & GOULD, K. L. 2002. Proteomics analysis reveals stable multiprotein complexes in both fission and budding yeasts containing Myb-related Cdc5p/Cef1p, novel pre-mRNA splicing factors, and snRNAs. *Mol Cell Biol,* 22**,** 2011-24.

ONICHTCHOUK, D., CHEN, Y. G., DOSCH, R., GAWANTKA, V., DELIUS, H., MASSAGUE, J. & NIEHRS, C. 1999. Silencing of TGF-beta signalling by the pseudoreceptor BAMBI. *Nature,* 401**,** 480-5.

OXTOBY, E. & JOWETT, T. 1993. Cloning of the zebrafish krox-20 gene (krx-20) and its expression during hindbrain development. *Nucleic Acids Res,* 21**,** 1087-95.

PANDUR, P. D., SULLIVAN, S. A. & MOODY, S. A. 2002. Multiple maternal influences on dorsal-ventral fate of Xenopus animal blastomeres. *Dev Dyn,* 225**,** 581-7.

PATTHEY, C., EDLUND, T. & GUNHAGA, L. 2009. Wnt-regulated temporal control of BMP exposure directs the choice between neural plate border and epidermal fate. *Development,* 136**,** 73-83.

PERA, E. M., IKEDA, A., EIVERS, E. & DE ROBERTIS, E. M. 2003. Integration of IGF, FGF, and anti-BMP signals via Smad1 phosphorylation in neural induction. *Genes Dev,* 17**,** 3023-8.

PERROT, C. Y., JAVELAUD, D. & MAUVIEL, A. 2013. Overlapping activities of TGF-beta and Hedgehog signaling in cancer: therapeutic targets for cancer treatment. *Pharmacol Ther,* 137**,** 183-99.

PICCOLO, S., AGIUS, E., LU, B., GOODMAN, S., DALE, L. & DE ROBERTIS, E. M. 1997. Cleavage of Chordin by Xolloid metalloprotease suggests a role for proteolytic processing in the regulation of Spemann organizer activity. *Cell,* 91**,** 407-16.

PIEPER, M., AHRENS, K., RINK, E., PETER, A. & SCHLOSSER, G. 2012. Differential distribution of competence for panplacodal and neural crest induction to non-neural and neural ectoderm. *Development,* 139**,** 1175-87.

PILS, D., WITTINGER, M., PETZ, M., GUGERELL, A., GREGOR, W., ALFANZ, A., HORVAT, R., BRAICU, E. I., SEHOULI, J., ZEILLINGER, R., MIKULITS, W. & KRAINER, M. 2010. BAMBI is overexpressed in ovarian cancer and co-translocates with Smads into the nucleus upon TGF-beta treatment. *Gynecol Oncol,* 117**,** 189-97.

PLEISS, J. A., WHITWORTH, G. B., BERGKESSEL, M. & GUTHRIE, C. 2007. Transcript specificity in yeast pre-mRNA splicing revealed by mutations in core spliceosomal components. *PLoS Biol,* 5**,** e90.

POLIAKOV, A., COTRINA, M. L., PASINI, A. & WILKINSON, D. G. 2008. Regulation of EphB2 activation and cell repulsion by feedback control of the MAPK pathway. *J Cell Biol,* 183**,** 933-47.

PYATI, U. J., COOPER, M. S., DAVIDSON, A. J., NECHIPORUK, A. & KIMELMAN, D. 2006. Sustained Bmp signaling is essential for cloaca development in zebrafish. *Development,* 133**,** 2275-84.

PYROWOLAKIS, G., HARTMANN, B., MULLER, B., BASLER, K. & AFFOLTER, M. 2004. A simple molecular complex mediates widespread BMP-induced repression during Drosophila development. *Dev Cell,* 7**,** 229-40.

RAFTERY, L. A. & UMULIS, D. M. 2012. Regulation of BMP activity and range in Drosophila wing development. *Curr Opin Cell Biol,* 24**,** 158-65.

RAMEL, M. C. & HILL, C. S. 2012. Spatial regulation of BMP activity. *FEBS Lett,* 586**,** 1929-41.

RAMEL, M. C. & HILL, C. S. 2013. The ventral to dorsal BMP activity gradient in the early zebrafish embryo is determined by graded expression of BMP ligands
. *Dev Biol,* in press.

REICHERT, S., RANDALL, R. A. & HILL, C. S. 2013. A BMP regulatory network controls ectodermal cell fate decisions at the neural plate border. *Development,* in press.

REIM, G. & BRAND, M. 2006. Maternal control of vertebrate dorsoventral axis formation and epiboly by the POU domain protein Spg/Pou2/Oct4. *Development,* 133**,** 2757-70.

RENTZSCH, F., ZHANG, J., KRAMER, C., SEBALD, W. & HAMMERSCHMIDT, M. 2006. Crossveinless 2 is an essential positive feedback regulator of Bmp signaling during zebrafish gastrulation. *Development,* 133**,** 801-11.

ROBU, M. E., LARSON, J. D., NASEVICIUS, A., BEIRAGHI, S., BRENNER, C., FARBER, S. A. & EKKER, S. C. 2007. p53 activation by knockdown technologies. *PLoS Genet,* 3**,** e78.

SAINT-JEANNET, J. P., HE, X., VARMUS, H. E. & DAWID, I. B. 1997. Regulation of dorsal fate in the neuraxis by Wnt-1 and Wnt-3a. *Proc Natl Acad Sci U S A,* 94**,** 13713-8.

SANDER, J. D., CADE, L., KHAYTER, C., REYON, D., PETERSON, R. T., JOUNG, J. K. & YEH, J. R. 2011. Targeted gene disruption in somatic zebrafish cells using engineered TALENs. *Nat Biotechnol,* 29**,** 697-8.

SANVITALE, C. E., KERR, G., CHAIKUAD, A., RAMEL, M. C., MOHEDAS, A. H., REICHERT, S., WANG, Y., TRIFFITT, J. T., CUNY, G. D., YU, P. B., HILL, C. S. & BULLOCK, A. N. 2013. A new class of small molecule inhibitor of BMP signaling. *PLoS One,* 8**,** e62721.

SAPKOTA, G., ALARCON, C., SPAGNOLI, F. M., BRIVANLOU, A. H. & MASSAGUE, J. 2007. Balancing BMP signaling through integrated inputs into the Smad1 linker. *Mol Cell,* 25**,** 441-54.

SASAI, Y., LU, B., STEINBEISSER, H., GEISSERT, D., GONT, L. K. & DE ROBERTIS, E. M. 1994. Xenopus chordin: a novel dorsalizing factor activated by organizer-specific homeobox genes. *Cell,* 79**,** 779-90.

SATO, T., SASAI, N. & SASAI, Y. 2005. Neural crest determination by co-activation of Pax3 and Zic1 genes in Xenopus ectoderm. *Development,* 132**,** 2355-63.

SAUMWEBER, H., FRASCH, M. & KORGE, G. 1990. Two puff-specific proteins bind within the 2.5 kb upstream region of the Drosophila melanogaster Sgs-4 gene. *Chromosoma,* 99**,** 52-60.

SAXENA, A., PENG, B. N. & BRONNER, M. E. 2013. Sox10-dependent neural crest origin of olfactory microvillous neurons in zebrafish. *Elife,* 2**,** e00336.

SAYANI, S., JANIS, M., LEE, C. Y., TOESCA, I. & CHANFREAU, G. F. 2008. Widespread impact of nonsense-mediated mRNA decay on the yeast intronome. *Mol Cell,* 31**,** 360-70.

SCHIER, A. F. & TALBOT, W. S. 2005. Molecular genetics of axis formation in zebrafish. *Annu Rev Genet,* 39**,** 561-613.

SCHMID, B., FURTHAUER, M., CONNORS, S. A., TROUT, J., THISSE, B., THISSE, C. & MULLINS, M. C. 2000. Equivalent genetic roles for bmp7/snailhouse and bmp2b/swirl in dorsoventral pattern formation. *Development,* 127**,** 957-67.

SCHMIERER, B. & HILL, C. S. 2007. TGFbeta-SMAD signal transduction: molecular specificity and functional flexibility. *Nat Rev Mol Cell Biol,* 8**,** 970-82.

SCHUMACHER, J. A., HASHIGUCHI, M., NGUYEN, V. H. & MULLINS, M. C. 2011. An intermediate level of BMP signaling directly specifies cranial neural crest progenitor cells in zebrafish. *PLoS One,* 6**,** e27403.

SCHWANHAUSSER, B., BUSSE, D., LI, N., DITTMAR, G., SCHUCHHARDT, J., WOLF, J., CHEN, W. & SELBACH, M. 2011. Global quantification of mammalian gene expression control. *Nature,* 473**,** 337-42.

SEKELSKY, J. J., NEWFELD, S. J., RAFTERY, L. A., CHARTOFF, E. H. & GELBART, W. M. 1995. Genetic characterization and cloning of mothers against dpp, a gene required for decapentaplegic function in Drosophila melanogaster. *Genetics,* 139**,** 1347-58.

SELLECK, M. A., GARCIA-CASTRO, M. I., ARTINGER, K. B. & BRONNER-FRASER, M. 1998. Effects of Shh and Noggin on neural crest formation demonstrate that BMP is required in the neural tube but not ectoderm. *Development,* 125**,** 4919-30.

SERPE, M., UMULIS, D., RALSTON, A., CHEN, J., OLSON, D. J., AVANESOV, A., OTHMER, H., O'CONNOR, M. B. & BLAIR, S. S. 2008. The BMP-binding protein Crossveinless 2 is a short-range, concentration-dependent, biphasic modulator of BMP signaling in Drosophila. *Developmental cell,* 14**,** 940-53.

SHIMMI, O., UMULIS, D., OTHMER, H. & O'CONNOR, M. B. 2005. Facilitated transport of a Dpp/Scw heterodimer by Sog/Tsg leads to robust patterning of the Drosophila blastoderm embryo. *Cell,* 120**,** 873-86.

SIDI, S., GOUTEL, C., PEYRIERAS, N. & ROSA, F. M. 2003. Maternal induction of ventral fate by zebrafish radar. *Proc Natl Acad Sci U S A,* 100**,** 3315-20.

SIMS, R. J., 3RD, MILLHOUSE, S., CHEN, C. F., LEWIS, B. A., ERDJUMENT-BROMAGE, H., TEMPST, P., MANLEY, J. L. & REINBERG, D. 2007. Recognition of trimethylated histone H3 lysine 4 facilitates the recruitment of transcription postinitiation factors and pre-mRNA splicing. *Mol Cell,* 28**,** 665-76.

SJODAL, M., EDLUND, T. & GUNHAGA, L. 2007. Time of exposure to BMP signals plays a key role in the specification of the olfactory and lens placodes ex vivo. *Dev Cell,* 13**,** 141-9.

SKROMNE, I. & STERN, C. D. 2001. Interactions between Wnt and Vg1 signalling pathways initiate primitive streak formation in the chick embryo. *Development,* 128**,** 2915-27.

SMITH, W. C. & HARLAND, R. M. 1992. Expression cloning of noggin, a new dorsalizing factor localized to the Spemann organizer in Xenopus embryos. *Cell,* 70**,** 829-40.

SOLOMON, K. S. & FRITZ, A. 2002. Concerted action of two dlx paralogs in sensory placode formation. *Development,* 129**,** 3127-36.

SOPORY, S., KWON, S., WEHRLI, M. & CHRISTIAN, J. L. 2010. Regulation of Dpp activity by tissue-specific cleavage of an upstream site within the prodomain. *Dev Biol,* 346**,** 102-12.

SPOKONY, R. F., AOKI, Y., SAINT-GERMAIN, N., MAGNER-FINK, E. & SAINT-JEANNET, J. P. 2002. The transcription factor Sox9 is required for cranial neural crest development in Xenopus. *Development,* 129**,** 421-32.

STEVENTON, B., ARAYA, C., LINKER, C., KURIYAMA, S. & MAYOR, R. 2009. Differential requirements of BMP and Wnt signalling during gastrulation and neurulation define two steps in neural crest induction. *Development,* 136**,** 771-9.

STICKNEY, H. L., IMAI, Y., DRAPER, B., MOENS, C. & TALBOT, W. S. 2007. Zebrafish bmp4 functions during late gastrulation to specify ventroposterior cell fates. *Dev Biol,* 310**,** 71-84.

STOTTMANN, R. W., CHOI, M., MISHINA, Y., MEYERS, E. N. & KLINGENSMITH, J. 2004. BMP receptor IA is required in mammalian neural crest cells for development of the cardiac outflow tract and ventricular myocardium. *Development,* 131**,** 2205-18.

STREIT, A. 2007. The preplacodal region: an ectodermal domain with multipotential progenitors that contribute to sense organs and cranial sensory ganglia. *Int J Dev Biol,* 51**,** 447-61.

STUHLMILLER, T. J. & GARCIA-CASTRO, M. I. 2012a. Current perspectives of the signaling pathways directing neural crest induction. *Cell Mol Life Sci,* 69**,** 3715-37.

STUHLMILLER, T. J. & GARCIA-CASTRO, M. I. 2012b. FGF/MAPK signaling is required in the gastrula epiblast for avian neural crest induction. *Development,* 139**,** 289-300.

SUN, X., MEYERS, E. N., LEWANDOSKI, M. & MARTIN, G. R. 1999. Targeted disruption of Fgf8 causes failure of cell migration in the gastrulating mouse embryo. *Genes Dev,* 13**,** 1834-46.

TAMAI, K., SEMENOV, M., KATO, Y., SPOKONY, R., LIU, C., KATSUYAMA, Y., HESS, F., SAINT-JEANNET, J. P. & HE, X. 2000. LDL-receptor-related proteins in Wnt signal transduction. *Nature,* 407**,** 530-5.

TANAKA, M., KAMO, T., OTA, S. & SUGIMURA, H. 2003. Association of Dishevelled with Eph tyrosine kinase receptor and ephrin mediates cell repulsion. *EMBO J,* 22**,** 847-58.

THAWANI, J. P., WANG, A. C., THAN, K. D., LIN, C. Y., LA MARCA, F. & PARK, P. 2010. Bone morphogenetic proteins and cancer: review of the literature. *Neurosurgery,* 66**,** 233-46; discussion 246.

THISSE, B., PFLUMIO, S., FÜRTHAUER, M., LOPPIN, B., HEYER, V., DEGRAVE, A., WOEHL, R., LUX, A., STEFFAN, T., CHARBONNIER, X. Q. & THISSE, C. 2001. Expression of the zebrafish genome during embryogenesis (NIH R01 RR15402). *ZFIN Direct Data Submission (*http://zfin.org).

THISSE, C., THISSE, B., HALPERN, M. E. & POSTLETHWAIT, J. H. 1994. Goosecoid expression in neurectoderm and mesendoderm is disrupted in zebrafish cyclops gastrulas. *Dev Biol,* 164**,** 420-9.

THISSE, C., THISSE, B. & POSTLETHWAIT, J. H. 1995. Expression of snail2, a second member of the zebrafish snail family, in cephalic mesendoderm and presumptive neural crest of wild-type and spadetail mutant embryos. *Dev Biol,* 172**,** 86-99.

THOMPSON, P. D., JURUTKA, P. W., HAUSSLER, C. A., WHITFIELD, G. K. & HAUSSLER, M. R. 1998. Heterodimeric DNA binding by the vitamin D receptor and retinoid X receptors is enhanced by 1,25-dihydroxyvitamin D3 and inhibited by 9-cis-retinoic acid. Evidence for allosteric receptor interactions. *J Biol Chem,* 273**,** 8483-91.

TOGO, N., OHWADA, S., SAKURAI, S., TOYA, H., SAKAMOTO, I., YAMADA, T., NAKANO, T., MUROYA, K., TAKEYOSHI, I., NAKAJIMA, T., SEKIYA, T., YAMAZUMI, Y., NAKAMURA, T. & AKIYAMA, T. 2008. Prognostic significance

of BMP and activin membrane-bound inhibitor in colorectal cancer. *World J Gastroenterol,* 14**,** 4880-8.

TORRES-VAZQUEZ, J., WARRIOR, R. & ARORA, K. 2000. schnurri is required for dpp-dependent patterning of the Drosophila wing. *Dev Biol,* 227**,** 388-402.

TRIBULO, C., AYBAR, M. J., NGUYEN, V. H., MULLINS, M. C. & MAYOR, R. 2003. Regulation of Msx genes by a Bmp gradient is essential for neural crest specification. *Development,* 130**,** 6441-52.

TSANG, M., KIM, R., DE CAESTECKER, M. P., KUDOH, T., ROBERTS, A. B. & DAWID, I. B. 2000. Zebrafish nma is involved in TGFbeta family signaling. *Genesis,* 28**,** 47-57.

TUCKER, J. A., MINTZER, K. A. & MULLINS, M. C. 2008. The BMP signaling gradient patterns dorsoventral tissues in a temporally progressive manner along the anteroposterior axis. *Dev Cell,* 14**,** 108-19.

TURNER, N. & GROSE, R. 2010. Fibroblast growth factor signalling: from development to cancer. *Nat Rev Cancer,* 10**,** 116-29.

TYAGI, A., RYME, J., BRODIN, D., OSTLUND FARRANTS, A. K. & VISA, N. 2009. SWI/SNF associates with nascent pre-mRNPs and regulates alternative pre-mRNA processing. *PLoS Genet,* 5**,** e1000470.

TZAHOR, E. 2007. Wnt/beta-catenin signaling and cardiogenesis: timing does matter. *Dev Cell,* 13**,** 10-3.

UVERSKY, V. N., GILLESPIE, J. R. & FINK, A. L. 2000. Why are "natively unfolded" proteins unstructured under physiologic conditions? *Proteins,* 41**,** 415-27.

VALERA, E., ISAACS, M. J., KAWAKAMI, Y., IZPISUA BELMONTE, J. C. & CHOE, S. 2010. BMP-2/6 heterodimer is more effective than BMP-2 or BMP-6 homodimers as inductor of differentiation of human embryonic stem cells. *PLoS One,* 5**,** e11167.

VAN AMERONGEN, R. 2012. Alternative Wnt pathways and receptors. *Cold Spring Harb Perspect Biol,* 4.

VERMEULEN, M., MULDER, K. W., DENISSOV, S., PIJNAPPEL, W. W., VAN SCHAIK, F. M., VARIER, R. A., BALTISSEN, M. P., STUNNENBERG, H. G., MANN, M. & TIMMERS, H. T. 2007. Selective anchoring of TFIID to nucleosomes by trimethylation of histone H3 lysine 4. *Cell,* 131**,** 58-69.

WAKEFIELD, L. M. & HILL, C. S. 2013. Beyond TGFbeta: roles of other TGFbeta superfamily members in cancer. *Nat Rev Cancer,* 13**,** 328-41.

WANG, C., CHANG, J. Y., YANG, C., HUANG, Y., LIU, J., YOU, P., MCKEEHAN, W. L., WANG, F. & LI, X. 2013. Type 1 Fibroblast Growth Factor Receptor in Cranial Neural Crest Cell-derived Mesenchyme Is Required for Palatogenesis. *J Biol Chem,* 288**,** 22174-83.

WANG, G., MATSUURA, I., HE, D. & LIU, F. 2009. Transforming growth factor-{beta}-inducible phosphorylation of Smad3. *J Biol Chem,* 284**,** 9663-73.

WANG, J., NAGY, A., LARSSON, J., DUDAS, M., SUCOV, H. M. & KAARTINEN, V. 2006. Defective ALK5 signaling in the neural crest leads to increased postmigratory neural crest cell apoptosis and severe outflow tract defects. *BMC Dev Biol,* 6**,** 51.

WANG, W., MARIANI, F. V., HARLAND, R. M. & LUO, K. 2000. Ski represses bone morphogenic protein signaling in Xenopus and mammalian cells. *Proc Natl Acad Sci U S A,* 97**,** 14394-9.

WANG, X., HARRIS, R. E., BAYSTON, L. J. & ASHE, H. L. 2008. Type IV collagens regulate BMP signalling in Drosophila. *Nature,* 455**,** 72-7.

WANG, X., ZHANG, S., ZHANG, J., HUANG, X., XU, C., WANG, W., LIU, Z., WU, J. & SHI, Y. 2010a. A large intrinsically disordered region in SKIP and its disorder-order transition induced by PPIL1 binding revealed by NMR. *J Biol Chem,* 285**,** 4951-63.

WANG, Y., FU, Y., GAO, L., ZHU, G., LIANG, J., GAO, C., HUANG, B., FENGER, U., NIEHRS, C., CHEN, Y. G. & WU, W. 2010b. Xenopus skip modulates Wnt/beta-catenin signaling and functions in neural crest induction. *J Biol Chem,* 285**,** 10890-901.

WEINBERG, E. S., ALLENDE, M. L., KELLY, C. S., ABDELHAMID, A., MURAKAMI, T., ANDERMANN, P., DOERRE, O. G., GRUNWALD, D. J. & RIGGLEMAN, B. 1996. Developmental regulation of zebrafish MyoD in wild-type, no tail and spadetail embryos. *Development,* 122**,** 271-80.

WESTERFIELD, M. 2000. *The zebrafish book. A guide for the laboratory use of zebrafish*

(Danio rerio), Eugene, OR, University of Oregon Press.

WHARTON, S. J., BASU, S. P. & ASHE, H. L. 2004. Smad affinity can direct distinct readouts of the embryonic extracellular Dpp gradient in Drosophila. *Curr Biol,* 14**,** 1550-8.

WHITE, R. M., CECH, J., RATANASIRINTRAWOOT, S., LIN, C. Y., RAHL, P. B., BURKE, C. J., LANGDON, E., TOMLINSON, M. L., MOSHER, J., KAUFMAN, C., CHEN, F., LONG, H. K., KRAMER, M., DATTA, S., NEUBERG, D., GRANTER, S., YOUNG, R. A., MORRISON, S., WHEELER, G. N. & ZON, L. I. 2011. DHODH modulates transcriptional elongation in the neural crest and melanoma. *Nature,* 471**,** 518-22.

WILHELM, B. T., MARGUERAT, S., ALIGIANNI, S., CODLIN, S., WATT, S. & BAHLER, J. 2011. Differential patterns of intronic and exonic DNA regions with respect to RNA polymerase II occupancy, nucleosome density and H3K36me3 marking in fission yeast. *Genome Biol,* 12**,** R82.

WILSON, P. A., LAGNA, G., SUZUKI, A. & HEMMATI-BRIVANLOU, A. 1997. Concentration-dependent patterning of the Xenopus ectoderm by BMP4 and its signal transducer Smad1. *Development,* 124**,** 3177-84.

WILSON, S. I., RYDSTROM, A., TRIMBORN, T., WILLERT, K., NUSSE, R., JESSELL, T. M. & EDLUND, T. 2001. The status of Wnt signalling regulates neural and epidermal fates in the chick embryo. *Nature,* 411**,** 325-30.

WITZE, E. S., OLD, W. M., RESING, K. A. & AHN, N. G. 2007. Mapping protein post-translational modifications with mass spectrometry. *Nat Methods,* 4**,** 798-806.

WOLPERT, L., JESSELL, T., LAWRENCE, P., MEYEROWITZ, E., ROBERTSON, E. & SMITH, J. 2007. Principles of Development. *Oxford University Press, Oxford*.

WU, M. Y. & HILL, C. S. 2009. Tgf-beta superfamily signaling in embryonic development and homeostasis. *Dev Cell,* 16**,** 329-43.

WU, M. Y., RAMEL, M. C., HOWELL, M. & HILL, C. S. 2011. SNW1 is a critical regulator of spatial BMP activity, neural plate border formation, and neural crest specification in vertebrate embryos. *PLoS Biol,* 9**,** e1000593.

YAMAGUCHI, T. P. 2001. Heads or tails: Wnts and anterior-posterior patterning. *Curr Biol,* 11**,** R713-24.

YAMAGUCHI, T. P., HARPAL, K., HENKEMEYER, M. & ROSSANT, J. 1994. fgfr-1 is required for embryonic growth and mesodermal patterning during mouse gastrulation. *Genes Dev,* 8**,** 3032-44.

YUN, J. I., KIM, H. R., PARK, H., KIM, S. K. & LEE, J. 2012. Small molecule inhibitors of the hedgehog signaling pathway for the treatment of cancer. *Arch Pharm Res,* 35**,** 1317-33.

ZENG, Y. A., RAHNAMA, M., WANG, S., SOSU-SEDZORME, W. & VERHEYEN, E. M. 2007. Drosophila Nemo antagonizes BMP signaling by phosphorylation of Mad and inhibition of its nuclear accumulation. *Development,* 134**,** 2061-71.

ZHANG, C., BAUDINO, T. A., DOWD, D. R., TOKUMARU, H., WANG, W. & MACDONALD, P. N. 2001. Ternary complexes and cooperative interplay

between NCoA-62/Ski-interacting protein and steroid receptor coactivators in vitamin D receptor-mediated transcription. *J Biol Chem,* 276**,** 40614-20.

ZHANG, C., DOWD, D. R., STAAL, A., GU, C., LIAN, J. B., VAN WIJNEN, A. J., STEIN, G. S. & MACDONALD, P. N. 2003. Nuclear coactivator-62 kDa/Ski-interacting protein is a nuclear matrix-associated coactivator that may couple vitamin D receptor-mediated transcription and RNA splicing. *J Biol Chem,* 278**,** 35325-36.

ZHANG, J. L., PATTERSON, L. J., QIU, L. Y., GRAZIUSSI, D., SEBALD, W. & HAMMERSCHMIDT, M. 2010. Binding between Crossveinless-2 and Chordin von Willebrand factor type C domains promotes BMP signaling by blocking Chordin activity. *PLoS One,* 5**,** e12846.

ZHOU, A. J., ZHU, Z., CLOKIE, C. M. & PEEL, S. A. 2012a. Mutation of a cleavage site adjacent to the mature domain leads to increase in secreted mature BMP-2 with reduced activity. *Growth Factors,* 30**,** 267-75.

ZHOU, S., FUJIMURO, M., HSIEH, J. J., CHEN, L., MIYAMOTO, A., WEINMASTER, G. & HAYWARD, S. D. 2000. SKIP, a CBF1-associated protein, interacts with the ankyrin repeat domain of NotchIC To facilitate NotchIC function. *Mol Cell Biol,* 20**,** 2400-10.

ZHOU, S., LO, W. C., SUHALIM, J. L., DIGMAN, M. A., GRATTON, E., NIE, Q. & LANDER, A. D. 2012b. Free extracellular diffusion creates the Dpp morphogen gradient of the Drosophila wing disc. *Curr Biol,* 22**,** 668-75.

ZHOU, Z., LICKLIDER, L. J., GYGI, S. P. & REED, R. 2002. Comprehensive proteomic analysis of the human spliceosome. *Nature,* 419**,** 182-5.

ZIMMERMAN, L. B., DE JESUS-ESCOBAR, J. M. & HARLAND, R. M. 1996. The Spemann organizer signal noggin binds and inactivates bone morphogenetic protein 4. *Cell,* 86**,** 599-606.